Carbon Fiber Monocoque Development For a Formula SAE Racecar

Senior Project Design Report

Cal Poly Formula SAE
CPFSAE@gmail.com

Andrew Cunningham

Andrew Ferrell

Matthew Lee

Tony Loogman

Mechanical Engineering Department
California Polytechnic State University
San Luis Obispo, CA

Formula Monocoque Development would like to extend a note of gratitude to the companies and individuals below for their support. Without your belief in us, donations, and advice, this project would not have been possible.

Advisor: John Fabijanic
Dr. Joseph Mello
Dr. Dan Jansen
Patricia Larson
FSAE Composites Team & Kenneth Li
ME Student Fee Allocation Committee
AERO Student Fee Committee

Table of Contents

List of Figures

List of Tables

Statement of Disclaimer

Since this project is a result of a class assignment, it has been graded and accepted as fulfillment of the course requirements. Acceptance does not imply technical accuracy or reliability. Any use of information in this report is done at the risk of the user. These risks may include catastrophic failure of the device or infringement of patent or copyright laws. California Polytechnic State University at San Luis Obispo, its staff, and the authors of this paper cannot be held liable for any use or misuse of the project.

Executive Summary

Commissioned by Cal Poly Formula SAE, the Formula Monocoque Development (FMD) senior project designed, manufactured, and tested a carbon fiber driver's cell and structural nosecone. The effort built upon 2013's Formula Chassis Works (FCW) project, but with a narrowed scope to conserve time and resources. FCW's monocoque was also used in 2014 when the team added aerodynamics and a new engine.

FMD focused on specific stiffness; compliance with new rules; weight-saving manufacturing techniques; and incorporating changes in suspension and aerodynamics. Specific stiffness was the primary goal of the project. Lightweighting the vehicle was critical to success at competition as a sensitivity of 2.2 points/pound was found in the 2014 Lincoln results for similar vehicles. Stiffness was critical to achieving noticeable changes in vehicle dynamics from suspension-setting adjustments. Meeting SAE laminate rules, while still achieving specific stiffness targets, became tougher than in past years due to more-demanding criteria in the Structural Equivalency Spreadsheet (SES). Particularly the new SES regulated the cockpit floor, added a bending requirement to the front bulkhead and anti-intrusion plate, and required an energy absorption threshold for the front bulkhead—none of which were required previously. Beyond the required tests, FMD performed experiments to realize tub weight savings including testing the minimum number of plies required to join the two monocoque halves, short beam shear tests to eliminate 4 pounds of film adhesive, part strength comparisons from cures in and out of autoclave, and testing multiple prepregs. FMD also accounted for a switch to pullrod suspension and shed weight in aero mounting via attaching trusses directly to the nosecone.

Initial design began with advancing FCW's FEM by correlating it to a physical torsional test, correcting ply orientations, and by incorporating experimental material properties. With these changes, potential laminates were selected for specific stiffness and rules adherence via destructive tests specified by SAE's SES. Classical Lamination Theory (CLT) was then used for strength calculations of suspension pickups and nosecone mounting. Past experience showed physical testing provided an extremely high return on investment so FMD began testing laminates once material arrived.

FMD also produced an impact-attenuating nosecone constructed entirely of carbon fiber. Even with a 50.9% heavier nosecone, consolidated aerodynamic mounting allowed for a 5.2% system weight savings over the 2014 assembly. The nosecone also passed SAE impact requirements by dissipating 7390J of energy with a 21.9g peak and 7.8g average deceleration.

The prepreg monocoque was manufactured generally as described in the FCW report—with the major difference being a post-cure to increase its glass transition temperature in an effort to reduce hot-weather induced compliance as seen in the 2013 chassis.

Future work includes lightening the laminates through more physical testing of the front bulkhead and side impact structure. Additionally, weight can be saved through reduced ply overlap and manufacturing a mold with tighter template tolerances. Investigating Flex-Core, foaming core-splice, and multistage cures may also increase part quality.

As compared to the 2013 car, the 2015 chassis had a monocoque that was 14.9% lighter and had an 11.5% higher specific stiffness. The anti-intrusion plate also weighed 16.6% less. All rules were met or exceeded. The changes in suspension architecture were successfully incorporated with iteration and the aerodynamic mounting performed well in the available testing time. The team placed 18th out of 79 teams entered at the 2015 Lincoln competition.

Introduction

Sponsor Background and Needs

Formula SAE (FSAE) is a student design competition centered on the scenario that a fictional company has contracted a team to develop a Formula-style race car. Each team of university students designs, builds, and tests a car based on a set of rules established and enforced by SAE International. The teams enter their project in an international competition, in which a series of events—including cost, design, and dynamic performance—are used to evaluate the performance of the vehicle.

The Cal Poly Formula SAE team has been competing in FSAE competitions since the 1980's with varying levels of success. Recently the Cal Poly team has been climbing the ranks through continued development and knowledge transfer from previous teams.

Most recently, the team placed 26th out of 120 teams at the 2014 Michigan competition. Sustaining this continued increase in performance can be achieved through iterative design and advanced development of various vehicle subsystems.

An FSAE vehicle is composed of several distinct subsystems that are critical to the overall vehicle's performance. These subsystems include the chassis, suspension, engine, drivetrain, aerodynamics, driver controls, and electronics. All subsystems must operate in tandem for a high performing vehicle. The chassis is a critical subsystem for any high-performance race car, since it acts as an interface to connect all of the car's separate subsystems together. The chassis must be adequately stiff in order to transfer loading from the tires and provide tangible response to handling tuning done to the suspension. In addition, the chassis must but lightweight, since weight is a limiting factor in terms of acceleration-based performance.

The current Cal Poly FSAE hybrid chassis, developed by Formula Chassis Works for the 2013 car, is comprised of a carbon fiber monocoque joined to a steel space frame in the rear.

Formula Monocoque Development will design, manufacture, and test a new monocoque laminate and impact attenuator with the goals of maintaining adequate stiffness and reducing weight, while complying with the other subsystems of the car and meeting all of SAE's structural requirements and rules.

Problem Definition

The carbon fiber monocoque used by the Cal Poly FSAE team for the 2013 & 2014 seasons was unnecessarily overweight and insufficiently stiff for an aerodynamically-equipped race car. Due to inherent manufacturing errors, approximately 5 pounds of excessive weight was added to the monocoque. The measured torsional stiffness of the vehicle was within the range of the expected result, but still too soft for the increase in roll stiffness present in a car equipped with large amounts of aerodynamic downforce. The electronics placement below the driver in the old chassis resulted in an unnecessarily high CG of the driver, which accounts for approximately 30% of the total vehicle weight. Finally, limited manufacturing and testing time greatly limited the previous senior project team in developing the best possible chassis laminate.

The overall goal of the Formula Monocoque Development (FMD) team is to develop and build a high-performance carbon fiber chassis for the 2015 Cal Poly FSAE team. The primary goals for this chassis are low weight and high stiffness, which are directly correlated to the performance of the vehicle. Additionally, the chassis must comply with SAE safety and template rules. More specifically, FMD will increase the specific stiffness of the tub via development of the carbon fiber layup schedule, modifications to the geometry of the tub, and analysis of the rules requirements.

Detailed requirements for the 2014/2015 tub are outlined in Table 1. These requirements were developed via a Quality Function Deployment (QFD) (see Appendix B), which takes into account all quantitative customer requirements requested by Cal Poly FSAE.

Table 1. Engineering requirements for the 2015 Cal Poly FSAE carbon fiber tub. Specification importance is measured with risk (high, medium, or low). How each specification will be met is outlined under compliance (analysis, test, similarity to previous

Spec #	Description	Target	Tolerance	Risk	Compliance
1	Weight of monocoque only	25 lb	max	H	A,T
2	Torsional stiffness of monocoque and front suspension only, determined from torsion test displacements between front hub and aft of tub (see page 18 for more details)	2184 lb-ft/deg	min	H	A,T
3	Area of cockpit opening	440 in^2	± 10	L	I
4	Cross sectional area of front tub, based off of SAE rules (ref.)	195 in^2	min	L	I
5	Max operating temperature of carbon face sheets, based off of glass transition temperature	150 ^oF	min	M	A
6	Egress time from seated driving position	5 sec	max	L	T
7	Visual rating of appearance	9/10	± 1	L	I
8	Driver rating of comfort	9/10	± 1	M	S,I
9	Cost (Cost Report), manipulated by obtaining accurate measurements and using simplified processes	$3,500	max	M	A
10	Safety factors for primary loading from suspension pickup points, pedal box assembly mounting, aerodynamics mounting and joint to rear subframe	2	min	H	A,T
11	Energy absorption of nosecone, undergoing quasi-static loading	7350 J	min	M	A,T
12	Flat mounting regions, used for interfacing with other subsystems, primarily suspension, aerodynamics, and driver controls	1.5x required mounting area (for adjustability)	min	M	I
13	Strength requirements from FSAE rules, located at side-impact structure, front roll hoop bracing, and front bulkhead support	67 kN 35.9 kN 99 kN	min	H	A,T
14	Front bulkhead cutout, used for ease of accessibility for pedal box assembly changes	10" x 10"	min	M	I
15	Cable routing cutout for brake lines and DAQ wires, at side of monocoque near suspension	5/8" x 3/4"	min	L	I

Objective and Specification Development

As opposed to starting a chassis design from scratch, FMD chose to utilize the design resources, documentation, and tooling from the 2013 chassis team to create an improved iteration of their composite tub.

The 2013 FSAE chassis team designed a chassis with a wealth of design potential, but time and resource restraints prevented the extensive composites testing necessary to further refine the laminate. A large portion of their development time was spent designing and manufacturing the plaster tub mold, securing donations of core and prepreg, and learning the basics of composites manufacturing and design. Composite panel testing and iteration were rushed, and the laminate design was not as developed as they had hoped. Despite their stringent time constraints, the 2013 team was able to design and manufacture a composite tub that would last more than two competition seasons and extensive dynamic testing.

In order to build off of past experience, FMD kept the 2013 chassis team – John Waldrop, Matthew Hagan, John Rappolt, and Nick Henderson – in close contact. The 2013 team members also left behind extensive design documentation in the form of their senior project report, FEMs, Computer-Aided Design (CAD), and many other useful documents. It became very apparent early on that remaining in close correspondence with the 2013 team and constantly referencing their documentation would be invaluable in both the design and manufacturing process.

From the comments of the 2013 chassis team and further research into composite tub design, it was decided that the primary goals of the 2015 monocoque design would revolve around a greater volume of composites testing, improving the chassis finite element analysis (FEA) model, physically validating chassis stiffness, and adapting the tub to accommodate a new pullrod suspension. The FSAE governing body also released new chassis structural requirements that would necessitate different testing methods and a completely new laminate.

The team's goal for torsional stiffness was to design a monocoque that meets or exceeds the 2014 monocoque stiffness. In that sense, the stiffness of the monocoque must be isolated from the rest of the chassis in order to make an effective comparison between the 2014 and 2015 tubs. The team conducted a torsion test of the 2014 chassis (see pages 109-113), and deflection values were taken along the length of the chassis. These numbers were manipulated to yield the component stiffness values for the monocoque and front suspension combined, the subframe-to-tub joint, and the subframe. Considering the points taken, the team was unable to separate the monocoque stiffness from that of the front suspension. As a result, the closest thing to a target monocoque stiffness our team could obtain was the stiffness of the tub and front suspension combined, which was 2148 ft-lb/deg. Our team used this combined monocoque and front suspension stiffness as our effective stiffness goal.

Future teams should make sure to take deflection values at the front suspension pickups in order to separate the stiffness contribution of the front suspension, thus isolating the stiffness of the monocoque. Taking this approach would have yielded a more sensible stiffness goal.

Project Management

The large scope of designing, building, and testing a carbon fiber monocoque and impact-absorbing nosecone required clear responsibilities. To that effect, each team member was delegated roles as shown in Table 2. As Chassis Lead, Matthew Lee spearheaded FEA, testing analysis, and manufacturing. As Suspension Lead, Tony Loogman determined loadings on the chassis and assisted Mr. Lee with FEA and localized attachment analysis. Senior team member, Andrew Ferrell led CLT analysis and nosecone laminate development and manufacturing. In order to increase productivity and help future teams, Mr. Ferrell also acted as project archivist and CAD manager. Outgoing Team Lead Andrew Cunningham was responsible for FMD's pre-manufacturing scheduling, budgeting, and material acquisition. Additionally, as 2015 Aerodynamic Lead, Mr. Cunningham was responsible for providing aerodynamic loadings and flow considerations. While the four engineers on the project all had a demonstrated track record of commitment and results as members of Cal Poly Formula SAE, a formal contract was established to ensure responsibilities were met at a level of quality and in a manner of time that was acceptable to the sponsor.

Table 2. Member roles for the scope of the project. Each member was in charge of a major aspect of the project.

Matthew Lee	Tony Loogman	Andrew Ferrell	Andrew Cunningham
FEA	FEA	CLT Analysis	Nosecone Aerodynamics
Localized Attachment Analysis	Localized Attachment Analysis	Nosecone Design and Manufacturing	Impact Attenuator Testing
Manufacturing Lead	Suspension Loading	Archive Management	Hardware Analysis
Physical Testing and Analysis	Physical Testing and Analysis	Impact Attenuator Testing and Analysis	Scheduling and Budgeting
Build Scheduling		CAD Management	Material Sourcing

A project of this magnitude also required a detailed yet flexible schedule and well-allocated resources in order to meet its performance requirements in a timely manner. To that affect, a Gantt chart was used to track critical path items, labor requirements, and concurrent engineering leading up to manufacturing. Once heavy testing and construction began, the project direction was cemented and scheduling was performed via a spreadsheet. The project's major stages and milestone can be found below and detailed scheduling in Table 3.

Table 3. Major milestones in the monocoque design and manufacturing included problem definition, selection, materials acquisition, and laminate testing, and chassis manufacturing, nosecone production, and testing. The initial stages of the project were organized via a Gantt chart and this progressed to a spreadsheet as direction became self-evident.

Stage	Task	Start	End	Duration
Definition		5/1/2014	12/4/2014	217
	Design Specifications	5/1/2014	6/1/2014	31
Selection	FSAE Preliminary Design Review	8/10/2014	8/10/2014	0
	Conceptual Design Review	6/5/2014	6/5/2014	0
	Critical Design Review	12/4/2014	12/4/2014	0
Materials Acquisition		9/1/2014	1/15/2015	136
	Carbon-Fiber	9/1/2014	11/20/2014	80
	Core	12/15/2014	1/15/2015	31
	Film Adhesive	11/4/2014	1/4/2015	61
	Vacuum Bagging Materials	9/10/2014	10/22/2014	42
Laminate Testing		10/7/2014	1/16/2015	101
	2014 Rules Test Panels	10/7/2014	12/8/2014	62
	2015 Rules Test Panels	12/8/2014	1/16/2015	39
	In-mold Test Layups	12/17/2014	1/14/2015	28
	Pull-Out Test	1/14/2015	1/14/2015	0
	Short Beam Shear Tests	11/18/2014	11/20/2014	2
	Lap Joint	1/26/2015	1/27/2015	1
Chassis Manufacturing		1/15/2015	2/23/2015	39
	Prepare Core, Templates and other Materials	1/15/2015	1/17/2015	2
	Layup	1/17/2015	1/20/2015	3
	Cure	1/21/2015	1/21/2015	0
	Remove Excess Material	1/25/2015	1/26/2015	1
	Drill Suspension Holes	1/26/2015	1/28/2015	2
	Post Cure	1/28/2015	1/28/2015	0
	Bond halves	1/30/2015	2/8/2015	9
	Closeouts	2/21/2015	2/22/2015	1
	Carbon-Fiber Repair	2/18/2015	2/22/2015	4
	Final Material Removal	2/22/2015	2/23/2015	1
	Flattening Pedal Box and Pickups	4/18/2015	4/25/2015	7
	Vehicle Assembly	2/24/2015	4/7/2015	42
Nosecone Manufacturing		3/21/2015	3/31/2015	10
	Layup	3/21/2015	3/30/2015	9
	Impact Testing	3/26/2015	3/31/2015	5
	Mounting Holes	3/28/2015	3/29/2015	1
Testing		4/7/2015	5/28/2015	51
	First Drive	4/7/2015	4/7/2015	0
	Torsion Test	5/28/2015	5/28/2015	0

SAE's required document deadlines (Table 4) were factored into the schedule because these documents command a heavy point penalty for late submission. All data and analysis was completed on time and, except for the Notice of Intent for Alternative Frame Rules, passed upon the first submission. Of note is that the Alternative Frame Rules were abandoned in favor of the Structural Equivalency Spreadsheet for reasons explained later in this report.

.

Table 4. Deadlines for SAE chassis design, analysis, and costing are strictly enforced with a point penalty for late submission. All documents were submitted on time and met or exceeded SAE requirements.

Requirement	Date
Notice of Intent for Alternative Frame Rules	11/3/2014
Structural Equivalency Form	3/2/2015
Impact Attenuator Data	4/1/2015
Cost Report	4/1/2015

While the composite portion of the chassis was largely designed by the four members of FMD building upon FCW's foundation, a large and specialized labor pool was needed for the carbon fiber manufacturing. Recognizing this, a Composites subteam was formed under Cal Poly Formula SAE for the 2015 season. This team worked with Chassis and Aerodynamics to elevate part quality-assurance through studying successes and failures as well as developing standard operating procedures for test panels and other layups. The Composites subteam worked with FMD to produce over 120 test panels and assisted during the tub layup. As such, the team should be considered essential for future monocoque development. Beyond laminating skills, FMD also enlisted one of the team's CNC operators to machine the nosecone mold foam.

Material availability is always a large component in Formula SAE chassis senior projects due to the team's limited budget and the high cost of composite materials. Cal Poly Formula SAE is the sponsor of record, but industry partners are critical to the success of the project. Most notably, TenCate Advanced Materials, C&D Zodiac, Toray Composites of America, and SpaceX, Plascore, and Airtech International have been exceedingly generous with material donations. Material types, usages, and sources are detailed in Table 5. The team thanks these industry partners and hopes to provide a return on investment via media promotion during testing and competition as well as training to become highly-contributing future employees.

The Formula SAE team committed $3,000 to the project for all materials and other expenses not covered by industry partners. In total, the project cost the team only $215 due to FMD and team management seeking industry partners who donated $44,080 worth of materials and services (Table 5). This shows that by maintaining positive sponsor relations and putting forth significant effort in gaining new partners, a composite chassis can be produced for less than the cost of a steel-tube chassis' raw materials.

Table 5. The budget breakdown shows that a monocoque is only possible with large sponsorships.

Material/Item	Value	FMD Cost	Funding Source
Mold Tooling (From 2013)	$20,000	$0	C&D Zodiac
Carbon Fiber Prepreg	$18,000	$0	TenCate/Toray/SpaceX
Dry Carbon Fiber Cloth	$80	$0	Cal Poly MESFAC
Vacuum Bagging Materials	$3,000	$0	Airtech/C&D Zodiac
Core	$1,600	$0	Plascore
Low Temp Foam	$1,000	$0	Coastal Enterprises
Sealant Tape	$400	$0	General Sealants
Hardware	$165	$165	Formula SAE
End Grain Balsa	$50	$50	Formula SAE
Total	$44,295	$215	

Background

Team History

In 2011, the Cal Poly FSAE team built a new car from the ground up. The chassis was a full steel-tube frame, which was one aspect that led to an overweight car. Unfortunately, the car was not completed in time for the 2011 FSAE competition. In 2012, the car was completed and taken to the FSAE competition in Lincoln, Nebraska, and finished 36th out of 66 teams. Because the car was so heavy, one of the primary goals of the 2013 team was to make the car lighter. Formula Chassis Works, the senior project group who set out to redesign the chassis, originally planned to develop a full carbon fiber monocoque. Due to temperature and packaging issues, mostly regarding the engine, this plan was scrapped in favor of a hybrid chassis. Because the switch to a hybrid chassis occurred so late in the design phase, there was very little time for development. This was also the first carbon fiber tub these team members had built so there was not much experience. The Cal Poly FSAE team had built carbon fiber monocoques in the past; however, none of the previous driver's cells would have been strong enough to meet the new set of SAE rules. Due to unfamiliarity with composites, the team designed the 2013 tub with excessively high safety factors, which lead to unnecessary weight. In addition, manufacturing inexperience led the team to add approximately 5 extra pounds of honeycomb core during the layup. Problems also arose due to a lack of time.

For example, due to the last minute design change from a full monocoque to a hybrid chassis, there was not much time to develop the laminate to be lightweight. In addition to the laminate, the geometry of the monocoque was not developed in depth. This lead to a tub that was unnecessarily long, as well as more complicated than necessary. Lack of development time also lead to heavy mounting brackets. Finally, a shortage of development time for the strap joint that joins the two monocoque halves resulted in excess weight. Largely due to insufficient dynamic testing time (only 30 minutes of drive time total), the 2013 Cal Poly FSAE team placed 44th out of 62 teams at the Lincoln competition.

In 2014, the Cal Poly FSAE team used the same tub as the year prior in the interest of testing and development time. Minor changes were made to the vehicle, including the addition of an aerodynamics package and integration of a new engine. This allowed the car to be driving much sooner than in 2013, and 11 hours of testing time were logged. The result of this large increase in testing time allowed many problems to be worked out, most of which were reliability issues. With an improved and well tested car, Cal Poly FSAE competed in the Michigan FSAE competition and placed 26th out of 120 teams.

Resources

FMD's most valuable resource is the 2013 FSAE Chassis Report, written by Formula Chassis Works (Reference 4). This report documents how the 2013 chassis was designed, manufactured, and tested. It has a plethora of valuable information about the entire process of designing a monocoque, such as initial concepts and ideas, how they conducted their analysis, their decision making, and the manufacturing processes they used. The 2013 Chassis report also had suggestions for future work to improve the monocoque. They recommend using over-expanded core to help reduce the amount of excess core used, spending more time developing the layup schedule in order to save weight, and further developing the strap joint, the closeouts, and the nosecone. Ideally, FMD will be building upon this report, therefore advancing the current design. Having access to the 2013 Chassis Report and the lessons learned was a significant advantage to FMD.

Current State of the Art

The current state-of-the-art in regards to track vehicle racing is Formula 1 (F1), which is a single-seat auto racing competition organized by the FIA. It is very similar in design requirements to the Formula SAE competition, with an emphasis on maneuverability around an autocross-style course. While F1 cars do experience much higher loading conditions, certain design principles can still be applied to a FSAE racecar.

The chassis of a F1 racecar is composed primarily of a carbon fiber sandwich structure because of its superior specific stiffness. As visible in Figure 1, F1 chassis' use variable-thickness aluminum honeycomb core with CFRP face sheets. In previous years, the Cal Poly Racing team has used Nomex core in the interest of ease-of-manufacturing and due to availability. Table 6 shows the shear stiffness and density properties of Nomex and aluminum honeycomb core.

Figure 1. Formula 1 chassis, showing the use of carbon fiber and aluminum honeycomb core.

Table 6. Properties of possible core materials to be used in the 2015 monocoque.

	Density [lb/ft^3]	Shear Strength [psi]	Shear Modulus [ksi]
HRH-10 Nomex	3.0	175	6
PAMG Aluminum	3.1	210	70

Additionally, F1 chassis are cured in autoclaves, which allow the use of external pressure to improved carbon compaction, which is directly correlated to strong performance. Unfortunately, the autoclave located on the Cal Poly campus is far too small to fit the chassis molds, so the large oven must be used to cure the chassis, which doesn't allow the option of additional pressure. The Formula Monocoque team was able to gain access to Swift Engineering's autoclave, which would have allowed the use of a pressurized cure. Unfortunately, due to time constraints and logistical issues, this opportunity was abandoned.

Sandwich Structures

A composite sandwich structure is composed of core sandwiched by two face-sheets. The skins take the in-plane tensile and compressive forces, while the core takes the out of plane shear and compressive loading. The core also serves to increase the second area moment of inertia of the sandwich panel, thus increasing its bending stiffness.

An important laminate design consideration is the carbon fiber and its mechanical properties. When selecting prepreg carbon, the strength, stiffness, failure strain, fiber volume, weave type (or absence of weave), and resin type have to be taken into account. The fiber strength determines the permissible load on the fiber before failure, and the stiffness determines the amount of deflection the laminate sees given a certain load. Failure strain is a large concern in composites design, because laminates often reach their failure strains before their maximum fiber stress. The fiber volume (the volume of fiber versus the volume of resin) is also important, because excessive resin content will dilute the ply strength and stiffness in exchange for better adhesion and bonding.

Modern composites design strives for high strength and high stiffness at reduced weight. Depending on a composite part's geometry and load path, certain regions of the part may be stiffness dominated, strength driven, or in need of both high stiffness and strength. For example, high load areas like suspension pickups will require high strength to prevent failure and high stiffness to avoid roll stiffness compliance. However, there are other lightly loaded parts of the tub that do not require a great deal of strength, but must be stiff in order to promote chassis torsional stiffness. In the pursuit of high performance at minimal weight, the designer aims to tune the laminate to meet the unique requirements of each chassis region using various fiber types in different orientations at different locations. With these considerations in mind, FMD considered a variety of fiber types within the limitations of what was available from donations. FMD considered fibers like Toray M55J unidirectional tape ("uni") for its high fiber stiffness, as well as M46J and T800 for their high strength and superior surface finish. With a wide variety of fibers at our disposal, our goal was to minimize ply count by placing certain types of fibers in the direction of the load.

Core bonding

In order for a composite sandwich structure to function properly in bending, the face-sheets must be securely bonded to the core. This can be achieved using film adhesive designed for core bonding. Despite the high core-bonding strength film adhesives provide, these adhesives are very costly and still add weight to the laminate. An alternative to film adhesive is to use a prepreg with a resin system designed to be self-adhering to core. This method reduces laminate weight considerably, but the integrity of the core-skin bond may not be ideal. From a safety standpoint, it was suggested that film adhesive be used, even if it were a redundant measure against possible core-skin delamination. In order to justify the use or exclusion of film adhesive, composites testing is necessary to determine the bond strength of each core bonding method.

Temperature Resistance

The expected operating temperature of a composite part is also a large component of composites design. All resins are rated to a specific temperature for safe operation. If a cured resin is heated beyond its rated temperature, then it may soften and lead to delamination in the part. Since regions of the tub would be exposed to intense prolonged sunlight and radiant heat from the exhaust and engine, proper precautions would have to be taken to ensure that the tub is rated to the expected operating temperature. All resins have a suggested operating temperature, and some resins can be post-cured to further elevate the operating temperature.

Applicable Standards

Our laminate design is governed by the loads expected from the suspension, pedals (from the driver's feet), driver weight, and other considerations. In addition, the laminate must pass SAE's rules governing laminate properties and dimensions. The SAE-mandated tests are intended to isolate specific mechanical properties of the laminate, which are then compared to the properties of a baseline steel tube design. The properties considered are: bending stiffness (EI), yield strength, ultimate strength, and absorbed energy. Depending on the region of the tub, the laminate must meet or exceed the properties of one, two, or three baseline steel tubes.

There are three tests required by SAE regarding the chassis laminate: the 3-point bend test, perimeter shear test, and off-axis pullout test. The details of each test are summarized in Table 7. All of the composite tests were performed on an Instron tensile tester under the safety guidelines set forth by the Mechanical Engineering Department.

Table 7. SAE-mandated laminate tests

	Long beam 3-point bend	**Perimeter Shear**	**Off-axis Pullout**
Property Tested	• Skin strength • Skin stiffness	• Panel Shear Strength	• Harness pickup strength

The SAE tests cover a variety of loading conditions that are intended to replicate actual on-car loading. However, the Hexcel and ASTM tests provide more generalized laminate properties that are useful for design outside of the SAE requirements.

The ASTM D2344 short beam shear test is a 3-point bend test that isolates the interlaminar shear strength (ILSS) of a composite, coreless panel. The ILSS is essential to the integrity of the resin.

Hexcel’s short beam sandwich shear test is a 3-point bend test with a reduced support span. The test is designed to isolate the ILSS or core shear strength of the laminate, depending on the failure mode. Failures in delamination isolate the core-to-face-sheet bonding strength. If the core fails, then the test results isolate the core shear strength. If the panel experiences failure in the core before any delamination occurs, then the core-skin bond is sufficient.

SAE provides two chassis design rulesets: the Structural Equivalency Spreadsheet (SES) and the Alternative Frame Rules (AFR). The SES approach utilizes the composites testing data to determine if a laminate meets or exceeds the stiffness and strength of an established baseline steel design for a given region of the chassis. The AFR is more open-ended, in that it requires teams to use an FEA simulation to prove chassis strength and stiffness given a series of different loading conditions.

The SES is the older and more developed ruleset. The Structural Equivalency Spreadsheet compiles all of SAE’s chassis requirements into a large spreadsheet, complete with formulas and guidelines to quickly check laminate equivalence. Checking whether a laminate passes is almost instant, in that the user does not need to program any mechanical formulas. However, it does help to fully examine the formulas in order to extrapolate which laminate properties drive the design.

The Alterative Frame ruleset requires teams to produce a full chassis finite element model (FEM) using material properties derived from testing. The model is then subject to a series of loads that examine the structural integrity of the design. Alternative frame designs are exempt from several dimensional and loading requirements present in the main chassis ruleset, thus allowing for a greater freedom of chassis geometry. Despite these advantages, creating a functional, accurate FE model takes considerable time and a great deal of specialized expertise. In addition, some loading cases (especially for frontal impact) are very high, and will cause an imperfect model to break down. Since the AF ruleset is relatively new, SAE takes several weeks to respond to rules clarifications or analyze a submitted model. This added down-time significantly impedes the laminate iteration process.

At the start of the design phase, FMD explored the possibility of designing an AFR chassis by modifying a pre-existing chassis FEM. As FMD began altering the FEM to accommodate the AF loads, the team quickly realized that significant modifications needed to be made to the model in order to obtain feasible results. In addition, the rules clarifications and sample models submitted did not receive responses until weeks after submittal. Considering the team's manufacturing timeline, FMD felt that pursuing the AFR any further would severely impact the timely completion of the chassis. For that reason, FMD promptly switched to the SES ruleset.

Details on FMD's attempt to satisfy the AF rules can be found in Appendix T.

Design Conceptualization

Mold and Tooling

In order to devote design resources to laminate development and speed up manufacturing, the 2013 monocoque molds were reused. In 2013, C&D Zodiac machined the foam bucks on their 5-axis gantry mill. After hand-finishing by FSAE members, a plaster-hemp mold was pulled off of the bucks. Again, team members sanded and filled these tools to ensure a high-quality surface finish and C&D finished them with an industrial gelcoat. Details of the mold construction are covered in the FCW report. In total, it is estimated that these molds took 400 hours of team labor to produce, excluding design time. Moreover, the molds were rated for 3-5 heat cycles and only 2 had been used in 2013 for a test layup and the final part. For the aforementioned reasons, FMD did not see a positive return on investment coming from manufacturing new molds.

Target Stiffness

The primary concern when determining a target torsional stiffness for a performance vehicle is how well the chassis transfers loads between the front and rear suspension. The success of any race car is largely dependent on tuning made to the vehicle, both for specific courses and for specific track conditions. When tuning the suspension of a vehicle for steady-state handling and transient performance, the primary concern is the lateral load transfer, from the inside tires to the outside tires of the vehicle. This lateral load transfer determines the normal load on the tire, which is directly proportional to how much lateral grip the tire can create. More specifically, the distribution of the lateral load transfer between the front and the rear tires will determine the oversteer/understeer characteristic of the vehicle since the normal loads are responsible for how much grip is created at the front and rear of the vehicle. The lateral load transfer at the tires is primarily controlled by changing the roll stiffness distribution of the vehicle, which is typically adjusted via springs and anti-roll bars. In order for these adjustments to take effect, the chassis of the vehicle must be able to transfer the difference in loading between the front and rear suspension components. With an inadequately stiff chassis, changes made in the suspension parameters will have little to no effect on the actual lateral load transfer, since the chassis will absorb the energy transfer.

The front roll rate, chassis torsional stiffness, and rear roll rate act like successive springs in series and an increase in the roll rate of the suspension will require a proportional increase in the chassis stiffness to retain the same handling response. The previous tub was designed for a front and rear suspension roll rate of 130 and 135 lb*ft/deg, respectively. The addition of aerodynamics to the car required an increase of the front and rear roll rate to 450 and 330 lb*ft/deg, respectively, in order to meet the aerodynamics subsystems wing displacement requirements. As a result, a much stiffer chassis was required to adequately support the lateral load transfer.

In order to quantify the effects of torsional stiffness on the ability to tune suspension parameters, a model was developed that determines lateral load transfer based off of an input change in roll stiffness distribution for any given chassis torsional stiffness. This model is based off of several basic vehicle dynamics equations, as well as the constitutive relationship shown in Figure 2.[Ref 3]

$$m_f = K_{rollf}\emptyset_1 - K_{ch}\emptyset_3 \quad (1)$$

$$m_r = K_{rollr}\emptyset_2 + K_{ch}\emptyset_3 \quad (2)$$

$$\emptyset_1 + \emptyset_3 = \emptyset_2 \quad (3)$$

$$m_f = front\ mass$$

$$m_r = rear\ mass$$

$$K_{rollf} = front\ roll\ stiffness$$

$$K_{rollr} = rear\ roll\ stiffness$$

$$K_{ch} = chassis\ torsional\ stiffness$$

$$\phi_1 = front\ roll\ angle$$

$$\phi_2 = rear\ roll\ angle$$

$$\phi_3 = chassis\ twist\ angle$$

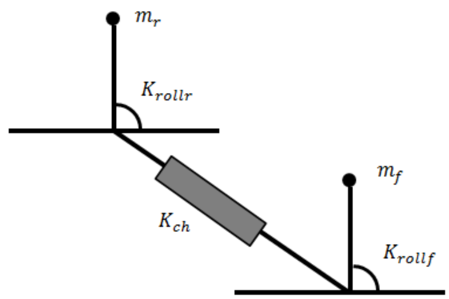

Figure 2. Relationship between suspension and chassis roll angles and roll rates.

The model takes any input chassis torsional stiffness and total suspension roll stiffness, and then creates an arbitrary roll moment to simultaneously solve the above equations for their respective roll angles. From the front and rear roll angles, the lateral load transfer distribution can be determined. With an insufficiently stiff chassis, excessive twist angle in the chassis causes the difference in roll angles between the front and rear suspension, which is the cause of poor lateral load transfer distribution. With the results of the model, the effect of different chassis torsional stiffnesses can be seen (Figure 3).

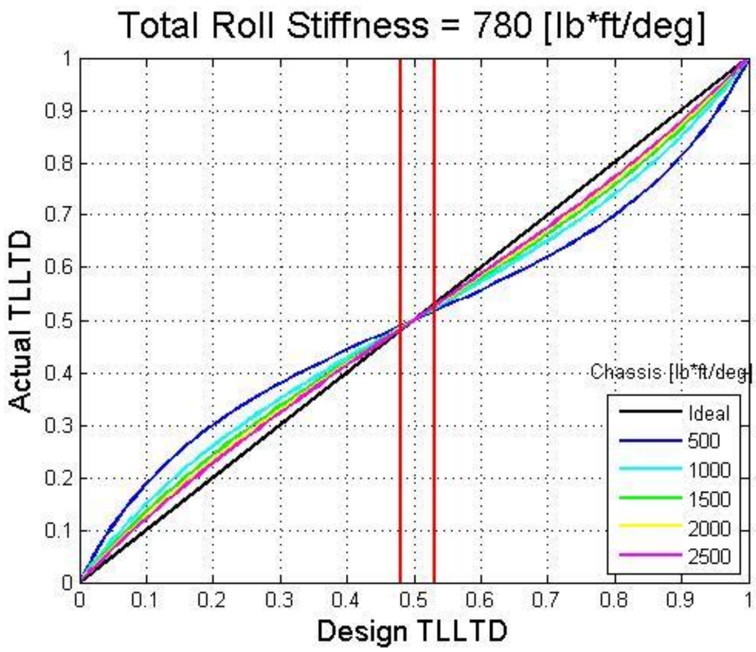

Figure 3. The effect of poor torsional stiffness on the correlation between roll stiffness distribution and lateral load transfer distribution. A stiffer chassis results in a more linear relationship.

The ideal race car would have a perfectly linear rate between the designed lateral load transfer distribution and the actual lateral load transfer distribution. With a linear relationship, any given change in the roll stiffness of the suspension would directly correlate to a change in the lateral load transfer distribution, thus affecting the tire grip. However, due to chassis flex, this is not the case. The nonlinearity means that a change in the roll stiffness distribution does not cause a direct change in the lateral load transfer distribution and does not cause the change that the race engineer is expecting.

As visible in Figure 3, a decrease in chassis stiffness results in a more nonlinear relationship between the desired total lateral load transfer distribution (TLLTD) and the actual TLLTD. As stiffness increases, the relationship becomes more linear, but the improvements are a case of diminishing returns. However, the complete plot can be misleading, because typically the suspension subsystem is only tuned in a certain range of TLLTD. Figure 4 shows a zoomed-in view of the tuning range that is desired by the suspension subsystem. Based off of the design of the suspension, the desired range of tuning was 0.48-0.53 TLLTD, which allowed a range of 10% greater rear lateral acceleration to 10% greater front acceleration, depending on the roll rates selected. A chassis stiffness of 500 lb*ft/deg is too little because the desired tuning range is greatly limited. With a torsional stiffness of only 500 lb*ft/deg, the TLLTD tuning range is restricted to 0.49-0.517, which is determined from the constitutive relationship presented in Figure 2. The lack of ability to tune the TLLTD with this little chassis torsional stiffness could seriously inhibit the ability to tune the handling of the car. However, chassis stiffnesses of 1500, 2000, and 2500 have been determined to be stiff enough, because the actual tuning range of the car is within 20% of the desired tuning range and this is a realistic goal based off of previous years' achievements. From these results, the FMD team determined that the stiffness of the 2015 chassis must be increased to a minimum of 1500 lb*ft/deg, with 1700 lb*ft/deg as an optimistic goal.

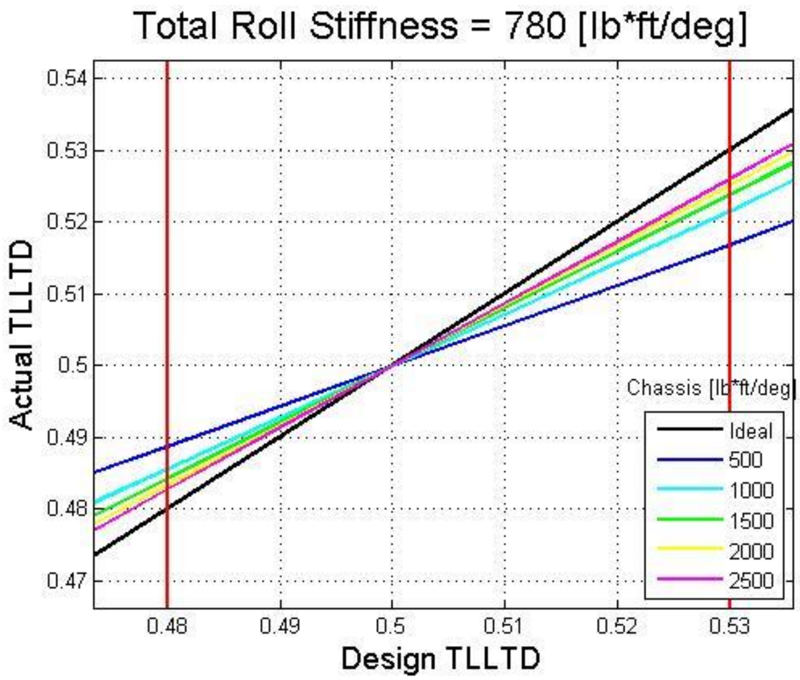

Figure 4. Zoomed-in view of planned TLLTD tuning range of 2015 vehicle.

Monocoque Shortening

Upon examining the 2013 tub, it became apparent that there was 1 inch of unused space at the front of the tub. Using the 2013 laminate weights, FMD predicted that eliminating this excess material would save about 0.8 pounds. In the event that the pedal box could be shortened by relocating the fluid reservoirs further rearward, the tub could be shortened by a total of 4 inches, thus saving 3.4 pounds.

Shortening the tub would require CNC machining of an MDF plug that would be bonded to the front end of the mold. Although conceptually simple, machining an MDF part to the contours of the tub would require CNC expertise, as well as considerable CAM, setup, and machining time. As the laminate design and testing went on, it was determined that manufacturing the tub shortening plug would divert crucial manpower away from composites testing and ultimately delay the final tub layup. Moreover, maintaining the existing length allowed for lower driver placement, which allowed for higher quality rear wing flow. It was thus ruled that shortening the tub presented more of a logistical problem than the weight savings would warrant.

Cockpit Cutout

Another potential weight-cutting measure was reducing the height of the driver cell sidewall and seat back. The SAE rules state that the side impact structure need only extend from the cockpit floor to a point 13.8 inches above the ground. This meant that the side impact structure of the 2013 tub was 5” too tall. Removing the excess material would save approximately 5.4 pounds. However, the driver’s cell is an open-section region that suffers from low stiffness compared to the closed-section front of the tub. Any reduction of material from the top of the driver’s cell will further impact chassis stiffness. Analyzing the effects of this change required a significant modification to the chassis FEA model. The current tub model would have to be replaced and re-meshed, and all the ties and constraints would have to be redone. FMD determined that making these FEM changes would adversely impact our design and manufacturing timeline, so the effort was dropped.

In order to effectively transfer the load between the skins along the top of the driver's cell, FMD decided that carbon prepreg closeouts needed to be bonded over the exposed core to bridge the gap between the discontinuous skins. A single ply at 45° was selected per recommendation from Dr. Mello as well as from the 2013 chassis team. The chassis FEM was not used in selecting a layup schedule because it did not capture the out of plane load transfer that the closeouts would pick up. This is due to the use of shell elements in the FEM.

Material Selection

Material selection began by assessing the mechanical properties of prepreg and core, and running a torsional stiffness test in ABAQUS to determine the performance of each possible arrangement.

Several types of carbon prepreg were obtained. According to the fiber datasheets, each prepreg has unique mechanical properties, as shown in Table 8. The goal was to design a laminate that satisfied the SAE testing standards and fulfilled the localized loading conditions from the pedal-box and suspension mounts. In order to make a final selection, FMD considered the laminate stiffness, strength, and density of each material. Fiber selection would ultimately be determined through laminate testing and iteration.

Table 8. The mechanical properties for the available fibers vary significantly, especially with respect to stiffness.

Fiber	Tensile Modulus (Msi)	Tensile Strength (ksi)
AS4	33.5	640
T800	42.7	796
M46J	63.3	611
M55J	78.2	583

In regards to core, a variety of Nomex paper core and aluminum core were considered. The 2013 team utilized 3.0 lb/ft^3 paper core to good effect. Nomex is easy to form and bend to complex geometry, resulting in parts with minimal bridging. Nomex is also easy to splice, because the partially crushed cells tend to spring out and expand into the crevice being filled. However, Nomex does not possess the stiffness and strength of aluminum core of similar density, as detailed in Table 9. Finite element simulations also show that aluminum core yields higher chassis stiffness compared to Nomex core of similar weight, mainly due to aluminum core's superior shear modulus. These numbers convinced FMD that using aluminum core would be a worthwhile upgrade with very little weight penalty.

Table 9. Nomex and Aluminum core comparison. All torsional stiffness simulations utilized the 2013 laminate.

	Density (lb/ft^3)	Shear Modulus (ksi)		Plate Shear Strength (psi)		FE Simulated Chassis Torsional Stiffness (lb-ft/deg)	Specific Chassis Stiffness WRT core density (lb-ft/deg)/(lb/ft^3)
		Ribbon	Transverse	Ribbon	Transverse		
HRH10 Nomex	3.0	6.0	3.5	175	155	1260	420
PAMG 5052 Aluminum Core	3.1	45.0	22.0	210	130	1407	469

One of the drawbacks of hexagonal-cell aluminum core is its poor formability and tendency to bridge over contours. When bent over a curve, aluminum core is too stiff to keep its bent shape. This results in frequent bridging over internal curves. The use of aluminum Flex-Core mitigates this problem by using elongated hexagonal cells to facilitate bending in one direction.

In addition, splicing aluminum core is difficult without expanding core-splice foam. Unlike Nomex (cells spring back after compression), aluminum core cells yield and thus do not expand to fill in empty spaces when splicing.

During the core selection process, the team was aware that Flex-Core would provide improved manufacturability over conventional-cell aluminum core. However, FMD was yet to discover that conventional-cell aluminum core would produce bridging and facesheet compaction problems.

Since there was no guarantee of obtaining Flex-Core from sponsors, FMD was open to the possibility of using the more readily available conventional-cell aluminum core. Finite element simulations showed that 3.1 lb/ft^3 PAMG-XR1 5052 conventional-cell aluminum core provided an 11.67% increase in both torsional stiffness and specific stiffness (Table 9). The team reasoned that using conventional-cell aluminum core would be worth the performance gain over Nomex, and that the manufacturing issues could be worked out with test layups.

The use of foaming core-splice adhesive was recommended by several sources in the industry. However, the cost of the recommended FM-410 adhesive was prohibitively expensive, with ten 8.5''x11'' sheets retailing for around $500. As an alternative to foaming adhesive, the team was advised to either use film adhesive or paste adhesive for core splicing. Paste adhesive would require a multistage cure according to Dr. Mello and was abandoned.

Using loading data from the 2013 team, it was determined that aluminum core would not have sufficient strength in areas of high out-of-plane loading such as the pedal box and suspension pickups. A perimeter shear test was conducted with two panels of identical skin layup – one with aluminum core and one with end-grain balsa core. The testing results (Table 10) show that balsa core panels have much higher perimeter shear strength than aluminum core panels. These results mean that balsa is a more suitable core material for monocoque regions with high out-of-plane loading. Balsa core was easily sourced from Specialized Balsa Wood.

Using Garolite G10 as a core material in areas of high out-of-plane loading was considered but not pursued, due mainly to the high density of G10 compared to end-grain balsa. The density of the balsa core used in the 2013 tub was 6.0 lb/ft^3, whereas G10 is 112 lb/ft^3. The use of end-grain balsa produced satisfactory perimeter shear testing results (Table 10), so the team did not feel that testing a G10 core panel was necessary.

Table 10. Perimeter shear comparison between balsa core and aluminum core panels.

	Balsa Core panel	Aluminum Core panel
Failure Load (lb)	4114.08	2000
Perimeter Shear (lb/in)	1309.52	636.62

Although the possibility of omitting film adhesive from the laminate design was considered, FMD felt that it would be prudent to obtain film adhesive anyways, in case the core-bonding strength of the prepreg resin was insufficient. Unfortunately, all of the existing film adhesive available to the team had terminally degraded. Since film adhesive was believed to be exceptionally expensive, FMD began reaching out to various suppliers for a donation. Late in the design phase, the team received a generous donation of TC-263 low-tack film adhesive from TenCate. Future testing would show that using film adhesive was not needed for an effective core-skin bond (see page 57). However, the team reasoned that keeping film adhesive on hand for core splicing would be prudent.

Driver Fitment

In addition to the laminate testing requirements, SAE mandates that the chassis design be sized to fit the 95th percentile male ("Percy") template. Following these requirements, the driver's cell must be proportioned so that Percy's feet can reach the pedals. In addition, the driver must be situated so that the subframe roll hoops and bracing members provide adequate protection in rollover. Since the 2013 tub molds were already sized to these requirements, the FMD tub had no problem passing the driver fitment rules.

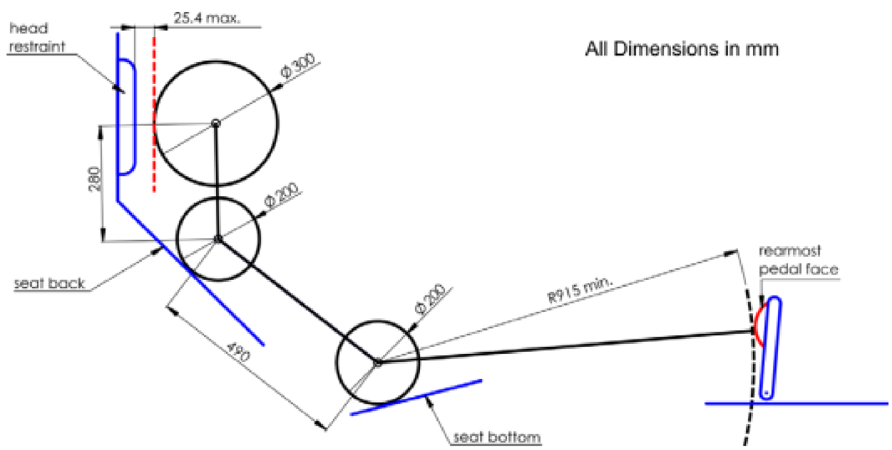

Figure 5. 95th percentile male template

To ensure that the driver harnesses properly protects the driver in case of collision, SAE requires that the harness mounting points fall within a certain region of the tub relative to the driver's hips. In 2013, the driver assumed an upright position because the driver sat on an elevated Plexiglas case that housed the electronics. In 2015, the electronics were moved outside of the cockpit, allowing a more reclined driver position. This arrangement brought the driver's weight lower, thus lowering the car's center of gravity. In accordance with SAE's rules, the lap belt and anti-submarine belt mounts were placed on the cockpit floor and moved further forward to better line up with the driver's hips. The harness clips were secured to the tub via 7/16"-20 eyebolts, and the backing plates were sized to a cross-sectional area of 0.093 in^2, as mandated by the rules.

Figure 6. Lap belt and anti-submarine harness attachment locations. This bracket arrangement is replicated on both sides of the cockpit floor.

Each front and rear roll hoop pickup is required to be 0.080” thick and sustain a 30 kN load before failure. In order to size the perimeter of each bracket, the perimeter shear value (shear load per inch) from laminate testing was taken and solved for the bracket perimeter, given a 30 kN load. As per SAE rules, the front roll hoop has two pickups on each side, and one along the top strap of the tub. The main roll hoop is secured with two pickups on each side. Each backing plate incorporates two AN5 bolts.

Geometry Layout

The geometry of the monocoque was designed to accommodate the driver, as well as the components attached. To accommodate the driver, it had to meet SAE rules as well as the team’s ergonomic requirements. One of the SAE rules requirements for the driver’s cell is that it must be large enough to fit a template of given geometry through it (SAE Rule section T3.10, see Appendix I). This ensures that the driver will have sufficient room inside while driving the car. It also ensures that in the event of a rollover, the drivers head will be protected by the main and front roll hoops.

Other considerations taken into account when designing the monocoque geometry were mounting. Components like the suspension, subframe, and pedal box all played a role. This is evident by the flat regions where most of these components mount. Another consideration was torsional stiffness. Shaping the monocoque like a tube is an efficient way to be torsionally stiff.

Integrated Front Roll Hoop

One design change that was looked into was integrating the front roll hoop into the monocoque (see Figure 7 for an example). This could be achieved by either integrating the roll hoop into the layup or by bonding the roll hoop to the tub after the initial layup. The thought process behind integrating the front roll hoop is that it would increase stiffness as well as reduce weight. Stiffness could be increased because the roll hoop would become a much more structural member (bonded to monocoque along its entire length, instead of being held in place by bolts). Weight could be saved because the mounting hardware would be replaced by much lighter epoxy resin.

While there could be benefits of successfully integrating the front roll hoop into the monocoque, there would also be disadvantages. The largest deterrent to pursuing an integrated front roll hoop is the increased manufacturing complexity. Moving forward with an integrated front roll hoop would also necessitate additional design and testing time to prove equivalency. Due to the increased complexities, added risks, and longer development time associated with an integrated front roll hoop, this design change was not pursued further.

Figure 7. Global Formula Racing uses a roll hoop bonded to the outside of their monocoque. A 0.3” circular indentation was made in the mold to locate the roll bar and provide additional bonding surface area. Relocating the roll hoop to the outside of the 2015 Cal Poly vehicle would increase tubing weight from 4.2 pounds to 7.5 pounds.

Front Access Cutout

In order to access components inside the front half of the monocoque, such as the pedal box, a front access window is needed. The 2013 monocoque utilized a rectangular cutout in the front bulkhead as an access point. While driving, the cutout was covered by the anti-intrusion plate, which was covered by the nosecone.

Concept 1a. Front cutout identical to 2013 monocoque.

The 2013 car had a front-facing cutout that was 9” wide and 7.5” tall (Figure 8). Using the same geometry for the 2015 monocoque is a viable option.

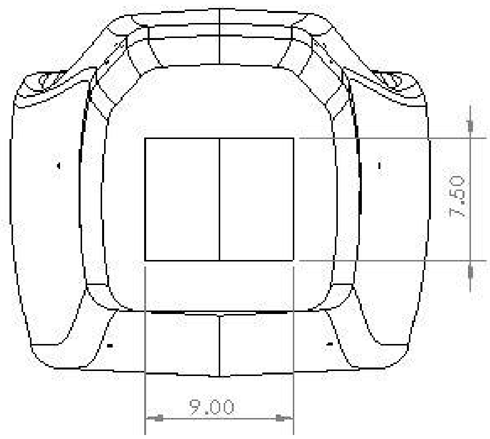

Figure 8. Solid model of 2013 monocoque showing cutout geometry and placement. .

Concept 1b. Front cutout of larger dimensions.

Due to a very thick front bulkhead laminate, the SES allowed for an increase in cutout size relative to 2013. Each square inch of front bulkhead weighs approximately 0.0185 pounds, so increasing the size to 11”x11” (Figure 9) would save 0.99 pounds over maintaining the previous dimensions. It is unknown what effect this would have on torsional stiffness.

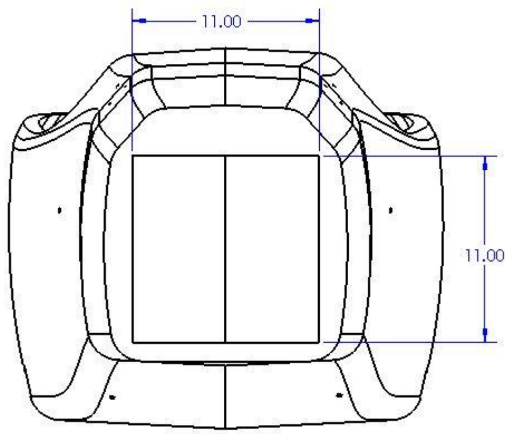

Figure 9. Solid model of monocoque showing new cutout dimensions and placement.

Concept 2. Top cutout.

Another option for a front access window would be to have a cutout on the top of the tub, most likely directly over the pedal box area (see Figure 10). A top cutout would allow the combination of the front bulkhead with the anti-intrusion plate. With this configuration, a single laminate could satisfy both requirements, saving weight. The main disadvantage to a top cutout would be its effect on torsional stiffness of the monocoque. Other disadvantages to a top cutout include increased difficulty in accessing components inside the monocoque as well as finding a new way to close the opening.

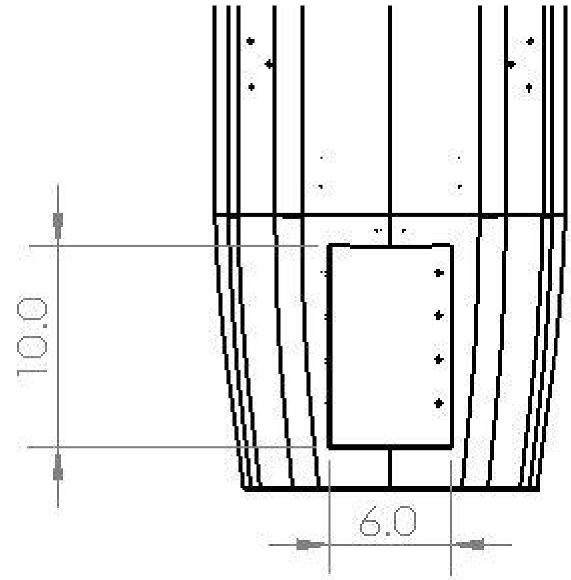

Figure 10. Solid model of the monocoque with a potential top cutout.

Cockpit Closeouts

In the sandwich structure used in the monocoque, the core carries the shear load well in the middle of the structure; however, near the edges extra reinforcement in the form of closeouts is often necessary. The 2013 monocoque utilized wet-layup carbon closeouts to connect the two face-sheets around the cockpit opening.

Concept 1. No closeouts.

Research indicated that one of the most important things to do when designing a sandwich structure is to use properly developed closeouts. Closeouts increase stiffness, strength, and help prevent delamination near the edges. They do add weight, but the benefit greatly outweighs the weight penalty. Due to these reasons, it would be unwise to not use closeouts.

Concept 2. Standard closeouts.

According to Mechanical Engineering composites specialist Dr. Joseph Mello, closeouts should be at least the same thickness as the face sheets. The amount of overlap area in order to have enough bonding surface is calculated from the shear stress in the laminate. As long as the closeouts are strong enough, they will transfer the shear flow between the two face sheets and greatly increase torsional stiffness around the cockpit opening. They also prevent delamination from occurring near the edges of the cockpit opening. Finally, they prevent water and other unwanted materials from degrading the core. See Figure 11 for an example of where a closeout is utilized.

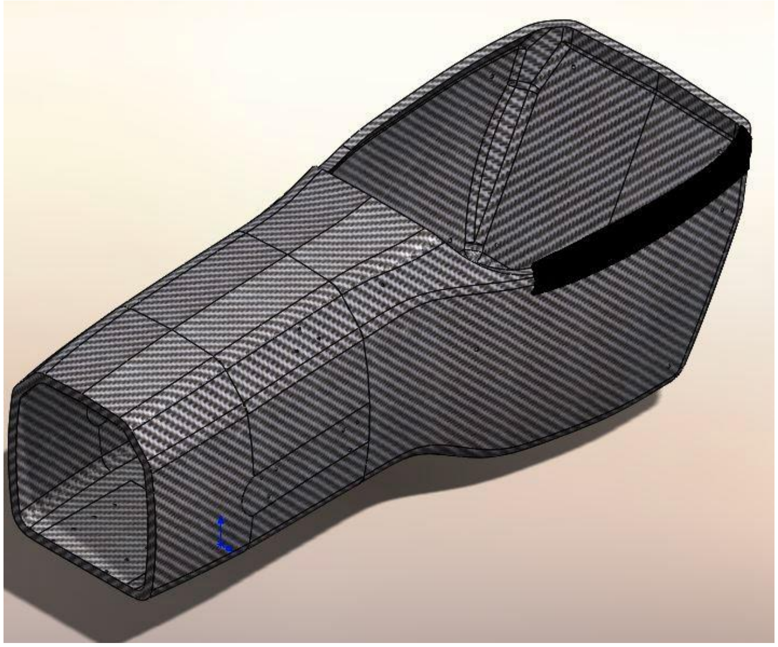

Figure 11. Example of size and location of closeout used on monocoque. The black strip represents where part of the closeout is located. Note how it wraps over the edge of the sandwich structure.

Concept 3. Large channels as closeouts.

At the 2014 FSAE competition in Michigan, a few teams had large channels around the edges of their cockpits where closeouts would be. It was originally believed that this was to promote torsional stiffness. However, after consulting Dr. Mello and further researching closeouts, it is believed that they serve as structural members so their monocoque does not fail during driver egress. Since thick carbon closeouts would be comprised of many layers of carbon laid up over the region, they would add quite a bit of weight (1.5 pounds per foot, assuming 10 plies). Because the monocoque will be strong enough to support driver egress with standard closeouts, thick carbon closeouts were an unnecessary weight addition and therefore were not used.

Nosecone Geometry

The nosecone of the car serves four different purposes. Primarily, it functions as the car's impact attenuator, and therefore must meet FSAE impact attenuation requirements (see Appendix C). Additionally, the nosecone provides mounting for the front wing, aids the car's overall aerodynamics by providing a smoother transition to the tub region, and covers the front bulkhead cutout along with the anti-intrusion plate.

Energy absorption considerations

Because the FSAE impact attenuation requirements are referenced to a head on impact, the nosecone must be able to attenuate high levels of energy in the axial direction. The 2013 nosecone accomplished this by having thick sides that were minimally angled. This allowed the fibers in the sides to take a high load in the axial direction of the fiber, where it is strongest. The consistent tapered geometry also allowed for a progressive failure as the impact transpires, and the effective crush area increases. See Figure 12 for the 2013 nosecone geometry.

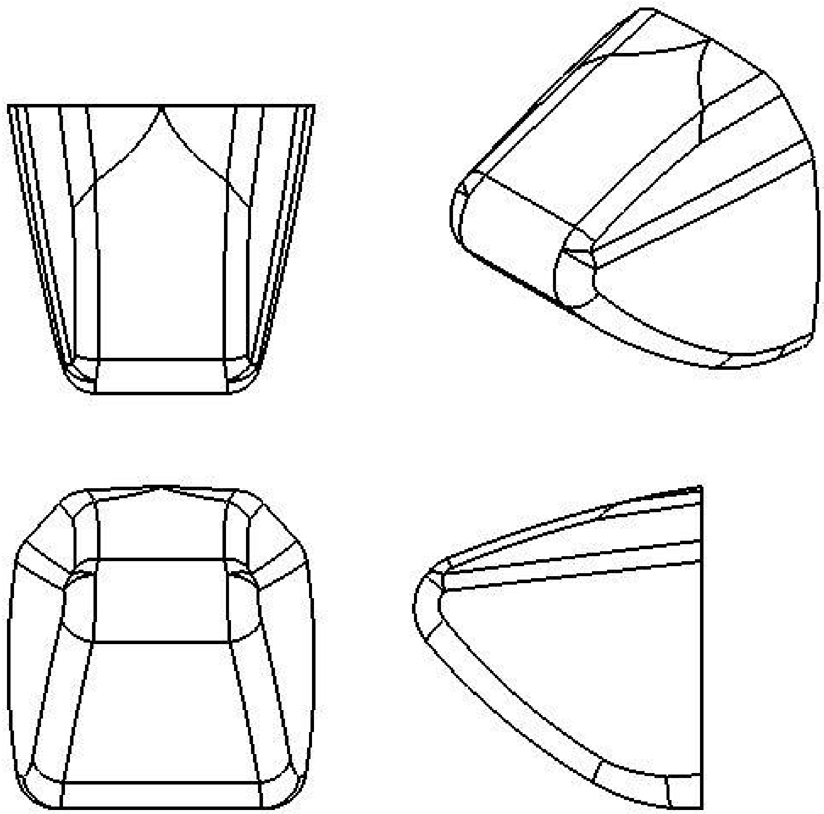

Figure 12. Solid model of 2013 nosecone. Note that bolt flanges are not included in this drawing, as they were not included in impact attenuation test.

Because this geometry proved to be effective at absorbing energy, a similar design was used. See Figure 13 for a potential 2015 nosecone geometry.

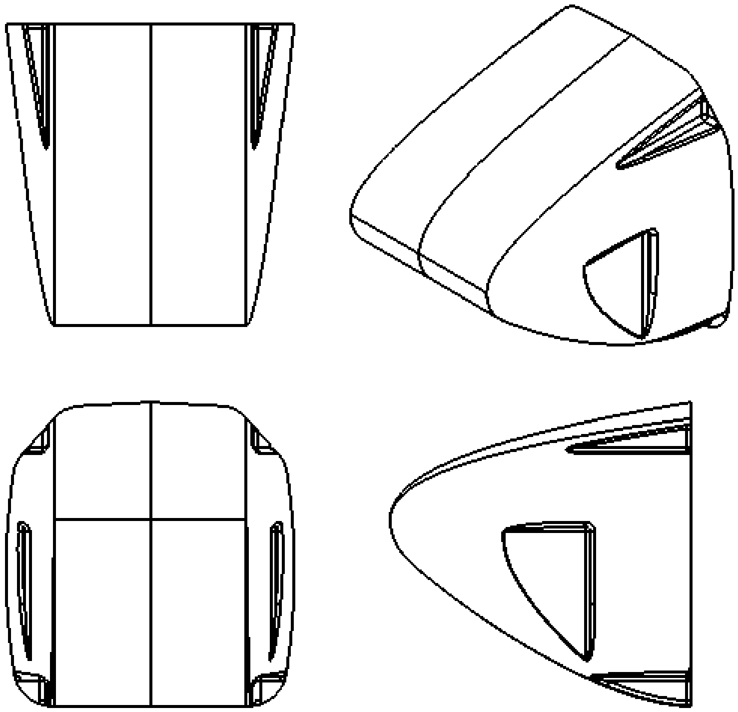

Figure 13. Proposed 2015 nosecone geometry. Note the flat regions where front wing mounting trusses mount.

Front wing mounting considerations

In 2013, the car was not designed or manufactured with an aerodynamics package. In 2014, an aerodynamics package consisting of front and rear wings was added to the car. Because the front wing was added on after the car was completed, it was inefficiently integrated. The 2014 front wing mounting amounted to 4.43 pounds. This year, one goal was to mount the front wing in a more weight efficient manner. Instead of having supports begin at the tub, they could be smaller and lighter by being mounted to the nosecone. These mounts would bolt to the nosecone at flat regions designed into the nosecone geometry (see Figure 14 for a potential design).

Figure 14. Potential nosecone design with integrated front wing mounting. Multiple holes are present to conduct ground clearance testing before producing a final version of the mount. Placing the additional holes in the mounts instead of the nosecone allows for less stress concentration introduction into the nosecone.

Local Ply Reinforcement

The use of additional tapered carbon fiber layers at localized areas of high load offers increased strength and stiffness (Figure 15). The theory behind pad-ups is directed from the line-moment distribution used in Classical Lamination Theory. The greater thickness of the face sheet helps to distribute the localized loads throughout the laminate.

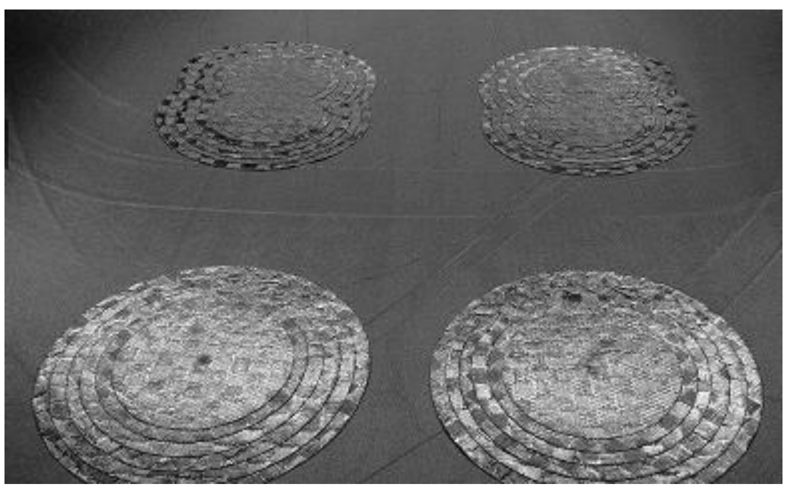

Figure 15. An example of pad-ups used to reinforce regions with excessive localized loading.

It was determined that pad-ups would be advantageous at the lower suspension pickups, which are the points of the greatest expected load. Two additional plies of cloth at these points act to help distribute the large localized loads. Based off of instinct, doubling the ply count in that region would provide sufficient support, hence why two plies were used. It would be useful for future teams to test the effectiveness of using pad ups for structural support.

Preliminary Analysis

Localized Loading Conditions

The monocoque must withstand loading from several of the vehicle's subassemblies, including the suspension, subframe, and pedal box. The chassis experiences localized loadings at suspension pickup points, pedal box assembly mounting points, and rear subframe attachment points, as well as loading from the driver upon egress. These are regions where excessive contact stresses and deflections have potential to develop, so special attention was given when designing the laminate at these regions.

Suspension loading occurs at several different pickup mounting locations, including lower A-arms, upper A-arms, rockers, and coilovers. Three loading cases were analyzed for the following suspension loads: a max lateral acceleration of 2.3 g, max braking deceleration of 1.6 g, and combined lateral/braking acceleration of 1.5 g and 0.5 g, respectively. These accelerations are based off of data collected from the 2014 FSAE vehicle, which has been scaled to represent the predicted performance of the 2015 car with improved aerodynamics and reduced overall weight. Individual A-arm forces were calculated based off of tire normal, lateral, and longitudinal forces acquired from Calspan tire-testing data. The tire forces are projected through the suspension members, assuming quasi-static loading. The lower A-arms see the largest loads, around a maximum of 1200 pounds (axial compression, per arm) for the combined loading case. This loading condition induces a combination of in-plane shear and bending moment on the chassis. The maximum loading case for the upper A-arms is 500 pounds (axial tension, per arm), inducing out-of-plane shear on the side of the monocoque, which can be modeled as a simply supported plate in bending. The rocker mounting location experiences loads of 500 pounds max, due to a combination of the pullrod force and spring displacement, which induces in-plane shear and bending moment on the monocoque. Similarly, the damper mount experiences 300 pounds (axial compression) of loading in extreme driving conditions. Finally, the anti-roll bar experiences forces of 300 pounds under pure lateral acceleration, which induces out-of-plane shear on the bottom of the tub. The laminate design at the front floor and front bulkhead was driven by the upper and lower A-arm forces and ARB forces, so these loading cases were incorporated into the CLT strength analysis code (explained below) and are depicted below in Figure 16.

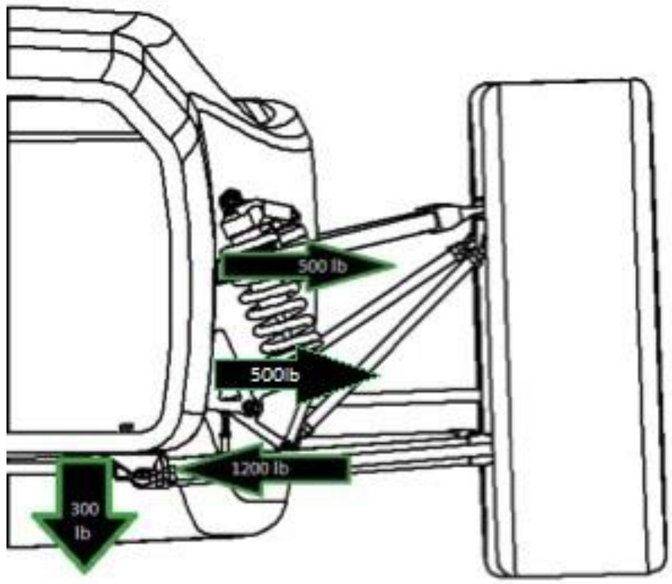

Figure 16. Suspension induced loads acting on the monocoque. The largest loading case occurs at the lower A-arms, which induce shear and a bending moment into the tub.

Stiffness requirements for the suspension mounts are based off of effects of deflection on the contact patch of the tire. The tolerance for camber change and toe change are 0.2^{o} and 0.02^{o}, respectively, determined by the suspension subsystem. Since the lower A-arm forces primarily load the chassis in-plane, which is relatively stiff, deflection of the upper A-arm mounting point was focused on, which acts as a plate in bending. To account for compliance stack-up in the chassis, suspension members, and uprights, the suspension system set a requirement of 0.1^{o} of camber change due to upright/suspension member compliance and 0.1^{o} of camber change due to monocoque compliance. This amount of camber change corresponds to 0.010" of deflection at the upper A-arm pickup point.

The pedal box assembly experiences force inputs from the driver during operation. Maximum forces occur under the case of threshold braking. Based on the strength of the driver, the largest input expected is 450 pounds, applied to the brake pedal, which is located 9" above the front floor panel. This force induces a large bending moment load and in-plane shear on the monocoque. Additionally, the cockpit floor experiences its most extreme loading condition upon driver egress. Assuming that the driver jumps out of the monocoque, a max load of 500 pounds at the cockpit floor is expected. Both of these loading conditions can be seen below in Figure 17.

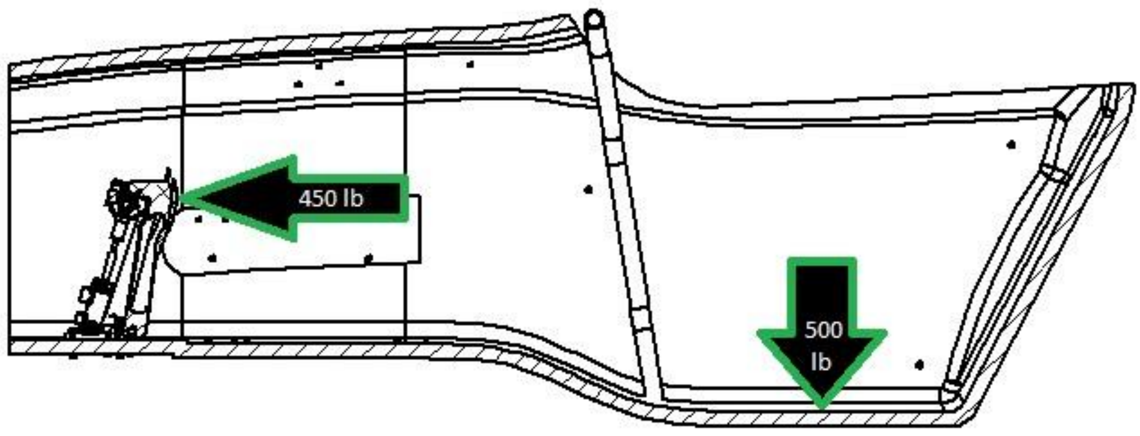

Figure 17. Pedal box assembly and driver egress forces applied to the front floor and cockpit floor of the monocoque.

The final major localized loading condition is experienced upon frontal impact in the case of a crash. Assuming quasi-static loading from a 40g deceleration in the case of front impact, a force of 20,000 pounds is applied across the perimeter of the front bulkhead,

The seat back laminate was originally validated with CLT. The seat back was modeled as a beam with a 15’’ span and an 18’’ width, with a 7000 pound load applied at the midspan. This loading was intended to simulate the seat back supporting the driver in the case of a 40g impact. The final seat back schedule of $[45c/0c/\bar{c}]_s$ was validated using this requirement (see Table 21), and the seat back was manufactured to this design. However, discussions with our advisor revealed that this loading condition was an inaccurate representation of frontal impact. In the case of frontal impact the chassis rapidly decelerates, and the driver moves forward relative to the chassis. The shoulder, lap, and anti-submarine harnesses are then pulled in tension to restrain the driver, thus resulting in an off-axis out-of-plane load at the tub’s harness pickups. This type of loading is represented by the SAE cockpit off-axis pullout test (see page 61 and Appendix M), which simulates loading through the harness, at an angle representative of the harness angle relative to the monocoque. The cockpit floor laminate was sized using this test.

Possible loading conditions for the seat back involve any forces going through the subframe pickups during driving. Applying these forces in the FEA model at the applicable pickup points will show how the seat back responds. The FEA model can be used to examine a variety of loading conditions, as was attempted in our pursuit of the Alternative Frame rules (Appendix T).

Loading conditions applied to the seatbelt harness attachments were based off of the requirement mandated by SAE rules, which is a 2900 pound load acting along the vector designated by the lap belt angle. Since inertial effects are relevant in this case, these are overly conservative estimates that help simplify the analysis process.

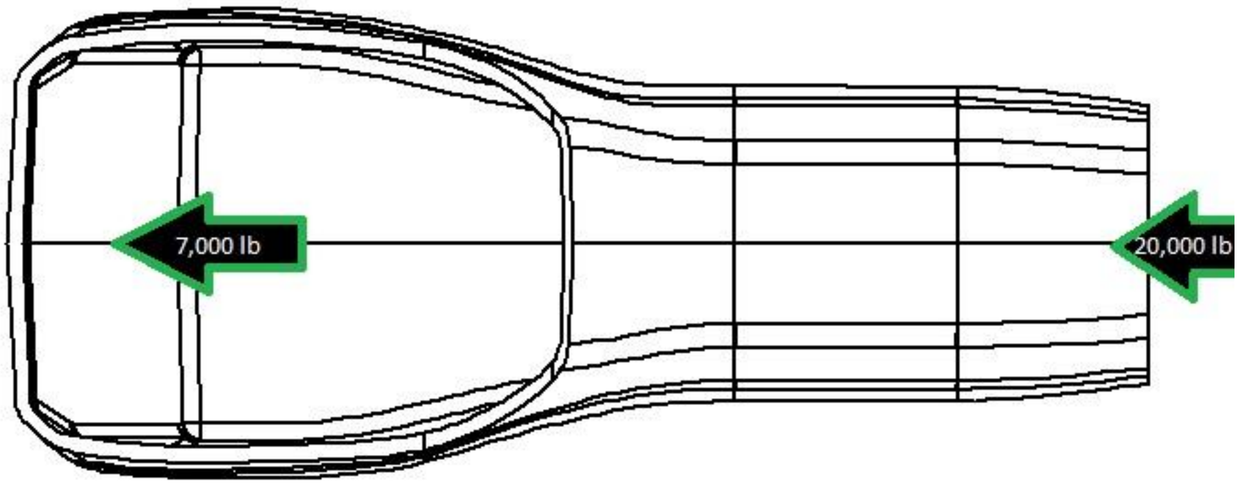

Figure 18. Front impact forces applied to the front bulkhead and seatback of the monocoque.

An additional localized loading region of potential concern is the junction of the monocoque and the rear subframe. Based on the preliminary design, this connection will be similar to previous designs, with backing plates held in place by several bolts. Two worst case scenarios were considered for this critical joint: 3 g's of bump loading and 3 g's of cornering. Tire forces under these conditions were projected to the joint using simple static relationships. The large amount of connectors used in the joint design (8 5/16" bolts) help distribute the stress over a large area, so both of these extreme loading cases resulted in negligible forces at any specific bolting location. The maximum load was determined to be 450 lbs of in-plane shear due to the 3g cornering condition. Based off of static tests, the strength of a basic honeycomb sandwich structure will be sufficient at these points since the loads act primarily in-plane.

Finite Element Analysis

A full-chassis ABAQUS FEM was used to analyze the torsional stiffness of the monocoque. This model is an assembly consisting of the monocoque, rear subframe, front roll hoop, suspension arms, uprights, and engine (Figure 19). The monocoque was modeled with thick shell elements with laminate properties. The subframe and front roll hoop were modeled as beam elements with appropriate steel material properties and tubular cross-section profiles. The control arms of the suspension were modeled as truss members in order to simulate the effect of heim joints, where moments are not reacted at the ends of each arm. Finally, the uprights were modeled as infinitely stiff beams to simplify the analysis.

Bolted connections between the tub and roll hoops were modeled as rigid connectors for simplicity. However, a more accurate approach would be to model the bolts as springs with stiffness values derived from testing or manufacturer data. Rigid connectors artificially increase the torsional stiffness performance of the chassis model. Considering this, developing the modeling of bolted connections is a worthwhile pursuit for future teams.

Unlike the suspension arms, suspension rockers were modeled as rigid connectors for simplicity, with forces applied at each joint to imitate the loading from a 1 pound upward force at the upright. In pursuit of a more accurate model, the team was advised to model the rocker as a volute, with rotation only being allowed along the axis of the rocker pivot. The rocker pivots was modeled using HINGE connectors. Unfortunately, the model encountered errors that proved too time-consuming to fix. Given more design time, refining the modeling of the rockers would be a worthwhile development.

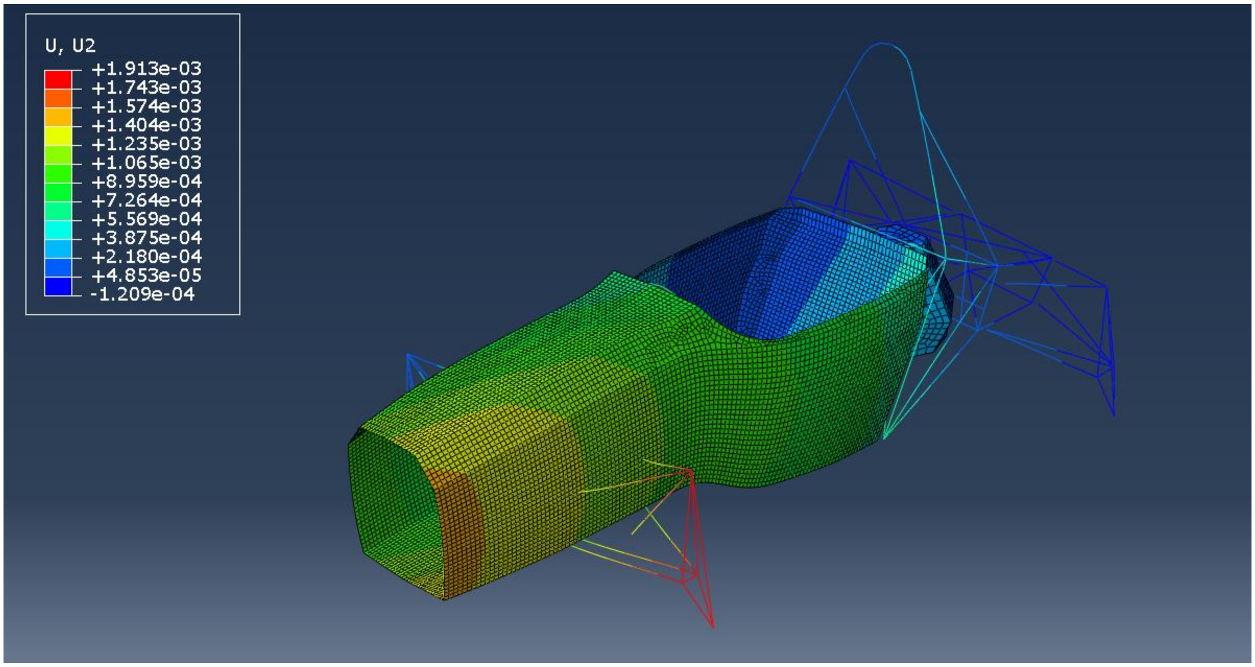

Figure 19. ABAQUS full chassis model subjected to a torsional load.

The individual components of the chassis assembly are tied together with rigid connectors. In the case of a torsional stiffness simulation, three of the four uprights were assigned partial constraints, with a downward load applied at the unconstrained upright. Constraints were configured so that the system was neither under-constrained nor over-constrained. Under-constrained systems do not adequately support an object in space, resulting in excessively high deflections. On the other hand, over-constrained systems output artificially-low deflection values due to the presence of redundant constraints. Since the torsional performance of the chassis will be physically tested, the FEA constraints (Figure 20) were configured so that a fixture could be feasibly manufactured to imitate the model.

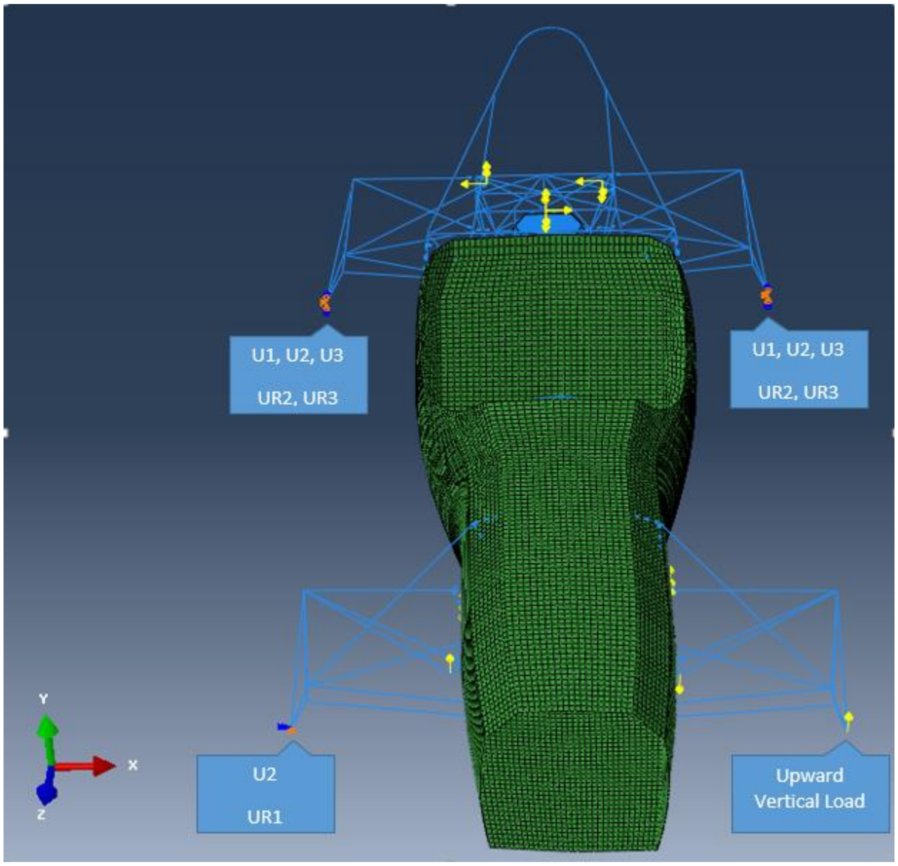

Figure 20. Torsional stiffness model with constraints. The X, Y, and Z directions correspond to the 1, 2, and 3 axes, respectively.

Manipulating the monocoque material properties in the FEA model resulted in the conclusion that the core shear moduli influenced torsional stiffness more than fiber stiffness. The 2013 skin laminate focused on uni fiber stiffness to increase chassis torsional stiffness (Figure 21).

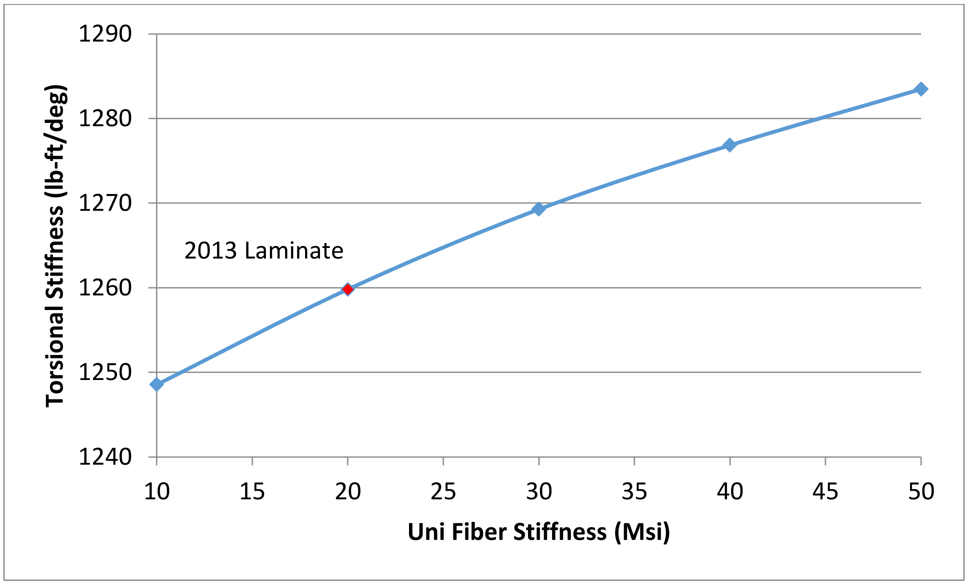

Figure 21. Chassis torsional stiffness response to unidirectional fiber stiffness.

Changing the core properties to reflect different honeycomb thicknesses yields a much more pronounced torsional stiffness response (Figure 22). According to the Hexcel datasheets, core thickness is directly related to the ribbon and transverse shear moduli (G13 and G23, respectively). Since torsional stiffness is so heavily influenced by core shear moduli, it was determined that using stiffer aluminum core was the most efficient way to increase chassis stiffness. However, thicker core means more difficulties in manufacturing. Thicker core is more difficult to bend into tight radii and corners. The monocoque geometry is already not very accommodating for 0.7” core, so increasing core thickness was not seriously considered.

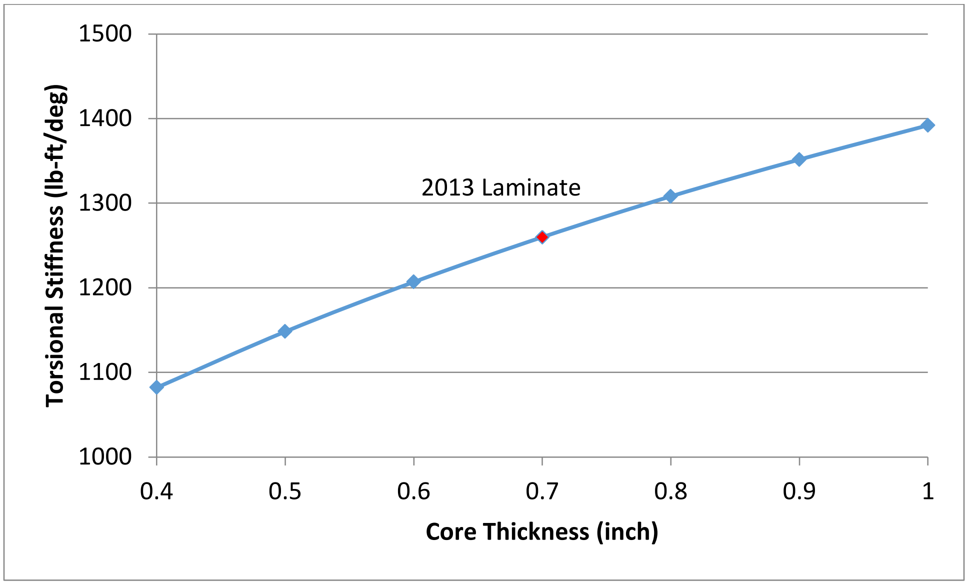

Figure 22. Chassis torsional stiffness response to core thickness (Nomex core).

Classical Laminate Theory Analysis

A CLT MATLAB script used in previous years was further developed for use in analyzing specific strength requirements at regions of high localized load. Each loading condition implemented in the CLT strength code is summarized below in Table 11. Simplifying assumptions were made to model the complex loading cases in a way that was easier to analyze. For example, the loading induced from the upper A-arm mounting locations was modeled as a plate in bending. Additional common CLT assumptions were employed, such as the core carrying all of the shear loading.

Table 11. Summary of loads used in CLT Analysis.

Loading Case	Laminate	Loading Specification
Front Impact	Front Bulkhead	20,000 pounds applied longitudinally across perimeter of front monocoque, to simulate 40g impact.
Seatback	Seatback	7,000 pounds applied across area of seatback experienced during front impact, to simulate seat back supporting driver in 40g impact.
Upper Suspension	Front Bulkhead Support	500 pounds applied to middle of plate beam with width and span corresponding to the front bulkhead support of monocoque
Lower Suspension	Front Floor	1200 pounds applied to plate in-plane with offset corresponding to eccentricity of suspension pickup points
Pedal Force	Front Floor	450 pounds applied at 9" eccentricity
Driver Egress	Cockpit Floor	500 pounds applied to middle of plate beam with cockpit floor dimensions
Anti-Roll Bar	Front Floor	300 pounds applied to middle of plate beam with front floor dimensions

With the above loading conditions implemented into a MATLAB script, the strength of the monocoque was theoretically analyzed. The carbon fiber and core material properties were inserted in the code, along with ply orientations at each section of the monocoque. The code uses CLT in order to determine the stiffness matrices of the composite, and uses these matrices along with a max-strain failure theory to determine the failure indices of each composite section. The results of the analysis are then summarized in a spreadsheet for ease of post-processing. The matrix failure indices, fiber failure indices, and failure loads for each iteration were summarized in the output. Additionally, all ply angles, thicknesses, and materials were recorded for later reference.

Because the nosecone was designed to have the front wing mounted to it, new loading conditions were introduced. CLT was used to analyze local bearing strength where the mounting truss bolts attached to the nosecone, as well as the bolt flats where the nosecone bolts to the monocoque. The bearing stress calculation was straightforward, and resulted in a safety factor of 6.8. This also meant that the bolt would fail before the carbon, so if the front wing were to hit a cone, the nosecone would not be damaged. The nosecone mounting bolt flats were assumed to be plates in bending, fixed on one side. Because it is actually fully fixed at two adjacent sides, this is a conservative assumption. The resulting safety factor on the bolt flat was 3.4.

Laminate Iteration

In order to pursue increases in torsional stiffness, iterations were performed using the CLT strength code and the FEA torsional stiffness test in conjunction. Plies were added and subtracted, ply angles were varied, and changes were made between unidirectional fibers and woven cloth fibers. However, all material properties stayed constant, since the team was limited to using the materials it had already acquired.

The iteration process is summarized below in Figure 23. Equations were added to the CLT code so that the torsional stiffness could easily be calculated and recorded along with the strength criteria results. Results were summarized in a spreadsheet for future reference.

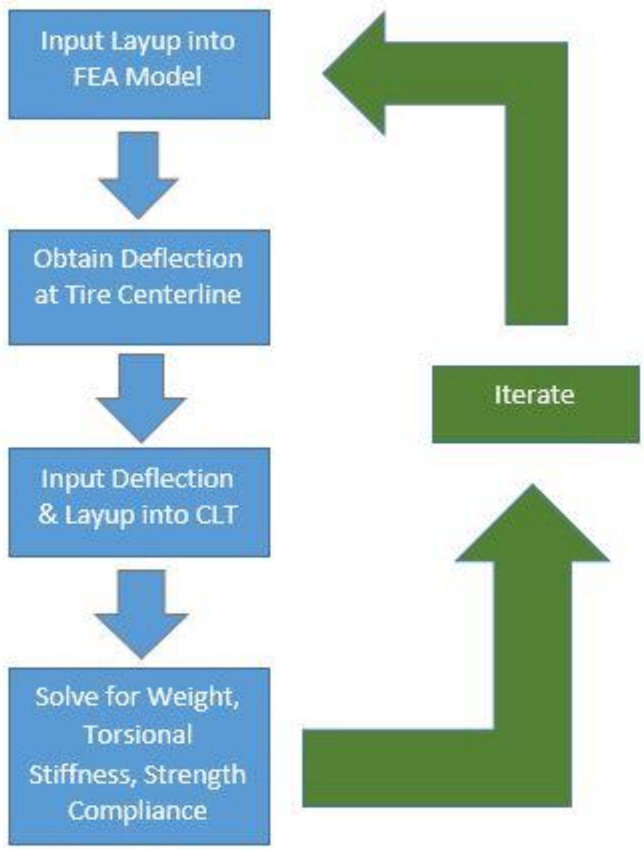

Figure 23. Laminate iteration process flowchart.

Results from the iteration are displayed below in Figure 24. Plies were added and ply orientations were varied in an attempt to stiffen the monocoque, however the overall torsional stiffness of the chassis increased only slightly. This lead to the specific stiffness of the chassis decreasing. Instead, if plies are removed in an attempt to save weight, the specific stiffness of the monocoque increased.

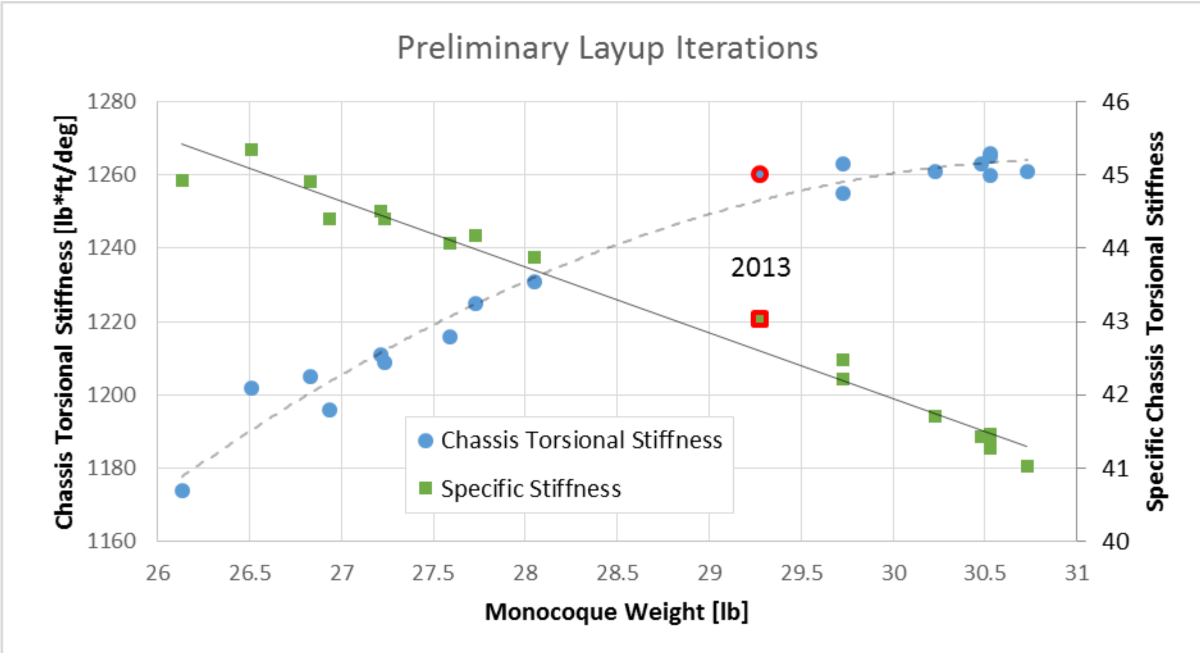

Figure 24. Primary laminate iteration results. Total chassis stiffnesses and specific chassis stiffness are plotted against the total monocoque weight.

In order to analyze where the major stiffness losses were located in the 2013 chassis, the FEA model was modified to analyze the torsional stiffness of three specific components: the suspension, the monocoque, and the rear subframe. With specific component torsional stiffnesses determined, the design of the tub torsional stiffness can be determined such that it will meet the overall chassis torsional stiffness requirement without adding unnecessary weight to the vehicle. Since these three components act as springs in series, having an exceptionally stiff monocoque with a highly compliant subframe would be unreasonable if it is possible to equalize the stiffness between the three aforementioned components.

The first analysis involved the torsional stiffness of the tub only. All other parts were set to infinite stiffness material properties. The resulting deflection corresponded to a torsional stiffness of 5060 lb*ft/deg. The second analysis involved the deflection due to only the subframe. The tub was modified to act as an infinitely-stiff shell. The result was a torsional stiffness of 3220 lb*ft/deg. Finally, the torsional stiffness of the suspension was determined. Again, the tub was defined as an infinitely-stiff shell and all other parts were also set to infinite stiffness. The suspension was found to have a torsional stiffness of 7730 lb*ft/deg. However, the theoretical torsional stiffness is expected to be greater than the actual torsional stiffness of the suspension subsystem, since the FEA model does not take into account bearing slop and deflection due to chassis pickup points and attachment bolts.

Table 12. Component stiffnesses of the chassis. The subframe offers the most room for improvement.

	Load [lb]	Moment Arm [in]	Deflection [in]	Torsional Stiffness [lb*ft/deg]
Tub Only	1	47	0.0006345	5061
Subframe Only	1	47	0.0009978	3218
Suspension Only	1	47	0.0004156	7727

By modeling these component stiffnesses as springs in series, a system stiffness of 1570 lb*ft/deg is obtained. The reason this value is different than the original FEA model's torsional stiffness of 1260 lb*ft/deg is because the subframe mounting tabs and front roll hoop were not included in the analysis. These components are included in the complete FEA model.

These results suggest that the highest potential gain for overall system stiffness lies in increasing the torsional stiffness of the rear subframe. Since the weakest spring in the group has the most influence on the overall chassis stiffness, it would be counterproductive to increase the stiffness of the monocoque if substantial increases in weight were required to do so. However, with a stiffened subframe, it could be possible to remove plies from the monocoque (and thus decrease its weight and stiffness) in order to better meet the holistic chassis torsional stiffness goal and team's weight goals.

In addition to FEA, a physical torsion test was performed on the 2013 chassis (with the new monocoque to subframe joint). The results can be viewed in Table 13. While physical testing results are more reliable than theoretical finite element results, the physical torsion test of the 2013 chassis was performed too late in the design phase to be of use. However, one lesson learned was that physical torsional stiffness will always be lower than theoretical torsional stiffness predicted by a FEM. This lesson was used when determining a target stiffness.

Table 13. Results of physical torsion test performed on 2013 chassis.

Component	Torsional Stiffness (ft-lb/deg)
Monocoque and front suspension	2148
Joint	36480
Subframe and rear suspension	2193
Total	**1054**

Since this project is primarily concerned with the performance of the monocoque, the relative stiffness of the monocoque was further analyzed. All components aside from the monocoque were stiffened so that the stiffness of the monocoque would dominate. Vertical deflections of the monocoque were probed along its longitudinal axis, and then transformed into rotations using the lateral distance from the centerline. Since the major concern is where large changes in rotation are occurring (e.g. where stiffness is lost), the derivative of the rotation was taken and analyzed. The results of this analysis can be seen below in Figure 25.

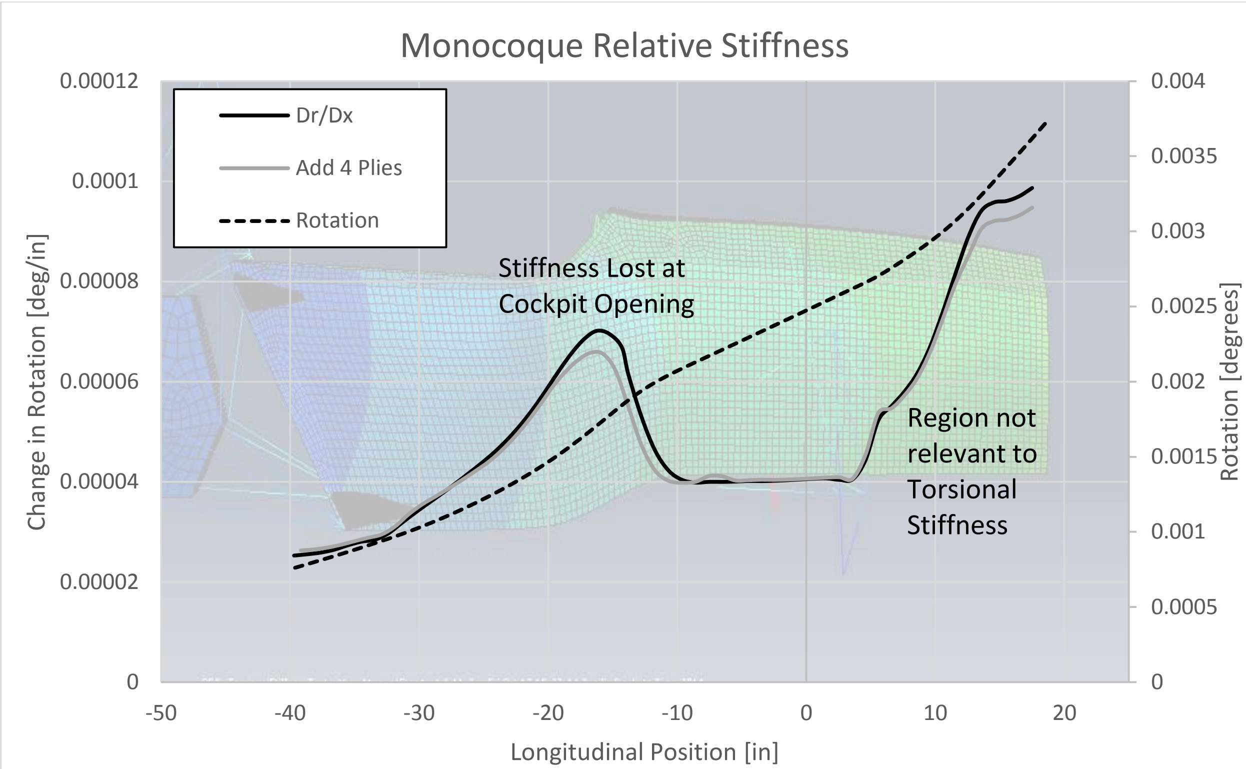

Figure 25. Relative stiffness of the monocoque with respect to the longitudinal axis. Results were obtained from probing the FEA model along the length of the chassis and determining the rotations about the chassis centerline from the results.

The largest change in rotation occurs at the start of the cockpit opening. This suggests that the primary region for improvement of the monocoque in terms of stiffness is stiffening the cockpit opening. The change in rotation between the front suspension and the start of the cockpit opening is relatively constant. The rotation also experiences a large jump fore of the front suspension, but the rotation of this region of the tub is not of primary importance because the torsional stiffness is quantified between the front and rear axles of the vehicle.

From the above results, it can be deduced that, if the torsional stiffness of the monocoque is to be increased, the area to focus on is the cockpit opening. The result of adding four +/- 45 degree plies at the side impact support are also shown in Figure 25. This change corresponds to a 7% increase in torsional stiffness, but an 8% increase in weight. Alternatively, there are other methods that will theoretically increase the stiffness in this area, such as increasing the size of the close-outs to improve shear flow around the cut out or increasing the girth of the front roll hoop in order to further restrict compliance. Unfortunately, FMD was limited to the geometry designed into the molds used for manufacturing the monocoque, so geometrical modifications were not pursued.

In the event that a new monocoque shape can be achieved through the manufacture of a new mold, several dimensions of the tub can be downsized to save weight and more closely adhere to the SAE template requirements.

Considering the template dimensions (Appendix I), the cockpit opening size can be further downsized. The template could be lowered past the minimum height (13.8 inches) above the ground. This remained the case, until a hand clutch was mounted to the side impact structure, thus obstructing the depth that the template can be lowered into the tub. Thankfully, the driver cell still passed the template test. In addition, inserting the cockpit opening template into the driver cell showed an approximately ½'' clearance (all around) between the template and the very top of the driver cell sidewalls. Considering these observations, the driver cell cutout can be downsized slightly. Future teams should consider the tradeoffs between cockpit size, driver comfort, and extra room for components mounted to the driver cell sidewall.

Currently, the cockpit internal cross-section (where the driver's legs lie) is significantly larger than the applicable template. The tub cross-section can be downsized in this region, at the expense of driver comfort and leg room. For future teams designing new mold geometry, a study should be conducted that examines driver comfort and leg positioning versus the height, width, and length of the front end of the tub.

The length of the monocoque can be further reduced, as the distance between the pedal face and Percy's feet is substantial. Future teams should consider shortening the monocoque, and then increasing the height of the monocoque so that the driver can place his or her knees higher. It would be worthwhile to examine the weight tradeoffs between shortening and raising the height of the monocoque, considering driver leg comfort.

Design Development

Film Adhesive

In order to evaluate whether sheet resin was needed for sufficient skin-to-core bonding, FMD laid up several short-beam shear panels – one with sheet resin, one with AS4 cloth only, and one with T800 cloth only. Depending on the failure load and failure mode of each panel, FMD could determine whether prepreg resin alone could effectively bond the skin to the core. Using aluminum core and AS4 cloth, the testing results (Table 14) were unexpected. The panels with film adhesive proved to be weaker than those without film adhesive. This proved the feasibility of omitting film adhesive from the layup schedule, saving approximately 4 pounds. Note that per Dr. Mello's recommendation, it was decided to still use film adhesive between core splices in order to transfer the shear between core sections. Hexcel standards detailing the test setup and calculations can be found in Appendix D. To further strengthen the bond, the aluminum core was scuffed with Scotch-Brite, blown clean of large particulate using a high-powered hair dryer, and wiped clean with acetone (see Appendix Q Part I for details). Note that compressed air from a shop compressor may contain moisture and oil and should not be used to clean aluminum core. The scuffing method was brought to the FMD's attention via a team member's internship at a major composites manufacturer. From short beam testing conducted by FMD, it was shown that scuffing increased interlaminar shear strength by 7.4%.

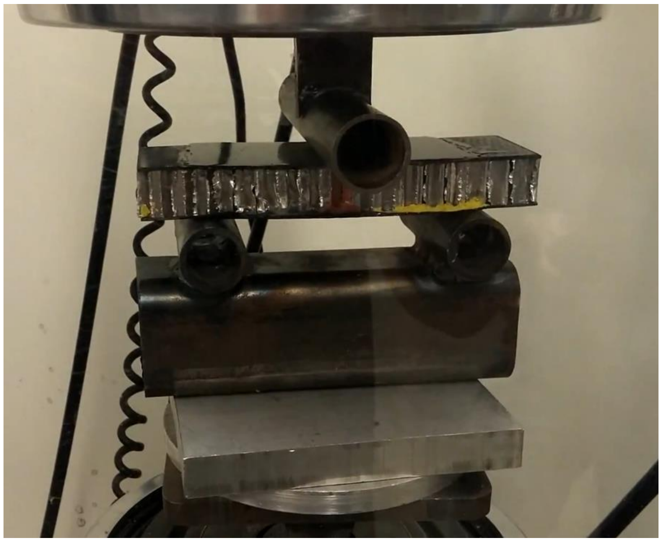

Figure 26. Short-beam shear test.

Table 14. Short beam shear test results verifying the viability of omitting film adhesive.

	Shear Stress (PSI)	Failure Mode
with Film Adhesive	107.49	Core shear failure
without Film Adhesive	95.15	Core shear failure
% Difference	11.48%	

Resin Integrity

The first step in validating our laminate was to verify the integrity of the prepreg resin. Considering that the majority of the donated prepreg received is more than a year old (expired by aerospace standards), checking resin properties was essential to building safe parts that do not delaminate unexpectedly. Prepreg resin typically retains its properties for multiple years, assuming proper storage.

To assess resin strength, the ASTM D2344 short beam shear test was utilized to isolate ILSS. These tests were conducted for all available prepreg types, as shown in Table 15. Testing details and formulas can be found in Appendix E.

Table 15. ILSS test results.

Fiber	**Resin**	**No. of Samples**	**Avg. Failure Load (lbs)**	**Avg. Tested ILSS (ksi)**	**Manufacturer Spec ILSS (ksi)**	**% Difference**
M55J uni	MTM 49	10	286.487	8.529	16.80	-49.2%
AS4 cloth	TC250	5	294.952	7.535	8.59	-12.3%
M46J	TC250	9	442.273	10.028	8.59	+16.7%

As the testing shows, the ILSS of the AS4 and M46J prepreg resins were similar to the manufacturer's specifications. The ILSS of the M55J prepreg proved to be very low compared to the manufacturer's specifications. Upon consulting Dr. Mello, it was determined that the manufacturer's specification was optimistic, and was indicative of perfect manufacturing and testing processes. Dr. Mello felt that the ILSS numbers were sufficient, and that the resins in FMD's prepregs were still good.

Laminate development

After verifying the integrity of the core bonding and the strength of the resin, FMD proceeded to develop the laminates to satisfy the SAE testing standards. These tests include the long beam 3-point bend, perimeter shear, and off-axis pullout tests.

The 3-point bend test (Figure 27) entails a composite beam loaded in bending along its midspan. The resulting load-deflection curve and failure load is then used to extrapolate the skin's bending strength and stiffness. The support span is significant enough that direct shear can be neglected, thus isolating the effect of the bending moment in the skins. Panels tested in this manner will experience skin compressive failure in the upper face-sheet.

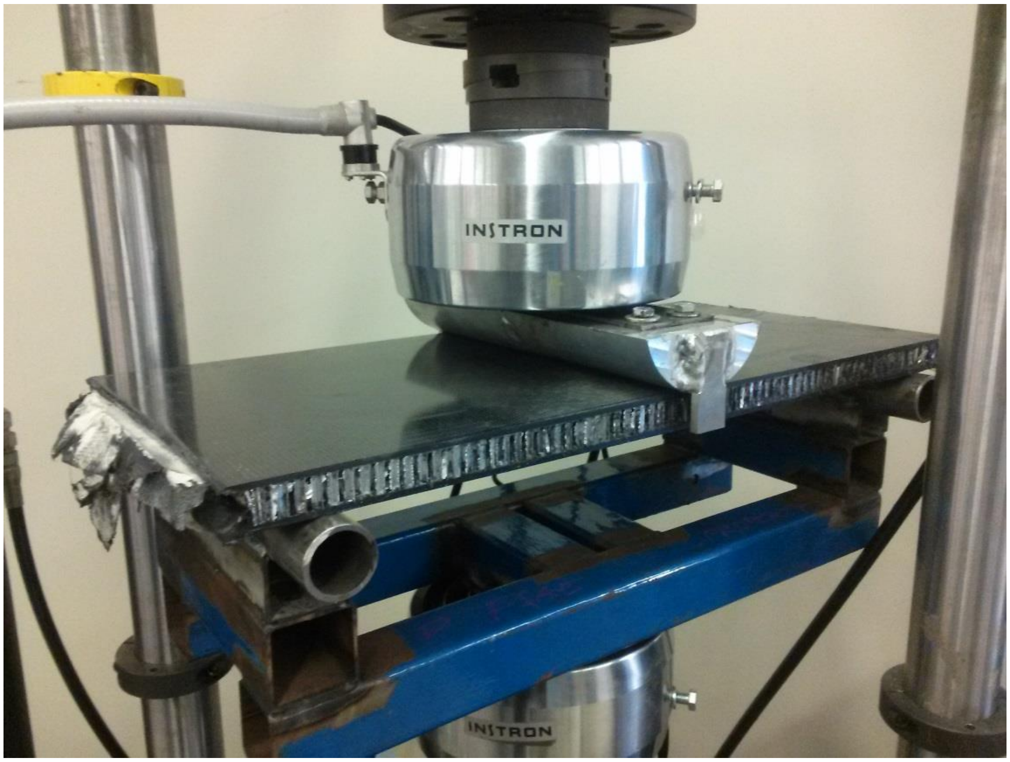

Figure 27. Long beam bend test. Safety tabs were welded onto both sides of the 4-inch diameter impactor to prevent specimens from sliding off the fixture.

One of the most critical SAE regulated regions, the side impact laminate, is required to have an energy absorption that is greater than or equal to that of two 1010 steel tubes (1"OD x 0.065 wall thickness). In order to establish a baseline for comparison, two of these tubes were tested in a long beam 3-point bend fixture (Figure 28) to a final displacement of 1". The force-displacement curve was then integrated to find energy absorption. The force-displacement long beam results from the side impact laminate results were also integrated, and the energy absorption values were compared. The comparative results (Table 16) showed that the side impact structure (SIS) laminate passed the SAE requirements by exceeding the steel tube energy absorption standard. This test was repeated until all SAE regulated region requirements were met.

Table 16. Energy absorption results for the SIS laminate and steel tube baseline

	Energy Absorption (J)
SIS laminate	66.5
Two 1010 steel tubes	40.9

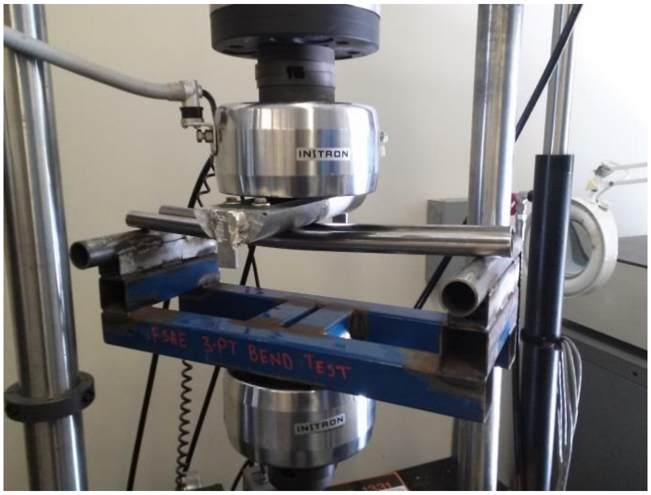

Figure 28. Long beam test of two 1010 steel tubes to establish an energy absorption standard for the side impact structure laminate.

The perimeter shear test (Figure 29) involves lowering a cylindrical impactor into a composite plate until the impactor punches through both skins. The plate support is configured so that the panel is stressed in direct shear. The failure load data is then used to determine the perimeter shear (shear load per inch) of the laminate for sizing the perimeter of brackets.

Figure 29. Perimeter shear test setup

Lastly, the off-axis pullout test (Figure 30) involves securing a panel in an angled jig that imitates a harness bracket undergoing an out-of-plane load at a specific angle. The panel is secured with tabs and fasteners, and is pulled in tension till the skins fail. Data from this test is used to determine whether the tub can sustain the load through the driver restraint harnesses in the case of impact. This test applies to regions of the tub where harness brackets are mounted. In this case, the performance of the cockpit floor laminate was validated using this test.

Figure 30. Off-axis pullout test.

In the early design phase, FMD developed a laminate in FEA to satisfy the Alternative Frame loadings. Considering the undeveloped nature of the FE model, the laminate was overbuilt in order to compensate for issues with proper constraints and element selection. To satisfy the SES requirements, testing began with the overbuilt AFR laminates, which were downsized as necessary. The laminates of each tub region were iterated over the course of two weeks in accordance to their applicable tests, until the layup schedule was finalized (Table 17, Figure 31, and Appendix X). This layup schedule presented resulted in a theoretical torsional stiffness of 1679 ft-lb/deg.

Table 17. Monocoque regions and their respective layups and SAE tests. Materials used are: AS4 cloth and M55J uni.

Tub Region	Layup Schedule	Applicable SAE Tests
Side Impact (vertical sidewall)	$[45c/0c/45/-45/0c/\bar{c}]_s$	• 3-point bend • Perimeter Shear
Front Bulkhead Support	$[45c/0c/\bar{c}]_s$	• 3-point bend
Front Roll Hoop Support	$[45c/0c/\bar{c}]_s$	• 3-point bend • Perimeter Shear
Cockpit Floor	$[45c/0c/\bar{c}]_s$	• 3-point bend • Off-axis pullout
Seat Back	$[45c/0c/\bar{c}]_s$	• N/A
Front Bulkhead	$[(45c/0c)_5/\bar{c}]_s$	• 3-point bend • Perimeter Shear

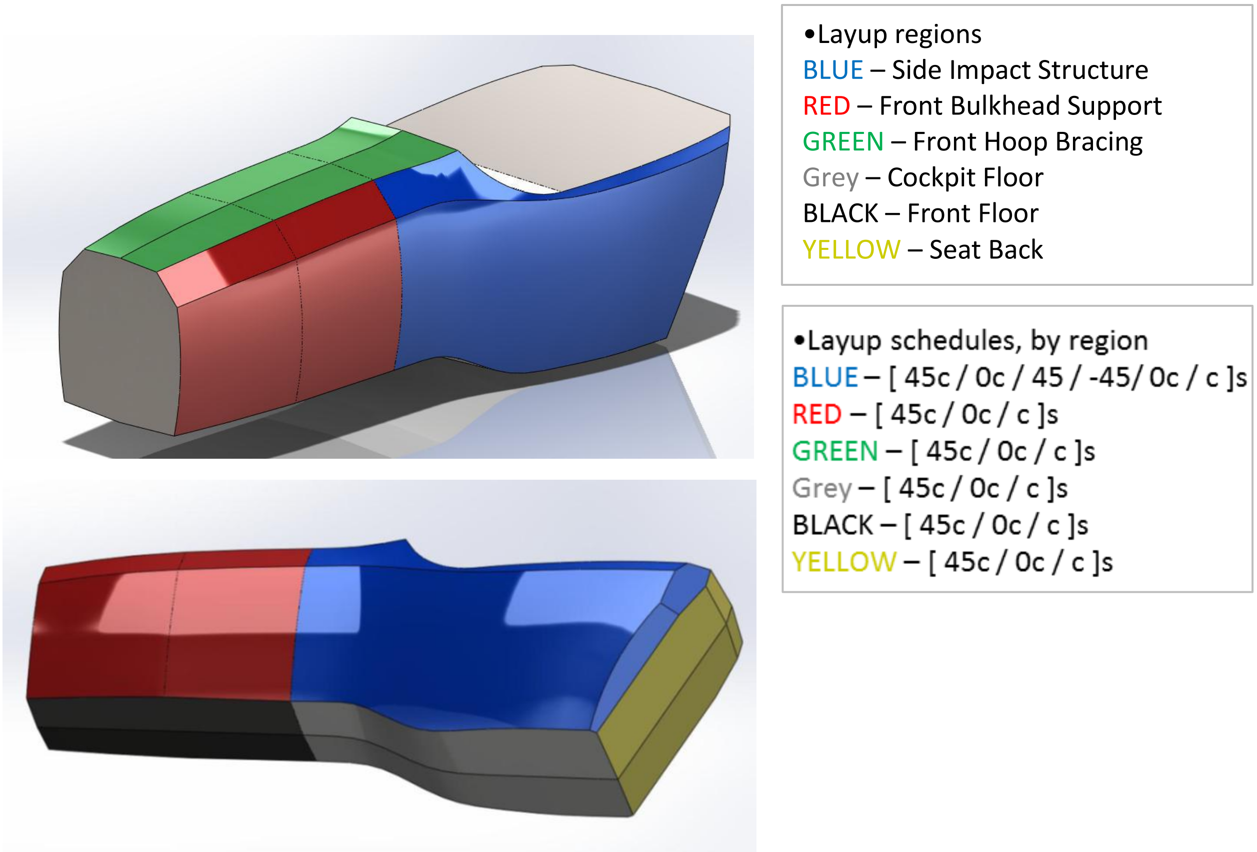

Figure 31. Layup schedule layout for each tub region.

Comparing AS4 and T800 cloth

The first round of laminates utilized AS4 cloth and M55J uni. Later laminates included the use of T800 cloth, but the results from these panels were underwhelming. Manufacturer data sheets showed that T800 fiber has superior strength, modulus, and failure strain values than AS4. Yet, long beams using AS4 cloth outperformed panels with T800 cloth, assuming the same layup schedule and uni selection. This situation enforces the importance of having a variety of prepreg types to test with, as the technically superior material may not always translate to better testing results.

A single ply of T800 cloth, however, is thinner than a single ply of AS4. In short, there are more fibers present in a single ply of AS4 cloth than in a ply of T800. Considering this, FMD predicted that increasing the T800 cloth ply count to more closely match the thickness (and thus fiber content) of a standard AS4 laminate would yield test results indicative of the mechanical superiority of T800 cloth. A single ply of T800 cloth weighs 0.00085 lb/in^2, compared to AS4's single ply weight of 0.00156 lb/in^2. Given these weights, FMD reasoned that two plies of T800 cloth would be equitable to one ply of AS4 in terms of fiber content. As shown in Table 18, long beam tests were conducted with several T800 cloth alternatives, and the results, again, showed that the AS4 panels performed better for the weight. Adding T800 plies in hopes of passing would have increased the area weight past that of a comparable AS4 panel that already passed.

Table 18. Test result comparison between T800 and AS4 cloths

Layup Schedule	Cloth Material	Uni Material	Area Weight (lb/in^2)	Failure Load (N)	Pass or Fail
[45c/0c/45/-45/0c/ $\bar{c}$]$_s$	T800	M55J	0.00796	5814	FAIL
	AS4	M55J	0.01222	11722	PASS
[45c/0c/0c/ $\bar{c}$]$_s$	T800	M55J	0.00636	4671	FAIL
[45c/0c/ $\bar{c}$]$_s$	AS4	M55J	0.0075	6093	PASS

It is believed that T800's poor testing performance is due to the nature of the 3-point bend test itself. Contrary to the FSAE standard 3-point bend test, composites industry leader Hexcel recommends a 4-point bend test. Compared to a 3-point test, the 4-point test distributes the load over two impactors (as opposed to one), thus decreasing the localized compressive load on the core and skin. Thus, a 4-point test is more suited to measuring the skin properties, because the localized compressive effects are spread more evenly between the two impactors. To this effect, it was observed that 3-point tests produced inconsistent failure modes, including skin failure, skin delamination, and core compressive failure. On the contrary, the few 4-point tests conducted produced very consistent skin compressive failure. Considering these points, there is reason to believe that the 3-point bend loading does a poor job of properly isolating the skin properties. Contrary to the 3-point tests, four-point tests show that T800 cloth produces superior skin strength and stiffness compared to AS4 panels of similar area weight, as detailed in Table 19.

Table 19. 4-point bend test results comparing AS4 cloth and T800 cloth. Both specimens utilized 1/8'' aluminum core.

	AS4 cloth, [0c/$\bar{c}$]$_s$	T800 cloth, [(0c)$_2$/$\bar{c}$]$_s$
Skin Strength (psi)	29437.04	39407.75
Skin Modulus (psi)	58.93	66.41
Skin area weight (lb/in^2)	0.00156	0.0017

The final laminates met the SAE 3-point bend and perimeter shear requirements as closely as possible while fulfilling the loading conditions in the CLT code. Due to the superior shear strength of the aluminum core, the perimeter shear requirements were very easily met. Load-deflection curves for several laminate tests can be referenced in Appendix F.

With nearly 120 panels tested, it became apparent how time consuming laminate design and testing is. Thankfully, a dedicated composites team diligently manufactured three to four panels a day for the iteration process.

Pressure Cure

During the laminate testing, Swift Engineering notified the team that their autoclave would be available for a pressure cure. The original plan was to cure the monocoque in the ME department oven with vacuum pressure (out-of-autoclave). Pressure cures involve pressurizing the environment around the composite part during the cure, thus exerting additional force evenly on the bagged part. The added pressure improves laminate compaction, thus decreasing void content and in turn increasing part strength and stiffness. Pressure-cured laminates also experience less core-bridging and better surface finish than out-of-autoclave parts.

In order to validate any potential strength and stiffness gains from a pressure cure, long beam bend performance was compared between two panels of equal layup – one cured at 30 PSI and the other cured with vacuum only.

Both panels were tested, and the panel that was cured without vacuum achieved a failure load of 1607 pounds, whereas the panel cured at 30 psi failed at only 1063 pounds. Considering these unexpected results, it was unclear whether this large gap in performance was due to the faults of the pressure or a manufacturing error. Before investigating further, it was determined that moving the molds and materials to Swift Engineering and performing the layup there would be a logistical hindrance that had the potential to severely impact the team's timeline. The possibility of a pressure cure was dropped in light of the test data and scheduling demands.

Post-cure

The issue of laminate operating temperature becomes an issue when the tub is in close proximity to hot exhaust runners or exposed to long periods of sun. To investigate the effects of heat, temperature stickers (260°F max readable temperature) were placed on various parts of the tub. During prolonged testing, the 2013 tub reached a top surface temperature of over 260°F near the exhaust tubing, even with the addition of heat-shielding foil. The effects of exhaust heat put the resin fairly close to its glass transition temperature (T_g) of 275°F, thus risking a compromise in laminate strength.

A post-cure involves re-curing a part at an elevated temperature to further increase the resin's T_g. Post-curing the TC250 resin involves completing an initial cure at 275°F, then curing the panel again at 350°F. The post-cure increases the T_g from 284°F to 347°F, thus making the tub temperature safe to surface temperatures well above what was measured on the 2013 tub.

In order to test whether a post-cure would introduce problems like warpage and laminate discoloration, FMD post-cured a sandwich panel at 350$^{\circ F}$. The panel came out of the oven as flat as it was before the post-cure, with a slightly dull orange sheen. Since the panel experienced no warpage, it was decided that the final monocoque layup would undergo a post-cure.

Strap Joint

The initial plan to bond the two cured monocoque halves was to apply high temperature resin and microballoons to the exposed core where each half meets, then lay up a carbon prepreg strip over the joint on both the inside and outside of the tub. The resin and microballoon slurry was mixed to a peanut butter consistency.

Applying stress analysis to the carbon joint would have proved difficult without a very robust FE model, so a short beam sandwich bend test was conducted to determine the minimal width of the carbon strip. The biggest concern involved the delamination of the prepreg strip from the surrounding laminate due to inadequate bond area or poor resin adhesion to pre-cured surfaces.

To test the bond strength, two short beam sandwich panels with prepreg strap joint widths of three inches and four inches were laid up (Figure 32).

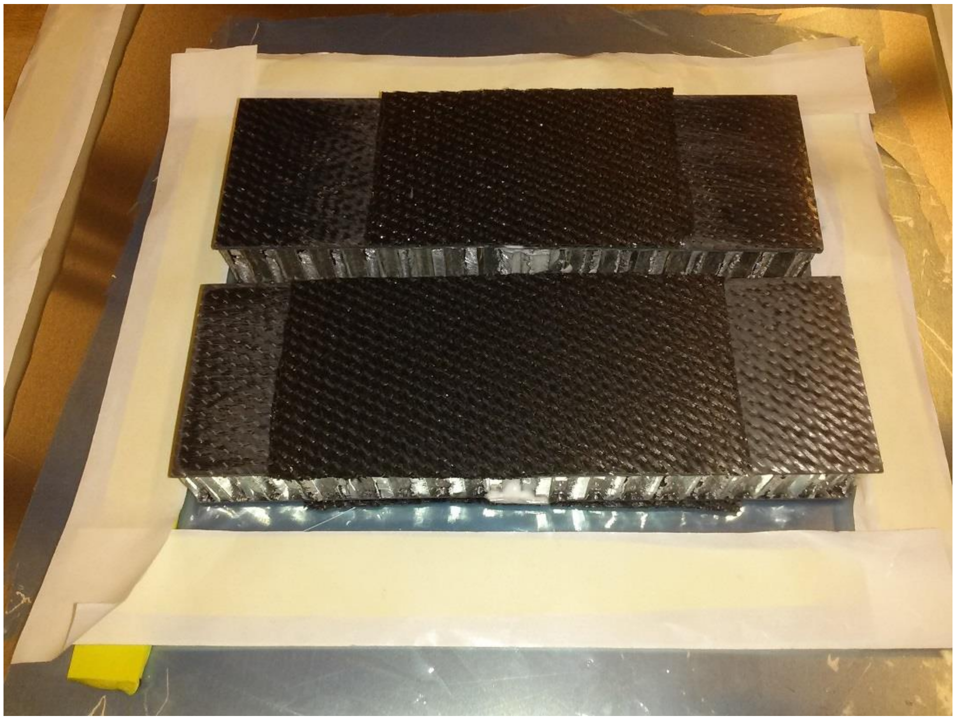

Figure 32. Short beam shear test panels for strap joint width design

For each panel, the two halves were bonded together with Fiberglast 3000 resin and 3120 hardener, held together with c-clamps, and cured at room temperature. Once the adhesive had cured, a prepreg strip of AS4 cloth was laid up on each side of the panel, with schedule [45c/0c]. This layup schedule was chosen so that torsional shear loading on the chassis could be most effectively transferred between the tub halves. In the case of simplified tube in torsion, the principal loading is ±45 degrees relative to the axis of the tub, so running fibers in that orientation would be most efficient. The 0-direction ply was included so that the strap joint replicated the surrounding monocoque laminate.

Short beam test results (Table 20) show that three inch and four inch joints provide roughly the same bond strength. For both panels, the core along the periphery of the strip failed in compression (Figure 33). This failure mode indicates that the joint reinforcement is stronger than the surrounding laminate in core shear. No delamination occurred in either of the specimens. In light of the results, it was concluded that a three inch strap joint would perform just as well as a four inch joint. To save weight, FMD chose to apply a three inch strap joint on the chassis. Considering the similar performance of the two panels, it would have been prudent to investigate the viability of a smaller width joint. However, the manufacturing scheduling did not allow for this development.

Table 20. Testing results comparing prepreg strap joint widths

Prepreg Joint Width (in)	Failure Load (lb)	Shear Strength (psi)
3	698.7	257.3
4	723.1	266.3

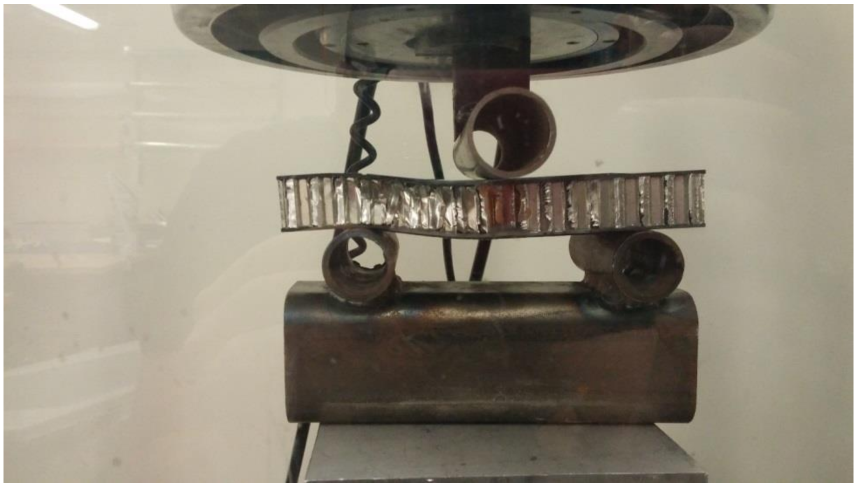

Figure 33. Core-shear failure on the periphery of the prepreg joint. Upon close examination, no delamination occurred in the panel.

Blob layups

Unlike Nomex, aluminum core is significantly more difficult to form to complex contours without bridging. In order to test the viability of using aluminum core in the tub molds, FMD laid up and cured several test layups (blob layups) in different regions of the mold. The team initially laid up on fairly flat surfaces, and then proceeded to layup on areas of simple and complex curvature (Figure 34).

Figure 34. Sample blob layup in a region of the tub mold with complex curvature.

Various core-splicing techniques were investigated in an attempt to mitigate bridging. For several blob specimens, the core was slit with a razor (halfway through core thickness) along the line of the desired bend so that the core cells would more easily fold into each other. In another experiment, a rotary tool was used to cut a slot along the bend line to make the honeycomb more pliable (see Figure 35). Specimens with slit core showed no bridging at the bends, whereas parts with slots along the bends showed a triangular gap in the core where the bent core bridged over itself. Core bridging was evidenced by local face-sheet resin dryness, suggesting that the face-sheets unsupported by core are subject to exaggerated resin flow. Regions with no bridging displayed shiny and smooth surface finishes with satisfactory resin content. Additionally, it was found that core splices needed to be spaced about three inches from any bend to avoid bridging.

Figure 35. Core bending results from an area of simple curvature

No loaded tests were conducted to assess the viability of laminates with bridging or low facesheet resin content; however they are advised and suggestions for how to do so are included in the Conclusions and Recommendations section.

Final Design Details

Layout and Design

Formula Monocoque Development is in charge of four unique components on the 2015 Cal Poly Formula SAE car: the monocoque, nosecone, anti-intrusion plate, and firewall. See Appendix G for an assembly drawing.

Monocoque

After the design phase, it was determined that the monocoque would be composed of TC250 AS4 8HS prepreg cloth, MTM49 M55J uni, and 0.7" thick 3.1 lb/ft^3 3/16" cell size 5052 aluminum honeycomb core, with a theoretical torsional stiffness of 1679 ft-lb/deg. Suspension and pedal-box mounting points would be reinforced with end grain balsa. Core splices would be positioned at least three inches from any radius or bend. Additionally, film adhesive would be omitted from the layup, except where joining core at splices. See Figure 36 for a solid model of the monocoque.

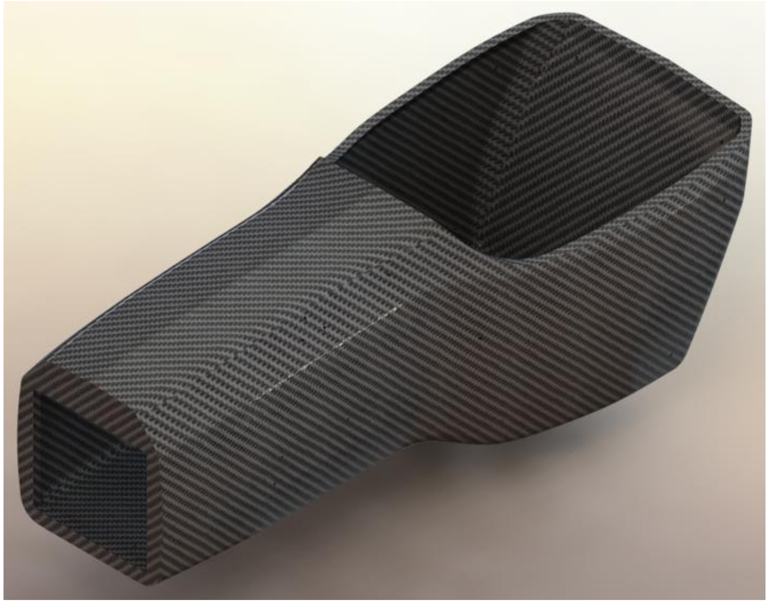

Figure 36. Isometric view of carbon fiber monocoque.

Nosecone

The nosecone would be a carbon fiber skin that mounts to the front of the monocoque. The nosecone serves as the car's impact attenuator while concurrently providing mounting for the front wing. Because it serves as the impact attenuator, it must comply with SAE rules. The SAE energy absorption standards state that the impact attenuator must absorb 7350 Jules of energy while not exceeding a 40 g peak deceleration or a 20 g average deceleration. This would be accomplished with a layup schedule of $[45_C/90/0_2/90/0_2/\overline{90}]_S$. CLT was used to verify that the layup was strong enough to support the front wing loads. The nosecone would mount to the front bulkhead by slipping over 4 studs installed in the monocoque. See Figure 37 for a solid model of the nosecone.

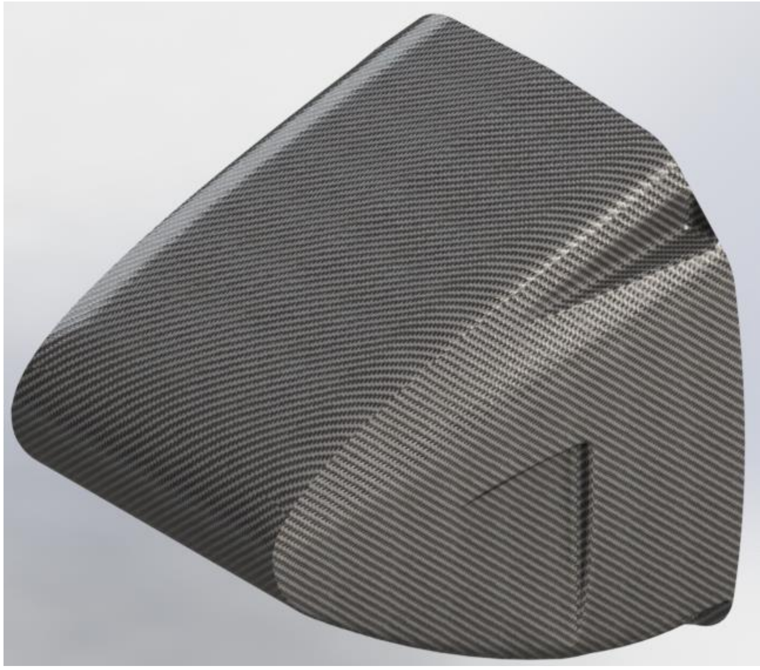

Figure 37. Isometric view of carbon fiber nosecone

Anti-Intrusion Plate

The anti-intrusion (AI) plate would be a flat composite plate composed of AS4 cloth, M55J uni, and 0.7” aluminum core. It would be mounted to the front bulkhead by being slipped onto the nosecone studs and being sandwiched between the nosecone and front bulkhead. It would be cut to the shape of the front bulkhead, so when mounted to the front of the monocoque the plate’s perimeter is flush with curvature of the tub. The AI plate would be mounted by slipping over 4 studs installed in the front bulkhead of the monocoque. The purpose of the anti-intrusion plate is to prevent foreign objects from entering through the front of the monocoque and injuring the driver. SAE mandates that the bending and shear properties of the AI plate laminate be comparable to a 0.063” mild steel plate. After a battery of laminate tests, a laminate of $[(45c/0c)_2/45/\text{-}45/0c/\overline{c}]_s$ was selected.

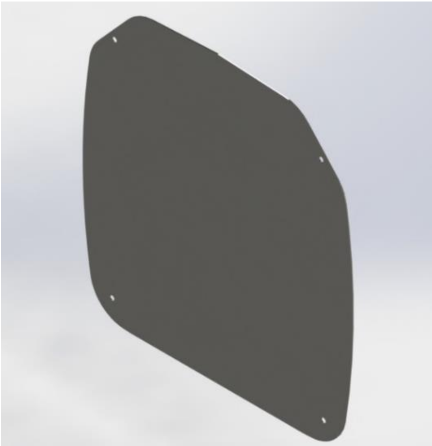

Figure 38. Isometric view of anti-intrusion plate.

Firewall

A firewall is required as per Formula SAE rule T4.5, which states, in part, that the cockpit must be sealed from fluid discharges and fire by a non-permeable, rigid, flame-resistant material. Rule T4.3.2 also requires that the driver compartment be shielded to an unspecified degree from convection, conduction, and radiation heat transfer. The FMD team would implement two provisions to meet these requirements. First, a shield that protects the driver's head and neck would be attached near the engine region. Second, a carbon sandwich structure would provide heat insulation behind the driver's torso, while the face sheet provides protection from flame due to carbon fiber's inherent fire-resistive qualities. Convective and radiative heat transfer would be prevented by the solid panel. Conduction would be limited by a 1" air gap between hot coolant lines, engine components and the seatback of the monocoque. Reflective Aerolite tape manufactured by Coast Fabrication (see Figure H4 in Appendix H for data sheet) would be bonded to the rear of the driver's cell addresses radiation and is 2.3 times lighter than the standard gold foil. See Figure 39 for a solid model of the firewall.

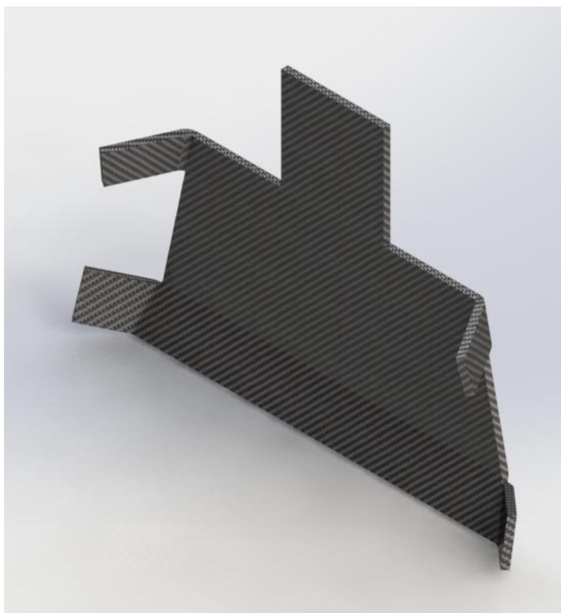

Figure 39. Isometric solid model view of firewall.

The firewall was designed to be laid up as a flat panel, cut in predetermined locations, folded using a jig to fit the chassis roll hoop geometry, and bonded into shape while in the jig. This method of construction is termed "cut-and-fold." Brackets welded to the steel rear subframe hold the firewall in place via AN3 bolts, all-metal locknuts, and fender washers to transmit the loads to the fiber. Inserts were not designed into the firewall, though they should have been in order to carry the clamping load of the bolts and distribute shear bearing forces over a larger area. The firewall was designed using a layup schedule of $[0c/45c/\underline{core}]_s$ where the 0° direction is the vertical. Prepreg Toray 2510-T800 was selected for the cloth and 3/8 inch thick, 3/16 inch cell $1.8 lb/ft^3$ Nomex was used selected for the core. Wet layup was selected for bonding the folded firewall into place. Two plies of 2x2 twill, 3K, 199GSM fabric from Soller Composites was chosen due to its high strength and strong past performance. Strips were chosen to be 2 inches wide and placed only on the side of the "cut" in the 0°/90° direction. West Systems 105 resin and

207 hardener were selected for the fabric. Unaccounted for in the initial design was the forward position that the driver's head would be placed in when the required padding was installed on the firewall. The final solution arrived at was to cut the upper portion of the firewall (the headrest), move it rearward using a piece of aluminum angle, and secure the headrest from rearward motion via two 5/16" OD 4130 steel rods.

Geometry Layout

The geometry of the monocoque was designed to accommodate the driver, as well as the components attached. To accommodate the driver, it had to meet SAE rules as well as the team's ergonomic requirements. One of the SAE rules requirements for the driver's cell is that it must be large enough to fit a template of given geometry through it (SAE Rule section T3.10, see Appendix I). This ensures that the driver will have sufficient room inside while driving the car. It also ensures that in the event of a rollover, the drivers head will be protected by the main and front roll hoops. Because the rules requirements were the same when the geometry was designed in 2013, using the same tub molds along with the same core thickness ensured that the monocoque would meet template.

Other considerations taken into account when designing the monocoque geometry were mounting. Components like the suspension, subframe, and pedal box all played a role. This is evident by the flat regions where most of these components mount. Another consideration was torsional stiffness. Shaping the monocoque like a tube is an efficient way to be torsionally stiff. Again, all of these considerations were the same in 2013, so using the same geometry ensured that all of these considerations would be met.

Laminate Design and Selection

The laminate used in the monocoque was chosen for reasons very similar to that of the geometry. Torsional stiffness, localized strength, and SAE rules requirements all influenced the design (Figure 23 on page 52). To satisfy SAE rules, potential laminates were laid up as flat panels and tested for strength and stiffness properties (description of testing procedures starts on page 58). A FEM of the chassis and suspension was used to analyze torsional stiffness of these different laminates used in different regions (description of finite element analysis starts on page 47). For example, it was shown that adding plies at ±45° at the side impact structure increased specific torsional stiffness more than adding ±45° plies elsewhere (see discussion on page 54). The FEM also showed that using stiffer aluminum honeycomb core increased specific torsional stiffness much more than adding plies of carbon fiber (Figure 22 on page 50). The final consideration was localized loading, mainly at suspension pickup points and pedal box mounting points. CLT was used to analyze failure indices and determine if the laminate selected would be strong enough (CLT discussion begins on page 50). In the end, a laminate was selected that met all of these criteria, and can be found on Table 17 on page 61.

Fastening Methods

All accessory components fastened to the monocoque utilize potted aluminum inserts. The aluminum inserts carry the clamping load of the bolt on the sandwich structure. Inserts also provide a larger bearing-stress area for in plane load transfer to the carbon facesheets. Backing plates on both facesheets where bolted joints are present help to carry out of plane loadings by transferring the load into the direction of the fiber. 3M DP420 structural adhesive (see Figure H5 in Appendix H for specification sheet) permanently anchors the insert within the monocoque. Due to the short lifecycle of the vehicle, aluminum-carbon galvanic corrosion is not a significant concern.

CLT Analysis Results

As previously explained starting on page 50, an automated CLT script was used to analyze the strength of the monocoque under numerous loading conditions seen during normal driving (review Table 11 on page 51). From this script, the failure loads for the final laminate were determined, and are summarized below in Table 21. This analysis step was part of the laminate iteration phase (review Figure 23).

Table 21. CLT analysis results for failure load of final laminate design.

	Seat Back	Upper Suspension	Lower Suspension	Pedal Box	Driver Egress	ARB
Failure Load [lb]:	12300	3650	7000	750	2080	2500
Safety Factor:	1.8	7.3	5.8	1.7	4.2	8.3

The minimum safety factor occurs at the pedal box, with a failure load of 750 pounds, concentrated at the base of the pedal-box. It is highly unlikely that the driver would be able to exert this amount of force on the pedal, so the likelihood of failure in this region is not a primary concern. Additionally, the safety factor of 1.8 on the seatback is under the assumed case of impact deceleration, so failure in this region is unlikely unless a crash occurs.

Cost Breakdown

As part of the SAE competition, the Formula team submits an itemized cost report that accounts for every component on the car. In order to reflect a mass-produced car, SAE provides hypothetical raw material, manufacturing, and assembly costs. Regardless of how the chassis is made, teams are free to creatively combine and simplify the manufacturing processes to lower the hypothetical cost. The items included in the cost report are comprehensive, including parts like roll hoop fasteners, inserts, carbon prepreg, and core, as well as manufacturing processes like cutting carbon, bonding inserts, and curing. In an effort to reduce costs, many processes were simplified. For example, the cost to physically cut each ply of carbon out of a roll is incredibly expensive since the length of cut is an itemized cost. To simplify the process, the claim was made that all similarly-shaped carbon plies were stacked and waterjet cut in one operation. Once all processes were streamlined, a hypothetical tub cost of $2927.38 was achieved. The cost breakdown (Table 22) details how the costs were distributed between materials, processes, fasteners, and tooling.

Table 22. Monocoque cost report breakdown.

Materials	Processes	Fasteners	Tooling	Total
$2017.50	$705.41	$2.80	$201.67	$2927.38

Although the results of the cost report are theoretical at best, it does provide some insight into the costs associated with mass production. Tooling costs are low, because it was claimed that the plaster molds could accommodate 10 cure cycles. This claim is untested in the context of the molds utilized but it is a realistic assumption for similar molds in a mass-production setting.

Safety Considerations

As with most manufacturing processes, working with carbon fiber entails its own safety considerations. Cutting and grinding cured carbon requires a respirator or dust mask to prevent inhalation of carbon dust. In order to prevent carbon dust from imbedding itself in clothing or skin, gloves and paper coveralls are recommended personal protective equipment.

Safety precautions also must be taken when conducting destructive laminate testing. Users must ensure that the testing machine is configured so that specimens do not slip off their fixtures at any point during the test. Test machine feed rates should be monitored so as to avoid crashing the machine. Unlike metals, carbon fiber parts fail catastrophically, ejecting carbon splinters in unpredictable directions. Although testing did not produce airborne debris, a Plexiglas shield was placed between the specimen and the user to avoid any potential safety risks.

Maintenance and Repair Considerations

Once completed, the tub requires very little maintenance under normal driving conditions. In the case of local failure, the failed section of the tub can be cut out and replaced with a post bond layup. In the case of a global failure, the best route would be to manufacture a new monocoque.

Four studs were installed longitudinally in the front bulkhead to allow mounting of the nosecone and AI plate. This means that both components will be removable, so if either gets damaged, they can easily be replaced. The removability of the AI plate and front bulkhead to reveal the front bulkhead cutout also promotes ease of maintenance for components inside the monocoque. A second nosecone was manufactured so if the one on the car gets damaged at competition, there will be a backup one available for replacement.

Product Realization

Flat Panels

In order to determine laminate properties, FMD manufactured flat panels. The use of a flat panel allowed for applying mechanics of materials to test data in order to calculate different strengths and stiffnesses. This is extremely valuable because composite parts are highly dependent on manufacturing methods. Being able to measure actual strengths and stiffnesses as opposed to theoretical values proved to be very important.

All flat panels were manufactured in the same general manner. An aluminum caul plate with dimensions that were slightly larger than that of the final part was selected. Then carbon and core (if necessary) were cut using the caul plate as a template. If the carbon did not have backing material on both sides and the plate had to be set directly on the carbon, it was thoroughly cleaned first. The carbon and core was then laid up on top of an aluminum tool with a sheet of Airtech PTFE-coated fiberglass slightly larger than the part. Note that while the caul plate doesn't need to be very thick, having a thicker tool greatly reduces the possibility of warping during curing. Finally, Teflon, the caul plate, and then breather cloth were placed on top of the carbon and the part was vacuum bagged. Panels were cured in the ME composites lab autoclave. Additional detailed methods and standard operating procedures (including a layup diagram and dimensions) for panel manufacturing can be found in Appendix Q.

When laying up composite parts, inconsistencies tend to occur close to the part edges. Therefore, it is recommended to lay up extra and trim to size after cure. Long beam panels, for example, needed to be 11 inches wide as per the SES. 12 inch wide panels were laid up, and a half inch of material was cut off of each side using the tile saw in the Bonderson machine shop (see Figure 41).

Figure 40. Test panel being cut on the tile saw.

Tub Layup

Layup Preparation

Once layup development and blob testing were completed, the tub layup was given the go-ahead. The layup was completed over a 3 day weekend in January in order to allow the team members to focus solely on the layup. The layup began Saturday morning with preparing the molds and creating templates. Mold preparation included cleaning, affixing the nylon stripping for the joint joggle, and applying release agent.

Cleaning was done by first vacuuming lose debris and dust from the molds using a shop-vacuum with the operator’s hand covering the hard plastic nozzle to prevent marring the mold surface. It should be noted that to prevent this type of contamination in the future, the molds were sealed with vacuum bag and sealant tape around the outside edge of the flange when placed in storage following the 2015 production period. Next acetone was applied to WypAll brand disposable towels and all gel-coated surfaces were lightly-scrubbed until no residue appeared on the towels.

Nylon stripping was applied to the mold surface next to act a joggle for the strap joint that was utilized post-cure to bond the two monocoque halves (Figure 41). The same high-temperature nylon and double-sided fiberglass tape was used as in 2013. Since the nylon strip resists in-plane bending, curves in the joggle, such as those around the cockpit, were accomplished by placing small, wedge-shaped pieces along the path of curvature. Once the nylon was in place, the release agent could be applied to the mold surface.

Coating the mold with release agent is vital in preserving the molds upon pulling the part and to the part quality. Loctite Frekote 770-NC was selected for the release agent as it was used successfully in 2013 and was available via donation from C&D Zodiac. To ensure proper application, the manufacturer’s technical datasheet was consulted. This process involved applying 5 coats with10 minutes between applications using WypAll towels. 30 minutes is required before applying the first layer of carbon-fiber. Frekote produces noxious airborne vapors and was applied wearing gloves and half-face respirators; and with both composites lab doors open. Since the doors have alarms that are triggered if left ajar, this required the Mechanical Engineering technician to come in on the weekend (when the coating was performed). See Appendix R for standard operating procedures on mold cleaning and release agent application.

Note that in order to save a large amount of development time and manufacturing time, the molds from 2013 were used.

Figure 41. Tub mold with nylon strap. Note that the nylon strap is applied right inside the scribe line, so the recess would be along the edge of the tub when joined. Release agent was applied after the nylon stripping was added.

Laying Up the Carbon

In order to cut and lay down plies of carbon consistently, templates were made before the tub molds were cleaned. Paper templates were initially made. Since paper doesn't drape like the carbon prepreg that would be used on the final part, the team decided fashion templates out of scrap prepreg. Slits were cut in the templates to allow them to lie flat in the molds. Regions of the monocoque defined by SAE rules (i.e. front bulkhead, side impact structure) were accounted for by shaping the template to cover the entire governed region. This ensured that the correct layup schedule would be applied to the region. The templates were cut so at least 1" of overlap would be present at each junction.

The AS4 prepreg was cut with a razor blade by placing the template on the carbon, then tracing the template with the blade. Slits in the templates were replicated on the ply. This was another big advantage of using templates, because cutting prepreg on a table is easier and more precise than cutting in the air. Each section was cut twice, with the template flipped over so a ply was cut for each tub half. Flipping the template was necessary because the AS4 cloth is a satin weave, which means that it is not symmetric about itself (meaning if the template was not flipped, a supposed 0° ply would actually be a 90°, and a 45° would be a -45°). Before each ply was laid down, the orientation was checked by at least one team member who understood the dual directionality of the satin weave.

Once a ply had been correctly assigned to a tub half, it was laid down. This was done by placing the ply inside the tub mold and lining it up. A small part of the ply was lifted up, and the poly (prepreg backing material) was removed. The bare carbon was then laid down for that small section, and the poly was progressively removed as the ply was pressed into the mold. This process was often done with 2, 3, or 4 team members working on one ply at once. Once the ply was completely laid down, the top layer of poly was removed. During the carbon layup process, all team members wore rubber gloves. See Figure 42 for team members working on laying down plies. At intermediate steps along the way, each tub was vacuum bagged and vacuum pressure was applied in order to compact the carbon against the mold (this process is called a debulk). Debulks were performed twice per face-sheet (both inner and outer), and once more after the core had been laid down.

Figure 42. The team hard at work laying down plies on the tub molds. Note that multiple people are working on a single ply.

Laying Up the Core

During the blob layups, by far the largest problem was getting desirable results with the aluminum core. Progress had been made and lessons had been learned from the blob layups, but a solid method that eliminated all problems had not been fully realized. Flat sections were easy, and sections that were slightly contoured didn't prove to be difficult. Difficulties were encountered when splicing core, particularly near radii. To make sure carbon didn't get sucked between two sections of core at a splice, extra core was cut and compressed into any cavities present. The compressed core was then re-expanded with picks to fill in any remaining gaps (Figure 43). To place the core over radii, the core was slowly bent into shape before being put into place. This took practice, patience, and time. Note that templates were used for cutting core. These templates were different than the carbon templates because core splices were located away from radii.

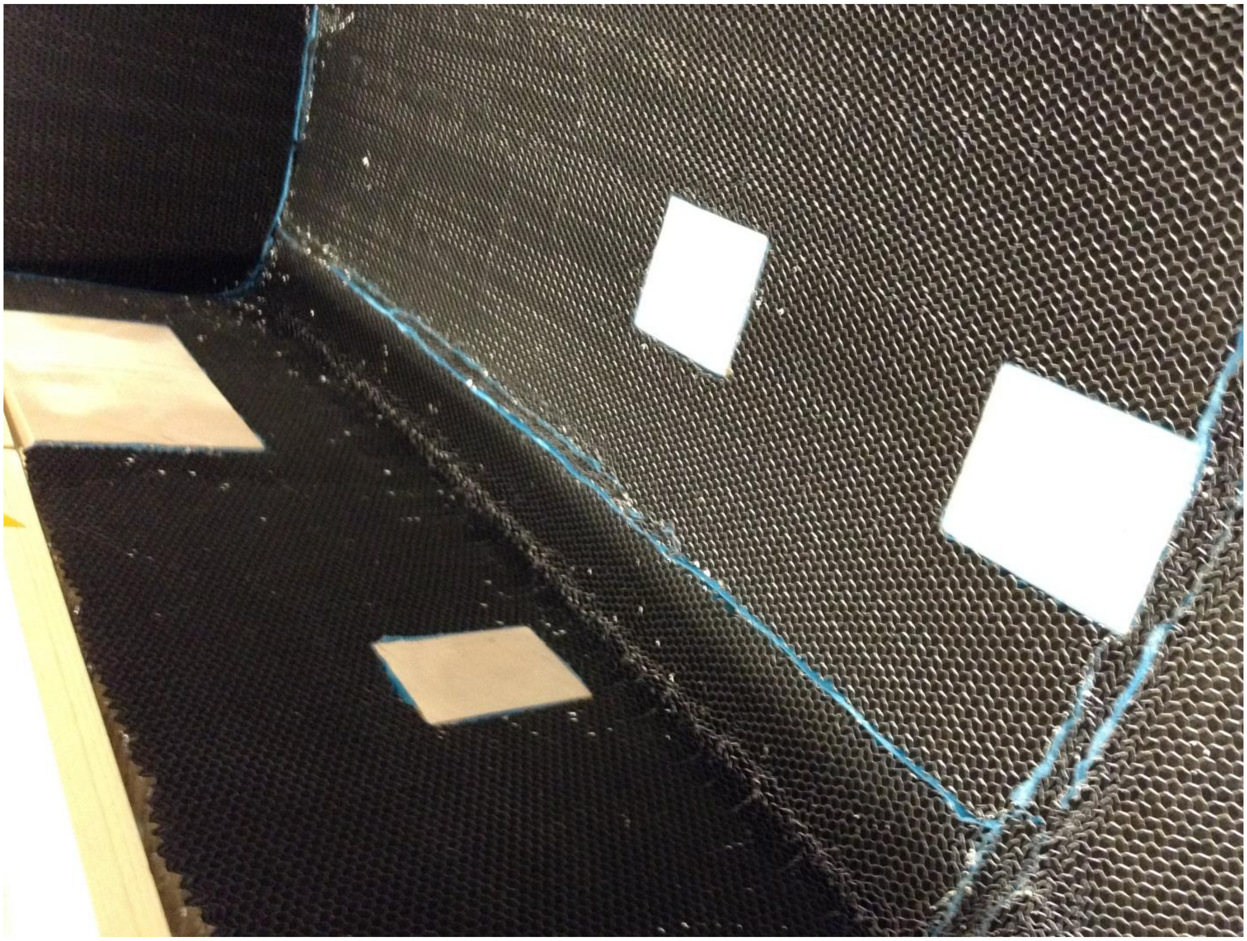

Figure 43. An example of how core splicing was taken care of. Note the placement of film adhesive between the core sections.

In order to avoid splicing core over contoured regions (including the entire SIS), it was decided to use one large piece of core to cover the entire SIS and the radii surrounding it, which included the compound radii of the bottom rear corner of the tub (Figure 44). Each piece was bent into shape by placing it in the mold and slowly working it by hand. This process took about 2.5 hours per tub half, but the end result was worth it. Due to diligence in core template design, no core splices were over contoured surfaces.

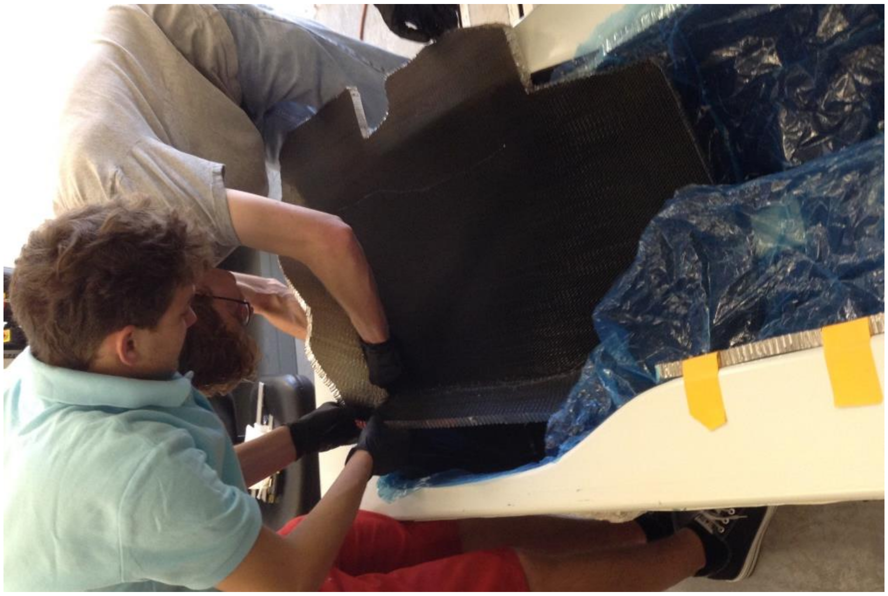

Figure 44. Large single core piece used in the SIS and surrounding radii.

Finally, balsa inserts were placed at suspension and pedal box mounting points. The balsa was sanded so it sat flush with the tub mold. To locate the balsa, suspension mounting points were marked on the tub molds by triangulating off the old suspension scribe marks (this was done before the layup began). When core templates were made, cutouts were made in the templates based off of these new marks. The aluminum core was cut out following the template profiles and replaced with balsa.

Cure and Post-cure

Once both tub halves were laid up, fluorinated ethylene propylene (FEP) was laid over the carbon. Breather was placed over the FEP, and the molds were bagged with high temperature vacuum bag. The team ensured that the bag did not bridge by incorporating pleats into the bag and by pressing the bag down in the areas prone to bridging (such as the corners) when first applying vacuum pressure. Bridging hinders vacuum pressure from being evenly distributed on the laminate, thus resulting in poor compaction and excess resin flow. Both of these scenarios result in a weakened or failed part.

Monocoque halves were cured in the Mechanical Engineering Composites Lab oven. Due to the large thermal mass of the molds, FMD knew that a high set point would be required in order to get the molds and part up to the desired 260°F. The set point on the oven was programmed to 325°F, which allowed the part to slowly get up to temperature. Oven air temperature is measured 1 foot above the upper flange of the mold surface at the side of the oven. During the cure, thermocouples were embedded in the facesheets in areas that were later cut off the final part. By placing thermocouples inside the part, it was possible to ensure adequate cure temperatures and soak durations. Two thermocouples were placed on the front bulkhead: one on the tool-side skin and one on the bag-side facesheet. Unfortunately, the bag-side thermocouple on the front bulkhead failed. However, an additional two thermocouples had been placed on the SIS—again one on the tool-side facesheet and one on the bag-side skin. The temperature deltas for the inside and the outside SIS facesheets are seen in Figure J2 in Appendix J and only varied by 5°F during the soak. The thermocouples were placed on the non-core side of the facesheets because the aluminum core's high thermal conductivity would result in similar temperatures for the two innermost layers. All thermocouples were labeled with Mylar tape ("flash tape") and their jack numbers recorded prior to starting the cure. Temperatures were recorded every 15 minutes in order to ensure that the parts were getting up to the temperatures that were required. Cool-down temperatures were a function of the thermal mass of the molds as the oven does not evacuate heat effectively and were not recorded. The exhaust and circulation fans were left on for an additional two hours after the cure's ramp-down commenced and one door was cracked 6 inches overnight to prevent thermal shock. According to C&D Zodiac, cracking induced from thermal shock is common if the tool is cooled too quickly. See Figure J1 in Appendix J for cure cycle data; and Figure 45 for a picture of the thermocouples and tub halves after being removed from the molds.

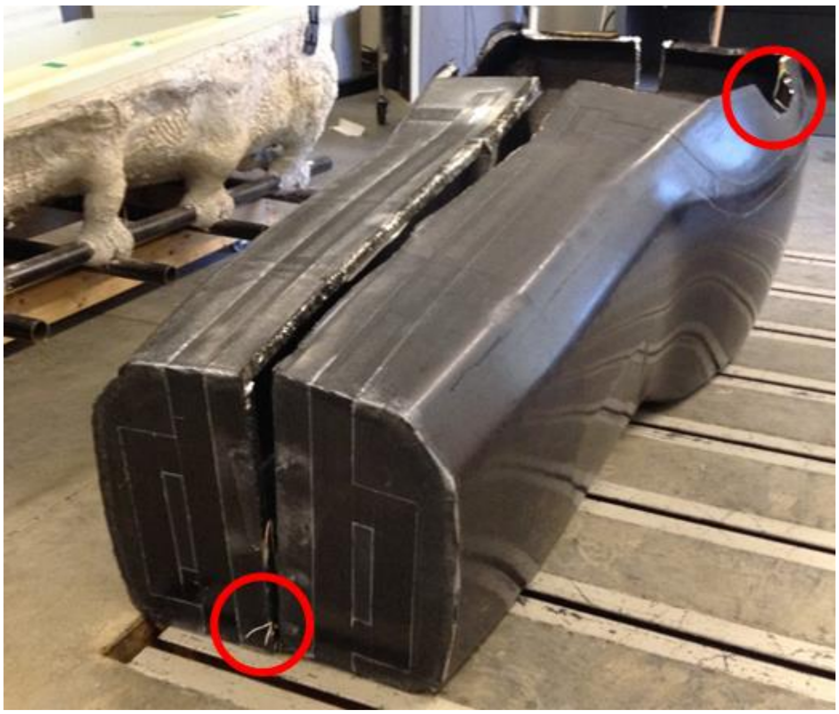

Figure 45. The two tub halves after being removed from the molds. Thermocouple locations are circled in red.

After the tub halves had been removed from the molds, they were post-cured freestanding in the oven to 350°F. The post-cure continued the resin crosslinking that was started in the standard cure. This increased the T_g of the resin, which means that a greater temperature would be required in order for the resin to begin losing strength and stiffness. Upon consultation with TenCate, a freestanding post-cure should have been possible with no part warpage. Assuming there would be no part warpage in a freestanding cure and knowing that the molds are only rated to 250°F, this post-cure method was pursued. Preserving the molds for a second 2015 part (if needed) and for possible use in 2016 was a priority.

Suspension Holes Locating and Drilling

Suspension attachment holes were drilled prior to bonding the two tub halves together in an attempt to save manufacturing time. Holes were located via triangulation from the previous year's suspension mounting locations. The previous year's suspension hole locations were scribed into the monocoque mold using a 5th axis Gantry mill, so it was trusted that their location was accurate. From the CAD model, distances were measured between these scribed holes and the location of the new suspension bolt locations. Using a compass, calipers and a fine-point sharpie, arcs were drawn around the scribe marks, and where the arcs intersected marked the location of the new suspension mounting hole (see Figure 46).

Figure 46. Positions of new suspension holes located via triangulation.

Once all of the bolt positions were located, a center punch was used to make a small indentation at each hole center. Then a center drill was used to pilot hole, before the holes were drilled using increasing drill bit sizes of 1/8”, 1/4”, and finally 3/8”.

Unfortunately, this method of locating holes proved to be less accurate than expected. As visible in figure 47, not all holes matched with the mounting brackets. The primary culprit of this error was the fact that center drilling the holes was not very accurate. Since no jig was used to locate the center drill, walking of the center drill was possible. Additionally, after the two halves had been bonded together, an 1/8” offset was measured between the right and left suspension mounting brackets, due to a poorly design jigging structure that relied on keeping the outer monocoque surfaces flush rather than keeping the suspension holes in the right position. While this error can partially be contributed to the possible warpage caused by the post-cure (discussed below), it could have been avoided if proper jigging was used to locate suspension holes after the two halves had been bonded together (see Future Recommendations section for further discussion).

Figure 47. Mismatch between the suspension bracket holes and tub inserts required additional machining on the brackets in order for them to fit.

Monocoque Half Bonding and Closeouts

The next step in manufacturing the monocoque was to bond the two halves together. The excess from the layup was cut off using a reciprocating saw with an abrasive blade. It is highly recommended that his method not be used in future years, since the reciprocating blade can delaminate the sandwich structure. Instead, an abrasive cutoff wheel should be used to trim the monocoque. Approximately 1/8" excess was left so the halves could be sanded flat. The two halves were sanded flat by sliding them back and forth over a layer of sandpaper taped to the frame table (see Figure 48). This did not get the halves completely flat, but it got them close enough to allow for hand sanding off the rest of extra material. Hand sanding was performed until the two halves lined up flush with each other.

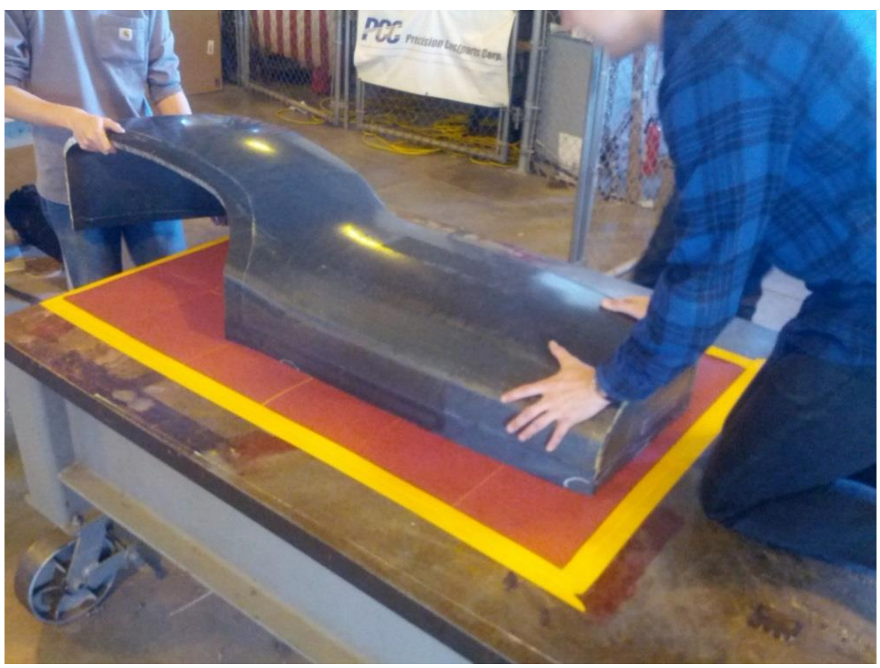

Figure 48. Tub half being sanded flat. Note the multiple pieces of sandpaper taped together on the frame table.

Once the two halves were flat, they were adhered together using a slurry of Fiberglast 3000 series high temperature resin and microballoons. Graphite powder was also added to the slurry to color it black. The slurry was first applied to both halves individually. The two halves were then pressed against each other, ratchet strapped together, and then aligned by making sure the surfaces lined up (see Figure 49). FEP was placed over the ratchet straps and inside the monocoque to keep the slurry from sticking to anything other than the bond surface. Although the slurry was thick enough to not run (due to its high microballoon content) and plenty of it was applied, a second application of slurry was still needed to fill in all gaps. Once the resin had fully cured, the excess was sanded off.

Figure 49. The monocoque while the resin slurry is curing. Note how FEP was placed between the monocoque and ratchet straps to prevent unwanted bonding.

With the monocoque now a single structure, the strap joint was laid up. The resin and microballoons held the two halves together during this process. With a glass transition temperature of 309°F, the high temperature resin bond would hold the two halves in alignment during the strap joint cure. However, the resin bond itself would not be strong enough to handle normal driving conditions. Therefore, a prepreg layup with the same layup schedule as the rest of the monocoque was laid up over the two halves (see Figure 49). The entire monocoque was then vacuum bagged and cured in the oven. In order to bag the monocoque, the structure was sandwiched between an inner vacuum bag and an outer vacuum bag, completely enclosing the tub. This was done after an initial attempt to bag to the surface of the monocoque. This method was unsuccessful because the surface finish of the tub was too porous to hold vacuum pressure. Since the post-cure was at 350°F, the new glass transition temperature of the part was 374°F according to TenCate's datasheet. With only a 260°F cure used on the strap joint, matrix crosslinking of the original part was minimally changed during the additional cure and part strength was maintained. [Ref 9]

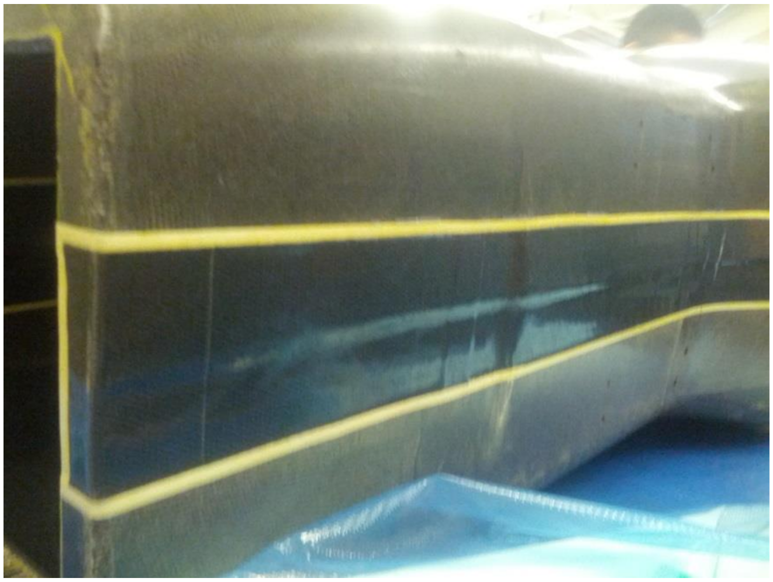

Figure 50. Carbon prepreg strap joint used to transfer load between the two tub halves.

Unlike the strap joint, the cockpit opening closeouts were only one ply of carbon prepreg. The closeouts were done as 4 separate pieces of carbon for ease of manufacturing.

Steering Rack Location & Cutout

In order to properly locate the steering rack relative to the suspension, a jigging plate was CNC'd in-house. The plate bolted to the underside of the monocoque at the suspension holes which had already been located. The plate was used to locate the steering rack mounting holes and cutout. The mounting holes were located using the jig and drilled using steel drill-guides to ensure holes were normal to the surface of the monocoque. The steering rack opening was cut using a diamond-tipped cutoff wheel on a rotary tool. The hole was filled with a resin-microballoon mixture to protect the core.

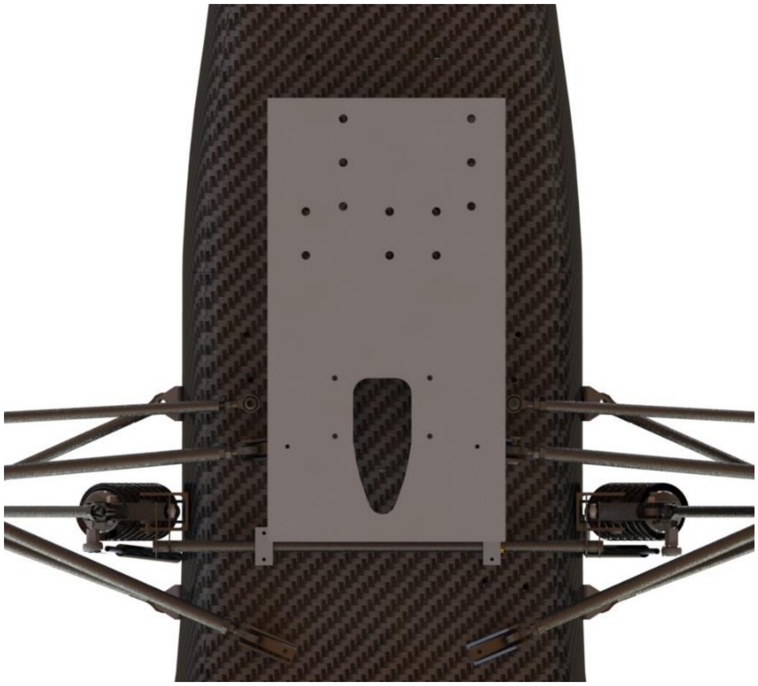

Figure 51. Jig plate located underneath the monocoque, used for drilling steering rack mounting holes and steering rack cutout.

Repair Patches and Pad-ups

After the tub halves were pulled out of the molds, it was apparent that there were a few defects. In some spots, the core was not formed well enough to the contour of the tub mold, and it didn't allow vacuum pressure to be applied to the outer face sheet. This resulted in resin dry spots (Figure 52 same as below). These were fixed by applying resin to the affected areas. Microballoons were not added to the repair resin because they reduce the structural integrity of the resin and prevent it from flowing freely into the dry fibers.

In addition to dry spots, the carbon had bridged over core splices in a few locations. This meant that the carbon in that area was no longer structurally sound (Figure 52). To fix these spots, resin and microballoons were applied into the recesses in order to make the surface flat. Then, carbon prepreg was laid over the affected spots and cured. Pad-ups were added at suspension mounting locations as well. See Figure 53 to see the locations of repair patches and pad-ups. The repair patches, pad-ups, and cockpit opening closeouts were laid up and cured at the same time to reduce thermal cycling on the monocoque.

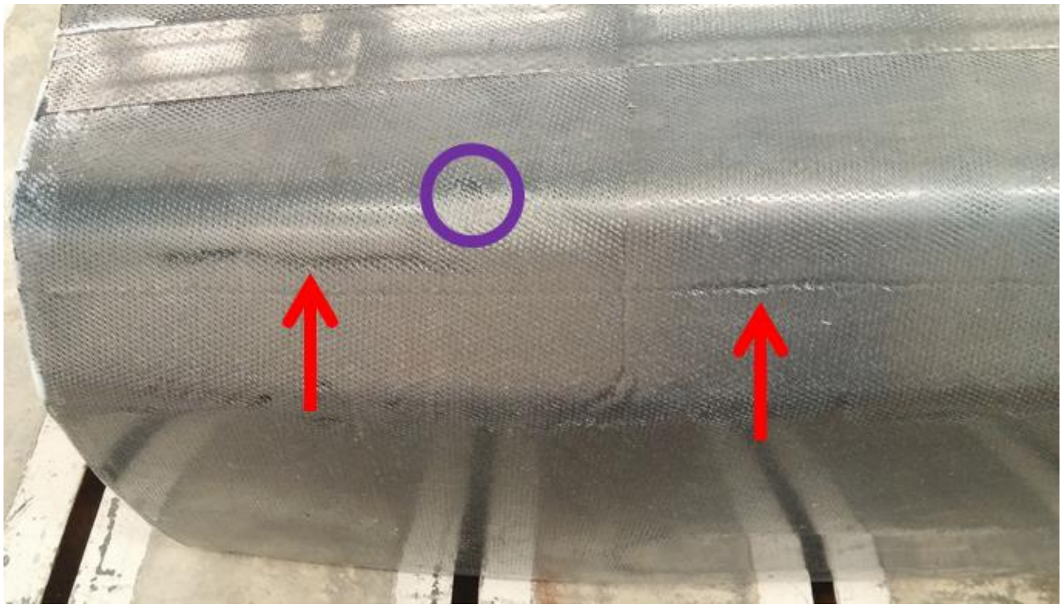

Figure 52. Dry spots occurred where the carbon fiber was not fully compressed into the mold by the core as shown inside the purple circle. Dry spots were corrected with the addition of high-temperature resin. Additionally, carbon bridging occurred at several core splice locations as indicate by red arrows. The cavities were filled with resin and microballoons, and then patched with carbon fiber.

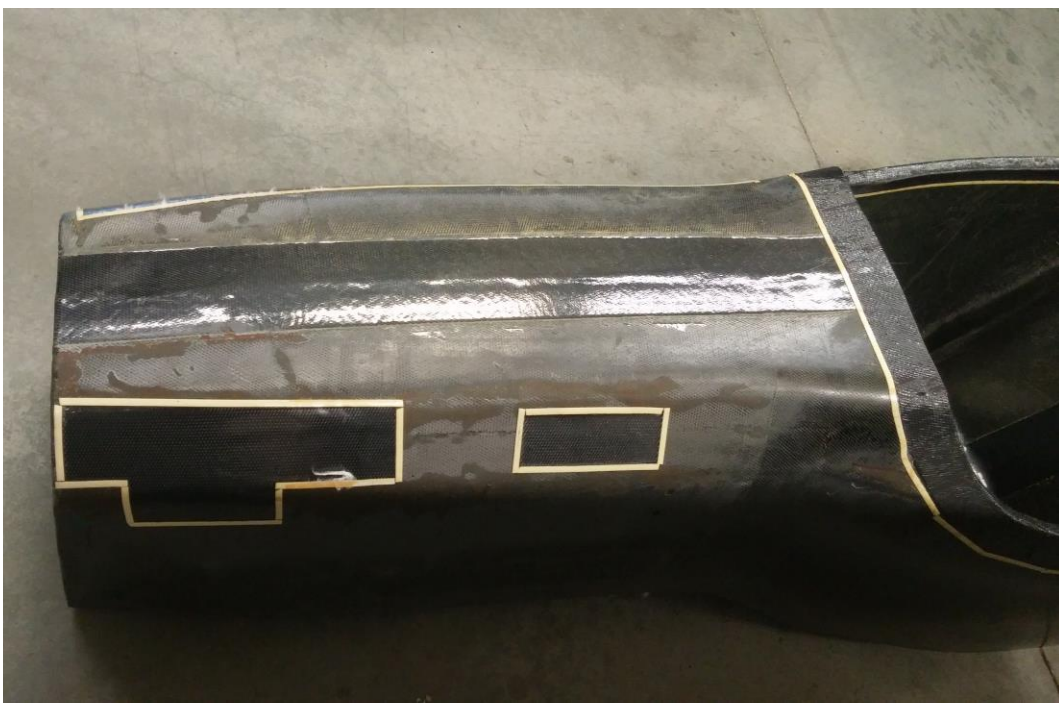

Figure 53. The dry spots pictured above are shown here coated with high-temperature resin. Additionally, the carbon bridging is shown with the repair patches. A minimal amount of material was used to save weight though an argument could be made, based on team goals, to use more material in single rectangular strops for aesthetic reasons.

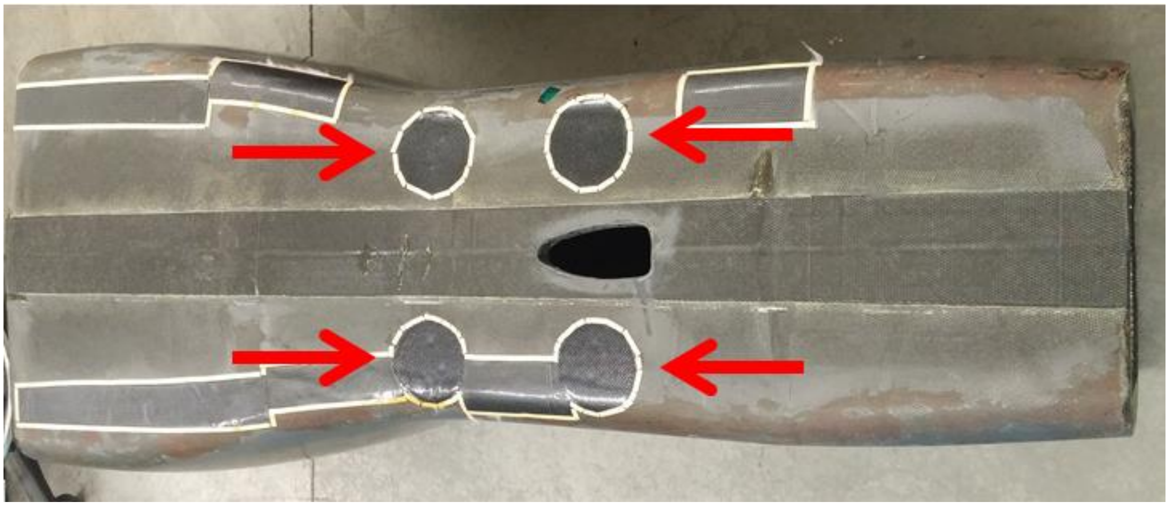

Figure 54. Pad-ups (shown with red arrows) were used at suspension mounting locations to increase the strength of the laminate in these areas of concentrated loading.

Flatness Repairs

Pedal Box Mounting

Upon bonding the two tub halves together, it became apparent that the halves were slightly warped relative to each other, which was most likely caused by the free-standing post-cure.

When bonding the two monocoque halves together, the team prioritized the width of each half. This allowed for the front suspension mounts to be as symmetrical as possible in the transverse direction (y-axis in SAE J760) about the longitudinal axis (x-axis) of the vehicle. The tub halves were cut very closely to the joggle line impression on the tub surface, ensuring that the width of the monocoque was kept true to the design. Moreover, the front of each half of the monocoque was aligned so not only would suspension pickups by transversely symmetric, but also longitudinally equal. Lining up the z-axis was more difficult as this is the direction in which the monocoque warped as evidenced by a visible (3/16”) step between the right and left halves. The left half has either expanded or the right half had contracted as the joggle lines were properly placed in the layup and the halves were carefully trimmed to these lines. The best overall fit between the seatback and front bulkhead was when the tops of the halves were aligned flush. This also was the most aesthetic when viewing the vehicle from eye-level; therefore this is the position in which the monocoque halves were aligned. However, aligning the top surface of the tub created a step at the bottom of the tub, which was later found to interfere with flush mounting of the pedal box and steering rack (see below). To ensure correct z-axis alignment in the future, a jig similar to that used by FCW should be used and the recommendations in the Drilling Holes subsection of this report’s Conclusions and Recommendations should be followed.

Due to the aforementioned issue, problems arose when attempts were made to bolt the pedal assembly to the front floor of the tub, as the pedal-box could not mount flush to the uneven surface. A flush fit is imperative for proper load transfer between the two systems, so metallic shims were applied to the uneven portion of the tub. The pedal-box mounting bolts were then routed through holes in the shims. After a day of testing, some of the shims started dislodging themselves, so a more permanent solution was necessary.

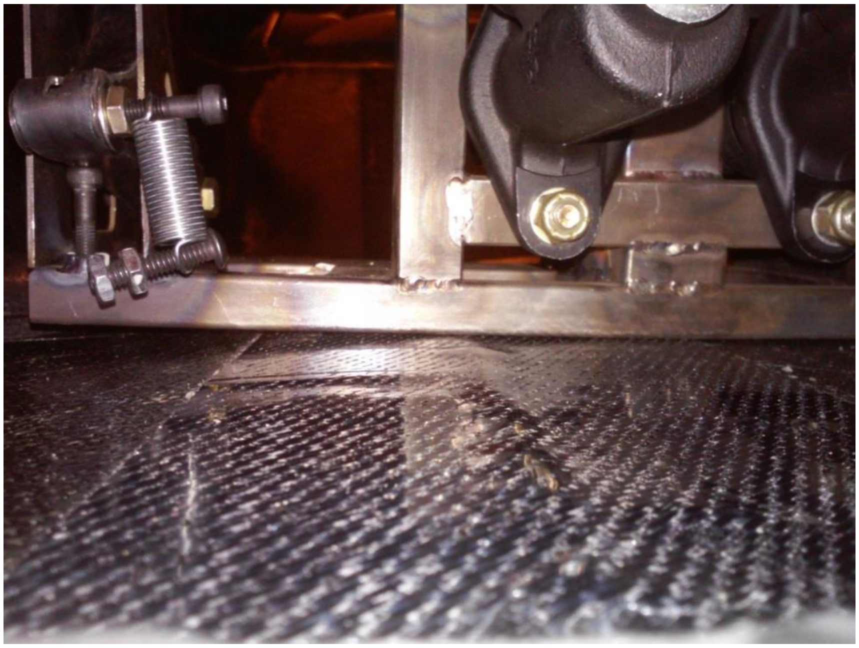

Figure 55. Pedal box placed on the uneven tub floor. A considerable gap between the pedal box and the tub is visible on the left. A visible step is present where the two halves of the tub join.

A resin and chopped fiberglass shim was the final solution to the aforementioned problem. The resin pools up and settles into a flat shape due to gravity, while the fiberglass increases the structural integrity of the cured mixture.

It was decided that physical testing was necessary to assess the compressive strength and cracking resistance of the shim, considering different fiber contents. Two test panels were manufactured: one with 20 grams and one with 30 grams of West Systems 105 resin (with the corresponding recommended hardener ratio). Each portion of resin was mixed with 1 tablespoon of chopped fiberglass and prepared on a flat plate (Figure 56). Both panels were drilled out to accept the mounting bolt, and a backing plate was bolted onto each panel with as much torque as could be managed by hand. Results showed no cracking in either of the panels. Considering these results, the team was confident that this arrangement would work. A ratio of one pump of resin to one tablespoon of fiber was selected for the final application.

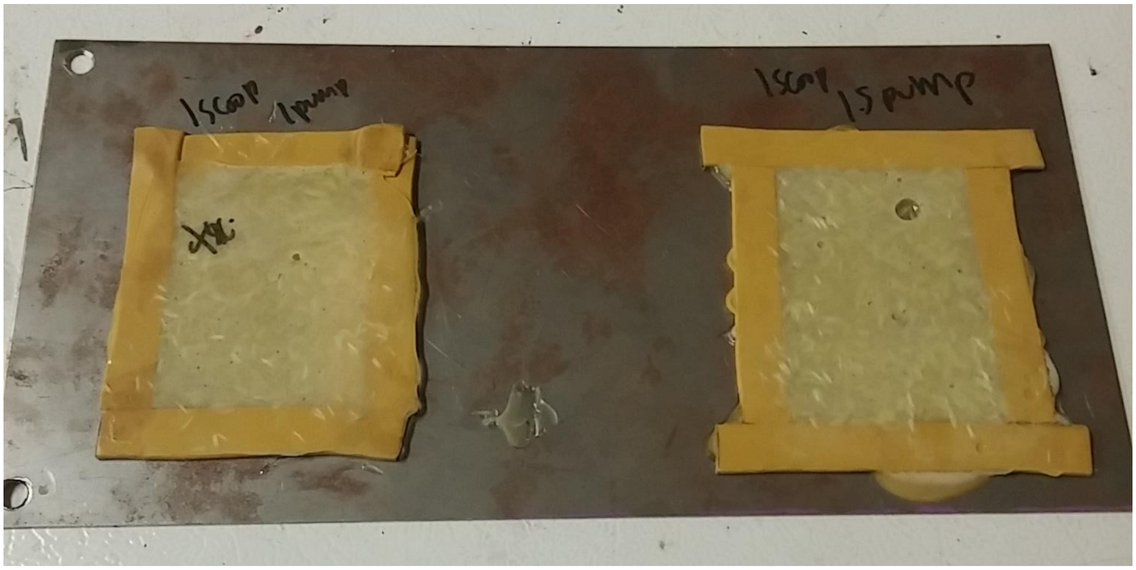

Figure 56. Two samples of the resin and chopped fiberglass mixture for the pedal box floor were prepared. Both had 1 tablespoon of chopped fiberglass, while one had 20 grams and the other 30 grams of West Systems 105 resin (with the corresponding recommended hardener ratio).

The area around the pedal-box was cleaned with acetone and dammed to prevent resin bleed. The slurry was poured in and allowed to cure for 24 hours. Since the resin settled flat from gravity, the resulting shim did not require much sanding to attain a perfectly flat mating surface for the pedal-box. Re-drilling the pedal-box mounting holes presented no difficulty, and did not crack the regions around the holes.

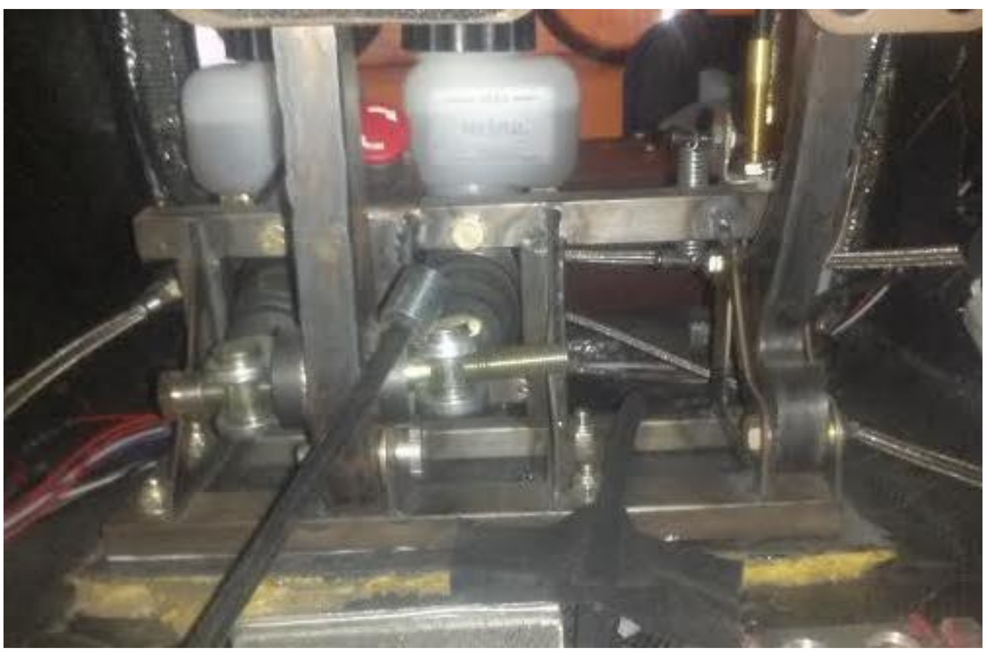

Figure 57. The resin and chopped fiber shim can be seen under the pedal-box. Graphite was added to the slurry to give it a black color. Remnants of yellow damming tape are visible along the periphery of the shim.

Subframe Mounting Surface

After applying the bridging repair patches, it was discovered that one of the patches produced a step along the rear of the tub, where the subframe was to be mounted. As with the pedal-box, this region of the tub needed to be flat.

Figure 58. The darker repair patch runs along the length of the subframe mounting surface, creating an uneven step that prevented flush mounting.

In order to avoid disassembling the suspension and running another cure cycle on the monocoque, a wet layup was applied along the seam to restore a flat mounting surface. Since pulling vacuum on the surface proved difficult, tensioned cling wrap was used to apply even pressure on the wet layup strip. The layup was allowed to cure at room temperature for 24 hours, and the resulting surface was flat with no noticeable seam where the flatness repair layup met the patch.

Rocker Mount Shim

The problem of flat mounting surfaces revealed itself again in the case of the front rocker mounts. During the car's initial shake down drive, it became clear that the area of the tub where the rocker mounted was deflecting much more than it should. The highest deflection was at the lower bolt. Deflections at the backing plate measured 0.017" while the monocoque surface surrounding the bracket showed a deflection of 0.030". Upon closer inspection, it was discovered that the bracket did not mount flush to the tub. The bracket was positioned low enough on the side of the tub that the lower half hung over a tub area of slight curvature. Since there was about 1/8" of clearance between the bracket and the tub in this area, the mounting bolt provided no clamping load on the tub. Due to the absence of clamping force between the outer and inner brackets, the backing plates could not properly distribute the bolt load. This caused a concentrated out-of-plane load at the bolt, which put the surrounding laminate in magnified plate bending. It is very likely that this unintended loading case caused progressive core failure, which was reflected in the high deflection measurements.

The solution to this issue was to shim the rocker bracket to the tub using structural aluminum repair putty. A sheet of FEP was taped to the tub, and aluminum putty was slathered onto the mating surface of the bracket. The puttied bracket was then pressed against the tub and bolted down, causing any excess putty to ooze out the side of the bracket (Figure 59). After 24 hours of cure time, the bracket was removed to reveal a perfectly contoured shim (Figure 60). Unfortunately, the shim did not reduce the deflection, so it was determined that the core had failed.

Figure 59. Structural aluminum putty was used to create a matching surface for the upper and lower suspension mounts. FEP was used to keep the adjacent areas clean during the process.

Figure 60. Rocker mount with cured aluminum paste shim. The grey aluminum paste shim is visible where the bracket meets the tub. The paste shim appears thicker than it actually is due to leftover residue adhering to the side of the bracket.

Core Failure Repairs

To permanently solve this deflection issue, the outer face sheet was cut off and the core was removed from a 4” square around the rocker mount area (see Figure 61). End grain balsa was sanded to shape and bonded in using resin and microballoons. Once the resin dried, the top of the balsa was sanded so it was flush with the tub, and a wet layup patch was placed over the area. To reduce risk of delamination, the patches were made using a similar tapering style as the pad-ups with an overlap of 0.75” and 1.0” for the inner and outer plies, respectively. See Appendix S for additional photos of the core failure repair process.

This rocker shim fix, along with the replacement of the local honeycomb with balsa, reduced the localized backing plate deflection from 0.017” to 0.007”. Deflection of the laminate around the backing plate was reduced from 0.030” to 0.005”. Measurements taken before and after driving sessions confirmed the same deflection numbers, thus ruling out the possibility of progressive failure. With the repairs in place, the entire backing plate showed similar deflection at different points, whereas before the repair most of the deflection was localized close to the bolt. These measurements indicated that sufficient clamping force was being provided, and that the balsa core had not experienced failure.

Figure 61. Location and size of repair section at front rocket mount. Note how both the outer face sheet and aluminum core have been cut out, but the inner face sheet was not.

Attachments

As previously stated, aluminum inserts were used at all points on the monocoque where accessory parts attached. Inserts were custom machined for each hole using aluminum rod. It is critical that the insert be the correct length so that the loading is distributed properly from the bolt to the laminate. Proper load transfer is reacted through the face sheets, so the inserts must be in good contact with both the inner and outer face sheet. Similar to previous years, 7/16” OD inserts were used for 1/4” fasteners and 3/8” diameter inserts were used for #10 fasteners, based off of insert pullout testing results and the expected loads (see Appendix F for testing results).

After the fit of each insert was checked for proper length, the inserts were bonded into the monocoque using 3M 420 Structural Adhesive, similar to the approach used in the test panels mentioned above. First, the core area and insert were scuffed using Scotch-Brite, and then cleaned with Acetone. The 3M adhesive was inserted into the hole cut into the monocoque using a mixing gun, and spread on the outside of the insert prior to final insert placement. After the inserts were placed inside of the monocoque, tape was placed over the inserts to prevent the inserts from dislodging themselves in the case that anyone moved the monocoque.

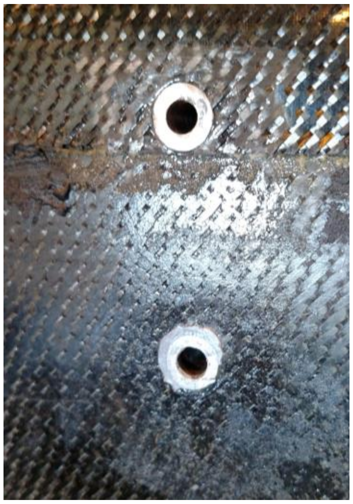

Figure 62. Aluminum inserts potted into the monocoque.

Backing plates were manufactured for each component being attached to the monocoque. The increased surface area covered by a backing plate helps to distribute the load across the laminate and limits stress concentrations. Backing plate surface area for each component was based off of perimeter shear testing data, which failed at a loading pressure of approximately 600 psi (see Appendix F). SAE rules mandates that all roll hoop backing plates be a minimum thickness of 0.080” steel. Ungoverned backing plates were manufactured out of 0.063” steel in order to save weight.

Figure 63. Backing plates used for the upper suspension mounts. Sizing was based off of perimeter shear testing results.

Front Bulkhead Cutout

Due to reasons discussed previously, a front bulkhead cutout was created to serve as an access window for the pedal box assembly. The maximum cutout size of the front bulkhead is determined by the SES, and a final cutout size of 11”x11” was chosen given the laminate testing properties. The geometry of the cutout was traced on the front bulkhead, and holes were drilled inside each of the four corners. The reciprocating saw was then used to cut out the square opening. As stated previously, this is not the preferred method of cutting through a carbon fiber sandwich structure. Once cutting was completed, resin and microballoons were applied to the exposed core in order to protect it.

Finishing

Aesthetic finishing was saved until just prior to competition in order to facilitate any chassis modifications or repairs that became evident during testing. The two primary options for improving the appearance of the vehicle were paint and vinyl covering. Properly executed painting produces a finer finish than vinyl. However, this level of quality is difficult to achieve and added 4.8 pounds to the 2013 monocoque. In addition, sponsor logos must be cut out and applied individually—a process taking approximately 10 man-hours when digitizing and application are considered. The advantages of a vinyl wrap are that it is lighter than paint, can be printed with partner logos, and conceals surface imperfections better than paint. The inherent advantages of vinyl combined with VE Signs offering to fully sponsor, design and apply this wrap, made choosing this option straightforward. Partner logos and chassis manufacturing drawings were sent to VE Signs designers to produce digital templates for the wrap. Beyond being aesthetically pleasing, a high-quality finish is important in gaining the confidence of design judges, securing additional industry support, and recruiting new students for the team.

Prior to the wrap's application, resin and microballoons were applied to the tub surface to fill any pinholes and steps in the carbon. The resin-microballoon slurry was applied in excess and then sanded down with 280 grit sandpaper to tangency in a manner similar to that of standard automotive body-filler. Only 0.1 pounds of the slurry was used on the 2015 monocoque, as opposed to the 2013 chassis which needed 0.3 pounds due to the vehicle being painted. From there, the vehicle was turned over to VE Signs for final finishing. As a professional company, their methods are beyond the scope of this report and it is suggested that future teams evaluate their resources before deciding on the best finishing method. The wrap itself added 0.6 pounds to the vehicle weight according to VE Signs. The end result was not as aesthetically pleasing as the 2013's vehicle's finish partially due to repair patches; however, it was sufficient for a racecar over 75% lighter (Figure 64).

Figure 64. The finish was over 75% lighter than in 2013 and had good aesthetics when on-course. The repair patches were still moderately visible under the vinyl wrap but not noticeable from a short distance.

Nosecone Manufacturing

Foam Molds

Because a controlled outer surface finish is desired for front wing mounting and mounting to the tub, a female mold was used for the nosecone. The front wing mounting flats necessitated a draft angle of 0°, which could make it more difficult to remove the part from a one-piece mold. Machinability of the mold was also an important consideration. The mold would need to be 15 inches deep due to the depth of the nosecone. Getting an end mill long enough to accurately machine was not feasible given the available resources. These two factors lead to the decision of using two separate mold halves, split down the centerline. This allowed the molds to be machined on their sides, which required a shallower depth of cut. It also allowed for the molds to be pulled apart once the cure was completed, so the part could be easily removed.

Two blocks of foam large enough for the molds were not available, so smaller blocks of 15 lb/ft^3 Coastal Enterprises Precision Board LT were glued together using PTM&W high-temperature epoxy foam glue. After bonding the foam was CNC machined on a Haas VF3 mill. In addition to the mold cavity, 4 alignment holes were also drilled with the CNC machine. Due to the high density of the foam, the machine didn't take out any chunks of foam, and left a finish that required little sanding. Next, the molds were sprayed with a Duratec Polyester Sealer, then 8 layers of Duratec Polyester Surfacing Primer. The first two layers of Duratec were dyed green, the rest were left white. If sanded down to green, it was obvious that most of the Duratec had been sanded through. The molds were sanded down to 600 grit sandpaper, which left a very smooth finish to lay up on. See Figure 65 for a view of the left nosecone mold.

The high density foam used for the molds worked extremely well. Not only did it machine easily, but it proved to be very durable. The team pulled 5 nosecones off of the same molds, and they still appear to be in good working condition. On the other hand, the team this year had multiple lower density (8lb/ft^3) molds for other components break during their first cure cycle.

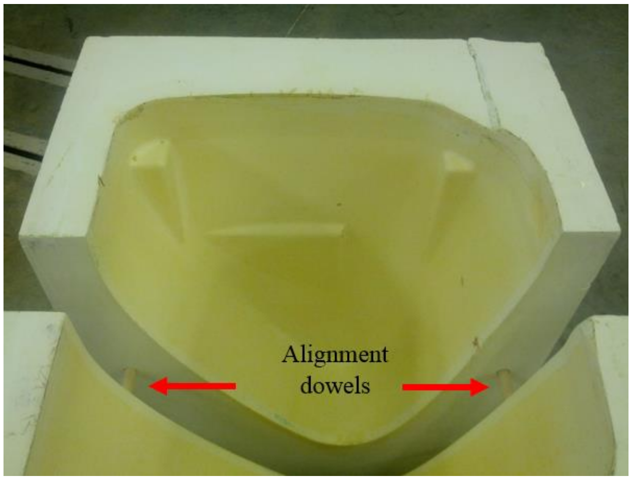

Figure 65. The two halves to the nosecone mold. Note the alignment dowels.

Layup

The nosecone layup was done in a similar manner to that of the monocoque layup. The molds were cleaned with acetone in the same manner as the monocoque molds, and then prepped with both Meguiar's Mold Release Wax #8 and Frekote (see Appendix R). For the first layup, a ply of carbon prepreg was cut in the general shape of the side, and then slowly trimmed down until it fit. The poly backing paper obtained off of the initial layer was then used as a template. Rectangular pieces of prepreg were used for the top and bottom. For the unidirectional prepreg, the roll was too narrow to cut side pieces as one piece. As a result, two pieces were cut and then placed side-by-side. Due to the nature of unidirectional carbon, splitting the ply in two parts parallel to the fiber direction would not affect part strength.

The top, bottom, and sides all had the same layup schedule. Both the T800 cloth and uni only had backing material on one side, so each ply was laid down by placing it on the mold at one location then slowly pushing down while moving across the ply. This proved to be the most consistent and time-efficient method. Due to the small opening on the top of the mold, it was most efficient for one team member to lay down the carbon at a time (Figure 66).

Figure 66. Laying down a ply on the side of the nosecone mold.

Due to temperature constraints of the foam molds and epoxy, the cure cycle had to be adjusted to a 200°F cure. This meant elongating the cure cycle to an 8 hour dwell in order to fully cure the resin as suggested by Dr. Mello. Thermocouples were used in order to monitor part temperature. Just like with the monocoque cure, temperatures were recorded every 15 minutes. See Figure J3 in Appendix J for cure cycle data.

Nosecone Hole Drilling

Prior to mounting the nosecone to the chassis and the front wing to the nosecone, holes were drilled in the carbon skin. To ensure proper alignment with the mounting studs protruding from the chassis, the monocoque stud inserts were placed prior to drilling the nosecone flanges. This pattern was transferred to a metal plate that was cut just smaller than the nosecone perimeter—thus allowing it to sit flat on the mounting flanges. After making holes for the 5/16” studs, the plate was then used as a template to drill holes in the flanges. A drill guide was used to keep the bit perpendicular to the 0.125” thick carbon present on the flanges.

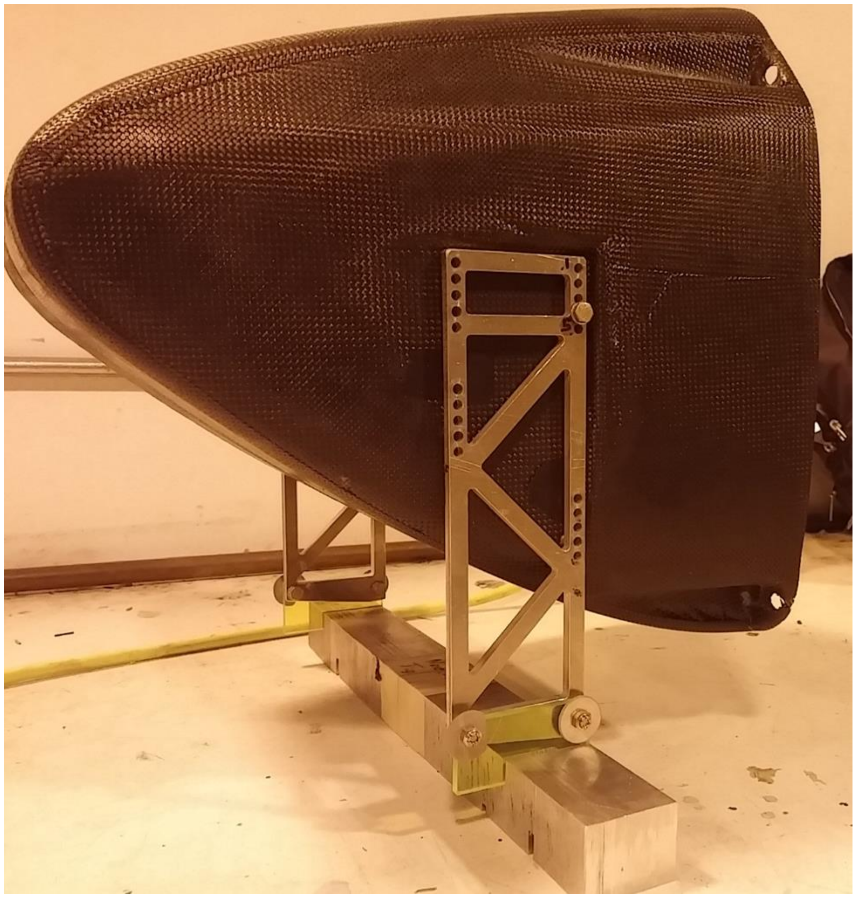

Figure 67. Fixture used to hold front wing mount truss structures in place while holes were drilled.

The flat sections present on the nosecone for aero mounting have a 90° guide at their top-back edge which allowed for level placement of the aluminum trusses. In order to ensure the trusses themselves were square with the ground plane and each other, a jig was machined out of a 2” x 2” aluminum bar with slots for the members. With the trusses secured in the jig, a sharp drill was spun by hand in the waterjet-cut holes in the trusses. The trusses were then removed and the holes were finished with a guide and hand drill. To facilitate testing of ground clearance and minimize the number of holes required to be drilled in the nosecone, the wing mount itself had multiple holes at 0.3” height increments.

Firewall

The firewall was manufactured first as a flat panel and folded into shaped as noted in the Final Design Details section. The jig required adjustment from the solid model design because not all features present on the vehicle were in the model and because of subframe variances between the model and real life. This process did not go smoothly and it is recommended that if a cut-and-fold firewall is used in the future, that care is taken to fully and accurately model that region of the vehicle prior to jig design. Moreover, compliance was introduced at the bend where the headrest portion was recessed to accommodate the driver’s helmet. This was solved via the 5/16” steel rods noted in the Final Design Details section, but the joint of the aluminum angle and the carbon fiber required bolts and washers—adding weight. Had this joint been accounted for initially, it could have been made via the stiffer and lighter cut-and-fold method. This section was extended when the gas tank was found to be too small and the fuel filler neck was extended upward to add capacity. Finally, it should be noted that 90° bends were found to strain the carbon fiber facesheet to failure, so future designs should test desired angles based on the specific layup to be used. The firewall is shown in Figure 68.

Figure 68. The cut-and-fold firewall as driven at competition. The aluminum shield on the right was added when the fuel filler neck height was increased.

Figure 69. The headrest section of the firewall was recessed to allow for the driver's helmet to be in a natural position. This feature was not part of the initial design and required the use of a (relatively) heavy aluminum bracket (red arrow). Steel tubes were added to connect the top of the headrest to the subframe to support the weight of the drivers head in a crash scenario (purple arrow).

Figure 70. Two plies of wet layup fabric were used to hold the folded panel in position. Mounts and washers with a large surface area were used to distribute the load along the facesheet though inserts were (incorrectly) omitted.

Recommendations for Future Manufacturing of Design

Core

One of the largest advances this year was the use of aluminum core. It theoretically allowed for an increase in torsional stiffness without adding weight and helped the laminates pass a stricter rule set. Unfortunately, several manufacturing difficulties arose due to the use of aluminum core. The two largest issues were the core bridging and core sections imperfectly butting together at splices.

When the aluminum core is not formed to exactly the same geometry as the mold, it does not lie down flat flush to the mold surface. The Nomex core used previously was much more formable and able to bend into the surface under vacuum pressure. Unfortunately, the stiffer aluminum core did not form to the complex geometry as well. Bridging of the core across the surface of the mold decreased the quality of surface finish because it hindered vacuum pressure from compacting the carbon.

When two sections of core meet up, it is imperative that there are no gaps between the two. Since, the Nomex used in 2013 springs back when compressed, extra core was compressed and forced into spliced regions, which acted to fill the gaps. The aluminum core, on the other hand, does not spring back so it was much more difficult to fill gaps at the spliced region. During the cure, the vacuum pressure would suck the carbon between the two core sections where gaps still existed (see Figure 71). This is the equivalent of a stress concentration, and needed to be repaired with patches when found on the monocoque.

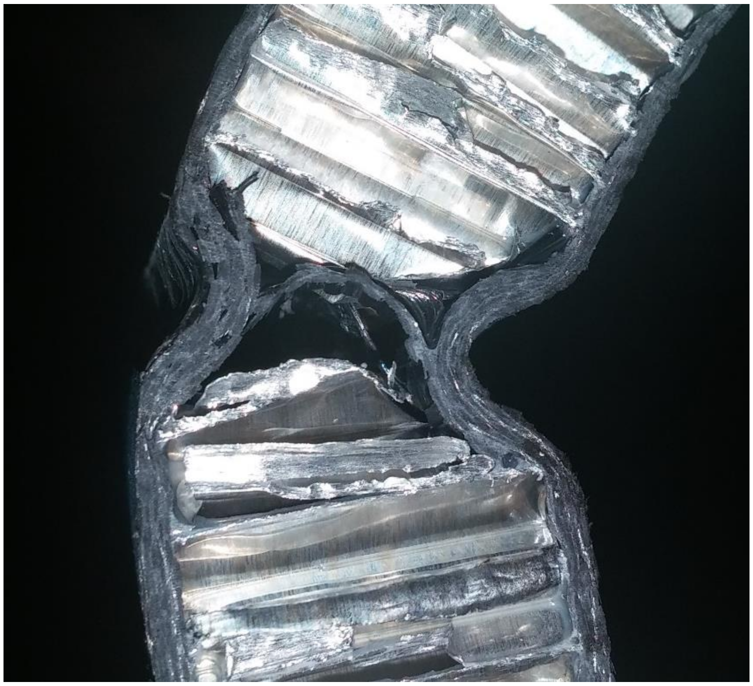

Figure 71. The effect of gaps between core sections. Note how the carbon has draped in between the two sections of core at the splice. Picture taken of a blob layup cut in half.

There are a few options to remedy these two manufacturing difficulties. Possible solutions include using aluminum Flex-Core, a smaller hex cell size, or thinner core. Any one of these would make it easier for the core to bend into contours and radii, but testing is necessary to determine the best solution in regards to strength and stiffness. In order to fill gaps between core splices, the team should look into expanding core splicing foam. Alternatively, Nomex core could be used in these regions since it naturally springs back and fills in gaps.

Harness Satin Weave

Another difficulty encountered was the use of a harness satin weave carbon cloth, in which the strand of carbon fiber is woven through the perpendicular strands once every 4 or 8 strands. The result is a cloth that is not symmetrical about itself, because it is predominantly 0° fibers on top and 90° fibers on the bottom. The top and bottom being different orientations means that extra care must be taken when determining the correct orientation of a satin weave cloth.

Satin weave cloths typically drape over contours easier and are stronger than plain weave cloths. However, figuring out how to deal with the asymmetry requires a solid understanding of the material. Therefore, the use of a harness satin weave cloth is only advised if the team has a solid understanding of the material and its effects on the laminate (asymmetry, warping, residual stresses, etc.).

Carbon Overlap

A significant amount of weight can be saved by incorporating less overlap between adjacent carbon sheets. After trimming both halves of the chassis, an almost 0.5 pounds difference between the two halves was measured. The most probable cause of this discrepancy is inconsistent amount of overlap used between the two halves.

Many aerospace manufacturers use a rule of 1:10, in which the overlap is approximately 10 times the thickness of the cloth or tape being used. Alternatively, a simple tensile test comparing the amount of overlap and the strength of a laminate can be conducted, to get a more accurate comparison of strength vs. weight due to overlap. It is projected that with a consistent amount of overlap enforced, the chassis could be approximately 1 pound lighter.

Multi-Stage Cure

Potential performance and aesthetic gains can be obtained by curing the monocoque in stages. A multi-stage cure entails curing the outer face-sheet, curing the core to the face-sheet, and then curing the inner face-sheet to the core. Increased compaction can greatly improve surface finish and the integrity of the laminate. Additionally, there is no risk of cavitation of the outer face sheet at core splices. However, there is a risk that the core may not fully bond to the facesheet, thus creating an interface incapable of transferring shear. Thus, if this method is pursued, non-destructive testing utilizing sample layups on *all* representative contours and/or ultrasonic inspection is recommended.

In order to minimize residual stresses within the laminate, the facesheet layup schedule would have to be designed to be symmetric about its own centerline so that no thermal warping occurred during each individual cure cycle.

Locating Suspension Holes

Suspension holes were located and drilled prior to bonding the two monocoque halves together. This resulted in geometrical consequences due to the apparent warpage of the two halves, most likely caused by the post-cure of the monocoque. It was observed after bonding the two halves together that one side of the suspension mounts was offset vertically approximately 1/8” from the opposite side. This error creates a difference in the kinematics of the suspension from the designed target and is disadvantageous to the vehicle’s handling. In order to avoid similar mistakes in the future, it is recommended that the suspension holes be drilled after the entire chassis is assembled using a jig to properly locate each point.

Nosecone Manufacturing

In an attempt to reduce weight of the front wing mounting, the front wing was mounted to the nosecone. While the front wing was successfully mounted to the nosecone, it brought up a few challenges as well. The largest issue with having flat spots to accommodate front wing mounts is the stress concentration that they cause (see Appendix P). The main reason that the 2015 nosecone is almost 1 pound heavier than the 2013 nosecone is because the sides are so much weaker. With a constant profile such as the 2013 impact attenuator, the load is able to follow a continuous path. In 2015, the transition of the flat spots cause the load to travel through a discontinuous load path, which puts the carbon skin in bending instead of in-plane compression and acts as a stress concentration. A carbon skin is much weaker in bending than it is with in plane compression, and as a result the layup schedule had to be increased in order to compensate. A second disadvantage to this mounting method was manufacturing. Getting the carbon to drape over the complex geometry was possible, but difficult.

A solution to these problems could be to mount the front wing differently. Other FSAE teams have mounts sticking through the nosecone that are attached to the chassis front bulkhead (see Figure 72). This would allow the geometry to be continuous like the 2013 nosecone, and would make the structure much stronger. One issue with this is the stress concentration introduced by drilling holes for the mounts to go through. However, these would most likely be much less significant than having a discontinuous geometry that introduces laminate bending.

Figure 72. University of Washington’s car. Note the front wing mounts coming through the nosecone, and how it allows the nosecone to maintain a continuous geometry.

An alternative mounting solution that would eliminate stress concentrations even further would be bonding wing trusses onto the exterior of the nosecone. This could be done easily by shaping the upper inboard portion of the wing trusses using a mold generated from the nosecone tool’s CAD. To allow for proper positioning of the truss, low-depth markings should be made on the nosecone mold via CNC during manufacturing as done for the 2013 monocoque suspension pickups. Since during impact testing the wing mounts do not need to be physically mounted, no stress concentrations would be added in the test. However, the force required to shear off the front wing must still be added mathematically to the testing results. Because the bonding shear strength of the team’s adhesive is approximately 3000 lb/in^2, it may be advantageous to use the lower bolts that secure the mounts to the wing for these calculations. While performing this trade-off analysis, it would be best to calculate the failure load for the adhesive using the front wing leading edge as the point of impact. This not only represents real-life crash conditions but allows the mathematically added forces to be reduced since they will include a moment.

Another aspect that should be investigated is the use of a male mold. A male mold would be much easier to layup on than a female mold. It would also potentially eliminate dry spots (Figure 73) because the carbon would not bridge like it does on the interior surface of a female mold.

Disadvantage to the use of a male mold would be an uncontrolled outer surface, which may be undesirable depending on what other purposes the nosecone has. Another possible problem with a male mold would be getting the mold out once the part has been cured. An alternative option would be to look into machining a male buck then pulling a plaster female mold off of it, similar to 2013. This would allow vacuum bag to be taped to the mold, instead of bagging the entire mold. Also, even though plaster is more dense than foam, much less plaster would be required to make the mold (a layer of plaster formed to the geometry, instead of large foam blocks). This would result in a lower thermal mass, which would help the part follow the cure cycle more closely.

Figure 73. Picture of nosecone dry spots, most likely caused by carbon bridging hindering vacuum pressure from pushing carbon against mold surface.

Design Verification and Testing

Drive Testing

In the early stages of drive testing in Cal Poly's H1 parking lot, the driver noticed a large degree of body roll through turns. This problem was mitigated by stiffening the suspension, but it was soon found that the region around the front rocker mounts had failed at the lower pickup. Details on the fixes can be found on pages 87-97.

Figure 74. The car rounding a cone at the Buttonwillow Raceway kart track where a combination of curbs, fast sweepers and medium-speed banked corners provide loadings somewhat higher than those expected at competition. These loadings quickly failed the core behind the rocker mounts where balsa wood was not present.

After the rocker deflection had been fixed, tuning the suspension was positive and repeatable based off of driver feedback, thus indicating a sufficiently stiff chassis. After each major drive day, bolts were checked for tightness and the tub examined for cracks or failures. As of writing this report, the car has logged over 5 hours of drive time without any additional incidents.

Mass Properties

Mass properties taken from the vehicle are presented in Table 23. Some mass properties from the 2013 report were not individually available and the weight of the cockpit closeout and repair patches was estimated (±0.5lb) for the 2015 vehicle.

Table 23. Mass properties for the 2013 and 2015 chassis. Some information was not broken out for the 2013 vehicle; however, the totals are correct.

Component	2015 Weight (lb)	2013 Weight (lb)	Change from 2013 (%)	Notes on 2015 Weight Values
Left half of monocoque	13.540	Unavailable	Unavailable	Excess trimmed, no closeouts, front bulkhead material not removed
Right half of monocoque	14.000	Unavailable	Unavailable	Excess trimmed, no closeouts, front bulkhead material not removed
Bulkhead removal	2.202	Unavailable	Unavailable	Weight removed from the 11" x 11" opening
Strap joint and all resin-microballoons	4.762	Unavailable	Unavailable	Includes resin-microballoons on cockpit opening but not cockpit closeout
Cockpit closeout and repair patches	2.4	Unavailable	Unavailable	±0.5lb
Monocoque without hardware	30.0	Unavailable	Unavailable	Includes inserts and vinyl wrap.
Hardware	2.5	3.20	-21.9%	±0.5lb. Roll hoop and harness harware and backing plate.
Monocoque total with hardware	**32.5**	**38.20**	**-14.9%**	±0.5lb/1.3%
Nosecone	3.160	2.094	50.9%	Fairing only
Nosecone hardware	0.150	0.138	8.7%	Nosecone to monocoque only
Aerodynamics hardware	0.215	0.352	-38.9%	Wing to truss and truss to nosecone only. Aero added in 2014.
Front wing trusses	0.690	1.860	-62.9%	Adjustable aluminum version for 2015. Aero added in 2014.
Nosecone and aero-mounts total	**4.215**	**4.444**	**-5.2%**	Includes nosecone, aero mounting, all associated hardware
Anti-intrusion plate	**2.160**	**2.59**	**-16.6%**	Composite version

Physical Torsion Test Results

In order to validate the theoretical chassis stiffness, a torsional stiffness test fixture was constructed. In order to maintain consistency with the FEM, the test fixture was designed with the same constraints. Three of the four wheel hubs were constrained, with the remaining hub loaded using weights cantilevered off of a tube slipped onto the axle stub. See page 47 for description of boundary conditions.

With the wheels still attached, the car was lifted and rolled onto the frame table. The front and rear of the car were then propped up with foam blocks, and the wheels and alignment pins removed to expose the hubs. In order to ensure that the rear fixtures mounted flush with the hubs, upright camber was set to zero with adjustment shims. Solid steel dummy shocks were installed in place of the coilovers, and the steering was locked with vice grips that were rigidly attached to the front roll hoop.

With the rear fixtures loosely bolted to the hubs, the car was lifted and a large steel I-beam was slipped under the fixtures. The fixtures were then bolted to the I-beam, and the I-beam was then c-clamped securely to the frame table (see Figure 75). This process was repeated for the I-beam and fixture arrangement in the front (Figure 76).

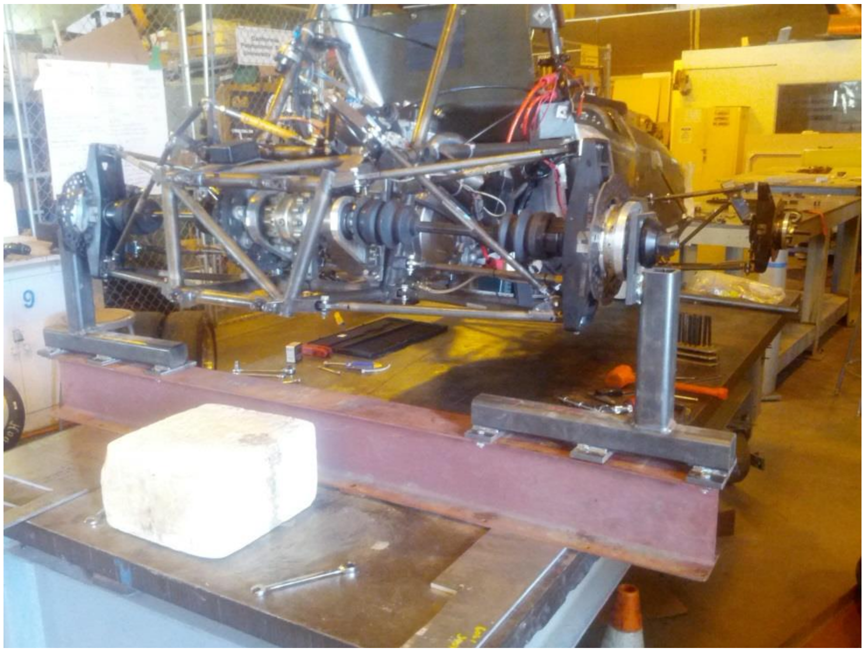

Figure 75. Torsion test rear view. The rear fixtures are shown bolted to the wheel hubs and the I-beam supports.

Figure 76. Torsion test front view. The front right upright is resting on a solid steel cylinder, while the front left upright is instrumented with a dial indicator and left unconstrained.

With the car fully suspended in the fixture, a dial indicator was placed at the upright of the unconstrained wheel hub. Varying weights were placed on the free hub, and deflection was recorded for each weight. The results were then averaged to yield a torsional system stiffness of 1224 ft-lb/deg (Table 24), which is a 16.6% increase over the 2013 chassis stiffness of 1050 ft-lb/deg. The 2015 chassis also has 24.4% improved specific stiffness, considering its lower weight (Table 25).

Table 24. Physical torsional stiffness results and deflections.

Weight Applied (lbs.)	Deflection at Upright (in.)	Torsional Stiffness (ft-lb/deg)
21.64	0.056	1329.02
45.06	0.129	1229.66
66.62	0.204	1174.53
89.98	0.278	1196.15
146.06	0.47	1190.78
	AVERAGE	1224.03

Table 25. 2013 vs. 2015 stiffness comparison

	Torsional Stiffness (ft-lb/deg)	Weight w/o Hardware (lb)	Specific Stiffness (ft-lb/deg-lb)
2013 Chassis	1050	32	32.8
2015 Chassis	1224	30	40.8
% Difference	16.6	6.7	24.4

However, the results shown above include some data points that should be disregarded for both of the 2013 and 2015 tests. The first data point likely includes slop in the mounting hardware and should therefore be omitted. The last data point was obtained with an extremely high load on the upright which it is believed, induced uncharacteristic behavior. These trends are shown in Figure 77. When the average of the remaining three points is taken, the 2015 chassis had an 11.5% higher specific stiffness than the 2013 version (Table 26).

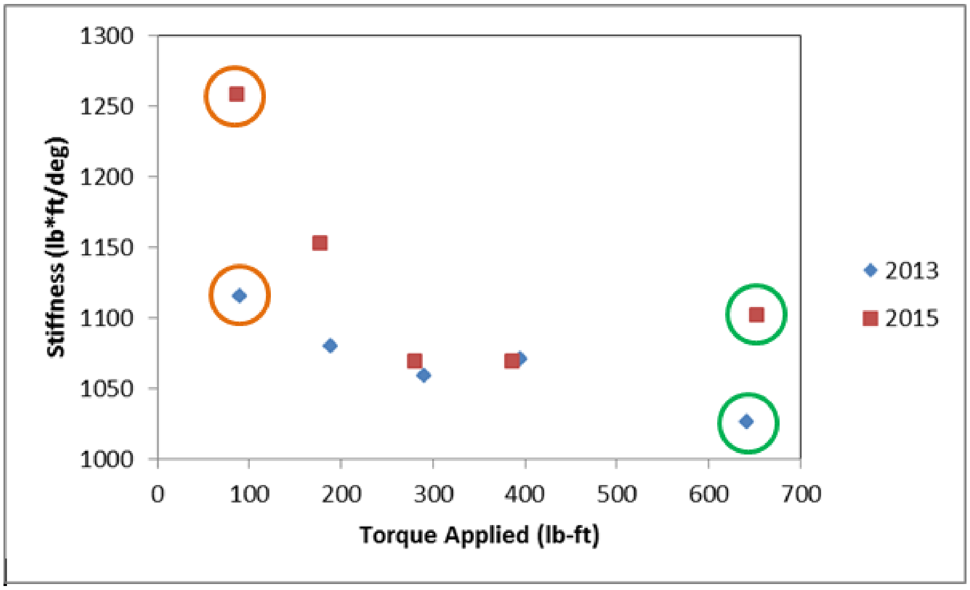

Figure 77. Data from the 2013 and 2015 vehicle torsional tests. The first data points (circled in orange) likely include slop in the bolted connections and should be omitted from analysis. The final data points (circled in green) were obtained with an extremely high load and may include uncharacteristic behavior. When these points are omitted, the average torsional stiffness of the 2015 chassis is 2.5% greater than the 2013 version.

Table 26. With the omission of the aforementioned data points, the 2015 chassis outperformed the 2013 version by 11.5% in terms of specific stiffness.

	Torsional Stiffness (ft-lb/deg)	Weight w/o Hardware (lb)	Specific Stiffness (ft-lb/deg-lb)
2013 Chassis	1070	32	32.8
2015 Chassis	1097	30	36.6
% Difference	2.5%	-6.3%	11.5%

These results are in line with our goals, but the chassis weight could have been further reduced if excessive bridging did not necessitate heavy repair patches and resin application.

During the physical torsion test, measurements were taken allowing the stiffness of the monocoque and the subframe to be calculated. These can be seen in Table 27. As can be seen, more stiffness is lost in the monocoque than the steel tube subframe. Ideally, these stiffnesses will be the same. However, that is not feasible for a real world chassis.

Table 27. Component stiffnesses calculated from the physical torsion test.

Component	2013 (ft-lb/deg)	2015 (ft-lb/deg)	Change
Monocoque and front suspension	2148	1982	-7.7%
Joint	36480	83433	128.7%
Subframe and rear suspension	2193	2670	21.7%
Total	**1070**	**1097**	**2.5%**

Unfortunately, the measured stiffness was lower than our predicted stiffness of 1679 ft-lb/deg. This discrepancy is most likely due to manufacturing difficulties with aluminum core, which caused bridging and localized resin dryness.

Note that sister senior project CP Speed also performed a torsional test on the 2013 and 2015 chassis. These results are believed to be slightly less accurate in relation to overall chassis stiffness though cover longitudinal stiffness in depth. These overall results are presented in Appendix W and the longitudinal results are in the CP Speed report itself. Results from this report include hysteresis of the 2015 chassis that are worthy of additional future examination.

Nosecone Results

As discussed previously, a quasi-static crush test was performed on the nosecone in order to ensure that it was sufficient as the car's impact attenuator (see Table 28 for results). The first nosecone (9 plies) only absorbed 2792 Jules of energy, which does not meet SAE's energy absorption requirement. The second nosecone (15 plies) absorbed 7391 Jules of energy, which meets the requirement. The nosecone also met both the peak and average deceleration requirements. Note that the peak deceleration requirement of 40 g is reduced by the front wing mounting bolts. See Appendix O for the Impact Attenuator Data sheet submitted to SAE.

Table 28. Quasi-static crush test results.

Specification	Requirement	9 Plies $[45_c/0_3/\ \overline{45}_c]_s$	15 Plies $[45_c/90/0_2/90/0_2/\ \overline{90}]_s$
Energy Absorbed	7350 J min	2792 J	7391 J
Average Deceleration	20 g max	3.196 g	7.759 g
Peak Deceleration	27.4 g max	11.351 g	21.873 g

The goal of mounting the front wing to the nosecone was to save weight compared to the 2014 mounting system. The front wing mounting flats had an adverse effect on energy absorption, leading to a heavier nosecone than 2014. However, the entire mounting system, including the nosecone, is lighter than 2014 by 0.23lb (see Table 28). Due to higher front wing loading, as well as stricter SAE rules requirements (front wing mounting failure load of 12.6g is subtracted from the allowable peak deceleration of 40g), decreasing the system weight is considered a success.

Table 29. Nosecone weight comparison.

Component	2014 Weight (lb)	2015 Weight (lb)	Change (lb)	Change %
Nosecone (2013-2014)	2.094	3.16	-1.066	51%
Trusses	1.846	0.69	1.156	-63%
Nosecone Mounting Hardware	0.138	0.138	0	0%
Aero Mounting Hardware	0.35	0.215	0.135	-39%
Total	**4.428**	**4.203**	**0.225**	**-5.1%**

Specification Verification Checklist

In order to quantify the achievements of the FMD team, the following specification verification checklist was made. All critical design specifications were met, which means that the monocoque successfully passed safety and drivability requirements. Unfortunately, some of the important performance goals set by FMD were not met, such as the final weight and torsional stiffness goals. While it is unfortunate that these goals were not met, the chassis has still performed well during testing and served its purpose as a lightweight racecar chassis.

Table 30. Design specification verification checklist, used to quantify the results of the project.

Spec #	Description	Target	Tolerance	Result	Specification Met (Y/N)
1	Weight of monocoque only	25 lb	max	30.0 lb	N
2	Torsional stiffness of monocoque and front suspension only, determined from torsion test displacements between front hub and aft of tub	2148 lb*ft/deg	min	1982 lb*ft/deg	N
3	Area of cockpit opening, which varies based on size of closeouts used around cockpit opening	440 in^2	± 10	595 in^2	Y
4	Cross sectional area of front tub, based off of SAE rules	195 in^2	min	235 in^2	Y
5	Max operating temperature of carbon face sheets, based off of glass transition temperature	150 ^oF	min	350 ^oF	Y
6	Egress time from seated driving position	5 sec	max	4 sec	Y
7	Visual rating of appearance	9/10	± 1	5	N
8	Driver rating of comfort	9/10	± 1	8	Y
9	Cost (Cost Report), manipulated by obtaining accurate measurements and using simplified processes	$3,500	max	$2,925	Y
10	Safety factors for primary loading from suspension pickup points, pedal box assembly mounting, and joint to rear subframe	2	min	1.7	N
11	Energy absorption of nosecone, undergoing quasi-static loading	7350 J	min	7391 J	Y
12	Flat mounting regions, used for interfacing with other subsystems, primarily suspension, aerodynamics, and driver controls	1.5x required mounting area (for adjustability)	min	Modular	Y
13	Strength requirements from FSAE rules, located at side-impact structure, front roll hoop bracing, and front bulkhead support	67 kN 35.9 kN 99 kN	min	201 kN 64 kN 145 kN	Y
14	Front bulkhead cutout, used for ease of accessibility for pedal box assembly changes	10" x 10"	min	11” x 11”	Y
15	Cable routing cutout for brake lines and DAQ wires	5/8" x 3/4"	min	Ø3/4"	Y

Conclusions and Recommendations

Time Management

Designing and manufacturing a composite monocoque necessitates enormous resources. Ensuring that these resources are in place by concrete deadlines is a requirement for a successful project.

Design must incorporate interfaces with other systems and their loads, a robust FEM, an understanding of manufacturing with composite materials, and quick flexibility that comes with an iterative design process such as a Formula SAE car.

Manufacturing also requires many areas of competency including rapid production of test samples, development of successful methods for every complex procedure on the final part, a large and skilled labor pool, and materials availability.

Effective time management of design and manufacturing requirements was successful in some areas of this project and lacking in several others. The first success was limiting the project scope to the monocoque laminate, nosecone, anti-intrusion plate, and firewall. This scope should have allowed sufficient time to develop all of these components. Maintaining this type of focus is recommended for future teams. Secondly, a group of skilled composites workers was rapidly developed at the start of the 2014 school year. This is discussed in more depth shortly, and is also recommended. Thirdly, a detailed Gantt chart schedule was created at the start of the project and incorporated all major and most minor milestones. Lastly, FMD rapidly developed laminates that met the SES upon its late-into-the-design-cycle release in December. Tapping a large reserve of resources at this time is what allowed for rapidly-developed laminates despite labor also being diverted to other manufacturing concerns.

While some successes in time management occurred, many more could have been implanted that would have allowed a high-quality product to be completed at an earlier date. Significant time was spent at the beginning of the project (Spring 2014) on improving the FEM instead of on other considerations such as improvements in the torsional test fixturing, monocoque geometry, and driver positioning. While many advancements were incorporated into the model, in the end, going into the summer months with a more comprehensive set of design requirements rather than one honed tool would have benefited the project. Additionally, having basic design near completion at this time would have allowed for testing of manufacturing methods over the summer and into the fall when only minor design changes from other systems' iterations could have otherwise been implemented. Thus, FMD recommends that basic design and model improvement is completed prior to the summer break. This could mean starting the design process earlier (i.e. winter quarter) and producing the same amount of design tool improvements, but given the manufacturing schedule of the prior year's Formula SAE car, this option is unlikely. Instead, prioritizing design tool capabilities and requirements should be performed at the embryonic stages of the project and given hard deadlines.

The above however assumes material availability, which was also problematic for FMD. Here some factors were out of the group's control such as the team's previous supplier of carbon fiber, core, and film adhesive backing out of their prior commitment for the 2015 vehicle. Prepreg carbon fiber was extremely difficult to procure. Several prepreg manufacturers and aerospace companies told FMD that they had high-modulus 350°F cloth and unidirectional tape available, but given the 250°F rating of the molds, this was unusable. See the recommendation below on using carbon fiber tooling as a means to take advantage of these materials in the future. Additionally, there are a highly-limited number of core manufacturers and suppliers. Of them, many are uninterested in supplying the small quantities required for a Formula SAE vehicle. Finally, film-adhesive and foaming core splice were believed to be beyond budget of the team, when in actuality, variants of them could have been purchased. All of the above and a freezer failure are good reasons for why material was unavailable for testing during the summer and fall; however, the major takeaway from the above is that *composite materials are difficult to source on a Formula SAE budget and provisions must be established to keep future chassis on schedule if materials are unavailable.*

Instead of producing a schedule of major milestones and modifying it when milestones are not achieved on time, contingencies must be established. For instance, if all composite materials required for testing manufacturing methods and SAE rules compliance are not obtained by a set date, then either the previous year's chassis is used (if applicable) or a steel-tube design is pursued. Another provision could include setting aside emergency funds to purchase the materials outright from an industry composites supplier. If this option is selected, it should be noted that some materials like core are custom order and have lead times. These lead times should be incorporated into the set date. A composite chassis cannot be manufactured without sample experimentation of manufacturing techniques such as core splicing and bends around compound radii. As such, if the materials are not present to perform these tests, the tests will need to be done at a later date and thus push back the final part's completion date. If these experiments are not performed, errors such as carbon bridging and dry spots will be present in the final part which will increase repair time and extend the project's completion date. A later chassis finish date most likely will be detrimental to the vehicle's dynamic testing program. With 68% of the available points at competition resulting from dynamic events, this delay could prove costly.

Additionally, future teams should consider SAE's timetable for releasing the SES when scheduling a monocoque's production. It should be noted here that the AFR timetable for review is unacceptable in producing a vehicle with sufficient dynamic testing time as noted in the Applicable Standards subheading of the Background section of this report. SAE releases new rules every two years in August, with the SES released in December. The SES in these two-year periods typically remains unchanged, and in the second year, it would be safe to assume parity and begin laminate development as soon as resources become available. However, when the two-year cycle expires, the SES can change dramatically and a laminate which met the old SES may no longer comply with the updated version. As such, during these transitory years, time spent developing a laminate (in depth) in the summer and fall is poorly utilized. Instead, it is recommended to perform manufacturing technique experimentation during this time and leave only the SES laminates to be developed during December when the rules are released.

The above issues of not establishing contingencies for missed deadlines (in design or material) and of developing SES laminates too early are the primary reasons for FMD's delay in finishing the monocoque and for the manufacturing errors covered previously in the report. Material delay led to concurrently developing manufacturing techniques and laminates. The results were techniques that were not entirely successful and laminates that were heavier than needed. To reiterate: had suitable materials been obtained earlier, testing on techniques such as core-splicing, compound radii core forming, lap-joint overlap widths, and other manufacturing methods could have been conducted in the summer and fall; and SES testing could have begun in December. While this is later than desired in terms of the Formula SAE's team Critical Design Review, potential laminate schedules are of little use without the rules specifications being known, so presenting an arbitrary laminate schedule at this review is not entirely useful. Moreover, now that the FEM has been dramatically improved, time can be spent in the spring improving SES rules models so that once the document is released, more work can be done analytically in terms of developing a laminate for strength and stiffness. Additionally, since materials will already be on-hand, actual mechanical properties can be evaluated via destructive testing and incorporated into the FEMs (as done late in Fall 2014)—further improving correlation.

Despite the problems mentioned above in material acquisition, it should be noted that the composite materials sponsors of this project including TenCate, Plascore, Toray, and SpaceX, and C&D Zodiac, and Airtech were all phenomenal in their service and speed in delivering products at low or no cost to the team. Once contact was made with these companies, they were quick to respond and rushed delivery of the requested materials.

Dedicated Composites Advisor and Sub-Team

Designing, testing, and building a composite chassis requires a large body of first-hand design experience, manufacturing knowledge and skilled physical labor. For these reasons, FMD recommends future teams secure one or more advisors with composites-specific experience and continue the Formula SAE Composites sub-team.

Frequent meetings or regular design reviews on topics such as mold production, finite element modeling, laminate construction, and more could be conducted with this advisor resulting in a high-quality part and increased knowledge transfer. Moreover, closer industry collaboration will lead to better trained graduates that are more capable of immediately contributing to composites companies during internships or upon graduation.

Additionally, recognizing the increased use of composites on the Cal Poly Formula SAE racecar, a Composites sub-team was created at the end of the 2014 season to assist with chassis, aerodynamic, and other systems' composites parts. FMD strongly recommends the continuation of this sub-team which significantly contributed knowledge and skilled labor toward passing rules and manufacturing the monocoque. Over 120 test panels were produced in order to pass rules, test core-forming, evaluate lap joint requirements, and more—and without the dedicated Composites team to share in manufacturing requirements, this large number of parts could not have been produced. Combining proven industry methods for designing and manufacturing composite parts with a skilled body of capable workers is yet another resource to ensure that future monocoques continue to progress.

Monocoque Strength

With the exception of the core failure at the front rocker mounts, the monocoque has not experienced any noticeable mechanical failures. Periodic inspection of the suspension, pedal-box, and roll hoop pickups showed no evidence of face-sheet cracking or any visible deflection characteristic of core failure. Considering the CLT analysis, the monocoque laminate is performing as expected, with no observable skin failures after approximately 5 hours of driving time.

Future teams should consider doing comparative long beam bend tests to assess the facesheet performance of core-bridged and resin-dry panels, compared to properly manufactured panels since it is likely at least a minimal amount of bridging or dryness will occur on the monocoque. For example: a long beam flat panel can be intentionally manufactured with a core bridge along the mid-span, which will likely result in local resin dryness. Long beam testing will isolate the flawed panel's facesheet stiffness and strength, which can be compared to values from a properly manufactured panel. This testing approach will at least provide insight into the impact of bridging on laminate performance. Similar tests can be conducted to examine the performance effects of core splicing, facesheet overlap, and splice filler material.

Monocoque Geometry

The geometry of the monocoque can be modified to ease manufacturing and post-processing. As noted earlier, one of the major obstacles experienced by the FMD team was contouring the aluminum core around radii, especially compound radii with multiple curvatures. Minimizing compound bends in the geometry would significantly ease manufacturing time and improve the final quality of the part. Bridging would be less likely to occur with less radii in the geometry of the mold. Any radii used should be large enough so that the core can easily be bent into the mold.

Additionally, all points where brackets are attached to the monocoque should be made perfectly flat. This allows balsa core to be easily placed in these regions, without additionally forming required. Additionally, areas that are highly loaded need to be flat to ensure maximum surface area contact between the load-bearing bracket and the monocoque. This should prevent the need for shims experienced by the FMD team at places like the suspension rocker mounting location.

As noted previously, decreasing the size of the cockpit opening has the potential to increase torsional stiffness. Future teams should conduct a weight vs. stiffness study on the size of the cockpit opening. A smaller cockpit opening offers better transfer of torsional load across the chassis, thus increasing torsional rigidity. Unfortunately, ergonomic requirements will restrict the opening from being decreased indefinitely. However, the oversized opening in the current chassis offers potential for improvement.

Carbon-Fiber Tooling

Utilization of prepreg tooling carbon-fiber to produce a female mold for the monocoque provides several key benefits for future teams.

The first benefit is matching coefficients of thermal expansion that would allow the use of 350°F cure carbon-fiber prepregs. When constructing a chassis intended to produce the highest specific stiffness with a suitable specific strength, the stiffest and strongest aerospace prepregs are the best choice. In the process of obtaining materials for the 2015 monocoque, sponsors offered several 350°F cure carbon-epoxy prepregs with moduli and ultimate strengths far exceeding the laminates used the actual layup, but their offers had to be declined given the available 250°F-safe tooling. Bringing the plaster-hemp molds past 250°F can lead to temperature-induced cracking and mold breakdown. Moreover, since the plaster molds expand with heat and contract with cooling at a greater rate than carbon-fiber tooling, the monocoque has residual stress that weakens the final part. Thus using carbon-fiber tooling with similar coefficients of thermal expansion solves two problems by allowing the use of even higher-grade base material and reducing residual stresses in the chassis.

The second benefit of a carbon-fiber tool is improved heat transfer rates between the oven surroundings and the part. The thickness of the plaster molds and the insulating properties of this ceramic material resulted in low and uneven heat transfer rates from the oven air to the part surface as measured by thermocouples. The result of which was uneven resin content and poor surface finish due to excess resin flow in some regions and insufficient movement in other zones. Moreover, cure cycles of over 10 hours were required which meant the manufacturer-recommended recipes could not be utilized. With the thinner mold and higher heat transfer rates that carbon tooling allows resin flow and cure cycling can be improved significantly, with the net result being a better-looking, higher-performance part.

The third set of benefits of carbon-fiber tooling is increased durability and transportability over the plaster-hemp molds. C&D Zodiac regularly obtains 3-5 heat cycles from the ceramic molds whereas carbon-tooling typically lasts at least 20 cures. Scaled sample layups ("blog layups") inside the actual mold are the best for experimenting with layup technique and the 3-5 heat cycle capability of the plaster molds is limiting here, especially if the molds are used for multiple years. Moreover, the plaster molds weigh 500 pounds each and are time consuming and potentially dangerous to move on campus or to offsite autoclave facilities (if desired). The longer life and reduced weight of carbon-fiber molds would again lead to higher part quality through increased experimentation and better allocation of team labor.

Lastly, C&D Zodiac has been extremely generous is donating time, expertise, and materials to several past Cal Poly Formula SAE teams that utilized their plaster-hemp molds to produce quality monocoques. With improvements in composites technology gained through FCW and FMD, tougher SAE rules, and a higher level of performance required at competition it is believed that the switch to carbon-tooling in imminent. Should C&D Zodiac be in a position to sponsor future molds, this type of construction would provide the benefit of reducing their cost as only plugs would need to be manufactured. For this reason and those above, FMD recommends future teams perform a proof of concept utilizing newly-acquired tooling carbon-fiber prepreg and begin seeking out ultra-high performance 350°F aerospace cloth and unidirectional tape.

Drilling Holes

The FMD team ran into problems several times when drilling holes for components that mounted to the monocoque. Holes were typically located by center-punching hole-centers through the component that was to be mounted, and then center drilling the punch before stepping up drill sizes to the final insert size. A steel drill guide was used to keep the holes normal to the monocoque surface. Unfortunately, sometimes the holes did not initially match so some additional machining was required to attach the accessory component. In order to allow the same brackets to be used, the holes on the attachments were slotted such that the bracket would fit without further alteration of the monocoque.

A more accurate way to locate holes would be to score the buck where bolt holes are required. Ideally, this would be done with the CNC router machining the buck. The score will show up in the final monocoque layup, and the holes can be drilled accurately with a center drill and drill guide. However, even with hole centers located through the mold, it is still recommended that jigs are used to properly locate holes once the tub is finally bonded and post-cured, in order to prevent error in between these steps. For example, see Formula Chassis Work's report on how suspension holes were located. [Ref. 4]

Surface Finish and Facesheet Continuity

The surface finish took on a dull and clouded appearance, with yellow colored concentrations of resin visible in certain areas. Before the repair patches were applied, resin dryness and exposed fibers were present in areas of bridging.

Contrary to the lackluster appearance of the tub, flat test panels were uniform and glossy. The improved surface finish of the flat panels is likely do to sufficient compaction of the face-sheets, which is easy to achieve with a flat tool and caul plate. For the tub layup, this degree of compaction was impossible to achieve considering the poor formability of standard hexagonal aluminum core. The vacuum cure did not sufficiently and evenly press the laminate tightly against the mold surface. This compromised skin compaction, producing visible resin pools and a muddy appearance. More important than aesthetics is the strength loss such a compromised compaction produces.

These surface finish and facesheet continuity issues could be remedied by using a more formable core material, like honeycomb Nomex or Flex-Core (aluminum or Nomex). It is considered essential by FMD that future monocoques utilize one of these formable core variants on radii. Honeycomb Nomex is relatively easy to compress and springs back against adjacent core sections, thus reducing bridging. However, this compaction adds weight as seen in 2013 and therefore using Flex-Core (aluminum or Nomex) for all simple radii corners is recommended. 2013 had good results with bridging and surface finish on compound radii by compressing honeycomb Nomex into these regions.

Speaking with a former Lotus F1 composites engineer, one of the Cal Poly Formula SAE team members also learned of a method where heat is used to loosen the core-ribbon adhesive in order to form the core to the mold. Flat sheets of core are placed over the mold and the whole unit is placed inside a vacuum bag. Next the unit is heated in an oven under slight vacuum pressure until the core adhesive begins to bond and the flat sheets starts to contour into the mold. The core is adjusted as needed and vacuum is increased until the core is formed to the tool. This is done in sections for the entire mold surface.

A pressure cure could have also produced better compaction and mitigated the severity of core bridging on the tool side, though good core-splicing is more important on the exposed facesheet with the addition of external pressure.

Finally, the use of the correct film-adhesive and foaming core-splice should be pursued with new sponsorships available to the team. Late in the year, contact was made with a major supplier that has provided samples of high-tack film adhesive and foaming epoxy core splice. High-tack adhesive will allow for better core to facesheet bonding. From speaking with FCW, this film-adhesive is much more difficult to work with given its propensity to quickly adhere, but given the complex geometry of a Formula SAE chassis, high-tack adhesive is required. If the prepreg used is not proven to be as self-adhering as the TC250-AS4, then this film-adhesive should be used on the entire facesheet. This will add weight but reduce the likelihood of delamination.

Lastly, foaming core splice, not film adhesive should be used between core sections. This epoxy product expands rapidly with heat and prevents carbon at core splices.

Using the Structural Equivalency Spreadsheet

During the laminate development phase, FMD assumed that using the structural equivalency spreadsheet would be straightforward and relatively free of ambiguity. SAE has iterated and improved on the SES for several years, but the most recent version had a multitude of revisions and additions that were not without flawed formulas. On several occasions, inputting laminate testing data would return questionable equivalency results. For instance, the equivalency formulas governing the cockpit floor required a skin thickness of 8 millimeters, which was entirely unfeasible. FMD submitted four SES formula corrections, all of which were acknowledged by SAE as legitimate claims. SAE fixed three of these four errors and updated the SES accordingly, while the fourth error is scheduled to be fixed in next year’s SES version. Collectively, these SES clarifications set the laminate design process back a week, and many potential laminates tested prior to the inquiries were later found to be overbuilt. In the event that the SES undergoes significant changes, it is highly recommend that FSAE teams start preliminary laminate testing early in order to identify potential formula errors. Laminates that have passed in previous years can be inputted into newer SES versions to check for any gross errors or unexpected results.

Appendix A

References

1. Bailie, J. A., Ley, R.P., & Pasricha, A. (1997). *A Summary and Review of Composite Laminate Design Guidelines*.

2. Cremens, W. S. (1980). *Thermal expansion molding process for aircraft composite structures.*

3. Crolla, David. (2000) "The Effect of Chassis Stiffness on Race Car Handling Balance"

4. Hagan, M., Rappolt, J., & Waldrop, J. (2013). *Formula SAE hybrid carbon fiber monocoque/steel tube frame chassis.*

5. Huschilt, T., Norris, C., Roberts, N., & Page, M. (2002). *Development of the Swift 014.a racecar for the CART Toyota Atlantic Championship Series.*

6. Levy, B. S., & Preban A. G. (1980). *The use of increased curvature to reduce weight of body panels.*

7. Riley, W. B., & George, A. R. (2002). *Design, analysis, and testing of a Formula SAE car chassis.*

8. "2014 Formula SAE Rules.". SAE International, 1 Jan. 2013. Web. 1 May 2014. <http://students.sae.org/cds/formulaseries/rules/2014_fsae_rules.pdf>.

9. Wright, Jonathan Macy. (2000). *Characterization of the Effects of Multiple Cure Cycles on a Carbon Fiber Epoxy Composite.*

Appendix B

House of Quality

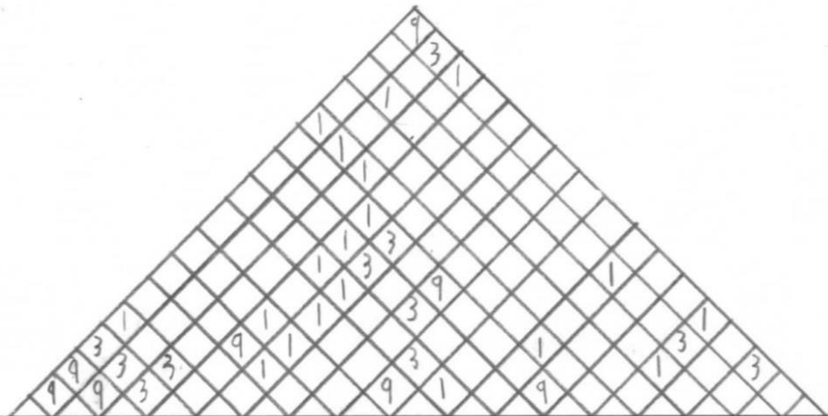

Benchmarks

Formula Monocoque Development

Customer (Step #1) Requirements (Whats) / Customer Requirements (Step #2)	Driver/Dynamic Performance	Manufacturer	Mechanics	Judges	Torsional Stiffness [lb*ft/deg]	Weight [lb]	Specific Stiffness ((lb*ft/degree)/lb)	Area of Cockpit Opening [in^2]	Cross sectional Area of Front Tub [in^2]	Max Operating Temperature [F]	Egress Time [s]	Drag Coefficient [Cd]	Lift Coefficient [Cl]	Visual Rating of Appearance [1-10 scale]	Driver Rating of Comfort [1-10 scale]	Range of Body Movement [inches]	Cost [$]	Difficulty of Accomplishing Task [%]	Safety Factor [#]	% of Available Space w/ Respect to Attachment	Energy Absorption [kJ]	2013/2014 Chassis		
Functional Performance																								
Sufficiently stiff	12	3	1	9	9	3	9	3	3											1	3	3		
Lightweight	12	3	3	9	3	9	9	1	1								1		3	3	3	2		
Weather resistance	6	3	1	2						9							1		1			2		
Road hazard resistance	5	3	1	3											1		1		1			2		
Least likely failure mode	1	3	8	7						3									9		3	1		
Minimal drag	4	3	1	4				1	3			9	9	3						3	3	2		
Design change flexibility	1	30	1	6					1			1	1	1				3	3	9		4		
Quick to egress	7	3	1	1				9	3		9	3	3	1	3	3		3				4		
Lift/Downforce	6	3	1	5					1			9	9	3							1	1		
Human Factors																								
Fits range of driver sizes	8	3	4	5				3	3		3				9	3	3	1				5		
Adequate support for drivers	10	3	1	5					3		3				9	9	1	1				2		
Comfortable	8	3	1	5				3	3		3			1	9	9	3	1				5		
Safe	8	3	1	9	1		1				9				1	3			9	3	9	5		
Looks fast	3	7	1	1				1	1			9	9	9		1	1			1	1	4		
Servicibility																								
Easy to attach components	1	3	13	3				1	3									9		3	1	2		
Easy to dettach components	1	3	13	2				1	3									9		3	1	2		
Easy to attach subframe	1	3	13	2														9				2		
Easy to dettach subframe	1	3	12	2														9				3		
Tool accessibility	1	3	19	5				1	3									9			1	4		
Rules																								
Meets templates	1	3	1	1				9	9		3				3	1						5		
Strength requirements	1	3	1	7	3	3	3		3	3									9	3	9	4		
Harness requirements	1	3	1	1							3				3	3		3				4		
Cheap	1	3	1	6	1	1	1							1			9		3			1		
	100	100	100	100																				
2013/2014 Chassis					4435	31	143	460	210	130	4			9	9	4	4880	100	10	70	9860			
Target					5000	31	157	440	195	175	5	Lower	Higher	9	9	2	3500	80	5	70	7600			

Appendix C

Impact Attenuator Data Requirement

T3.22 Impact Attenuator Data Requirement *T3.22.1 All teams, whether they are using their own design of IA or the "standard" FSAE Impact Attenuator, must submit an Impact Attenuator Data Report using the Impact Attenuator Data (IAD) Template found at "Downloads" at http://www.fsaeonline.com.*

T3.22.2 The team must submit test data to show that their Impact Attenuator *Assembly*, when mounted on the front of a vehicle with a total mass of 300 kg (661 lbs.) and run into a solid, non-yielding impact barrier with a velocity of impact of 7.0 meters/second (23.0 ft/sec), would give an average deceleration of the vehicle not to exceed 20 g's, with a peak deceleration less than or equal to 40 g's. Total energy absorbed must meet or exceed 7350 Joules.

> **NOTE 1**: These are the attenuator functional requirements not test requirements. Quasi-static testing is allowed.
>
> ***NOTE 2****: The calculations of how the reported absorbed energy, average deceleration, and peak deceleration figures have been derived from the test data MUST be included in the report and appended to the report template.*40
>

T3.22.3 Teams using a front wing must prove the combined Impact Attenuator Assembly and front wing do not exceed the peak deceleration of rule T3.22.2. Teams can use the following methods to show the designs does not exceed 300 kg times 40g or 120 kN:

a. Physical testing of the Impact Attenuator Assembly with wing mounts, links, vertical plates, and a structural representation of the aerofoil section to determine the peak force. See fsaeonline.com FAQs for an example of the structure to be included in the test.

b. Combine the peak force from physical testing of the Impact Attenuator Assembly with the wing mount failure load calculated from fastener shear and/or link buckling.

c. Combine the Standard Impact Attenuator peak load of 95kN with the wing mount failure load calculated from fastener shear and/or link buckling.

T3.22.4 When using acceleration data, the average deceleration must be calculated based on the raw data. The peak deceleration can be assessed based on the raw data, and if peaks above the 40g limit are apparent in the data, it can then be filtered with a Channel Filter Class (CFC) 60 (100 Hz) filter per SAE Recommended Practice J211 "Instrumentation for Impact Test", or a 100 Hz, 3rd order, low pass Butterworth (-3dB at 100 Hz) filter.

Appendix D

Hexcel Short Beam Sandwich Shear Test

Short Beam Shear Test

The typical span for this test is 4 inches (See Fig. 2). Although there are several possible failure modes for this test, the typical failure mode is a shear failure in the core.

From the short beam flexure test, provided the failure occurs in the core, the core shear strength (average shear stress) can be calculated by the following equation:

$$\text{shear stress } \tau = \frac{P}{2cw}$$

where: P = total load
c = core thickness
w = width of panel

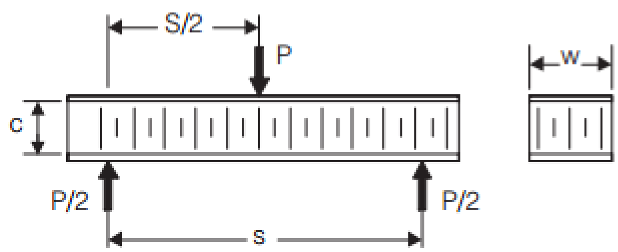

Figure 2

Figure D1. Hexcel short-beam shear test details.

Appendix E

ASTM D2344 Short Beam Shear Test

Test Fixture Requirements:

Support span: 0.5’’

Panel dimensions: 1’’ x 0.25’’

ILSS calculations:

$$ILSS = \frac{0.75 * P}{t * w}$$

P: panel failure load (in.)

t: panel thickness (in.)

w: panel width (in.), as measured with calipers

ILSS: Interlaminar Shear Stress (ksi)

Appendix F

Performance Curves for Final FSAE Laminates

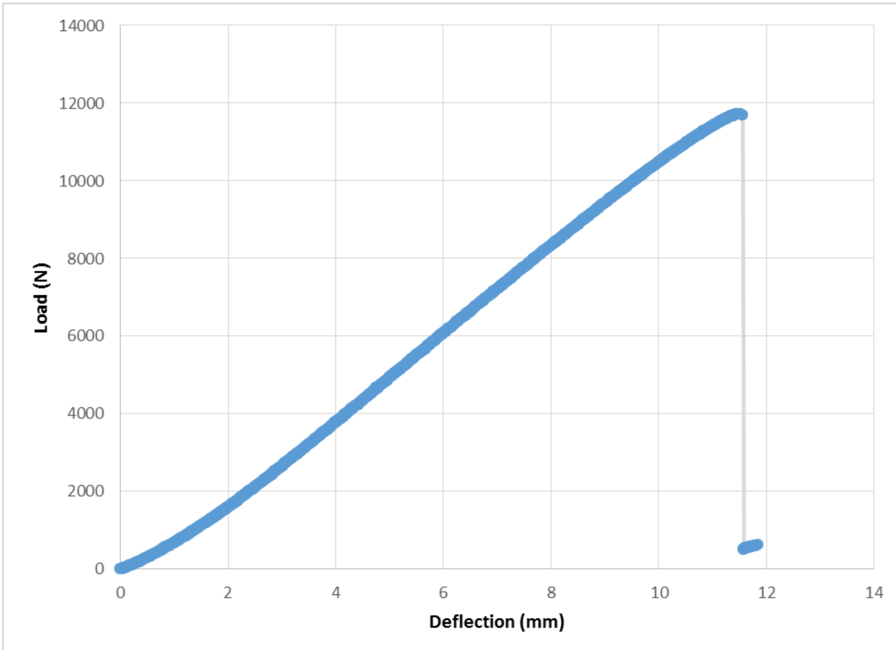

Figure F1: Long beam 3-point bend test results for the side impact structure laminate. Load-deflection behavior is fairly linear until sudden facesheet failure. The upper facesheet fails in compression.

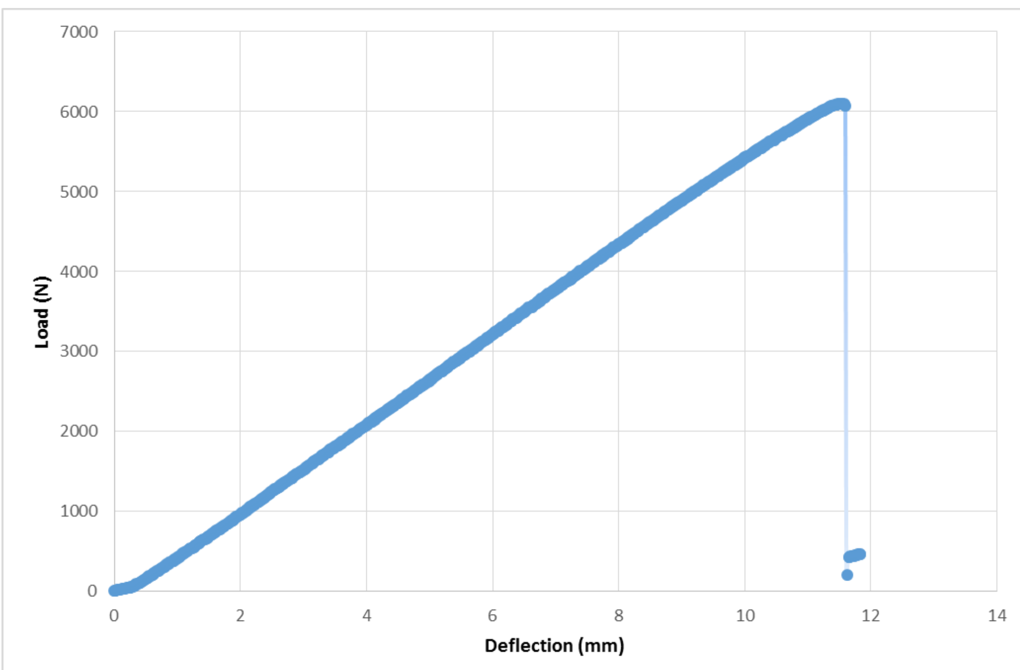

Figure F2: Long beam 3-point bend test results for the cockpit floor, front floor, seat back, front hoop bracing, and front bulkhead support laminates.

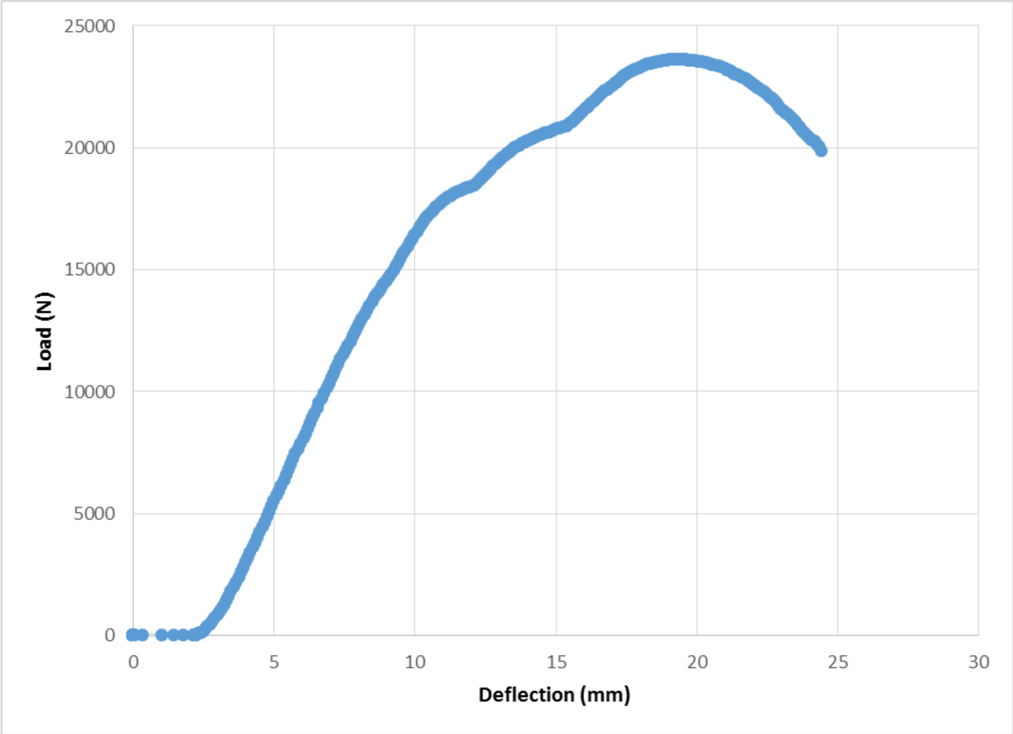

Figure F3: Long beam 3-point bend test results for the front bulkhead.

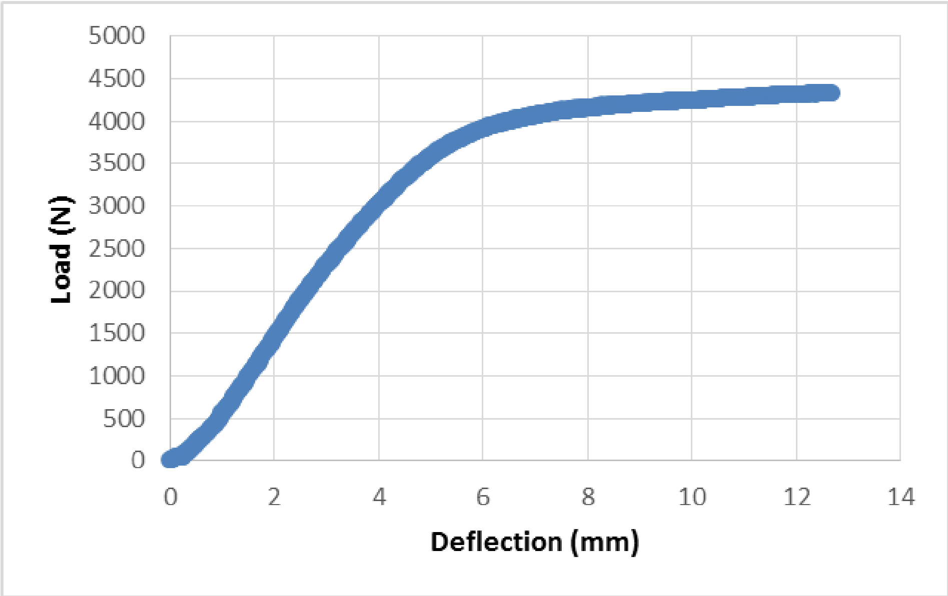

Figure F4: Long beam 3-point bend test results for two 1010 steel tubes, 1’’OD x 065 Wall.

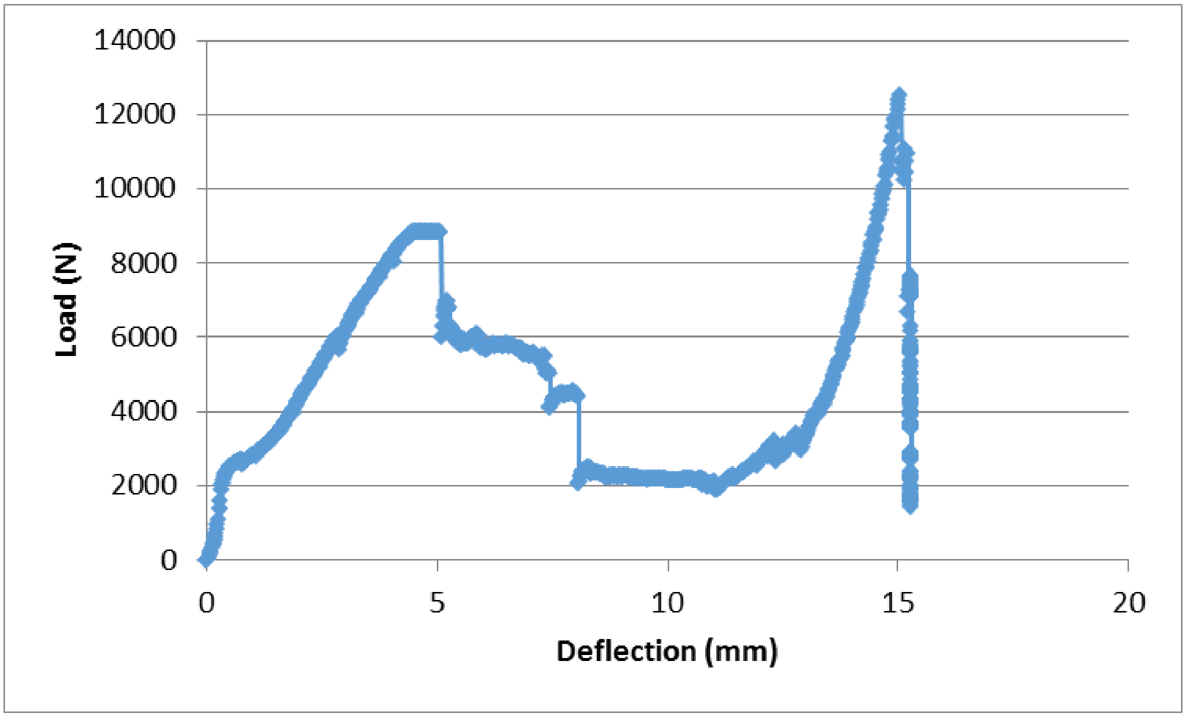

Figure F5. Perimeter shear test results for the side impact structure laminate. The first peak represents the failure of the first facesheet, and the second peak indicates the failure of the second facesheet.

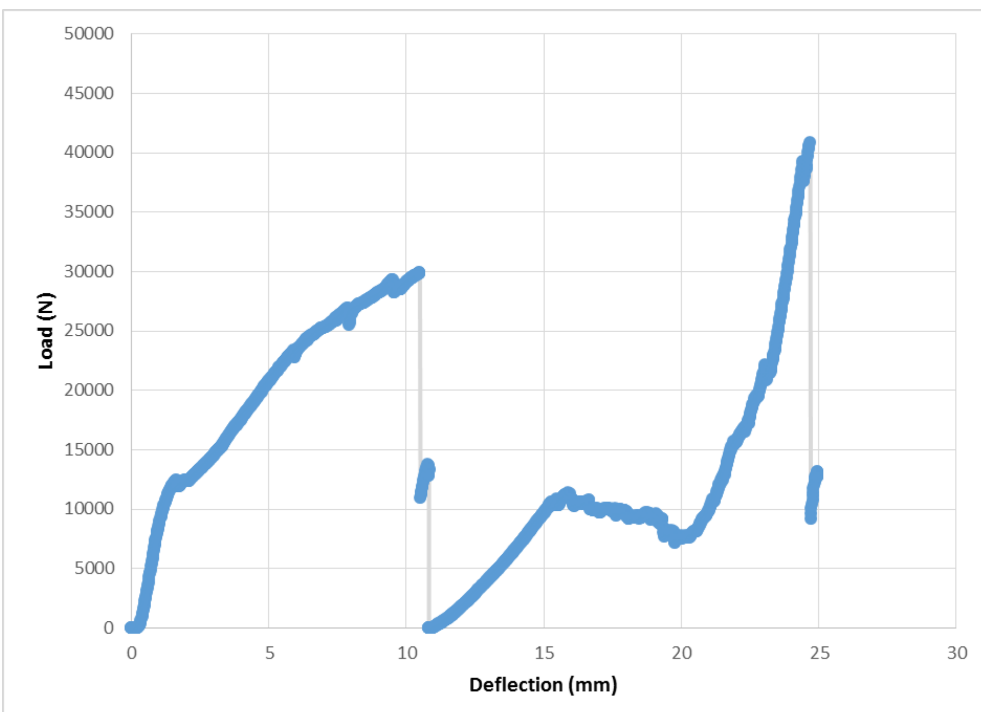

Figure F6: Perimeter shear test results for the front bulkhead laminate.

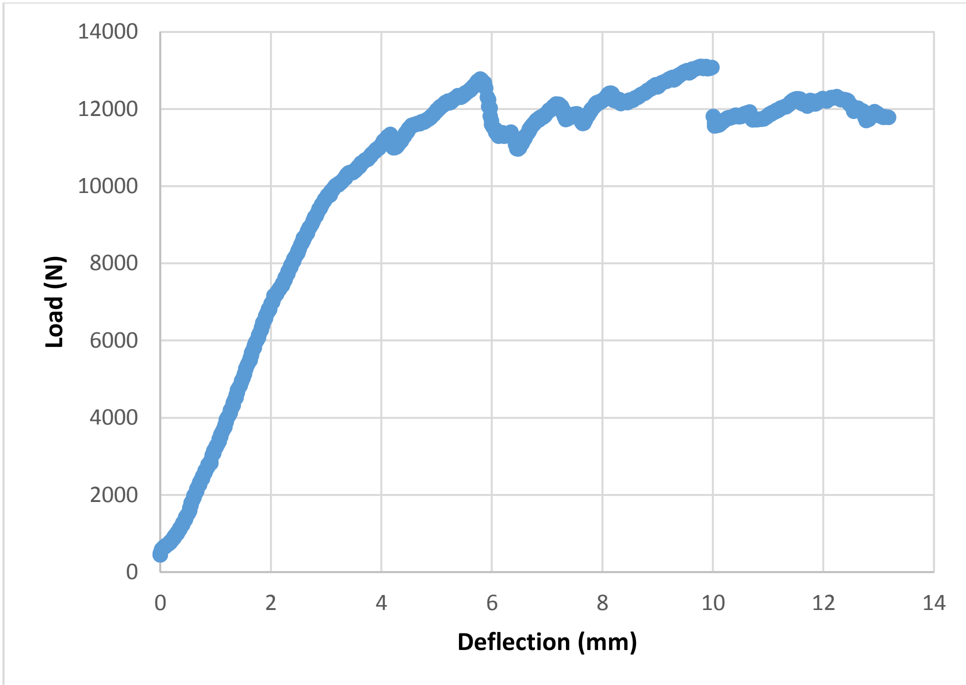

Figure F7. Cockpit pullout test results for the cockpit floor laminate.

Appendix G

Assembly Layout Drawing

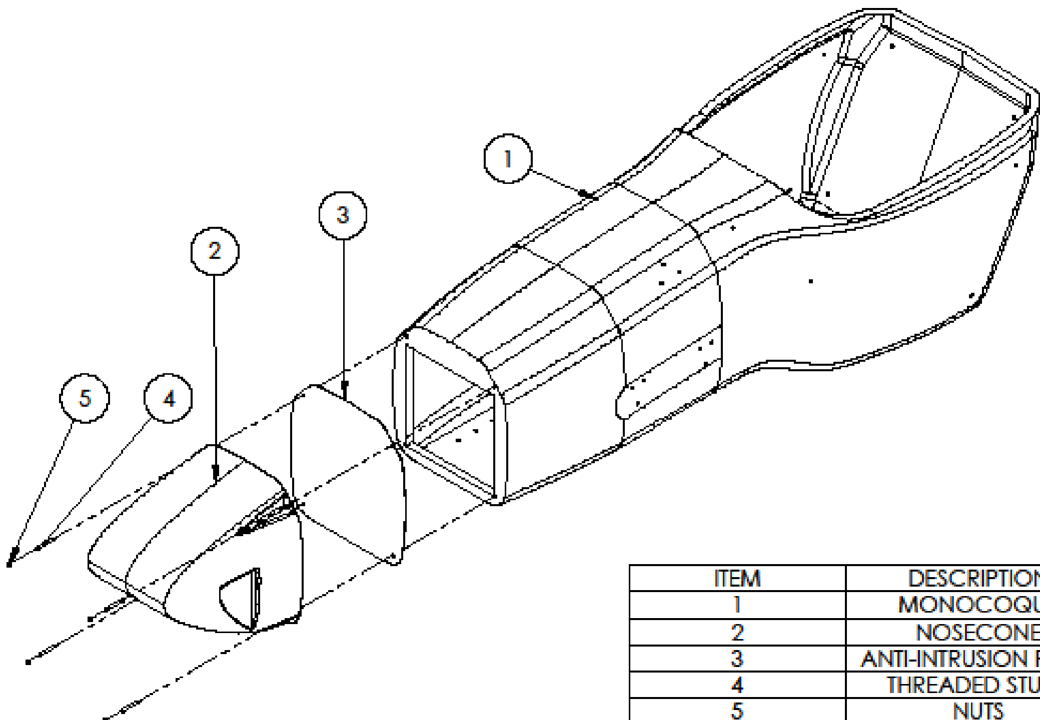

ITEM	DESCRIPTION	QUANTITY
1	MONOCOQUE	1
2	NOSECONE	1
3	ANTI-INTRUSION PLATE	1
4	THREADED STUDS	4
5	NUTS	4

UNLESS OTHERWISE SPECIFIED:
DIMENSIONS ARE IN INCHES
TOLERANCES:
FRACTIONAL±
ANGULAR: MACH± BEND ±
TWO PLACE DECIMAL ±
THREE PLACE DECIMAL ±
INTERPRET GEOMETRIC TOLERANCING PER:
MATERIAL
FINISH
DO NOT SCALE DRAWING

	NAME	DATE
DRAWN		
CHECKED		
ENG APPR.		
MFG APPR.		
Q.A.		

COMMENTS:

TITLE: FRONT CHASSIS ASSEMBLY

SIZE A | DWG. NO. | REV A

SCALE:12 | WEIGHT: | SHEET 1 OF 1

NEXT ASSY | USED ON
APPLICATION

PROPRIETARY AND CONFIDENTIAL
THE INFORMATION CONTAINED IN THIS DRAWING IS THE SOLE PROPERTY OF <INSERT COMPANY NAME HERE>. ANY REPRODUCTION IN PART OR AS A WHOLE WITHOUT THE WRITTEN PERMISSION OF <INSERT COMPANY NAME HERE> IS PROHIBITED.

5 4 3 2 1

Appendix H

Material Data Sheets

Figure H1. AS4 Data sheet.

Figure H2. TC250 Data sheet.

Figure H3. T800 Data sheet.

Figure H4. 2510 Data sheet.

Figure H5. M55J Data sheet.

Figure H6. MTM49 Data sheet.

Figure H7. Aluminum Core Data sheet.

Figure H8. Reflective Tape Data sheet.

Figure H9. 3M DP420 structural adhesive Data sheet.

HexTow® AS4

Carbon Fiber

Product Data

HexTow® AS4 carbon fiber is a continuous, high strength, high strain, PAN based fiber available in 3,000 (3K), 6,000 (6K) and 12,000 (12K) filament count tows. This fiber has been surface treated and can be sized to improve its interlaminar shear properties, handling characteristics, and structural properties, and is suggested for use in weaving, prepregging, filament winding, braiding, and pultrusion.

AS4-GP 3k (1%), AS4-GP 12k (0.9%), and AS4 12k carbon fibers have been qualified to NMS 818 Carbon Fiber Specification (NCAMP). This allows customers to call out an industry standard, aerospace grade carbon fiber without the need to write and maintain their own specification.

Typical Fiber Properties	U.S. Units	SI Units
Tensile Strength		
3K	670 ksi	4,620 MPa
6K	640 ksi	4,410 MPa
12K	640 ksi	4,410 MPa
Tensile Modulus (Chord 6000-1000)	33.5 Msi	231 GPa
Ultimate Elongation at Failure		
3K	1.8%	1.8%
6K	1.7%	1.7%
12K	1.7%	1.7%
Density	0.0647 lb/in^3	1.79 g/cm^3
Weight/Length		
3K	11.8×10^{-6} lb/in	0.210 g/m
6K	23.9×10^{-6} lb/in	0.427 g/m
12K	48.0×10^{-6} lb/in	0.858 g/m
Approximate Yield		
3K	7,086 ft/lb	4.76 m/g
6K	3,485 ft/lb	2.34 m/g
12K	1,734 ft/lb	1.17 m/g
Tow Cross-Sectional Area		
3K	1.82×10^{-4} in^2	0.12 mm^2
6K	3.70×10^{-4} in^2	0.24 mm^2
12K	7.43×10^{-4} in^2	0.48 mm^2
Filament Diameter	0.280 mil	7.1 microns
Carbon Content	94.0%	94.0%
Twist	Never Twisted	Never Twisted

Typical HexPly 8552 Composite Properties (at Room Temperature)	U.S. Units	SI Units	Test Method
0º Tensile Strength	320 ksi	2,205 MPa	ASTM D3039
0º Tensile Modulus	20.5 Msi	141 GPa	
0º Tensile Strain	1.55%	1.55%	
0º Flexural Strength	274 ksi	1,889 MPa	ASTM D790
0º Flexural Modulus	18.4 Msi	127 GPa	
0º Short Beam Shear Strength	18.5 ksi	128 MPa	ASTM D2344
0º Compressive Strength	222 ksi	1,530 MPa	ASTM Mod. D695
0º Compressive Modulus	18.6 Msi	128 GPa	
0˚ Open Hole Tensile Strength	64 ksi	438 MPa	ASTM D5766
90º Tensile Strength	11.7 ksi	81 MPa	ASTM D3039
Fiber Volume	60%	60%	

HEXCEL®

Yarn/Tow Characteristics	U.S. Units	SI Units
Specific Heat	0.28 Btu/lb-°F	0.27 cal/g-°C
Electrical Resistivity	5.6×10^{-5} ohm-ft	1.7×10^{-3} ohm-cm
Coefficient of Thermal Expansion	-0.35 ppm/ºF	-0.63 ppm/ºC
Thermal Conductivity	3.95 Btu/hr-ft-ºF	6.83 W/m-ºK

Carbon Fiber Certification

This carbon fiber is manufactured to Hexcel aerospace grade specification HS-CP-5000. A copy of this specification is available upon request. A Certification of Analysis will be provided with each shipment.

Available Sizing

Sizing compatible with various resin systems, based on application are available to improve handling characteristics and structural properties. Please see additional information on available Sizes on our website or contact our technical team for additional information.

Packaging

Standard packaging of HexTow® AS4 is as follows:

Filament Count	Nominal Weight		Nominal Length	
	(lb)	(kg)	(ft)	(m)
3K	4.0	1.8	28,340	8,640
6K	4.0	1.8	13,940	4,250
12K	8.0	3.6	13,870	4,230

Other package sizes may be available on request. The fiber is wound on a 3-inch ID by 11-inch long cardboard tube and overwrapped with plastic film.

Safety Information

Obtain, read, and understand the Material Safety Data Sheet (MSDS) before use of this product.

Important

Hexcel Corporation believes, in good faith, that the technical data and other information provided herein is materially accurate as of the date this document is prepared. Hexcel reserves the right to modify such information at any time. The performance values in this data sheet are considered representative but do not and should not constitute specification minima. The only obligations of Hexcel, including warranties, if any, will be set forth in a contract signed by Hexcel or in Hexcel's then current standard Terms and Conditions of Sale as set forth on the back of Hexcel's Order Acknowledgement.

For more information

Hexcel is a leading worldwide supplier of composite materials to aerospace and other demanding industries. Our comprehensive product range includes:

- Carbon Fiber
- RTM Materials
- Honeycomb Cores
- Carbon, Glass, Aramid and Hybrid Prepregs
- Structural Film Adhesives
- Honeycomb Sandwich Panels
- Special Process Honeycombs
- Reinforced Fabrics

For US quotes, orders and product information call toll-free 1-866-556-2662 and 1-800-987-0658.
For other worldwide sales office telephone numbers and a full address list, please click here:
http://www.hexcel.com/contact/salesoffice

February 2014

HEXCEL®

TENCATE

TENCATE ADVANCED COMPOSITES

TC250 Resin System

PRODUCT TYPE

265°F (130°C) Cure
Toughened Epoxy Resin System

TYPICAL APPLICATIONS

- Aircraft Structures
- Space Structures
- Radomes and Antennae
- Reflectors

SHELF LIFE

Tack Life
45 days at 75°F (24°C)

Out Life
60 days at 75°F (24°C)

Frozen Storage Life
12 months at <0°F (-18°C)

Tack life is the time during which the prepreg retains enough tack, drape and handling for easy component lay-up.

Out life is the maximum time allowed at room temperature before cure.

PRODUCT DESCRIPTION

TC250 is a member of TenCate Advanced Composites' newly derived TC family of toughened matrices for structural advanced composite applications. TC250 offers an excellent balance of toughness, mechanical property translation and hot/wet performance and is easily processed via vacuum bag/oven, autoclave, or press curing operations. Although TC250 is a 265°F (130°C) cure system, it develops very high dry and wet Tg values which enhance the product's elevated temperature performance. TC250 can also be cured or free standing post cured to 350°F (177°C) to increase its high temperature performance.

TC250 is available with virtually all fiber reinforcements in unidirectional tape, slit unidirectional tape, woven and nonwoven prepreg formats.

PRODUCT BENEFITS/FEATURES

- Excellent Mechanical Property Translation
- Can Be Initially Cured at 180°F (82°C) and post cured free standing to 265°F (130°C) or 350°F (177°C) for Prototyping with Low Cost Tooling
- Good Toughness
- Good Surfacing Properties
- Low Laminate Void Content with Low Pressure Vacuum Curing
- NCAMP Tested
- Easy Processing
- Self-Adhesive to Core

NEAT RESIN PHYSICAL PROPERTIES

Density ....1.21 g/cc
Dry Tg...285°F (140°C) cured at 265°F (130°C)
Wet Tg ....257°F (125°C) cured at 265°F (130°C)

Dry Tg ....356°F (180°C) post cured at 350°F (177°C)
Gel Time ....6-10 min. at 265°F (130°C)

STANDARD MODULUS UNITAPE LAMINATE PROPERTIES

Laminate data used UD Tape Prepreg Laminate - HTS-40 12k Carbon Fiber, 150 gsm FAW.
The data below represents limited lot data.

Property	Condition	Method	Results	
Tensile Strength 0°	RTD	ASTM D 3039	305 ksi	2,103 MPa
Tensile Modulus 0°	RTD	ASTM D 3039	20.3 Msi	140 GPa
Tensile Strength 0°	ETW	ASTM D 3039	303 ksi	2,089 MPa
Tensile Modulus 0°	ETW	ASTM D 3039	19.5 Msi	134.4 GPa
Tensile Strength 0°	CTD	ASTM D 3039	293 ksi	2,018 MPa
Tensile Modulus 0°	CTD	ASTM D 3039	20 Msi	138 GPa
Poisson's Ratio	RTD		0.3	
Poisson's Ratio	ETW		0.29	
Poisson's Ratio	CTD		0.35	

Vacuum bag oven cure at 14.5 psi, normalized to 60% fiber volume, ETW: 180°F (82°C) Wet, CTD: -65°F (-54°C)
* Wet conditioning done at 145°F (63°C) and 85% RH until complete saturation

Continue to page 2.

TORAYCOMPOSITES

2510 RECOMMENDED CURE CYCLE

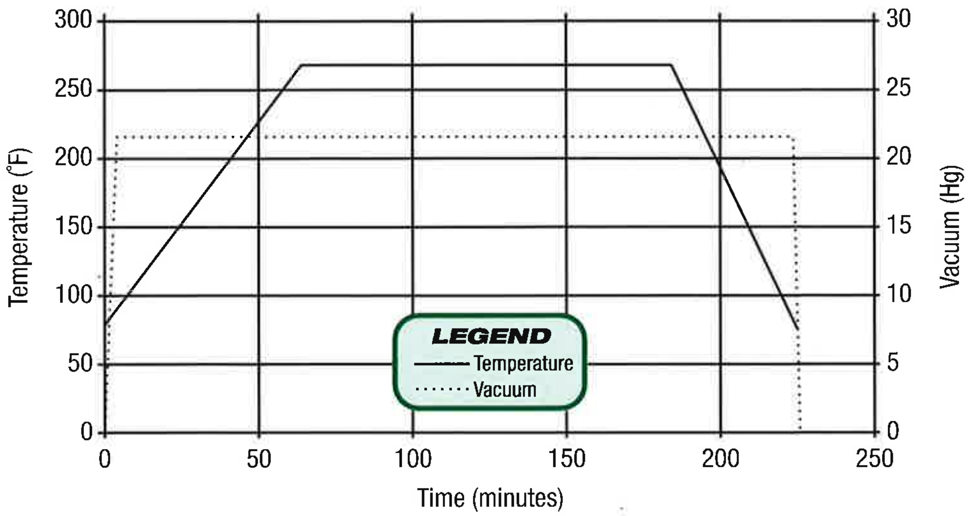

Heat-Up Rate (°F/minute)	Cure Temp. (°F)	Vacuum (in Hg)	Cure Time (minutes)	Cool Down Rate (°F/minute)
3.0 ± 1.0	270 ± 3	22 ± 2	120 + 10/-0	4.5 ± 0.5

NOTES:

1. Apply 22 inches Hg minimum vacuum to the vacuum bag assembly and check for leak prior to the beginning of the cure cycle. The leak rate shall be less than 2.0 in. Hg over 5 minutes.
2. Apply the temperature ramp from ambient to 270 ± 10°F at rate of 3.0 ± 1.0°F per minute.
3. Maintain the cure temperature at 270 ± 3°F for 120-130 minutes.
4. Cool down the temperature to 170°F or lower at a rate of 4.5 ± 0.5°F per minute before removing vacuum.
5. Remove the bagged laminates from the autoclave and de-bag for inspection.

TORAY COMPOSITES AMERICA, INC.

TECHNICAL DATA SHEET
No. CFA-017

TORAYCA®

M55J DATA SHEET

MJ type high modulus fiber with enhanced tensile and compressive strength over *M* series fibers. Mainly used for premium sporting goods, aerospace, and industrial applications.

FIBER PROPERTIES

	English	Metric	Test Method
Tensile Strength	583 ksi	4,020 MPa	TY-030B-01
Tensile Modulus	78.2 Msi	540 GPa	TY-030B-01
Strain	0.8 %	0.8 %	TY-030B-01
Density	0.069 lbs/in^3	1.91 g/cm^3	TY-030B-02
Filament Diameter	2.0E-04 in.	5 µm	
Yield 6K	6,833 ft/lbs	218 g/1000m	TY-030B-03
Sizing Type & Amount 50B		1.0 %	TY-030B-05
Twist	Untwisted		

FUNCTIONAL PROPERTIES

CTE	-1.1 $\alpha \cdot 10^{-6}/^\circ C$
Specific Heat	0.17 $Cal/g \cdot ^\circ C$
Thermal Conductivity	0.372 $Cal/cm \cdot s \cdot ^\circ C$
Electric Resistivity	0.8 x 10^{-3} $\Omega \cdot cm$
Chemical Composition: Carbon	>99 %
Na + K	<50 ppm

COMPOSITE PROPERTIES*

	English	Metric	Test Method
Tensile Strength	290 ksi	2,010 MPa	ASTM D-3039
Tensile Modulus	49.0 Msi	340 GPa	ASTM D-3039
Tensile Strain	0.6 %	0.6 %	ASTM D-3039
Compressive Strength	130 ksi	880 MPa	ASTM D-695
Flexural Strength	180 ksi	1,230 MPa	ASTM D-790
Flexural Modulus	40.5 Msi	280 GPa	ASTM D-790
ILSS	10.0 ksi	7 kgf/mm^2	ASTM D-2344
90° Tensile Strength	5.0 ksi	34 MPa	ASTM D-3039

* Toray 250°F Epoxy Resin. Normalized to 60% fiber volume.

M55J

COMPOSITE PROPERTIES**

Tensile Strength	270 ksi	1,860 MPa	ASTM D-3039
Tensile Modulus	43.5 Msi	300 GPa	ASTM D-3039
Tensile Strain	0.6 %	0.6 %	ASTM D-3039
Compressive Strength	120 ksi	835 MPa	ASTM D-695
Compressive Modulus	41.5 Msi	285 GPa	ASTM D-695
In-Plane Shear Strength	6.5 ksi	44 MPa	ASTM D-3518
ILSS	10.5 ksi	7.5 kgf/mm^2	ASTM D-2344
90° Tensile Strength	5.0 ksi	35 MPa	ASTM D-3039

** Toray Semi-Toughened 350°F Epoxy Resin. Normalized to 60% fiber volume.

See Section 4 for Safety & Handling information. The above properties do not constitute any warranty or guarantee of values. These values are for material selection purposes only. For applications requiring guaranteed values, contact our sales and technical team to establish a material specification document.

PACKAGING

The table below summarizes the tow sizes, twists, sizing types, and packaging available for standard material. Other bobbin sizes may be available on a limited basis.

Tow Sizes	Twist[1]	Sizing	Bobbin Net Weight (kg)	Bobbin Type[2]	Bobbin Size (mm)					Spools per Case	Case Net Weight (kg)
					a	b	c	d	e		
6K	B	50B	0.5	II	76	82	192	107	156	24	12

1 **Twist** A: Twisted yarn B: Untwisted yarn made from a twisted yarn through an untwisting process C: Never twisted yarn
2 **Bobbin Type** See Diagram below

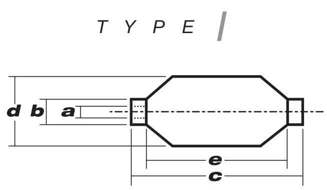

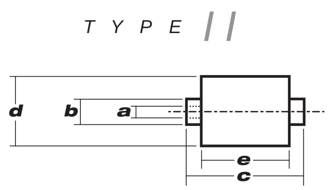

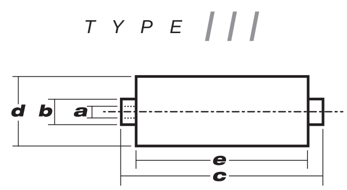

TORAY CARBON FIBERS AMERICA, INC.
6 Hutton Centre Drive, Suite #1270, Santa Ana, CA 92707 TEL: (714) 431-2320 FAX: (714) 424-0750
Sales@Toraycfa.com Technical@Toraycfa.com www.torayusa.com

MTM® 49-3

MTM49-3 is an 80 to 160°C (176 to 320°F) curing, toughened epoxy prepreg resin system developed specifically for the manufacture of components.

MTM49-3 prepregs exhibit excellent ambient and hot mechanical performance combined with good impact resistance after only moderate cure cycles making them ideal for use in the motorsport industry.

Features

- Autoclave and press curable
- 60 days out life at 21°C (70°F)
- 12 months storage at -18°C (0°F)
- Versatile cure temperatures
- 190°C Tg
- Bonds directly to Nomex core in bodywork type applications

Product variants

- MTM49-3: High Tg and moderate toughness
- MTM49-3B: Black pigmented variant of MTM49-3
- MTM49-3BB: Black pigmented variant of MTM49-3 (higher pigment loading)
- MTM49-3BD: Black dyed variant of MTM49-3

Related documents

- De-bulking guidelines (TDS1036)
- Autoclave processing – lay-up and bagging guidelines (TDS1037)

Related products

- MTA240 adhesive film (PDS1166)
- MTF246 surface improvement film (PDS1240)

Cure cycle

Autoclave cure

Vacuum bag pressure	Minimum of 980mbar (29"Hg)*
Autoclave pressure	6.2 bar (90 psi)†
Ramp rate	1 to 3°C (1.8 to 5.4°F)/minute
Recommended cure cycle	90 minutes at 135°C +5°C/-0°C (275°F, +9°F/-0°F)**
Cool down	Maximum of 3°C (5.4°F)/minute to 60°C (140°F)

*This is the ideal vacuum level, however, it is recognised that it is not always possible to attain. If in doubt, please contact our technical support staff for advice.

†If producing sandwich panels, apply the maximum pressure allowable for the honeycomb type.

**This is an industry standard cure cycle, however it is possible to cure at 135°C in a shorter time. Consult our technical support staff for further information.

Press cure

Mould tools should restrain the flow sufficiently under moulding conditions to avoid fabric or fibre distortion.

Press pressure	Minimum of 2.8 bar (40 psi)
Ramp rate	A suitable rate (dependant on mould tooling)
Recommended cure cycle	90 minutes at 135°C +5°C/-0°C (275°F, +9°F/-0°F)*
Cool down	A suitable rate (dependant on mould tooling) to 60°C (140°F)

*This is an industry standard cure cycle, however it is possible to cure at 135°C in a shorter time. Consult our technical support staff for further information.

Note:
- Demoulding at the cure temperature may be possible if the tooling is suitably designed. A specific trial is recommended.

Alternative cure cycles

Temperature	Duration
70°C (158°F)	24 hours
80°C (176°F)	16 hours
100°C (212°F)	4 hours
120°C (248°F)	1 hour
140°C (284°F)	25 minutes
160°C (320°F)	7 minutes

Post-cure

In applications demanding maximum temperature or environmental resistance, it is essential that the component is post-cured to fully develop the glass transition temperature.

Ramp rate	0.3°C (0.5°F)/minute
Post-cure cycle	2 hours at 180°C -0/+5°C (356°F -0/+9°F)
Cool down	Maximum of 3°C (5.4°F)/minute to 60°C (140°F)

* Temperature must be measured by the lagging thermocouple attached to the part.

Notes:
- Parts may be loaded into a pre-heated oven or heated at 3°C (5.4°F)/minute to the initial cure temperature.
- Large components should be adequately supported to avoid distortion.
- Post-cures from 100 to 200°C (212 to 392°F) may be used to suit specific applications. Please consult our technical support staff if you require assistance in determining the correct cure cycle for your application.

Physical properties

Test	Sample conditions	Results
Cured resin density	90 minutes at 135°C (275°F)	1.22 g/cm^3
DMA E' onset Tg	16 hours at 80°C (176°F), dry 90 minutes at 135°C (275°F), dry Maximum dry Tg Maximum wet Tg*	95°C (203°F) 140°C (284°F) 190°C (356°F) 115°C (240°F)

* Wet conditioning – 14 days immersion at 70°C (158°F)

Mechanical properties

Cure cycle: 90 minutes at 135°C (275°F), 6.2 bar (90 psi)
Test conditions: Room temperature, dry

Test	Test method	Units	Material		
			MTM49-3/ M46J-124-36%	MTM49-3/ T1000 GB - 124-36%	MTM49-3/ T800 GB -124-36%
0° Tensile strength	ASTM D3039	MPa (ksi)	1709 (248)	2999 (435)	2211 (321)
0° Tensile modulus		GPa (msi)	235 (34.1)	155 (22.5)	149 (21.6)
90° Tensile strength		MPa (ksi)	25.8 (3.74)	19.3 (2.80)	-
90° Tensile modulus		GPa (msi)	6.87 (1.00)	6.80 (0.99)	-
0° Compressive strength	SACMA SRM01R94	MPa (ksi)	875 (127)	1431 (208)	1396 (202)
0° Compressive modulus		GPa (msi)	201 (29.2)	127 (18.4)	122 (17.7)
90° Compressive strength		MPa (ksi)	189 (27.4)	199 (28.9)	-
90° Compressive modulus		GPa (msi)	7.59 (1.10)	7.51 (1.09)	-
In-plane shear strength (IPSS)	ASTM D3518	MPa (ksi)	69.0 (10.0)	132 (19.1)	107 (15.5)
In-plane shear modulus (IPSM)		GPa (msi)	4.09 (0.59)	3.09 (0.45)	3.10 (0.45)
0° Interlaminar shear strength (ILSS)	ASTM D2344	MPa (ksi)	88.2 (12.8)	105 (15.2)	107 (15.5)

Data normalised to 55%Vf except for ILSS and IPSS & IPSM.

Cure cycle: 90 minutes at 135°C (275°F), 6.2 bar (90 psi)
Test conditions: Room temperature, dry

Test	Test method	Units	Material		
			MTM49-3/ CF2115*-42%	MTM49-3/ CF4534†-42%	MTM49-3/ CF1218**-42%
0° Tensile strength	ASTM D3039	MPa (ksi)	590 (85.6)	1065 (155)	870 (126.2)
0° Tensile modulus		GPa (msi)	104 (15.1)	72.0 (10.4)	67.0 (9.72)
90° Tensile strength		MPa (ksi)	573 (83.1)	1035 (150)	834 (121)
90° Tensile modulus		GPa (msi)	102 (14.8)	70.0 (10.2)	65.0 (9.43)
0° Compressive strength	SACMA SRM01R94	MPa (ksi)	400 (58.0)	640 (92.8)	630 (91.3)
0° Compressive modulus		GPa (msi)	89.0 (12.9)	59.0 (8.56)	59.0 (8.56)
90° Compressive strength		MPa (ksi)	370 (53.7)	610 (88.5)	580 (84.1)
90° Compressive modulus		GPa (msi)	87.0 (12.6)	57.0 (8.27)	57.0 (8.27)
In-plane shear strength (IPSS)	ASTM D3518	MPa (ksi)	82.7 (12.0)	108 (15.7)	123 (17.8)
In-plane shear modulus (IPSM)		GPa (msi)	3.98 (0.58)	3.74 (0.54)	4.39 (0.64)
0° Interlaminar shear strength (ILSS)	ASTM D2344	MPa (ksi)	50.2 (7.28)	64.2 (9.31)	78.3 (11.4)

Data normalised to 48%Vf except for ILSS and IPSS & IPSM

*CF2115 is a 200g/m^2 2x2 twill fabric with 6k M46J fibres
†CF4534 is a 283g/m^2 5HS fabric with 12k T1000 type fibres
**CF1218 is a 200g/m^2 2x2 twill fabric with 6k T800HB fibres

Availability

MTM49-3 prepregs are available on all key motorsport reinforcements (fabrics and unidirectional tapes).

Storage

Out life* at 21°C (70°F)	60 days
Storage at -18°C (0°F)	12 months from date of manufacture

*Out life refers to accumulated time out of the freezer before the part is cured.

Note:
The actual freezer storage life and out life are dependent on a number of factors, including; fibre type, format and application. For certain formats, it may be possible for the storage life and out life to be longer than stated. Please contact our technical support staff for advice.

Exotherm

MTM49-3 prepregs are reactive formulations which can undergo severe exothermic heat up during the initial curing process if incorrect curing procedures are followed.

Great care must be taken to ensure that safe heating rates, dwell temperatures and lay-up/bagging procedures are adhered to, especially when moulding solid laminates in excess of 10mm (0.4in) thickness. The risk of exotherm increases with lay-up thickness and increasing cure temperature. It is strongly recommended that trials, representative of all the relevant circumstances, are carried out by the user to allow a safe cure cycle to be specified. It is also important to recognise that the model or tool material and its thermal mass, combined with the insulating effect of breather/bagging materials can affect the risk of exotherm in particular cases.

Please contact our technical department for further information on exotherm behaviour of these systems.

Health & safety

MTM49-3 resins contain epoxy resins which can cause allergic reaction on prolonged or repeated skin contact. Avoid contact with the skin. Gloves and protective clothing must be worn.

Wash skin thoroughly with soap and water or resin removing cream after handling. Do not use solvents for cleaning the skin.

Use mechanical exhaust ventilation when heat curing the resin system. Exhaust from vacuum pumps should be vented to external atmosphere and not into the work place.

For further information, consult Cytec Safety Data Sheet numbers:

MTM49-3:	SDS 291
MTM49-3B:	SDS 291
MTM49-3BB:	SDS 291
MTM49-3BD	SDS 449

PLASCORE®

PAMG-XR1 5052 Aluminum Honeycomb

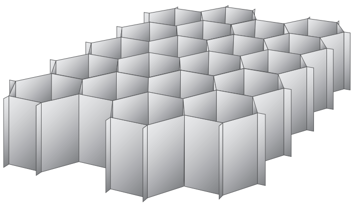

Description:

PAMG-XR1 5052 aerospace grade aluminum honeycomb is a lightweight core material which offers superior strength and corrosion resistance over commercial grade aluminum honeycomb. PAMG-XR1 5052 honeycomb is made from 5052 aluminum alloy foil and meets all the requirements of AMS C7438 Rev A.

Applications:

PAMG-XR1 5052 honeycomb uses include aircraft floors, aircraft leading and trailing edges, missile wings, fan casings, fuel cells, fuselage components, helicopter rotor blades and navy bulkhead joiner panels, energy absorption, air/light directionalization and EMI/RFI shielding. PAMG-XR1 5052 honeycomb is suitable for applications where materials conforming to AMS C7438 Rev A are required.

Features:

- Elevated use temperatures
- High thermal conductivity
- Flame resistant
- Excellent moisture and corrosion resistance
- Fungi resistant
- Low weight / High strength

Availability:

PAMG-XR1 5052 honeycomb is available in four forms: unexpanded blocks, unexpanded slices, untrimmed expanded sheets and cut to size expanded sheets. It is also available with or without cell perforations to facilitate cell venting for certain applications.

Cell Sizes:	1/8" - 3/8"	
Densities:	1.0 pcf - 8.1 pcf	
Sheet "Ribbon" (L):	48" typical	
Sheet "Transverse" (W):	96" typical	
Tolerances:	Length:	+ 6", - 0"
	Width:	+ 6", - 0"
	Thickness:	± .005" (under 4" thick)
	Density:	± 10%
	Cell Size:	± 10%

NOTE: Special dimensions, sizes, tolerances, CNC machining and die cut to size can be provided upon request.

PAMG-XR1 5052 aluminum honeycomb is specified as follows:

Material - Density - Cell Size - Foil Thickness - Perforation - Alloy - Corrosion Level

Designates aluminum military grade

The nominal density in pounds per cubic foot

Designates the foil thickness in inches

Indicates corrosion level

Example: **PAMG - XR1 - 3.0 - 3/8 - .002 - HP - 5052 - CL2**

Designates XR1 corrosion coating

Cell size in inches

Indicates cell walls are highly perforated (HP); not perforated (N)

Designates the alloy of the foil

PAMG-XR1 5052 Mechanical Properties

PLASCORE® Honeycomb Designation			Bare Compressive		Plate Shear			
					STRENGTH PSI		MODULUS KSI	
CELL SIZE	FOIL GAUGE	NOMINAL DENSITY PCF	STRENGTH PSI	MODULUS KSI	"L"	"W"	"L"	"W"
1/8	.0007	3.1	270	75	210	130	45	22
1/8	.001	4.5	520	150	340	220	70	31
1/8	.0015	6.1	870	240	505	320	98	41
1/8	.002	8.1	1400	350	725	455	135	54
3/16	.001	3.1	270	75	210	130	45	22
3/16	.0015	4.4	500	145	330	215	68	30
3/16	.002	5.7	770	220	460	300	90	38
3/16	.0025	6.9	1080	285	590	375	114	46
3/16	.003	8.1	1400	350	725	455	135	54
1/4	.0007	1.6	85	20	85	50	21	11
1/4	.001	2.3	165	45	140	85	32	16
1/4	.0015	3.4	320	90	235	150	50	24
1/4	.002	4.3	480	140	320	210	66	29
1/4	.0025	5.2	670	190	410	265	82	35
1/4	.003	6.0	850	235	495	315	96	40
1/4	.004	7.9	1360	340	700	440	130	52
3/8	.0007	1.0	30	10	45	30	12	7
3/8	.0015	2.3	165	45	140	85	32	16
3/8	.002	3.0	260	70	200	125	43	21
3/8	.0025	3.7	370	105	260	170	55	26
3/8	.003	4.2	460	135	310	200	65	29
3/8	.004	5.4	720	200	430	280	86	36

Tested at 0.625" per AMS C7438 Rev A at room temperature.

PLASCORE®

Corporate Headquarters

Plascore Incorporated
615 N. Fairview St.
Zeeland, MI 49464-0170

Phone (616) 772-1220
Toll Free (800) 630-9257
Fax (616) 772-1289
Email sales@plascore.com
Web www.plascore.com

Europe

Plascore GmbH&CoKG
Feldborn 6
D-55444 Waldlaubersheim
Germany

Phone +49(0) 6707-9143 0
Fax +49(0) 6707-9143 40
Email sales.europe@plascore.com
Web www.plascore.de

Coast Fabrication, Inc.
16761 Burke Lane, Huntington Beach CA 92647
Ph: (714) 842-2603
Fax: (714) 847-1824
info@coastfab.com
www.coastfab.com

HEAT REFLECTIVE TAPES

-- Definitions and Data –

- Tapes are a passive thermal control system. Their purpose is to minimize heat transfer through the panel or surface being protected by the tape.

- For aerospace, tapes are defined by an emittance number. The lower the number, the less heat actually transferred through.
  1. Real Gold: emittance = 0.02
  2. Aluminum mirror: emittance = 0.03

- In space, the gold material is used primarily to keep hear inside a satellite. This, 0.02 to 0.03 emittance difference is on the order of 50%: important in a 30 year life satellite . Gold is also completely inert. Gamma rays will not pass through it which is why it is also used on exterior surfaces in space.

- On earth where we are heating by both conduction and radiance, the 0.02 to 0.03 emittance difference is that between 98% and 97% of heat reflected (i.e. not passed through.)

- Coast Aerolite tape is composed of multiple layers:

  1. Acrylic overcoat: resistance to humidity, chemicals, salt fog
  2. Aluminum mirror; 0.001” thickness: heat reflection
  3. Polymide Kapton; 0.001” thickness: heat insulation and burn resistance to 750°F
  4. Acrylic overcoat: see #1
  5. 3M high-temperature Pressure-Sensitive Adhesive (PSA)

  Total thickness < 0.005”
  Weight 98g/m^2 or 2.9oz./square yard

Coast Fabrication, Inc.
16761 Burke Lane, Huntington Beach CA 92647
Ph: (714) 842-2603   Fax: (714) 847-1824   info@coastfab.com

COAST FABRICATION HEAT REFLECTIVE TAPE COMPARISION

Coast Fabrication Inc. is pleased to announce the latest addition to its line of heat-reflective tapes; test results are detailed below. Material is in stock for immediate delivery and may also be obtained through Earls Indianapolis (317-241-0318; mark@earlsindy.com).

In order to get an apples-to-apples comparison between our tapes and the corrugated "gold" material that is in universal circulation, we performed the following tests. The tapes were applied to an aluminum panel (.063" 3003H14). A constant heat source was fixtured at the noted distance and heat was applied to the front (tape) side and temperature measured on the backside.

☠ PLEASE NOTE THE FOLLOWING ☠

Several samples of the corrugated "gold" tape were tested and performance was very inconsistent. The material referenced in the tables below was the **HIGHEST PERFORMING** samples. The performance of other samples we tested barely exceeded bare metal. We were unable to identify any visual differences between the "good" and "bad" material. **OUR RECOMMEDATION IS TO AVOID THIS MATERIAL UNLESS YOU VERIFY ITS PERFORMANCE WITH YOUR OWN TESTS.**

Heat Source: 1,000° F; Fixture 2.38" from panel; Ambient 80° F; Panel 80°-85°F

Tape	Seconds to 180° F	Seconds to 210° F	Seconds to 240° F
Coast Fab USA (Aerolite)	17.5	28.0	46.0
Corrugated "gold"	18.9	31.9	49.3
Coast Fab USA Plus (Aerolite Plus)	26.5	41.8	66.0

Heat Source: 1,000° F; Fixture 4.38" from panel; Ambient 80° F; Panel 80°-85°F

Tape	Seconds to 180° F	Seconds to 210° F	Seconds to 240° F
Coast Fab USA (Aerolite)	35.4	60.0	116.0
Corrugated "gold"	42.0	65.0	125.0
Coast Fab USA Plus (Aerolite Plus)	49.3	85.0	151.0

Material Specifications

Tape	Material Specifications	weight oz./yd²	weight g/m²
Coast Fab USA (Aerolite)	Protected Aluminum with 1 mil Kapton and Acrylic PSA	2.9	98
Coast Fab USA Plus (Aerolite Plus)	Aluminized dual mirror, aramid cloth, PSA	8.5	288
Corrugated "gold"	Gold colored film over aluminum, Kapton, PSA	6.8	230

3M

Scotch-Weld™

Epoxy Adhesive

DP420 Black • DP420 NS Black • DP420 Off-White • DP420 LH

Technical Data **May, 2015**

Product Description

3M™ Scotch-Weld™ Epoxy Adhesives are high performance, two-part epoxy adhesives offering outstanding shear and peel adhesion, and very high levels of durability.

Features

- High shear strength
- High peel strength
- Outstanding environmental performance
- Easy mixing
- 20 minute worklife
- Controlled flow (3M™ Scotch-Weld™ Epoxy Adhesive DP420 NS Black)
- Recognized as meeting UL 94 HB – Underwriters Laboratory Horizontal Burn Flammability Test (3M™ Scotch-Weld™ Epoxy Adhesive DP420 Off-White)
- Low halogen content (3M™ Scotch-Weld™ Epoxy Adhesive DP420 LH)

Typical Uncured Physical Properties

Note: The following technical information and data should be considered representative or typical only and should not be used for specification purposes.

Product		3M™ Scotch-Weld™ Epoxy Adhesive			
		DP420 Black	DP420 NS Black	DP420 Off-White	DP420 LH
Viscosity (approx.) @ 73°F (23°C)	Base Accelerator	20,000-50,000 cP 8,000-14,000 cP	190,000-270,000 cP 60,000-130,000 cP	20,000-50,000 cP 8,000-14,000 cP	20,000-50,000 cP 8,000-14,000 cP
Base Resin	Base Accelerator	epoxy amine	epoxy amine	epoxy amine	epoxy amine
Color	Base Accelerator	black amber	black amber	white amber	white amber
Net Weight Lbs./Gallon	Base Accelerator	9.3-9.7 9.0-9.4	9.4-9.8 9.1-9.5	9.3-9.7 9.0-9.4	9.3-9.7 9.0-9.4
Mix Ratio (B:A)	Volume Weight	2:1 2:0.97	2:1 2:0.97	2:1 2:0.97	2:1 2:0.97
Worklife, 73°F (23°C)	20 g mixed 10 g mixed 5 g mixed	15 minutes 20 minutes 30 minutes	— — —	15 minutes 20 minutes 30 minutes	15 minutes 20 minutes 30 minutes

Appendix I

SAE Rules Requirements

T3.10 Main and Front Roll Hoops – General Requirements

T3.10.1 The driver's head and hands must not contact the ground in any rollover attitude.

T3.10.2 The Frame must include both a Main Hoop and a Front Hoop as shown in Figure 1.

T3.10.3 When seated normally and restrained by the Driver's Restraint System, the helmet of a 95th percentile male (anthropometrical data) and all of the team's drivers must:

a. Be a minimum of 50.8 mm (2 inches) from the straight line drawn from the top of the main hoop to the top of the front hoop. (Figure 1a)

b. Be a minimum of 50.8 mm (2 inches) from the straight line drawn from the top of the main hoop to the lower end of the main hoop bracing if the bracing extends rearwards. (Figure 1b)

c. Be no further rearwards than the rear surface of the main hoop if the main hoop bracing extends forwards. (Figure 1c).

95th Percentile Male Template Dimensions

A two dimensional template used to represent the 95th percentile male is made to the following dimensions:

• A circle of diameter 200 mm (7.87 inch) will represent the hips and buttocks.

• A circle of diameter 200 mm (7.87 inch) will represent the shoulder/cervical region.

• A circle of diameter 300 mm (11.81 inch) will represent the head (with helmet).

• A straight line measuring 490 mm (19.29 inch) will connect the centers of the two 200 mm circles.

• A straight line measuring 280 mm (11.02 inch) will connect the centers of the upper 200 mm circle and the 300 mm head circle.

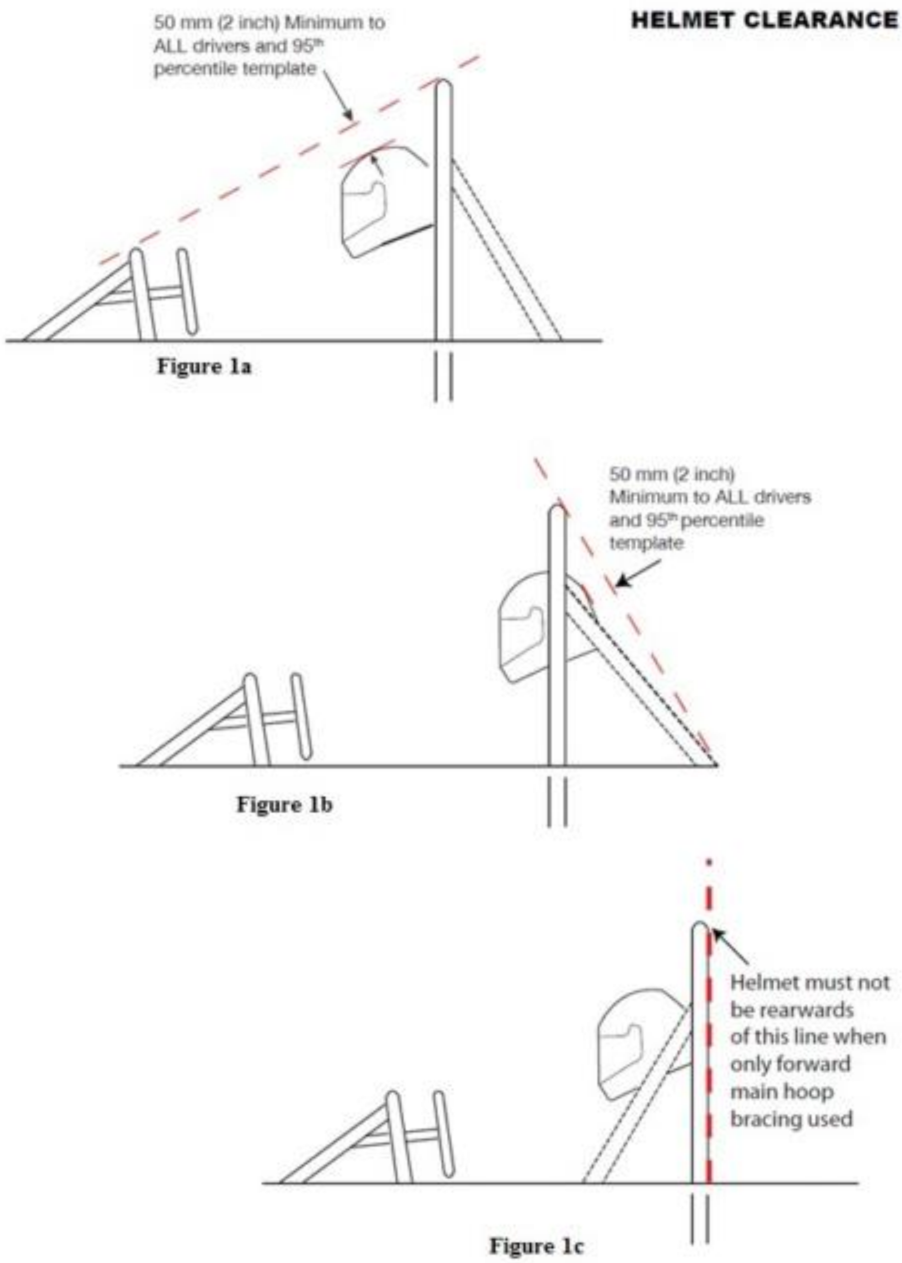

Figure I1. Helmet clearance requirements.

Monocoque Geometry Templates

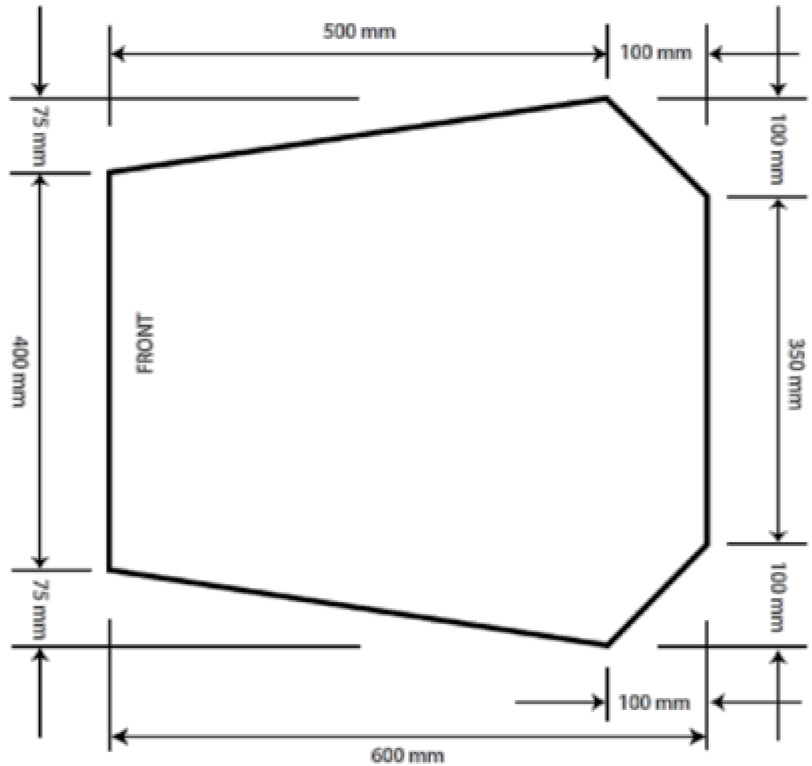

Figure I2. Cockpit Opening Template

T4.1.1 “In order to ensure that the opening giving access to the cockpit is of adequate size, a template shown (above) will be inserted into the cockpit opening. It will be held horizontally and inserted vertically until it has passed below the top bar of the Side Impact Structure (or until it is 350 mm (13.8 inches) above the ground for monocoque cars). No fore and aft translation of the template will be permitted during insertion.”

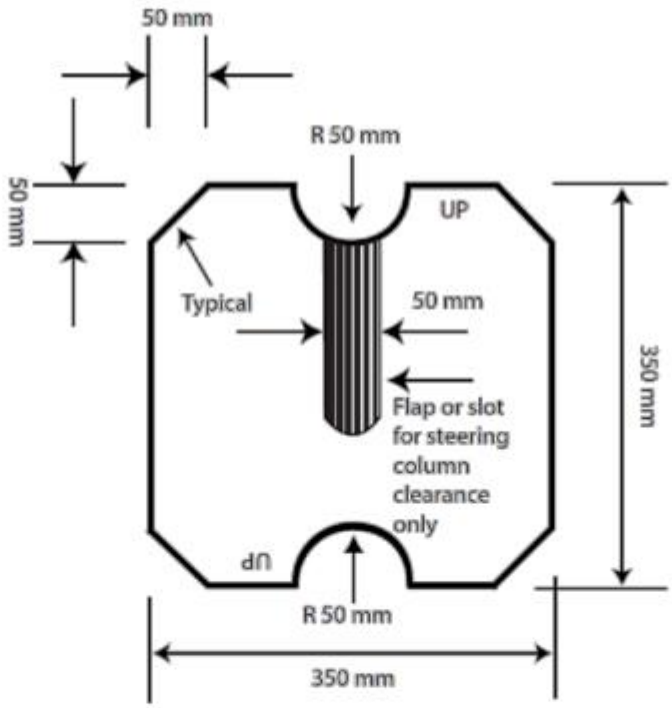

Figure I3. Cockpit Internal Cross Section

T4.2.1 "A free vertical cross section, which allows the template shown (above) to be passed horizontally through the cockpit to a point 100 mm (4 inches) rearwards of the face of the rearmost pedal when in the inoperative position, must be maintained over its entire length. If the pedals are adjustable, they will be put in their most forward position." (FSAE Rules, page 46-47)

Appendix J

Cure Temperature Data

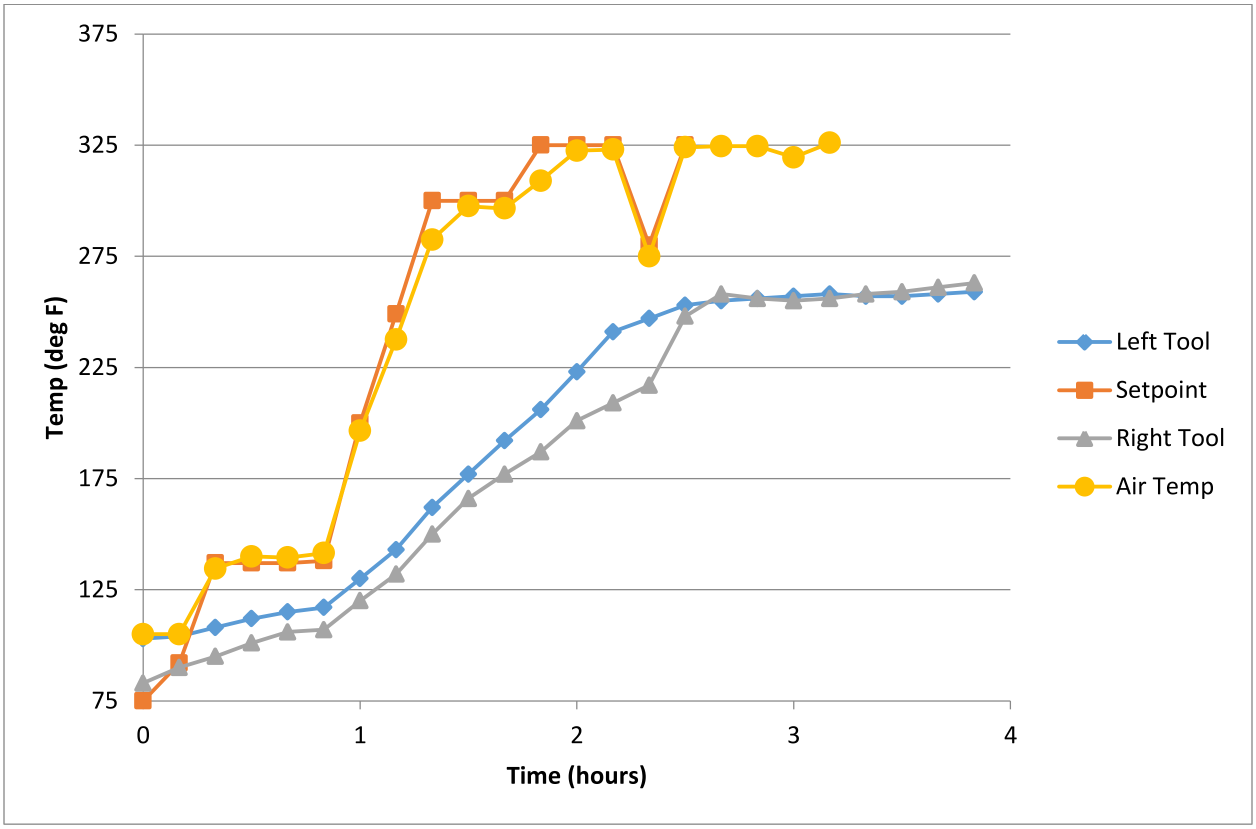

Figure J1. Final monocoque cure temperature trends.

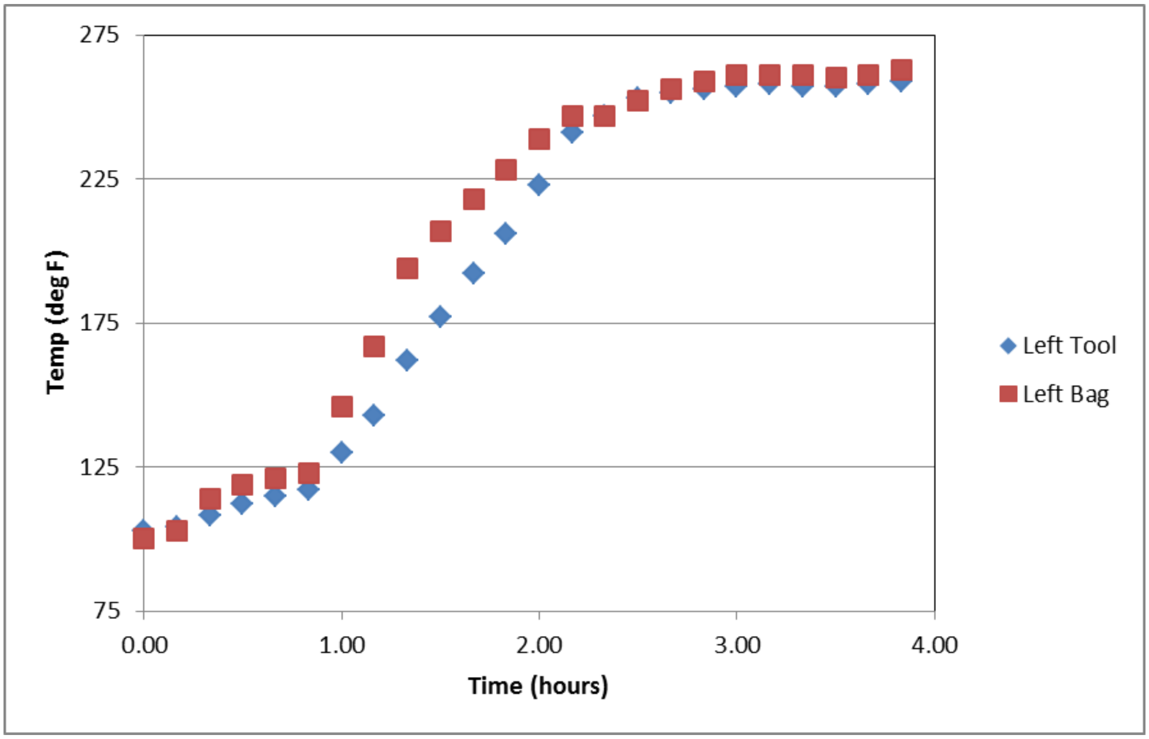

Figure J2. Final monocoque layup temperature deltas between the inner and outer facesheets equalized to within 5°F by the time the soak started.

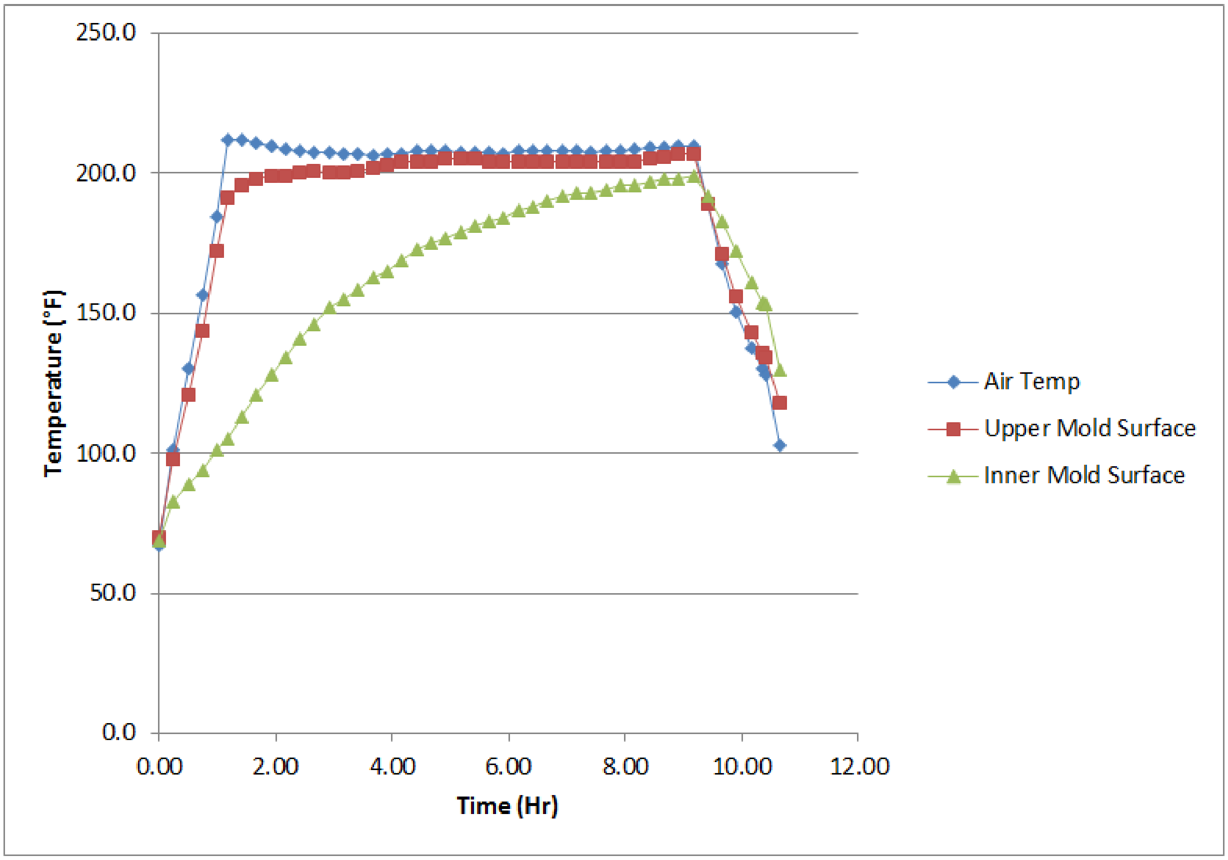

Figure J3. Nosecone cure data.

Appendix K

Chassis Mass Properties

Table K1. Mass properties of monocoque, anti-intrusion plate, and nosecone with aero mounting.

Component	2015 Weight (lb)	2013 Weight (lb)	Change from 2013 (%)	Notes on 2015 Weight Values
Left half of monocoque	13.540	Unavailable	Unavailable	Excess trimmed, no closeouts, front bulkhead material not removed
Right half of monocoque	14.000	Unavailable	Unavailable	Excess trimmed, no closeouts, front bulkhead material not removed
Bulkhead removal	2.202	Unavailable	Unavailable	Weight removed from the 11" x 11" opening
Strap joint and all resin-microballoons	4.762	Unavailable	Unavailable	Includes resin-microballoons on cockpit opening but not cockpit closeout
Cockpit closeout and repair patches	2.4	Unavailable	Unavailable	±0.5lb
Monocoque without hardware	30.0	Unavailable	Unavailable	Includes inserts and vinyl wrap.
Hardware	2.5	3.20	-21.9%	±0.5lb. Roll hoop and harness harware and backing plate.
Monocoque total with hardware	**32.5**	**38.20**	**-14.9%**	±0.5lb/1.3%
Nosecone	3.160	2.094	50.9%	Fairing only
Nosecone hardware	0.150	0.138	8.7%	Nosecone to monocoque only
Aerodynamics hardware	0.215	0.352	-38.9%	Wing to truss and truss to nosecone only. Aero added in 2014.
Front wing trusses	0.690	1.860	-62.9%	Adjustable aluminum version for 2015. Aero added in 2014.
Nosecone and aero-mounts total	**4.215**	**4.444**	**-5.2%**	Includes nosecone, aero mounting, all associated hardware
Anti-intrusion plate	**2.160**	**2.59**	**-16.6%**	Composite version

Appendix L

Technical Drawings

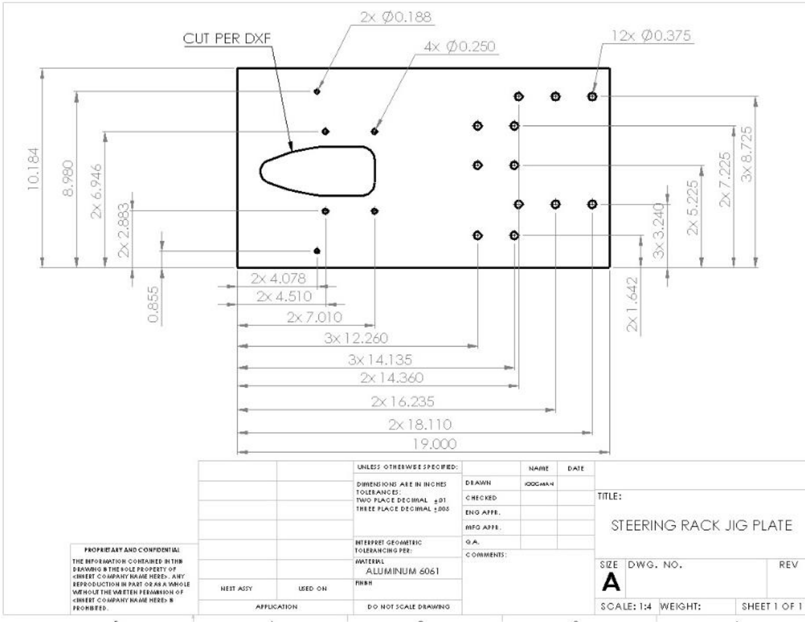

Figure L1. Drawing of Steering Rack Jig Plate.

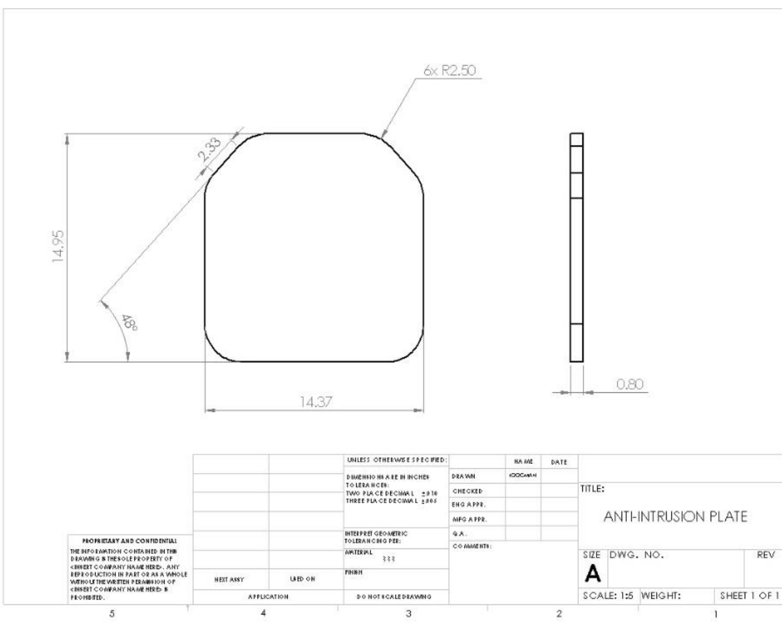

Figure L2. Drawing of Anti-Intrusion Plate

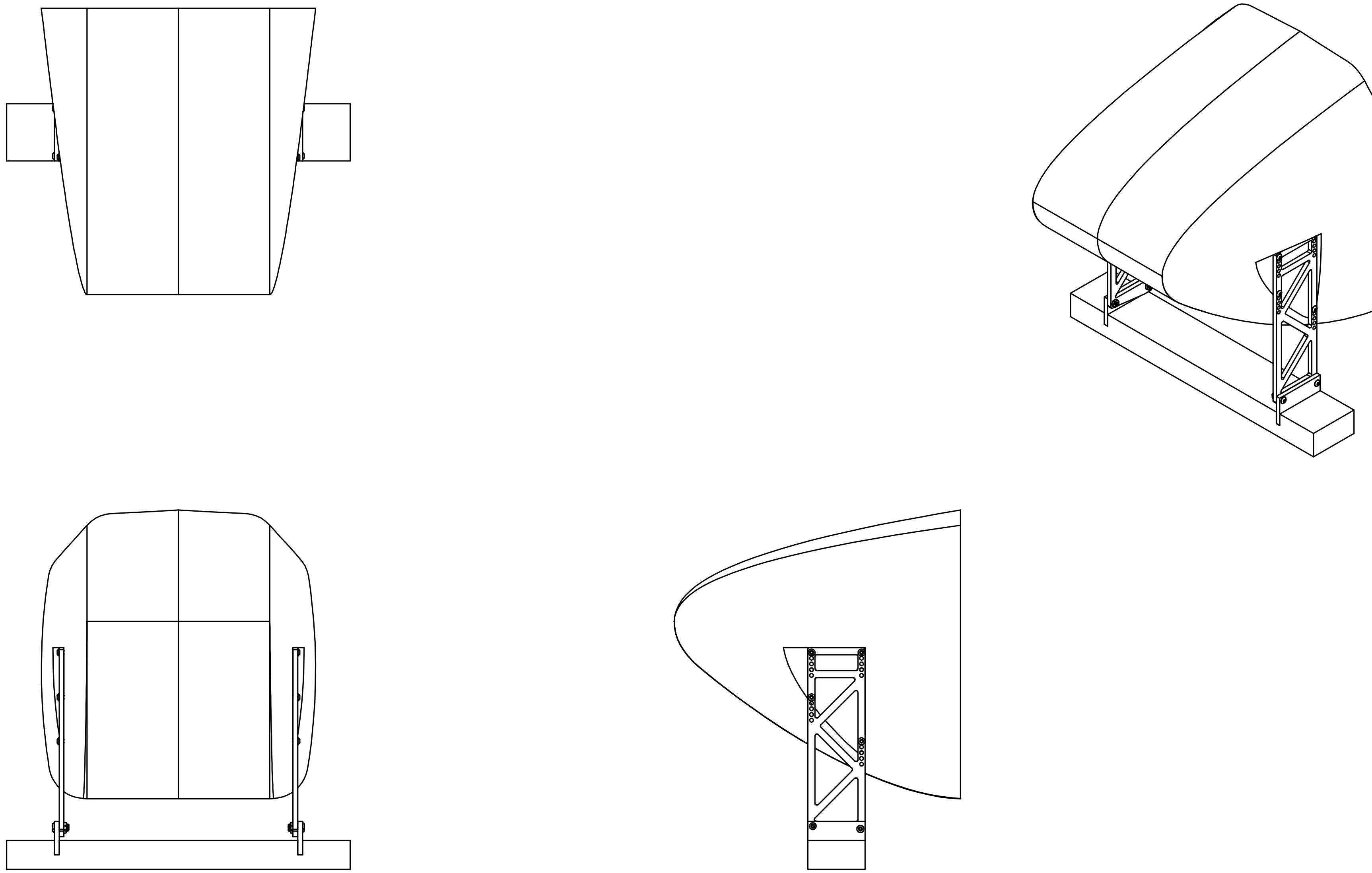

NEXT ASSY	USED ON
APPLICATION	

UNLESS OTHERWISE SPECIFIED:

DIMENSIONS ARE IN INCHES
TOLERANCES:
FRACTIONAL ±
ANGULAR: MACH ± BEND ±
TWO PLACE DECIMAL ±
THREE PLACE DECIMAL ±

INTERPRET GEOMETRIC TOLERANCING PER:

MATERIAL

FINISH

DO NOT SCALE DRAWING

	NAME	DATE
DRAWN	AC	
CHECKED		
ENG APPR.		
MFG APPR.		
Q.A.		

COMMENTS:

TITLE:

AERO MOUNTING JIG OVERVIEW

SIZE	DWG. NO.	REV
A		

SCALE: 1:8 WEIGHT: SHEET 1 OF 4

5 4 3 2 1

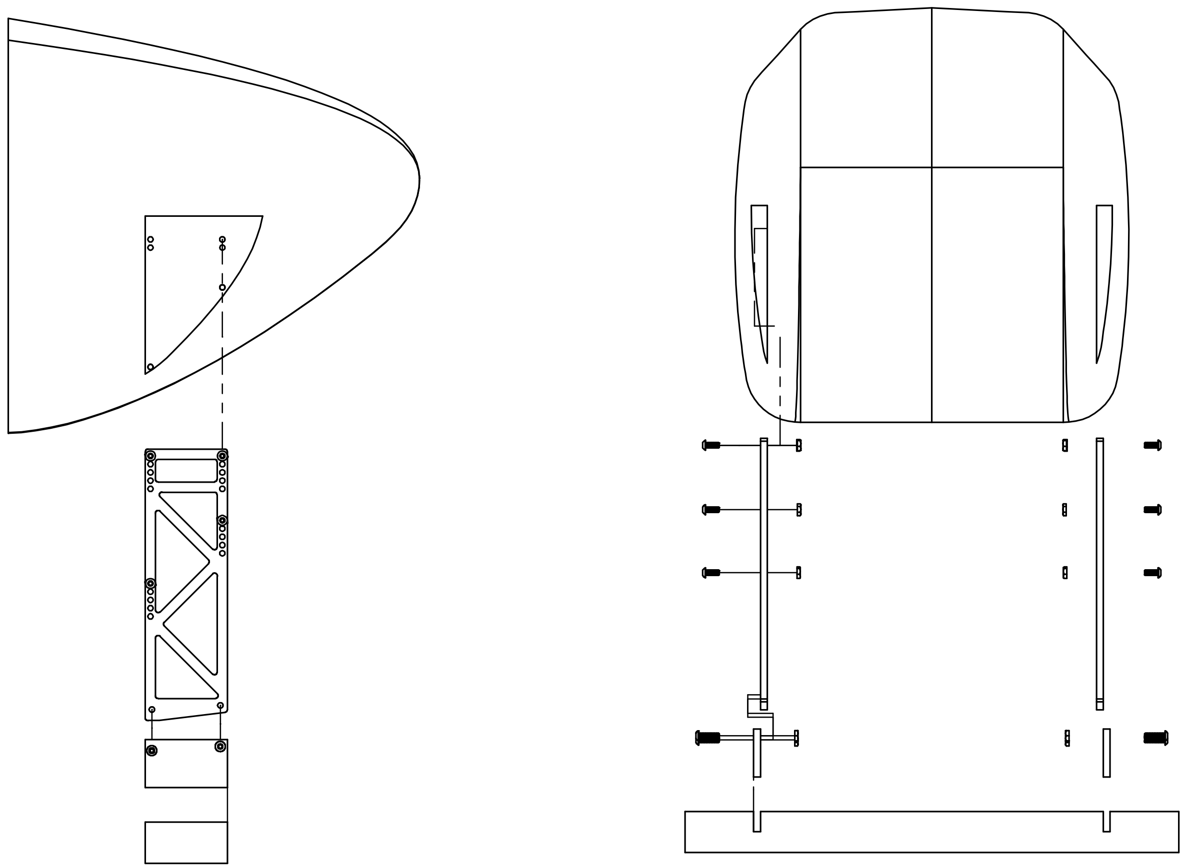

NOTE: ONLY USE LOWER FASTENERS WHEN DRILLING NOSECONE HOLES. ALIGN REAR EDGE OF PLEXIGLASS WTIH REAR EDGE OF ALUMINUM BAR. ALIGN TOP REAR CORNER OF MOUNT WITH NOSECONE RECESS.

		UNLESS OTHERWISE SPECIFIED:
		DIMENSIONS ARE IN INCHES TOLERANCES: FRACTIONAL ± ANGULAR: MACH ± BEND ± TWO PLACE DECIMAL ± THREE PLACE DECIMAL ±
		INTERPRET GEOMETRIC TOLERANCING PER:
		MATERIAL
NEXT ASSY	USED ON	FINISH
APPLICATION		DO NOT SCALE DRAWING

	NAME	DATE
DRAWN	AC	
CHECKED		
ENG APPR.		
MFG APPR.		
Q.A.		
COMMENTS:		

TITLE:

AERO MOUNTING JIG ASSY

SIZE	DWG. NO.	REV
A		

SCALE: 1:7

SHEET 2 OF 4

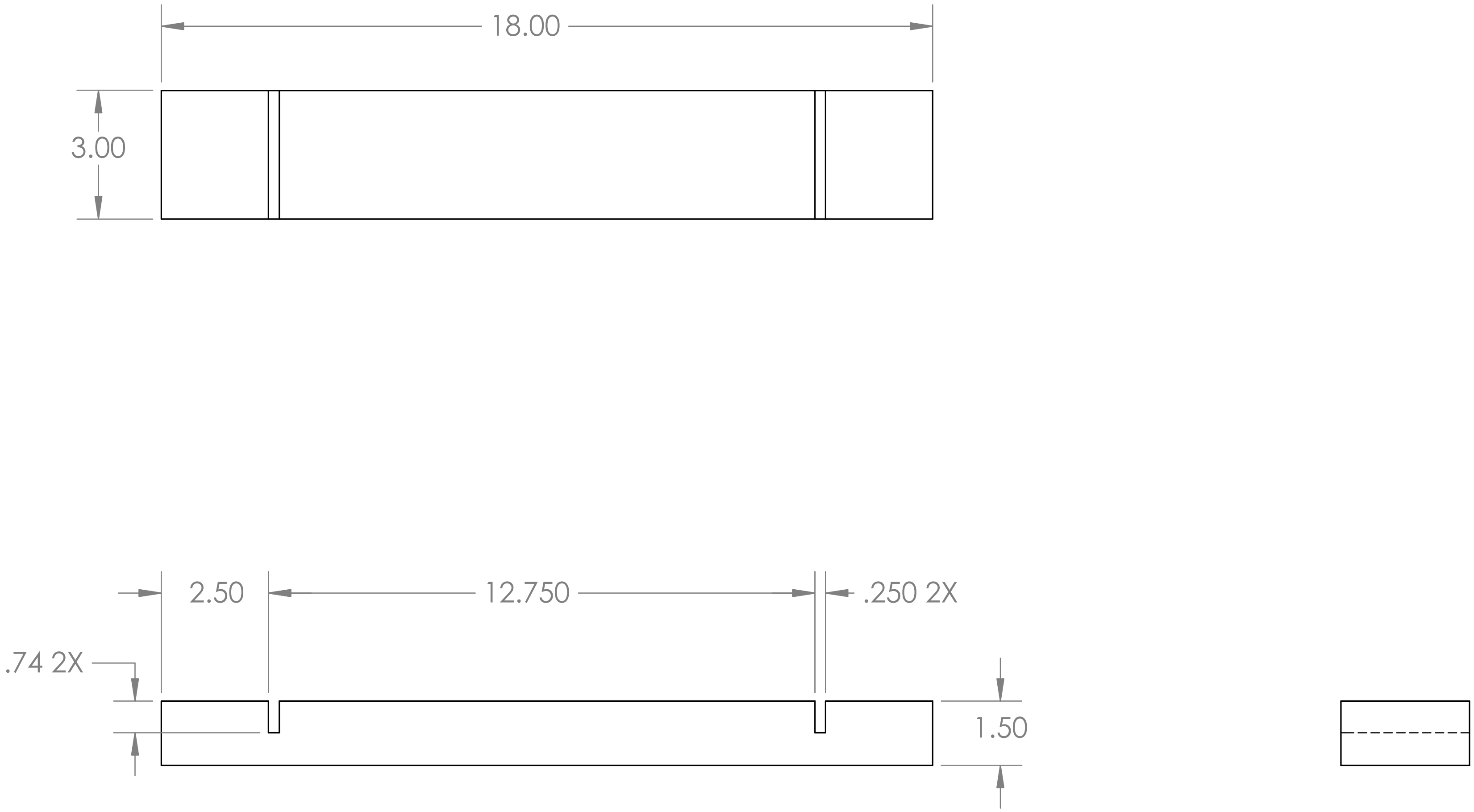

		UNLESS OTHERWISE SPECIFIED:		NAME	DATE	
		DIMENSIONS ARE IN INCHES TOLERANCES: FRACTIONAL ± ANGULAR: MACH ± BEND ± TWO PLACE DECIMAL ± THREE PLACE DECIMAL ±	DRAWN	AC		TITLE:
			CHECKED			ALUMINUM JIG BASE
			ENG APPR.			
			MFG APPR.			
		INTERPRET GEOMETRIC TOLERANCING PER:	Q.A.			
		MATERIAL 6061	COMMENTS:			SIZE A · DWG. NO. · REV
NEXT ASSY	USED ON	FINISH				
APPLICATION		DO NOT SCALE DRAWING				SCALE: 1:4 · WEIGHT: · SHEET 3 OF 4

5 4 3 2 1

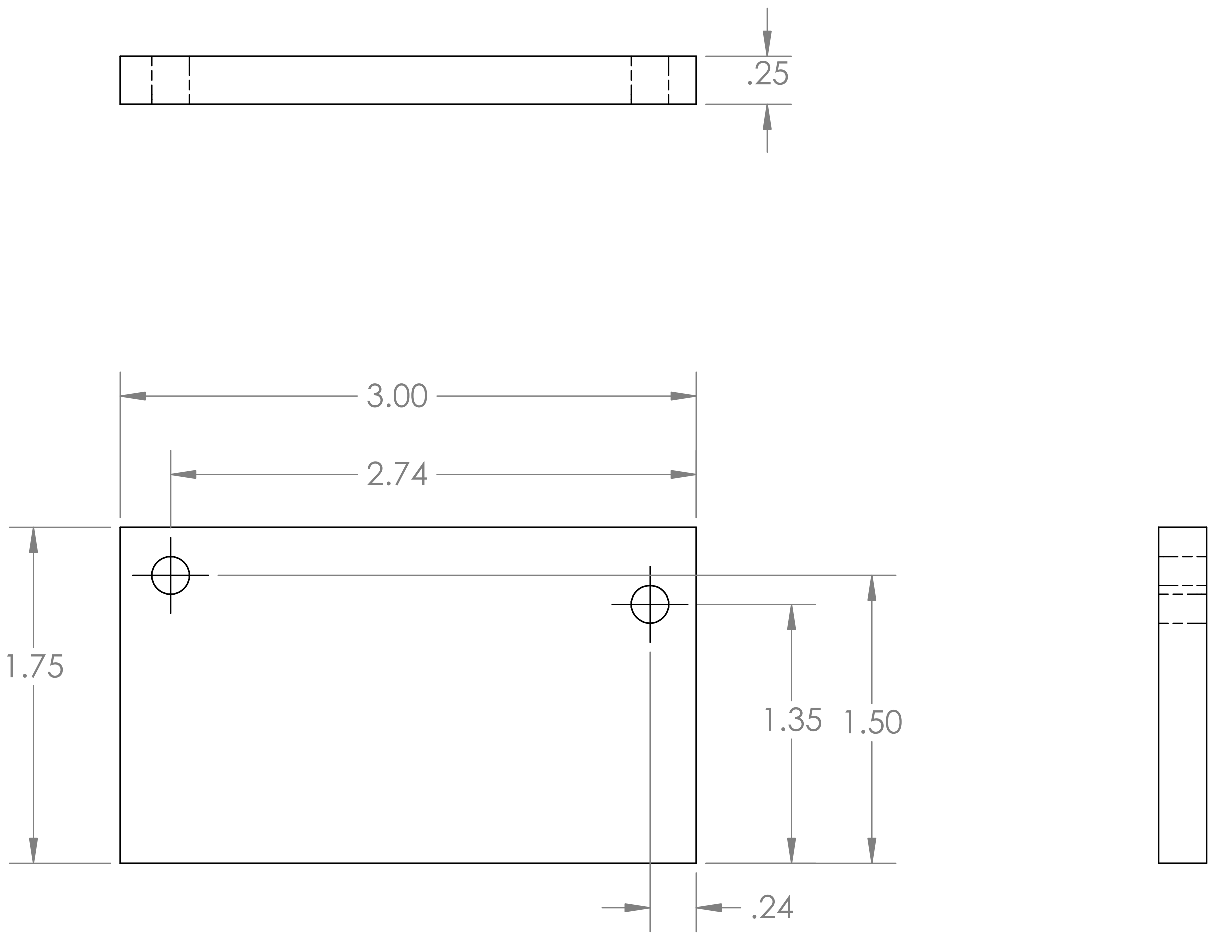

		UNLESS OTHERWISE SPECIFIED:		NAME	DATE	
		DIMENSIONS ARE IN INCHES TOLERANCES: FRACTIONAL ± ANGULAR: MACH ± BEND ± TWO PLACE DECIMAL ± THREE PLACE DECIMAL ±	DRAWN	AC		TITLE:
			CHECKED			ALIGNMENT PLATES
			ENG APPR.			
			MFG APPR.			
		INTERPRET GEOMETRIC TOLERANCING PER:	Q.A.			
		MATERIAL PLEXIGLASS	COMMENTS:			SIZE A DWG. NO. REV
NEXT ASSY	USED ON	FINISH				
APPLICATION		DO NOT SCALE DRAWING				SCALE: 1:1 SHEET 4 OF 4

5 4 3 2 1

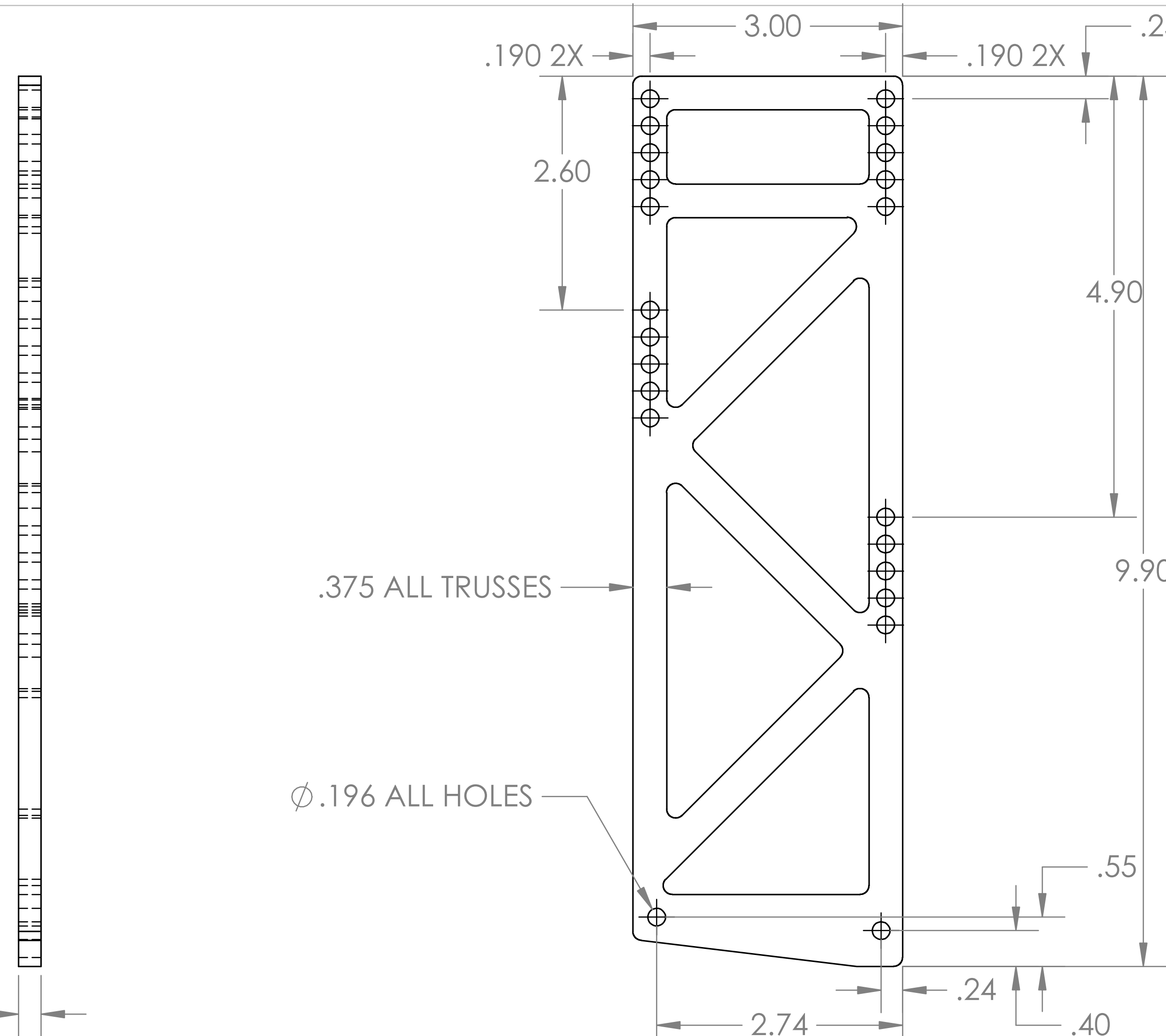

VERTICAL SPACING ON ALL HOLE ARRAYS IS 0.300".

POSITION HOLE LOCATIONS VIA MOUNTING JIG AND RECESS IN NOSECONE.

UNLESS OTHERWISE SPECIFIED:		NAME / DATE
DIMENSIONS ARE IN INCHES TOLERANCES: FRACTIONAL ± ANGULAR: MACH ± BEND ± TWO PLACE DECIMAL ± THREE PLACE DECIMAL ±	DRAWN	AC
	CHECKED	
	ENG APPR.	
	MFG APPR.	
INTERPRET GEOMETRIC TOLERANCING PER:	Q.A.	
MATERIAL 6061 AL	COMMENTS:	
FINISH		
DO NOT SCALE DRAWING		

NEXT ASSY | USED ON

APPLICATION

TITLE:

FRONT WING MOUNT (TESTING VER.)

SIZE A | DWG. NO. | REV

SCALE: 1:2 | WEIGHT: | SHEET 1 OF 1

5 4 3 2 1

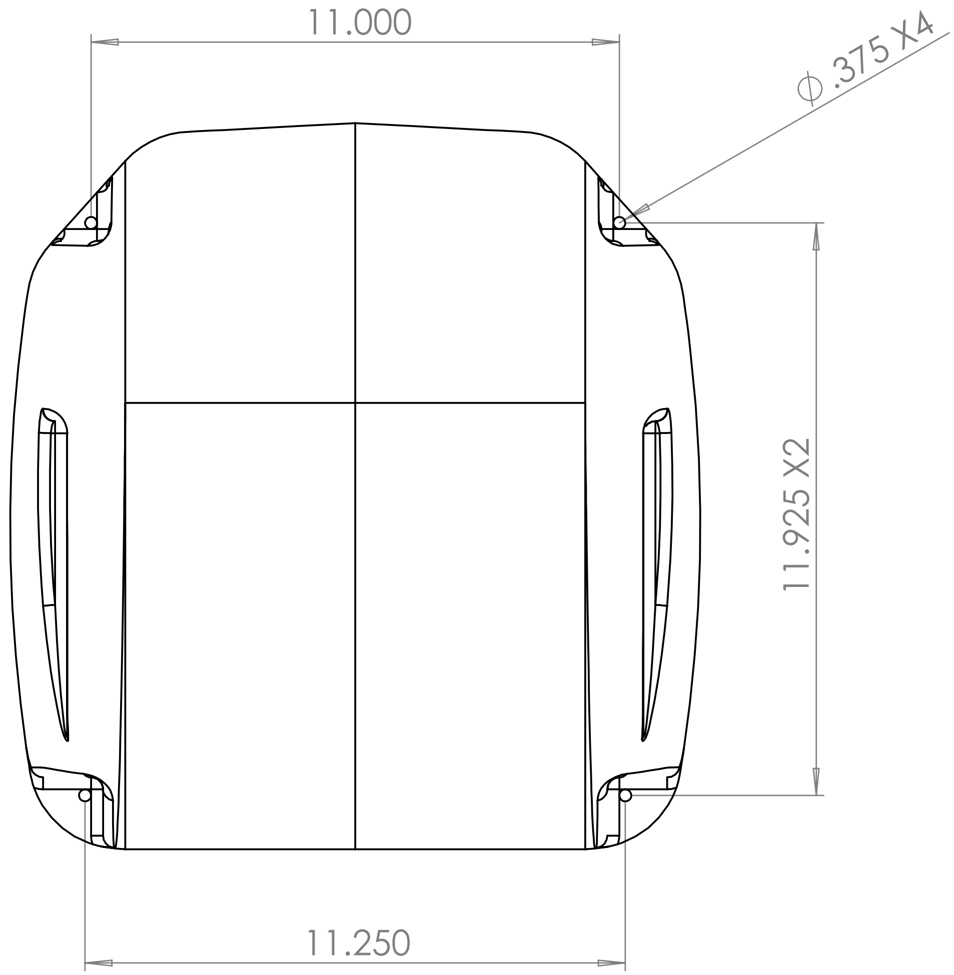

NOSECONE MOUNTING HOLES

	NAME	DATE
DRAWN	FERRELL	4/15/15
CHECKED		
ENG APPR.		
MFG APPR.		
Q.A.		

COMMENTS:

UNLESS OTHERWISE SPECIFIED:

DIMENSIONS ARE IN INCHES
TOLERANCES:
FRACTIONAL ± 1/16
ANGULAR: BEND ± 1°
TWO PLACE DECIMAL ± .01
THREE PLACE DECIMAL ± .005

MATERIAL
T800 CLOTH AND T800 UNI

FINISH

DO NOT SCALE DRAWING

NEXT ASSY | USED ON

APPLICATION

TITLE:
NOSECONE MOUNTING HOLES

SIZE A | DWG. NO. | REV

SCALE: 1:10 | SHEET 1 OF 1

5 4 3 2 1

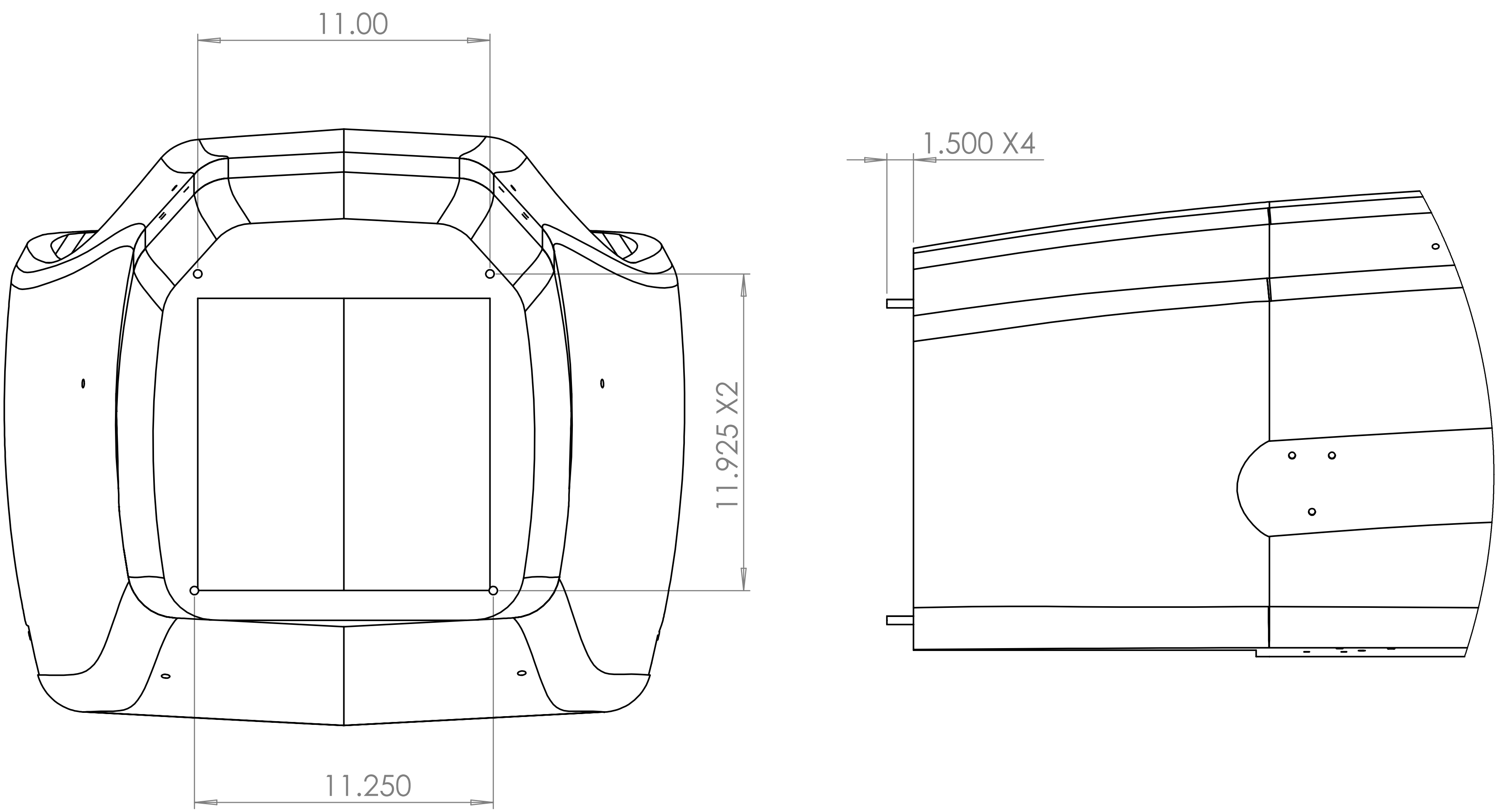

UNLESS OTHERWISE SPECIFIED:		NAME	DATE		
DIMENSIONS ARE IN INCHES TOLERANCES: FRACTIONAL ± 1/16 ANGULAR: BEND ± 1° TWO PLACE DECIMAL ± .01 THREE PLACE DECIMAL ± .005	DRAWN	FERRELL	4/15/15	TITLE:	
	CHECKED			NOSECONE MOUNTING STUD INSTALLATION	
	ENG APPR.				
	MFG APPR.				
	Q.A.				
MATERIAL STEEL	COMMENTS:			SIZE A	DWG. NO. / REV
FINISH					
DO NOT SCALE DRAWING				SCALE: 6:1 WEIGHT:	SHEET 1 OF 1

NEXT ASSY	USED ON
APPLICATION	

PROPRIETARY AND CONFIDENTIAL

THE INFORMATION CONTAINED IN THIS DRAWING IS THE SOLE PROPERTY OF <INSERT COMPANY NAME HERE>. ANY REPRODUCTION IN PART OR AS A WHOLE WITHOUT THE WRITTEN PERMISSION OF <INSERT COMPANY NAME HERE> IS PROHIBITED.

5 4 3 2 1

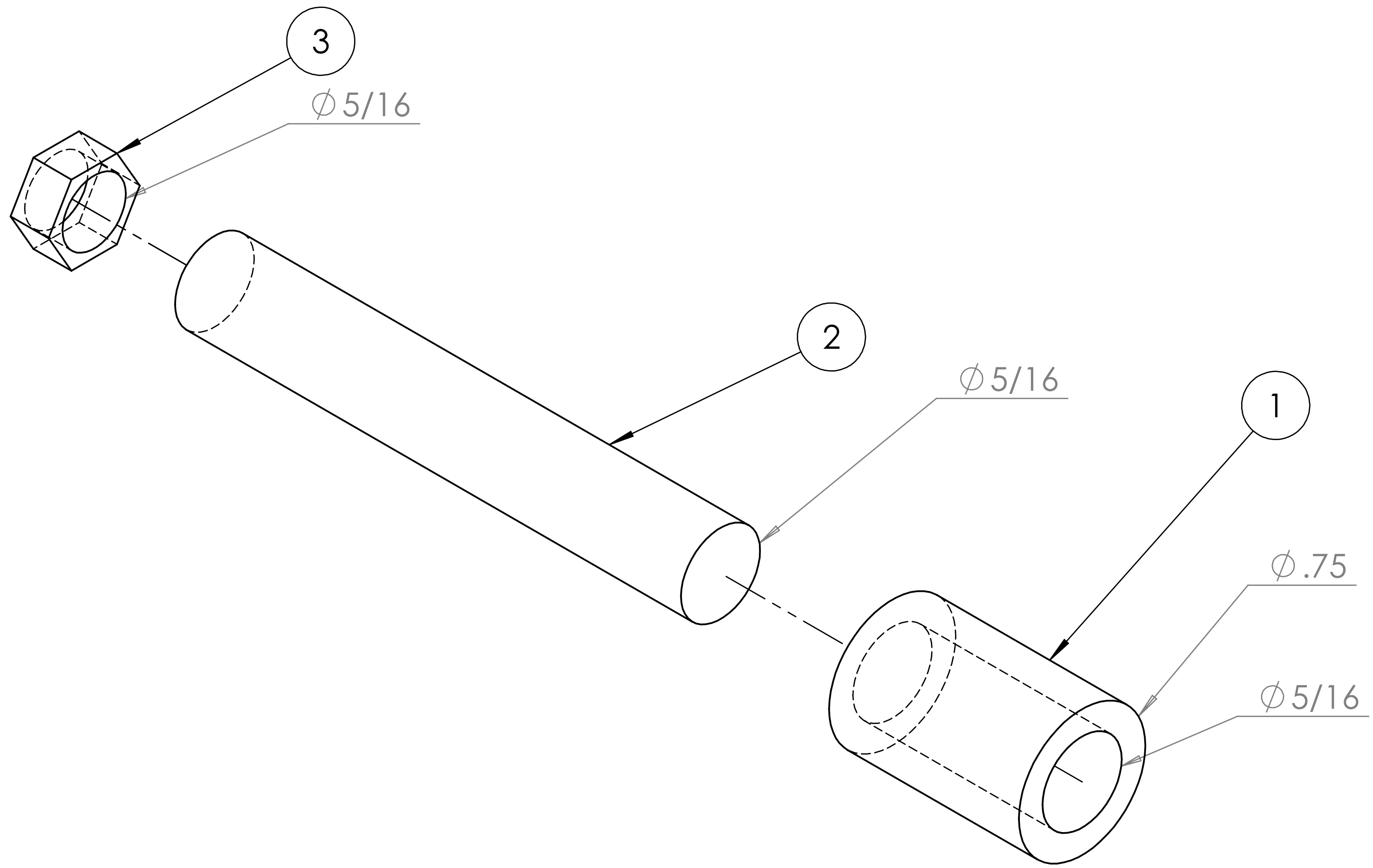

NUMBER	COMPONENT
1	INSERT
2	THREADED STUD
3	NUT

UNLESS OTHERWISE SPECIFIED:

DIMENSIONS ARE IN INCHES
TOLERANCES:
FRACTIONAL ± 1/16
ANGULAR: BEND ± 1°
TWO PLACE DECIMAL ± .01
THREE PLACE DECIMAL ± .005

	NAME	DATE
DRAWN	FERRELL	4/15/15
CHECKED		
ENG APPR.		
MFG APPR.		
Q.A.		

COMMENTS:

TITLE: NOSECONE MOUNTING HARDWARE

MATERIAL STEEL

FINISH

NEXT ASSY | USED ON

APPLICATION

DO NOT SCALE DRAWING

SIZE A | DWG. NO. | REV

SCALE: 1:1 | SHEET 1 OF 1

5 4 3 2 1

NOTE: QTY. 8
GRIND TO EXACT SANDWICH THICKNESS

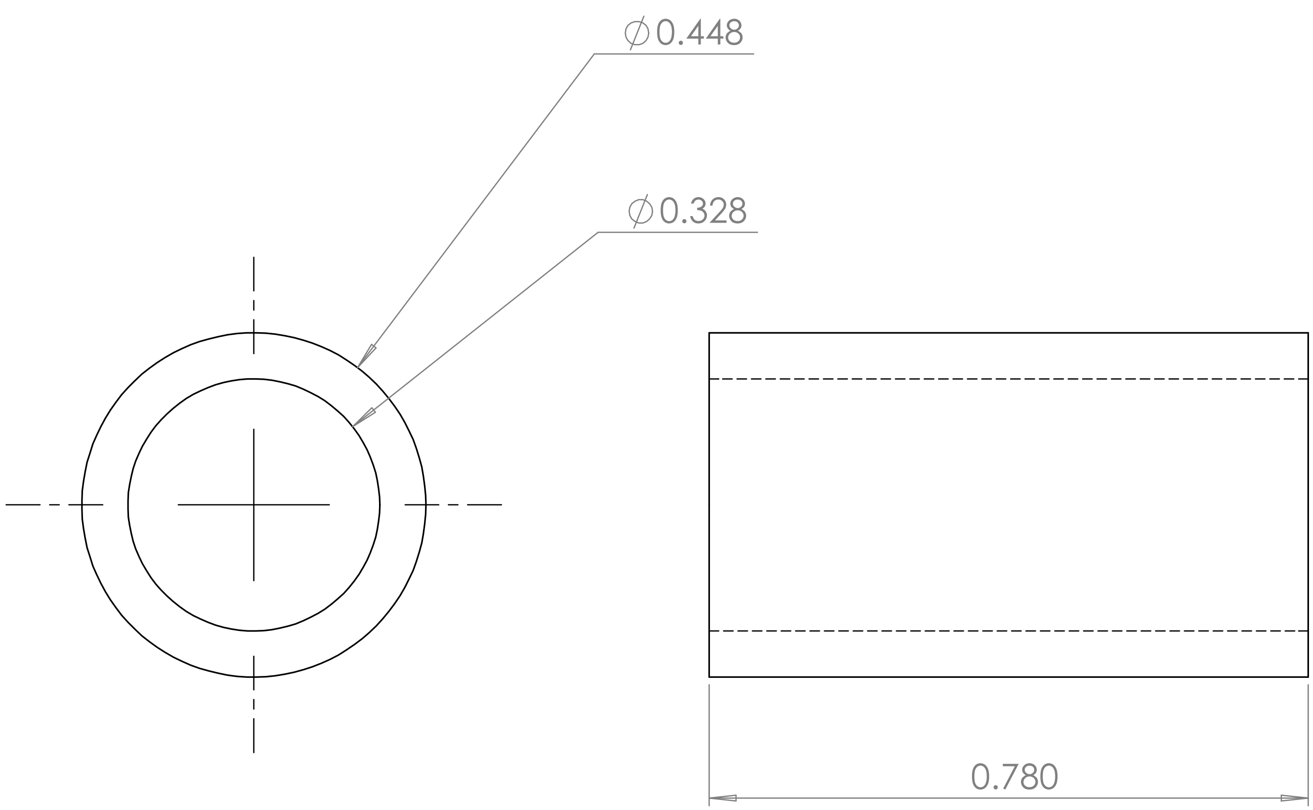

		UNLESS OTHERWISE SPECIFIED:		NAME	DATE	
		DIMENSIONS ARE IN INCHES TOLERANCES: FRACTIONAL ± 1/16 ANGULAR: BEND ± 1° TWO PLACE DECIMAL ± .01 THREE PLACE DECIMAL ± .005	DRAWN	AC		TITLE: FRONT ROLL HOOP INSERT
			CHECKED			
			ENG APPR.			
			MFG APPR.			
			Q.A.			
		MATERIAL 6061 ALUMINUM	COMMENTS:			SIZE A / DWG. NO. / REV
NEXT ASSY	USED ON	FINISH				
APPLICATION		DO NOT SCALE DRAWING				SCALE: 4:1 / WEIGHT: / SHEET 1 OF 1

5 4 3 2 1

NOTE: QTY. 4

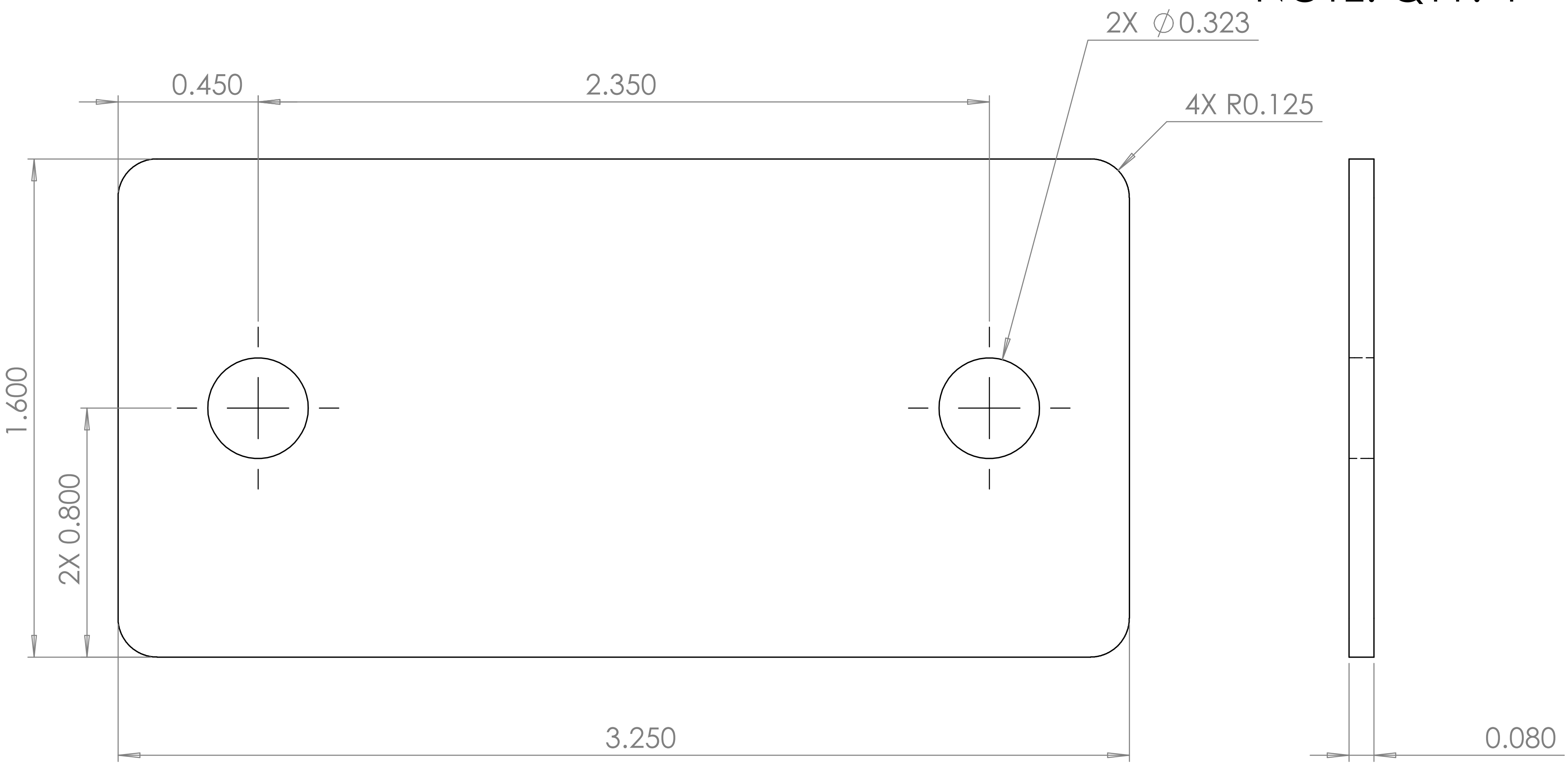

		UNLESS OTHERWISE SPECIFIED:		NAME	DATE		
		DIMENSIONS ARE IN INCHES TOLERANCES: FRACTIONAL ± 1/16 ANGULAR: BEND ± 1° TWO PLACE DECIMAL ± .01 THREE PLACE DECIMAL ± .005	DRAWN	AC			
			CHECKED			TITLE: FRONT ROLL HOOP BACKING PLATE	
			ENG APPR.				
			MFG APPR.				
			Q.A.				
		MATERIAL 4130 STEEL	COMMENTS:			SIZE A	DWG. NO.	REV
NEXT ASSY	USED ON	FINISH					
APPLICATION		DO NOT SCALE DRAWING				SCALE: 2:1	WEIGHT:	SHEET 1 OF 1

5 4 3 2 1

NOTE: QTY. 1
ROUND ALL CORNERS 0.13''
BEND AT CENTERLINE TO TUB CURVATURE
POSITION LOWER EDGE AT CENTER OF ROLL HOOP TUBE

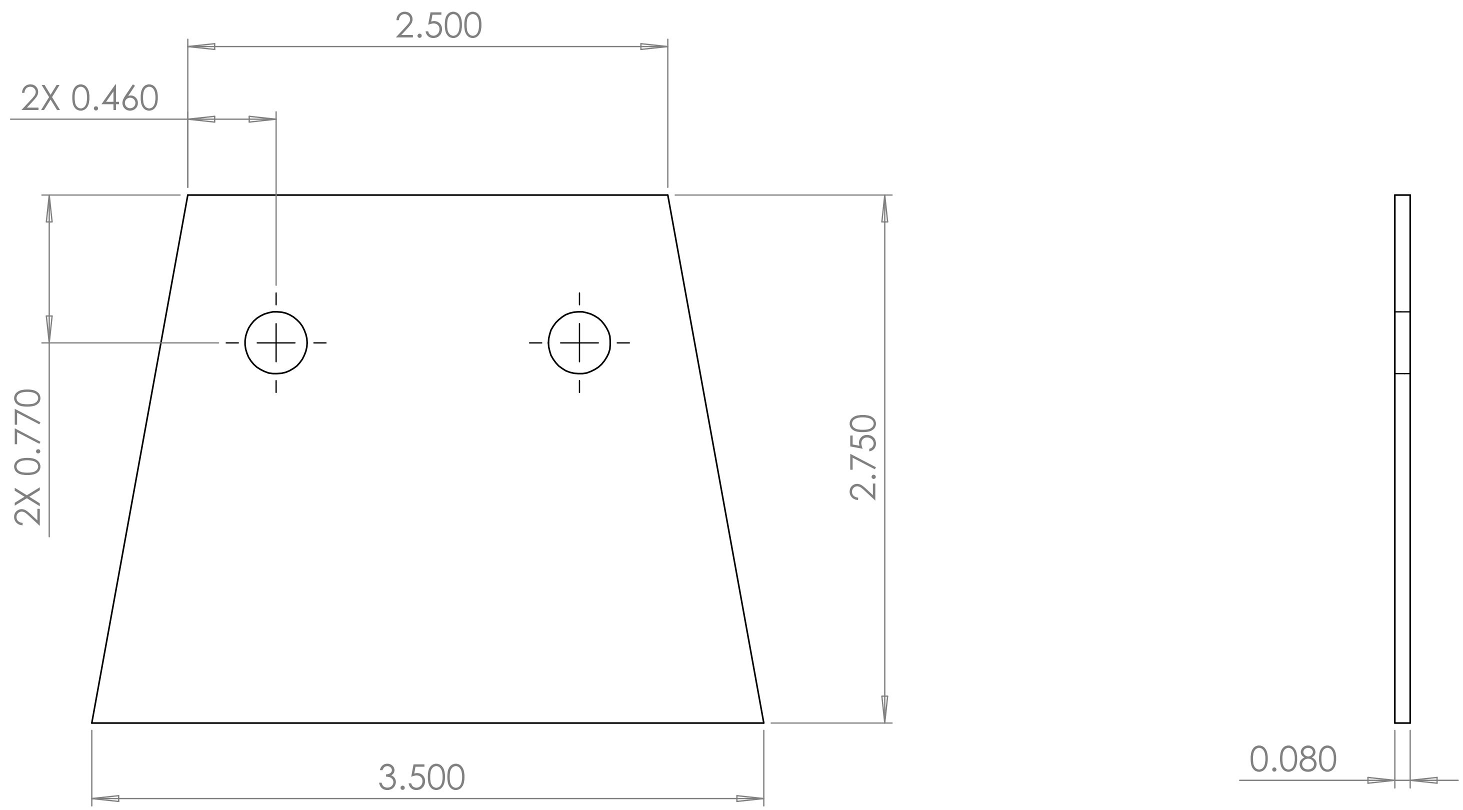

UNLESS OTHERWISE SPECIFIED:		NAME	DATE	
DIMENSIONS ARE IN INCHES TOLERANCES: FRACTIONAL ± 1/16 ANGULAR: BEND ± 1° TWO PLACE DECIMAL ± .01 THREE PLACE DECIMAL ± .005	DRAWN	AC		TITLE:
	CHECKED			FRONT ROLL HOOP CENTER MOUNT PLATE
	ENG APPR.			
	MFG APPR.			
	Q.A.			
MATERIAL 4130 STEEL	COMMENTS:			SIZE A — DWG. NO. — REV
FINISH				
DO NOT SCALE DRAWING				SCALE: 1:1 — WEIGHT: — SHEET 1 OF 1

NEXT ASSY	USED ON
APPLICATION	

5 4 3 2 1

NOTE: QTY. 8

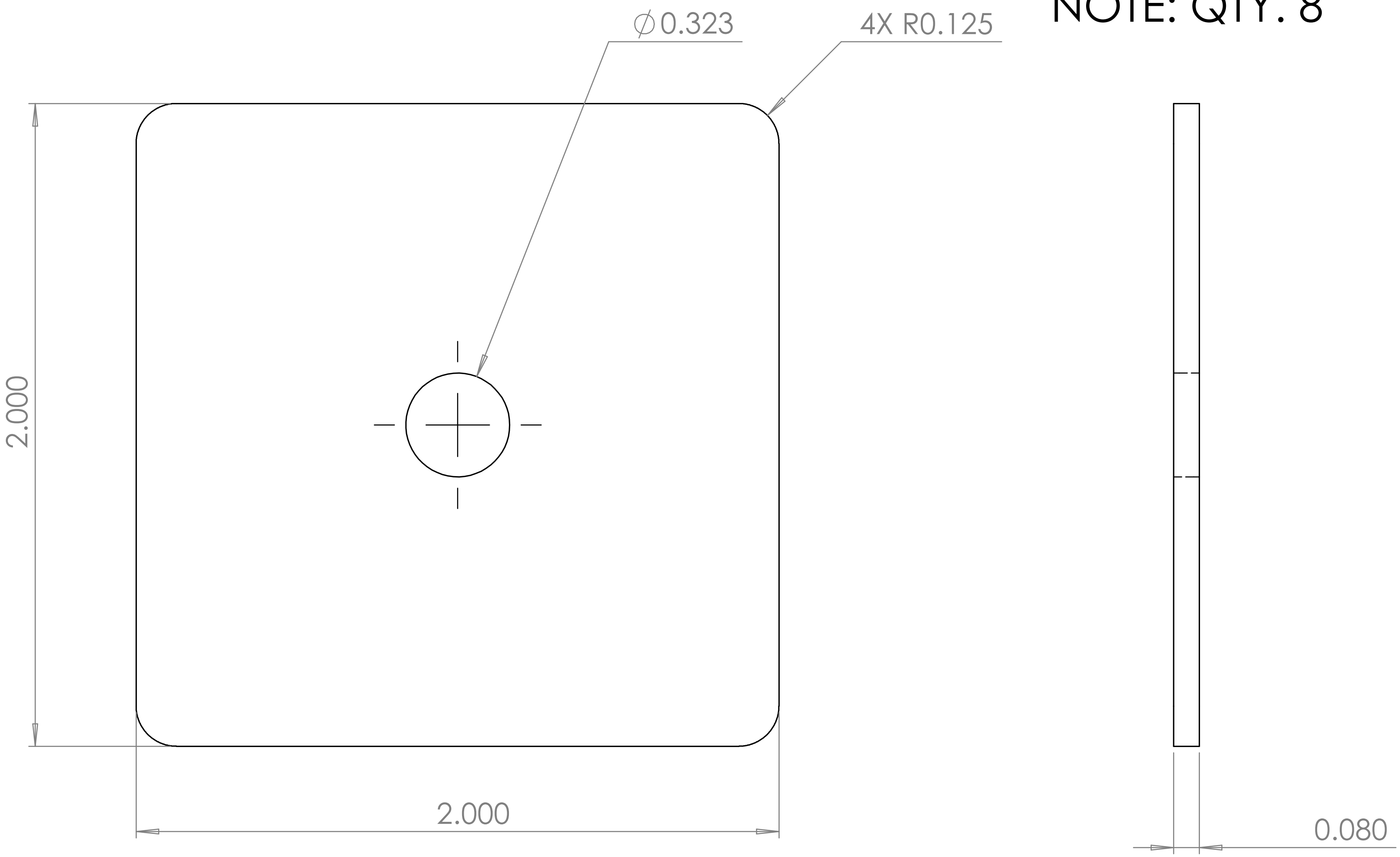

		UNLESS OTHERWISE SPECIFIED:		NAME	DATE	
		DIMENSIONS ARE IN INCHES TOLERANCES: FRACTIONAL ± 1/16 ANGULAR: BEND ± 1° TWO PLACE DECIMAL ± .01 THREE PLACE DECIMAL ± .005	DRAWN	AC		TITLE:
			CHECKED			HARNESS BACKING PLATE
			ENG APPR.			
			MFG APPR.			
			Q.A.			
		MATERIAL 4130 STEEL	COMMENTS:			SIZE A / DWG. NO. / REV
NEXT ASSY	USED ON	FINISH				
APPLICATION		DO NOT SCALE DRAWING				SCALE: 2:1 / WEIGHT: / SHEET 1 OF 1

5 4 3 2 1

NOTE: QTY. 8

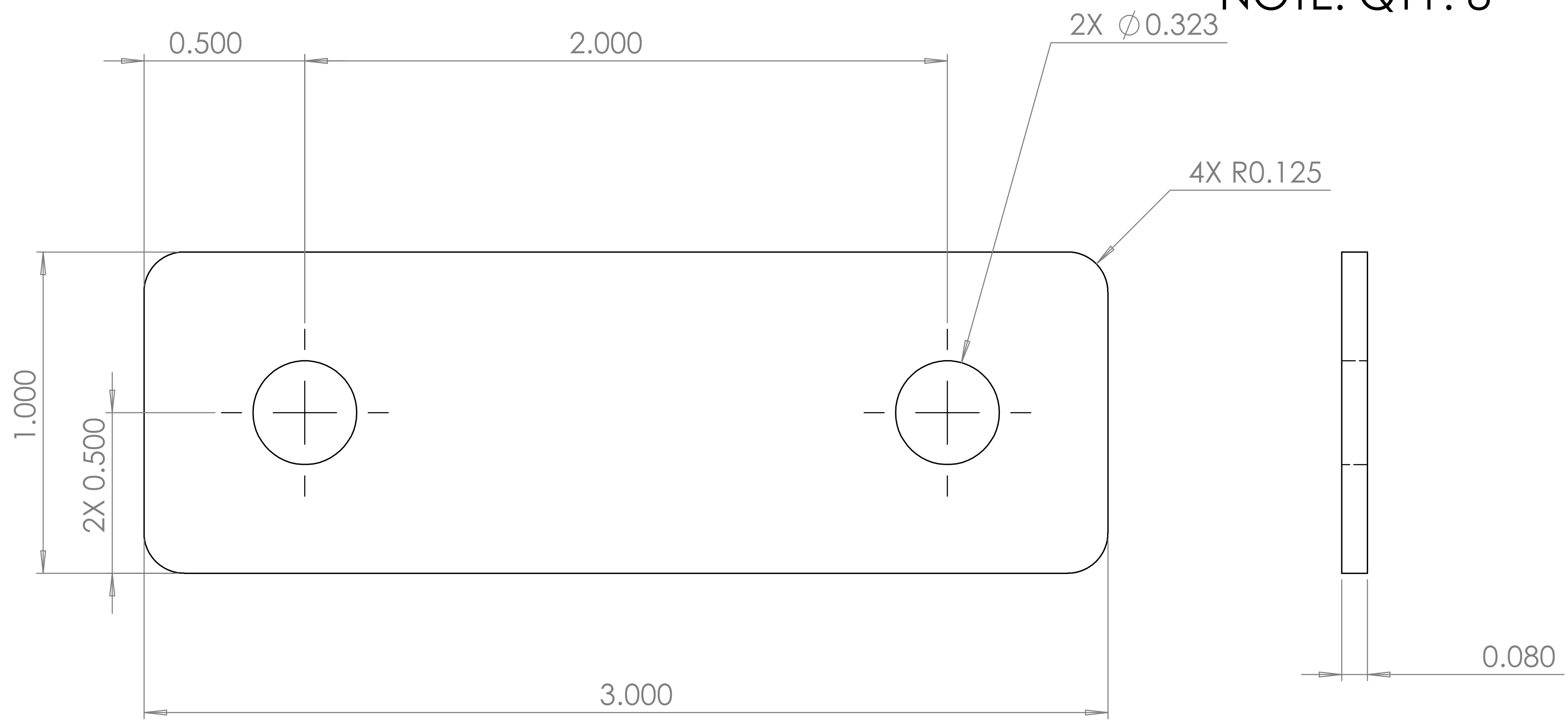

		UNLESS OTHERWISE SPECIFIED:		NAME	DATE
		DIMENSIONS ARE IN INCHES TOLERANCES: FRACTIONAL ± 1/16 ANGULAR: BEND ± 1° TWO PLACE DECIMAL ± .01 THREE PLACE DECIMAL ± .005	DRAWN	AC	
			CHECKED		
			ENG APPR.		
			MFG APPR.		
			Q.A.		
		MATERIAL 4130 STEEL	COMMENTS:		
NEXT ASSY	USED ON	FINISH			
APPLICATION		DO NOT SCALE DRAWING			

TITLE:

MAIN ROLL HOOP BACKING PLATE

SIZE	DWG. NO.	REV
A		

SCALE: 2:1 WEIGHT: SHEET 1 OF 1

5 4 3 2 1

NOTE: QTY. #2

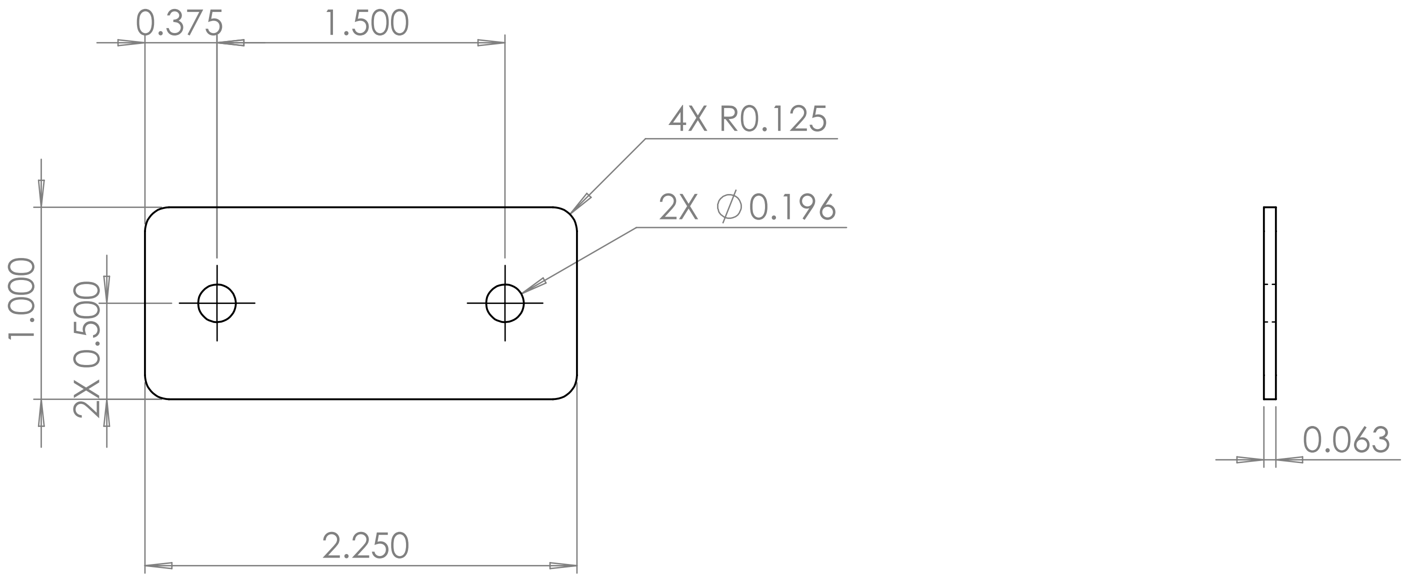

	NAME	DATE
DRAWN	LOOGMAN	12/15/14
CHECKED		
ENG APPR.		
MFG APPR.		
Q.A.		
COMMENTS:		

UNLESS OTHERWISE SPECIFIED:

DIMENSIONS ARE IN INCHES
TOLERANCES:
FRACTIONAL ± 1/16
ANGULAR: BEND ± 1°
TWO PLACE DECIMAL ± .01
THREE PLACE DECIMAL ± .005

MATERIAL
4130 STEEL

FINISH

NEXT ASSY | USED ON

APPLICATION

DO NOT SCALE DRAWING

TITLE:
COILOVER BACKING PLATE

SIZE A | DWG. NO. | REV

SCALE: 1:1 | WEIGHT: | SHEET 1 OF 1

5 4 3 2 1

NOTE: QTY. #4

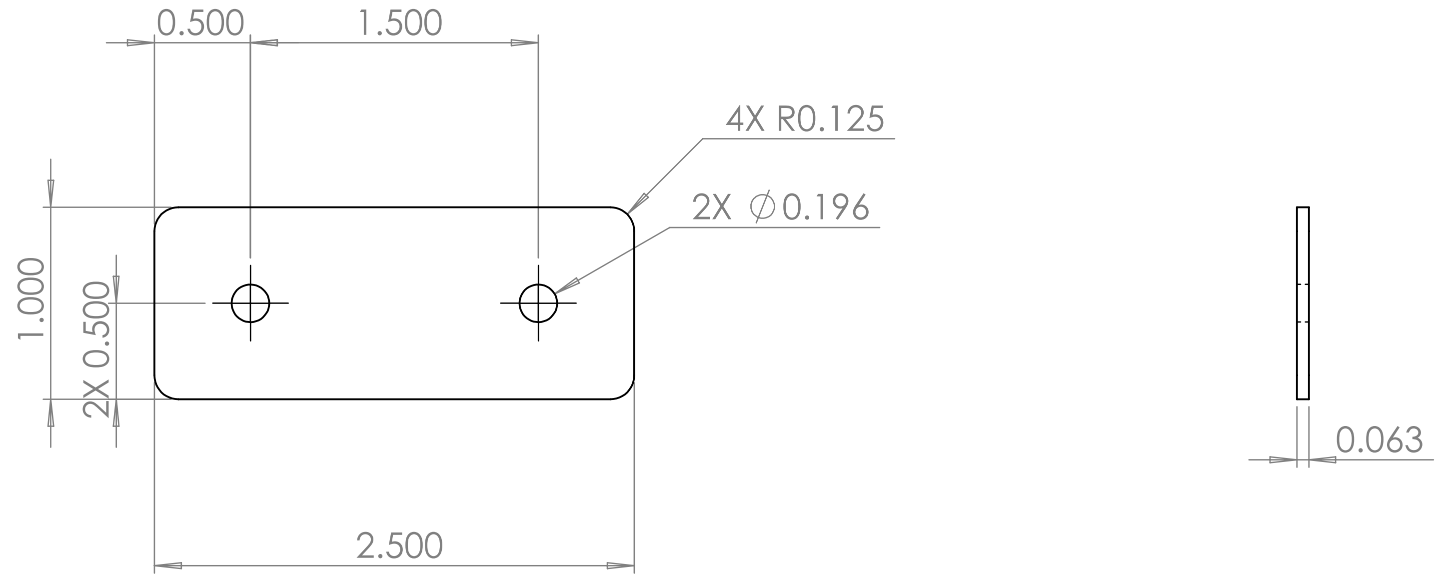

UNLESS OTHERWISE SPECIFIED:		
DIMENSIONS ARE IN INCHES TOLERANCES: FRACTIONAL ± 1/16 ANGULAR: BEND ± 1° TWO PLACE DECIMAL ± .01 THREE PLACE DECIMAL ± .005		
MATERIAL 4130 STEEL		
FINISH		
NEXT ASSY	USED ON	
APPLICATION		DO NOT SCALE DRAWING

	NAME	DATE
DRAWN	LOOGMAN	12/15/14
CHECKED		
ENG APPR.		
MFG APPR.		
Q.A.		
COMMENTS:		

TITLE:

LOWER A-ARM BACKING PLATE

SIZE	DWG. NO.	REV
A		
SCALE: 1:1	WEIGHT:	SHEET 1 OF 1

5 4 3 2 1

NOTE: QTY. #4

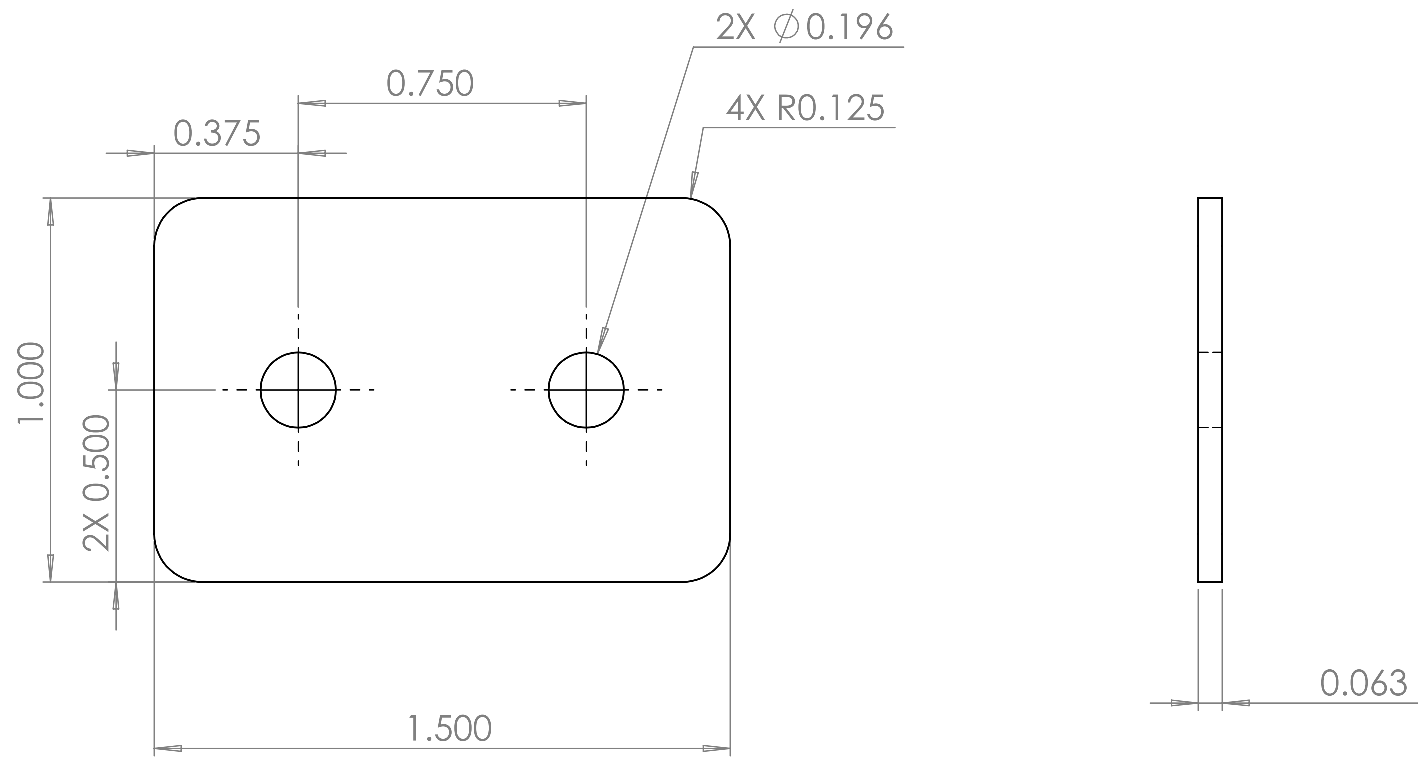

		UNLESS OTHERWISE SPECIFIED:		NAME	DATE
		DIMENSIONS ARE IN INCHES TOLERANCES: FRACTIONAL ± 1/16 ANGULAR: BEND ± 1° TWO PLACE DECIMAL ± .01 THREE PLACE DECIMAL ± .005	DRAWN	LOOGMAN	12/15/14
			CHECKED		
			ENG APPR.		
			MFG APPR.		
			Q.A.		
		MATERIAL 4130 STEEL	COMMENTS:		
NEXT ASSY	USED ON	FINISH			
APPLICATION		DO NOT SCALE DRAWING			

TITLE:
Upper Suspension Backing Plate

SIZE A | DWG. NO. | REV

SCALE: 2:1 | WEIGHT: | SHEET 1 OF 1

5 4 3 2 1

NOTE: QTY. #8

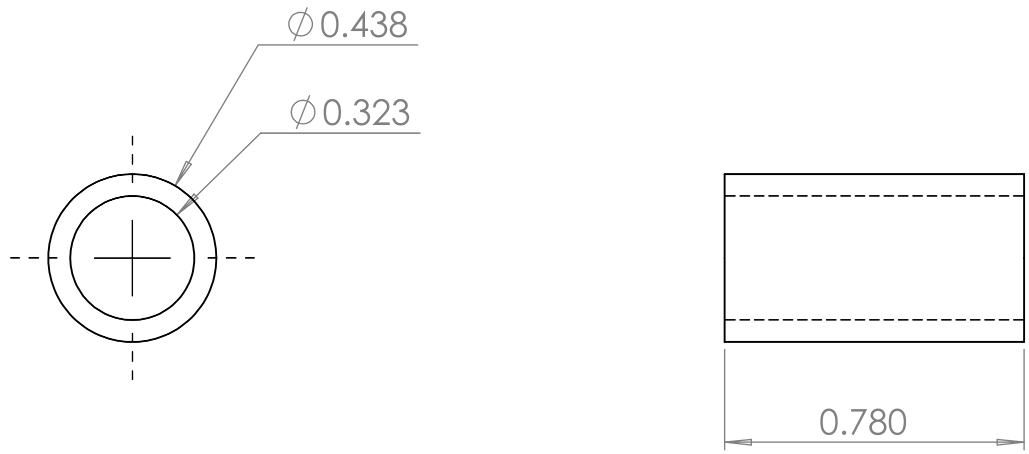

		UNLESS OTHERWISE SPECIFIED:		NAME	DATE
		DIMENSIONS ARE IN INCHES TOLERANCES: FRACTIONAL ± 1/16 ANGULAR: BEND ± 1° TWO PLACE DECIMAL ± .01 THREE PLACE DECIMAL ± .005	DRAWN	LOOGMAN	12/15/14
			CHECKED		
			ENG APPR.		
			MFG APPR.		
			Q.A.		
		MATERIAL 6061 ALUMINUM	COMMENTS:		
NEXT ASSY	USED ON	FINISH			
APPLICATION		DO NOT SCALE DRAWING			

TITLE:

HARNESS INSERT

SIZE **A** DWG. NO. REV

SCALE: 2:1 WEIGHT: SHEET 1 OF 1

PROPRIETARY AND CONFIDENTIAL

THE INFORMATION CONTAINED IN THIS DRAWING IS THE SOLE PROPERTY OF <INSERT COMPANY NAME HERE>. ANY REPRODUCTION IN PART OR AS A WHOLE WITHOUT THE WRITTEN PERMISSION OF <INSERT COMPANY NAME HERE> IS PROHIBITED.

5 4 3 2 1

NOTE: QTY. 24

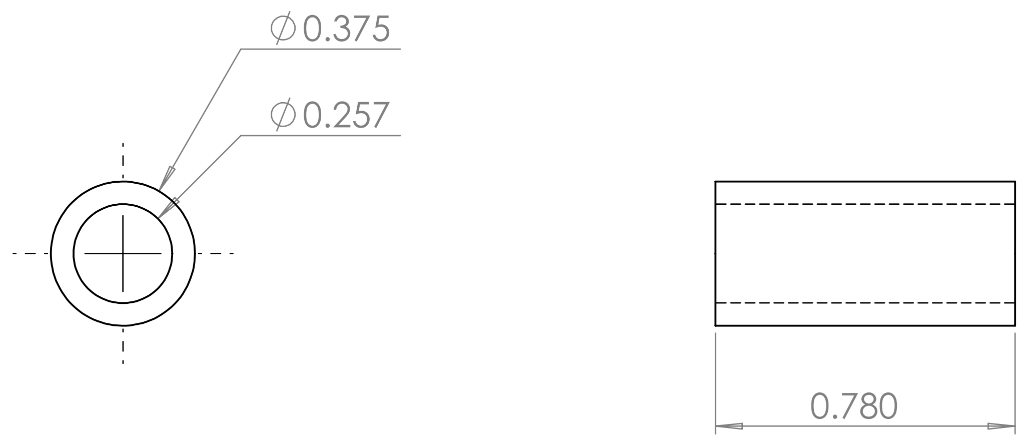

UNLESS OTHERWISE SPECIFIED:

DIMENSIONS ARE IN INCHES
TOLERANCES:
FRACTIONAL ± 1/16
ANGULAR: BEND ± 1°
TWO PLACE DECIMAL ± .01
THREE PLACE DECIMAL ± .005

	NAME	DATE
DRAWN	LOOGMAN	12/15/14
CHECKED		
ENG APPR.		
MFG APPR.		
Q.A.		

COMMENTS:

MATERIAL
6061 ALUMINUM

FINISH

NEXT ASSY | USED ON

APPLICATION

DO NOT SCALE DRAWING

TITLE:

Suspension Insert

SIZE A | DWG. NO. | REV

SCALE: 2:1 | WEIGHT: | SHEET 1 OF 1

5 4 3 2 1

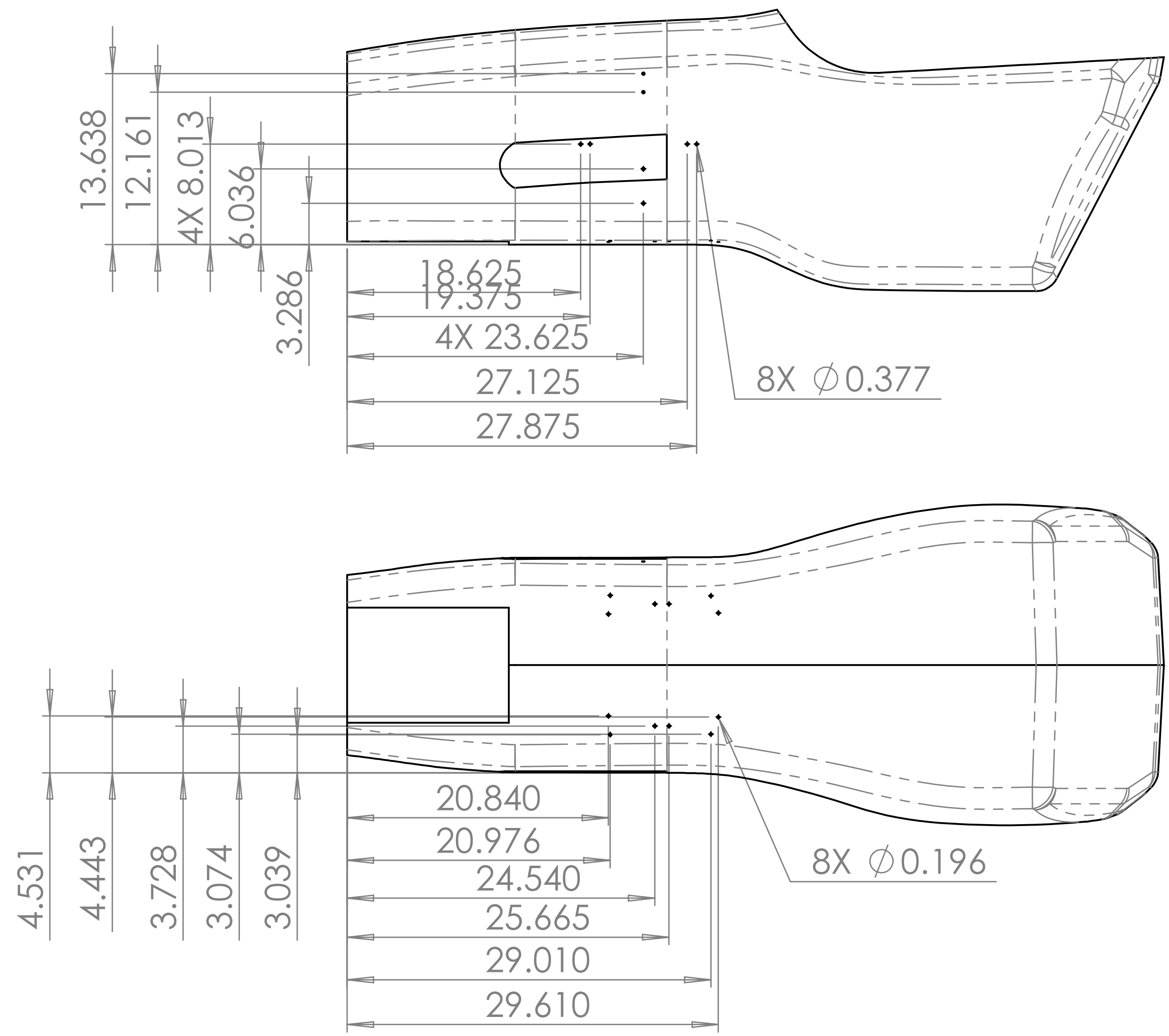

UNLESS OTHERWISE SPECIFIED:

DIMENSIONS ARE IN INCHES
TOLERANCES:
FRACTIONAL ± 1/16
ANGULAR: BEND ± 1°
TWO PLACE DECIMAL ± .01
THREE PLACE DECIMAL ± .005

	NAME	DATE
DRAWN	LOOGMAN	12/15/14
CHECKED		
ENG APPR.		
MFG APPR.		
Q.A.		

COMMENTS:

TITLE:

SUSPENSION HOLE LOCATIONS

MATERIAL
CFRP SANDWICH

FINISH

NEXT ASSY | USED ON

APPLICATION

DO NOT SCALE DRAWING

SIZE A | DWG. NO. | REV

SCALE: 1:15 | WEIGHT: | SHEET 1 OF 1

5 4 3 2 1

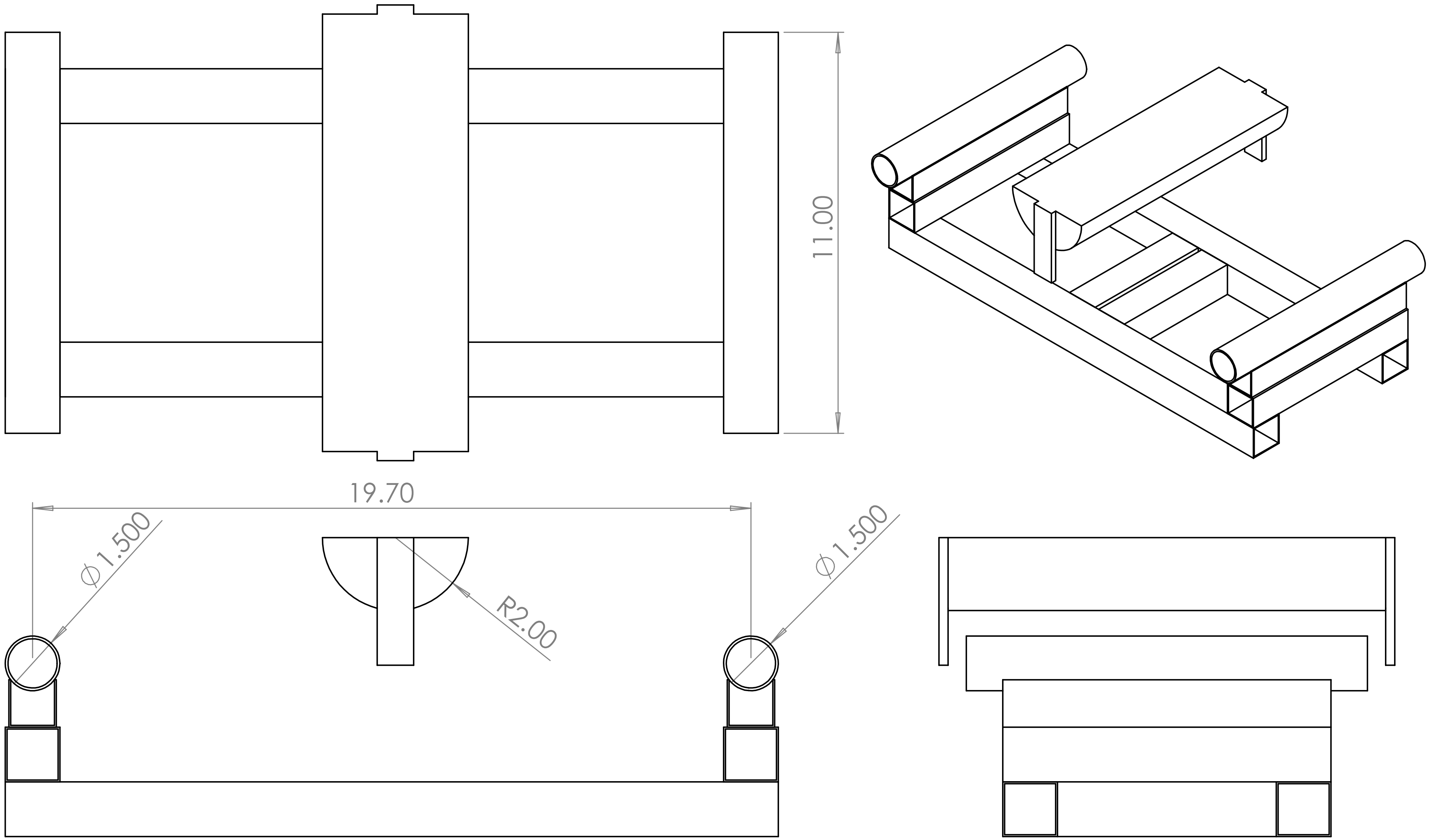

		UNLESS OTHERWISE SPECIFIED:		NAME	DATE
		DIMENSIONS ARE IN INCHES TOLERANCES: FRACTIONAL ± 1/16 ANGULAR: BEND ± 1° TWO PLACE DECIMAL ± .01 THREE PLACE DECIMAL ± .005	DRAWN	FERRELL	7/15/15
			CHECKED		
			ENG APPR.		
			MFG APPR.		
			Q.A.		
		MATERIAL 6061 ALUMINUM	COMMENTS:		
NEXT ASSY	USED ON	FINISH			
APPLICATION		DO NOT SCALE DRAWING			

TITLE: LONG BEAM TEST FIXTURE

SIZE	DWG. NO.	REV
A		

SCALE: 4

SHEET 1 OF 1

5 4 3 2 1

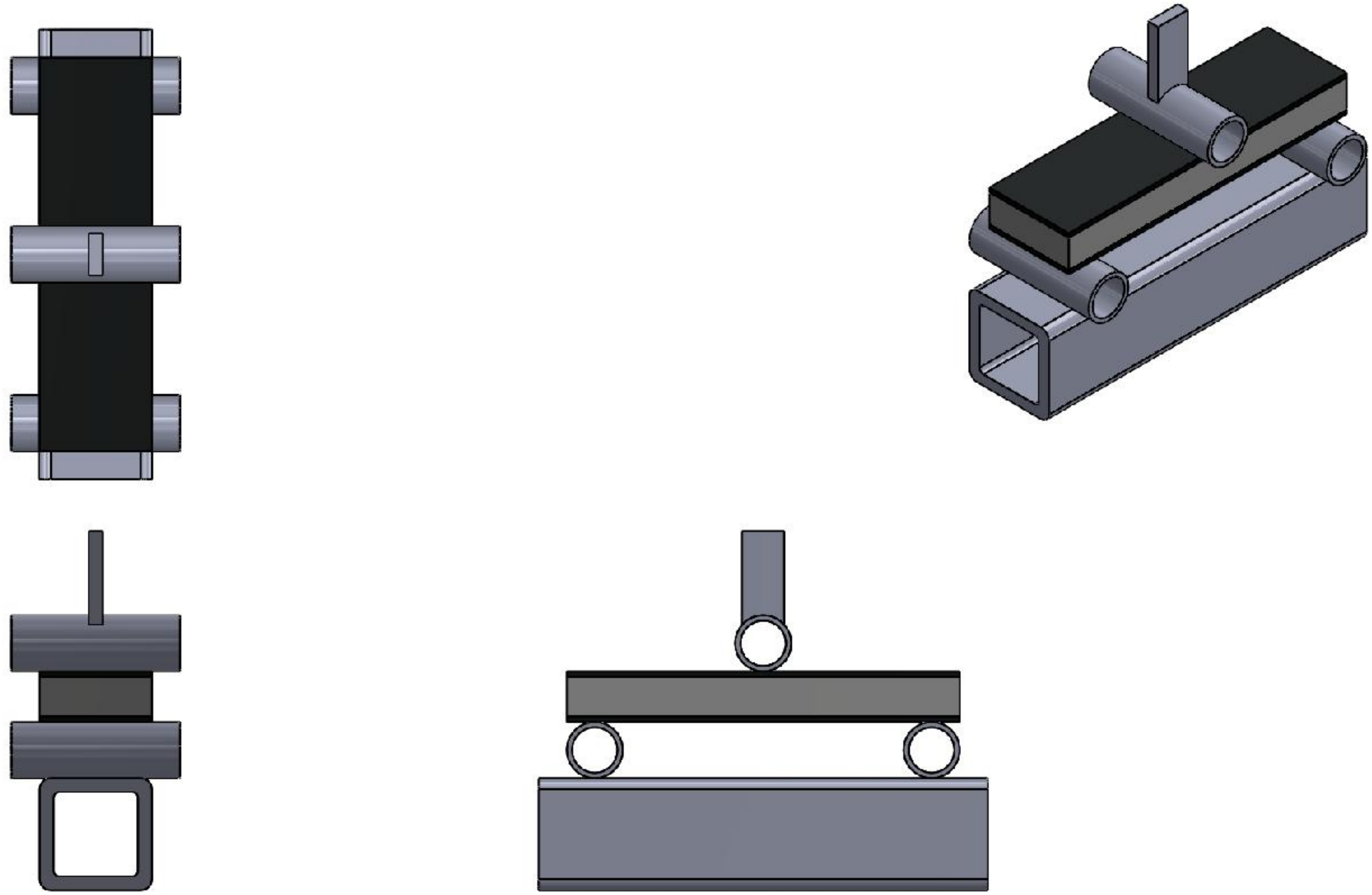

		UNLESS OTHERWISE SPECIFIED:		NAME	DATE	
		DIMENSIONS ARE IN INCHES TOLERANCES: FRACTIONAL ± ANGULAR: MACH ± BEND ± TWO PLACE DECIMAL ± THREE PLACE DECIMAL ±	DRAWN	AC		TITLE:
			CHECKED			SHORT BEAM FIXTURE AND PANEL
			ENG APPR.			
			MFG APPR.			
		INTERPRET GEOMETRIC TOLERANCING PER:	Q.A.			
		MATERIAL	COMMENTS:			SIZE A	DWG. NO.	REV
NEXT ASSY	USED ON	FINISH				
APPLICATION		DO NOT SCALE DRAWING				SCALE: 1:3	WEIGHT:	SHEET 1 OF 3

5 4 3 2 1

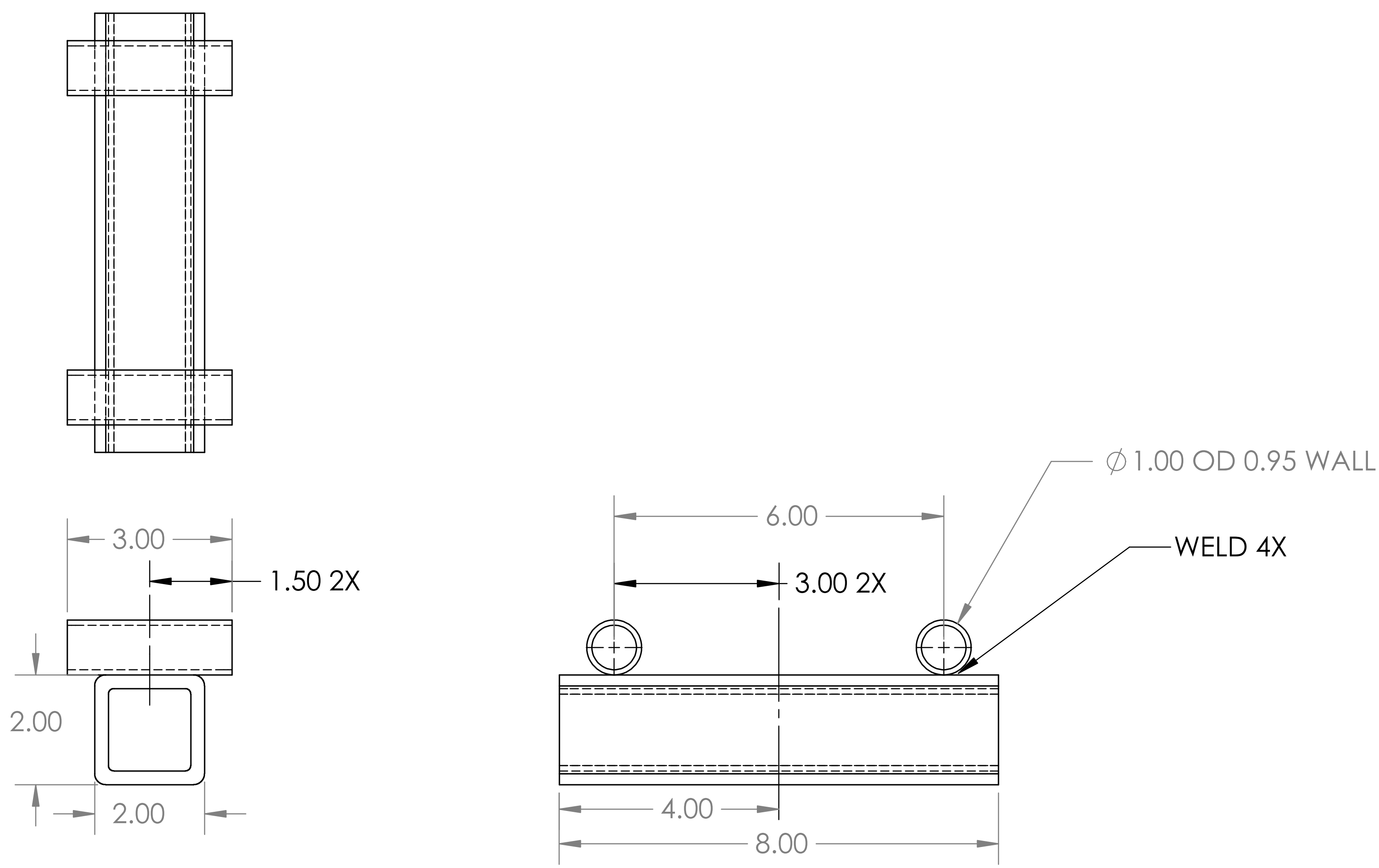

		UNLESS OTHERWISE SPECIFIED:		NAME	DATE	
		DIMENSIONS ARE IN INCHES TOLERANCES: FRACTIONAL ± ANGULAR: MACH ± BEND ± TWO PLACE DECIMAL ± THREE PLACE DECIMAL ±	DRAWN	AC		TITLE:
			CHECKED			SHORT BEAM BASE
			ENG APPR.			
			MFG APPR.			
		INTERPRET GEOMETRIC TOLERANCING PER:	Q.A.			
		MATERIAL STEEL	COMMENTS:			SIZE A / DWG. NO. / REV
NEXT ASSY	USED ON	FINISH				
APPLICATION		DO NOT SCALE DRAWING				SCALE: 1:3 / WEIGHT: / SHEET 2 OF 3

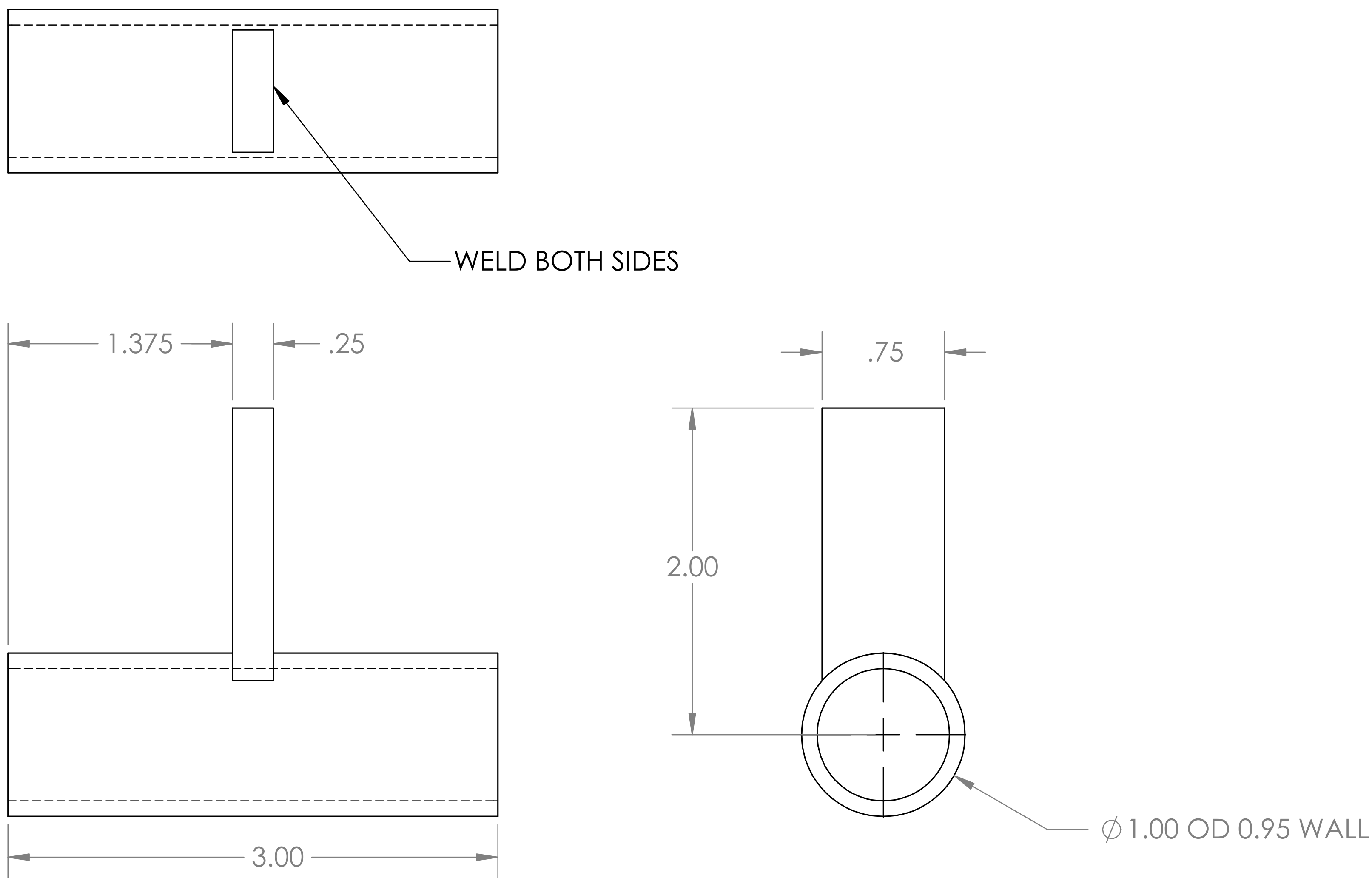

		UNLESS OTHERWISE SPECIFIED:		NAME	DATE	
		DIMENSIONS ARE IN INCHES TOLERANCES: FRACTIONAL ± ANGULAR: MACH ± BEND ± TWO PLACE DECIMAL ± THREE PLACE DECIMAL ±	DRAWN	AC		TITLE: SHORT BEAM IMPACTOR
			CHECKED			
			ENG APPR.			
			MFG APPR.			
		INTERPRET GEOMETRIC TOLERANCING PER:	Q.A.			
		MATERIAL STEEL	COMMENTS:			SIZE A · DWG. NO. · REV
NEXT ASSY	USED ON	FINISH				
APPLICATION		DO NOT SCALE DRAWING				SCALE: 1:1 · WEIGHT: · SHEET 3 OF 3

5 4 3 2 1

Appendix M

Cockpit Pullout Test Fixture Detail Images

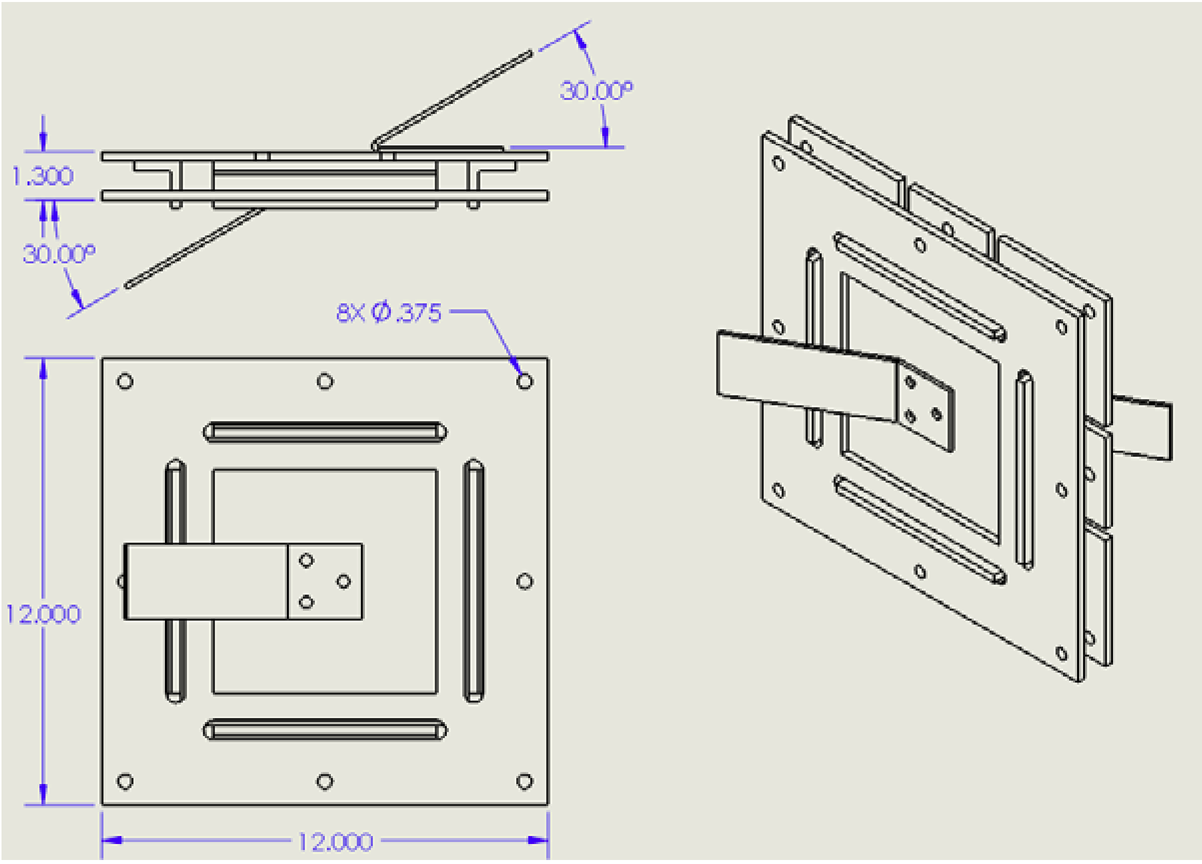

Figure M1. *Cockpit pullout test fixture dimensions.*

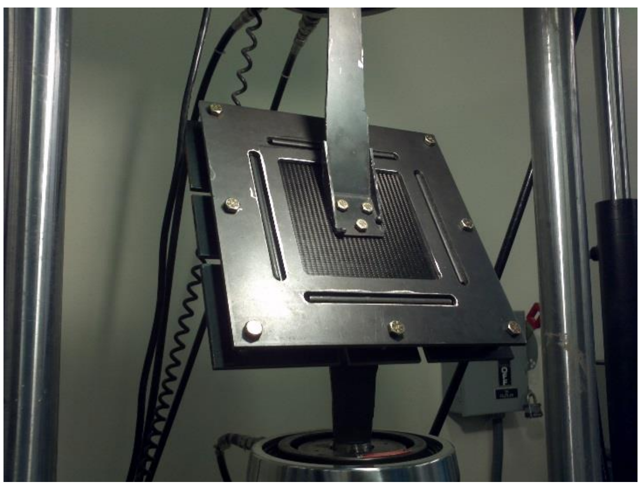

Figure M2. *Test laminate set up in the cockpit pullout test fixture.*

Appendix N

Gantt Chart

Table N1. A Gantt chart developed in Microsoft Project® is used for scheduling and forecasting. Predecessors are utilized in the manufacturing phase to automatically reschedule tasks should delays occur.

Task Name	Duration	Start	Finish	Predecessors
Start	0 days	Sun 6/1/14	Sun 6/1/14	
Definition	**37.47 days**	**Thu 5/1/14**	**Sun 6/1/14**	
Design specifications submitted, draft 1	0 days	Thu 5/1/14	Thu 5/1/14	
Discuss design specifications with sponsor	1 day	Sun 6/1/14	Sun 6/1/14	
Design specifications submitted, draft 2	0 days	Sun 6/1/14	Sun 6/1/14	
Selection	**36.98 days**	**Wed 4/30/14**	**Sat 5/31/14**	
Preliminary Design Review (with Formula SAE team)	1 day	Sat 6/28/14	Sat 6/28/14	
Project Proposal submitted to sponsor	0 days	Thu 5/1/14	Thu 5/1/14	
Develop pool of potential laminates	11 days	Mon 6/2/14	Tue 6/10/14	
Conceptual Design Report draft submitted to sponsor	0 days	Tue 6/3/14	Tue 6/3/14	
Conceptual Design Report Presentation	1 day	Thu 6/5/14	Thu 6/5/14	
Torsion test for 2013-2014 Monocoque (on hold)	**75.95 days**	**Mon 6/16/14**	**Sun 8/17/14**	
Design of monocoque (only) torsion tester	22 days	Mon 6/16/14	Fri 7/4/14	
Construction of monocoque torsional tester	23 days	Wed 7/16/14	Mon 8/4/14	
Torsional test of 2013-2014 monocoque	2 days	Sat 8/16/14	Sun 8/17/14	
Materials Acquisition	**3.5 days**	**Fri 10/31/14**	**Mon 11/3/14**	

Obtain all prepreg material to be used in test and final laminates	0 days	Sat 11/1/14	Sat 11/1/14	
Obtain all core materials to be used in test and final sandwich structures	0 days	Mon 11/3/14	Mon 11/3/14	
Obtain layup materials: vacuum bag, breather, tacky tape, etc.	0 days	Fri 10/31/14	Fri 10/31/14	
Layup Testing	**217.34 days?**	**Sat 10/18/14**	**Tue 4/14/15**	
Test Material Properties	4 wks	Sat 10/18/14	Mon 11/3/14	
Prepare in tub layup test samples	4 days	Mon 11/3/14	Thu 11/6/14	
Test in tub sample layups	2 days	Thu 11/6/14	Sat 11/8/14	26
Prepare rules test layups	2 days	Thu 11/6/14	Fri 11/7/14	
Test rules layups	2 days	Sat 11/8/14	Sun 11/9/14	28
Make final layup selection	0 days	Mon 11/10/14	Mon 11/10/14	
Critical Design Review (with Formula SAE team)	0 days	Sun 11/2/14	Sun 11/2/14	
Design changes from CDR feedback	11 days	Mon 11/3/14	Tue 11/11/14	31FS+2 days
Final Design Report due	0 days	Thu 10/30/14	Thu 10/30/14	
Monocoque Manufacturing	**10 days**	**Tue 11/11/14**	**Thu 11/20/14**	
Template cutting	1 day	Tue 11/11/14	Wed 11/12/14	32
Core cutting	1 day	Tue 11/11/14	Wed 11/12/14	32

Outer skin layup	0.4 days	Wed 11/12/14	Wed 11/12/14	36
Core placement	0.2 days	Wed 11/12/14	Thu 11/13/14	37
Inner skin layup	0.4 days	Thu 11/13/14	Thu 11/13/14	38
Oven cure	1 day	Thu 11/13/14	Fri 11/14/14	39
Trimming joint edges and bulkhead	2 days	Fri 11/14/14	Sun 11/16/14	40
Align halves	1 day	Sun 11/16/14	Mon 11/17/14	41
Join halves	0.5 days	Mon 11/17/14	Mon 11/17/14	42
Cockpit and bulkhead closeout	2 days	Mon 11/17/14	Tue 11/18/14	43
Additional post-bonding (if required)	1 day	Tue 11/18/14	Wed 11/19/14	44
Drill insert holes	0.5 days	Wed 11/19/14	Thu 11/20/14	45
Manufacture inserts	4 days	Tue 11/11/14	Sun 11/16/14	32
Bore suspension and steering cutouts	0.5 days	Tue 11/18/14	Wed 11/19/14	44
Mass properties without inserts but with all cutouts, post bonding structures, closeouts, etc.	1 day	Wed 11/19/14	Thu 11/20/14	48,45
Bond potted inserts	0.5 days	Thu 11/20/14	Fri 11/21/14	49
Torsion Test for 2015 Monocoque	**4 days**	**Sun 11/23/14**	**Tue 11/25/14**	
Prepare equipment and monocoque for torsional test	1 day	Fri 10/24/14	Sat 10/25/14	

Torsional test of 2015 monocoque	1 day	Sun 11/23/14	Sun 11/23/14	52FS+1 day
Monocoque ready to accept sub-system assemblies	0 days	Mon 11/24/14	Mon 11/24/14	53FS+1 day
Nosecone/Impact Attenuator	**31 days**	**Mon 11/3/14**	**Fri 11/28/14**	
Nosecone manufacturing	7 days	Thu 11/20/14	Tue 11/25/14	34
Impact attenuator testing	2 days	Tue 11/25/14	Thu 11/27/14	56
Impact attenuator analysis and report construction	1 day	Thu 11/27/14	Fri 11/28/14	57
Impact attenuator report submitted	0 days	TBD		
AFR Intent Due	0 days	Mon 11/3/14	Mon 11/3/14	
Structural Equivalency Spreadsheet (Incl. AFR)	**154.38 days**	**Sun 10/26/14**	**Mon 3/2/15**	**29**
Structural equivalency spreadsheet testing, perimeter shear, 3-point bend, harness attachment, fixture compliance	7 days	Sun 10/26/14	Fri 10/31/14	28
SES analysis and report construction	2 days	Sun 11/9/14	Mon 11/10/14	62
Submit SES	0 days	Mon 3/2/15	Mon 3/2/15	
Finish and Paint	**2 days**	**Fri 5/1/15**	**Sun 5/3/15**	
Paint monocoque	2 days	Thu 5/1/14	Fri 5/2/14	
Apply signage to monocoque	1 day	Sat 5/3/14	Sun 5/4/14	66
Vehicle assembly	0 days	Fri 2/14/14	Fri 2/14/14	
First drive	0 days	Sat 2/15/14	Sat 2/15/14	68
2015 Lincoln competition	4 days	Thu 6/18/15	Sun 6/21/15	
Finish Project	0 days			

Appendix O

Impact Attenuator Data Sheet Submitted to SAE

2015 FSAE® IMPACT ATTENTUATOR DATA REPORT

This form must be completed and submitted by **all teams no later than the date specified in the Action Deadlines on specific event website**. The FSAE Technical Committee will review all submissions which deviate from the FSAE® rules and reply with a decision about the requested deviation. All requests will have a confirmation of receipt sent to the team. Impact Attenuator Data (IAD) and supporting calculations must be submitted electronically in Adobe Acrobat Format (*.pdf). The submissions must be named as follows: schoolname_IAD.pdf using the complete school name. **Submit the IAD report as instructed on the event website. For Michigan and Lincoln events submit through fsaeonline.com.**

*In the event that the FSAE Technical Committee requests additional information or calculations, teams have **one week from the date of the request** to submit the requested information or ask for a deadline extension.

University Name: California Polytechnic State Univ - SLO Car Number(s) & Event(s): 025 FSAE Lincoln
Team Contact: Henrique Chan E-mail Address: henryk242@gmail.com
Faculty Advisor: John Fabijanic E-mail Address: jfabijan@calpoly.edu

Material(s) Used	Unidirectional and woven carbon fiber prepreg
Description of form/shape	Pyramidal skin with front wing mount flats
IA to Anti-Intrusion Plate mounting method	IA fastened using four (4) axial M8x1.25 Grade 8.8 bolts to Front Bulkhead (AI plate is clamped between IA and Front Bulkhead)
Anti-Intrusion Plate to Front Bulkhead mounting method	IA fastened using four (4) axial M8x1.25 Grade 8.8 bolts to Front Bulkhead (AI plate is clamped between IA and Front Bulkhead)
Peak deceleration (<= 40 g's)	21.873
Average deceleration (<= 20 g's)	7.759

Confirm that the attenuator contains the minimum volume 200mm wide x 100mm high x 200mm long yes

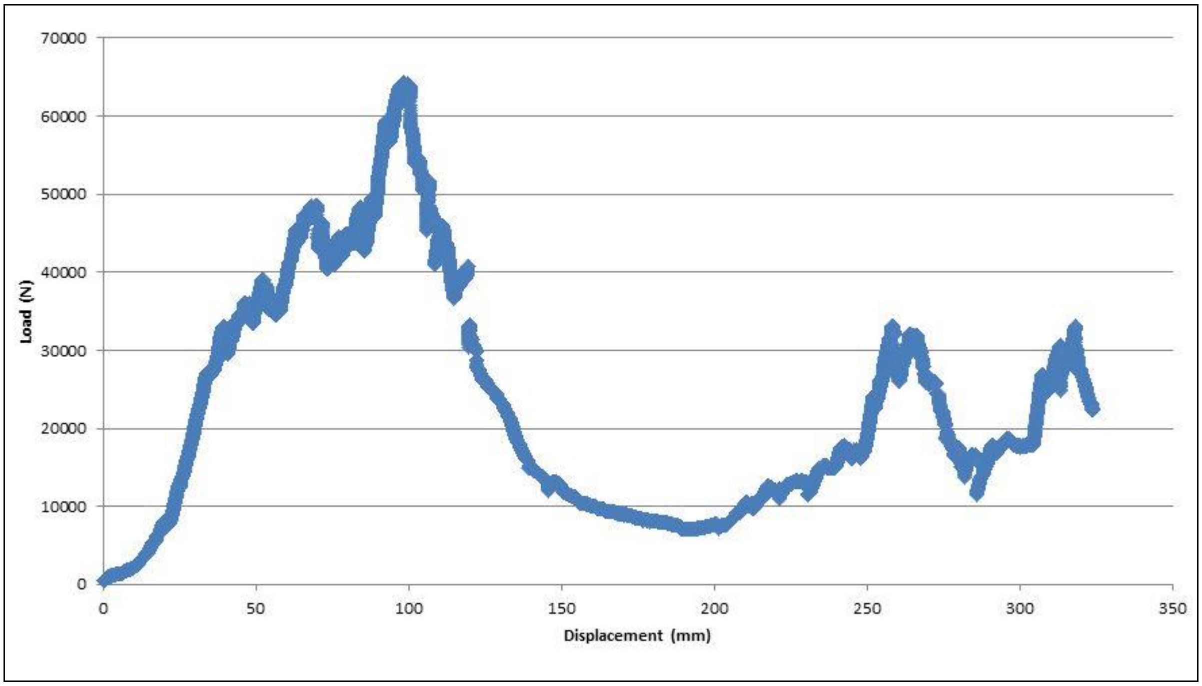

Figure 1: Force-Displacement Curve (dynamic tests must show displacement during collision and after the point v=0 and until force becomes = 0)

ATTACH PROOF OF EQUIVALENCY

TECHNICAL COMMITTEE DECISION/COMMENTS

Approved by____ Date_____________

NOTE: THIS FORM AND THE APPROVED COPY OF THE SUBMISSION MUST BE PRESENTED AT TECHNICAL INSPECTION AT EVERY FORMULA SAE EVENT ENTERED

University Name: California Polytechnic State Univ - SLO Car Number(s) & Event(s): 025 FSAE Lincoln

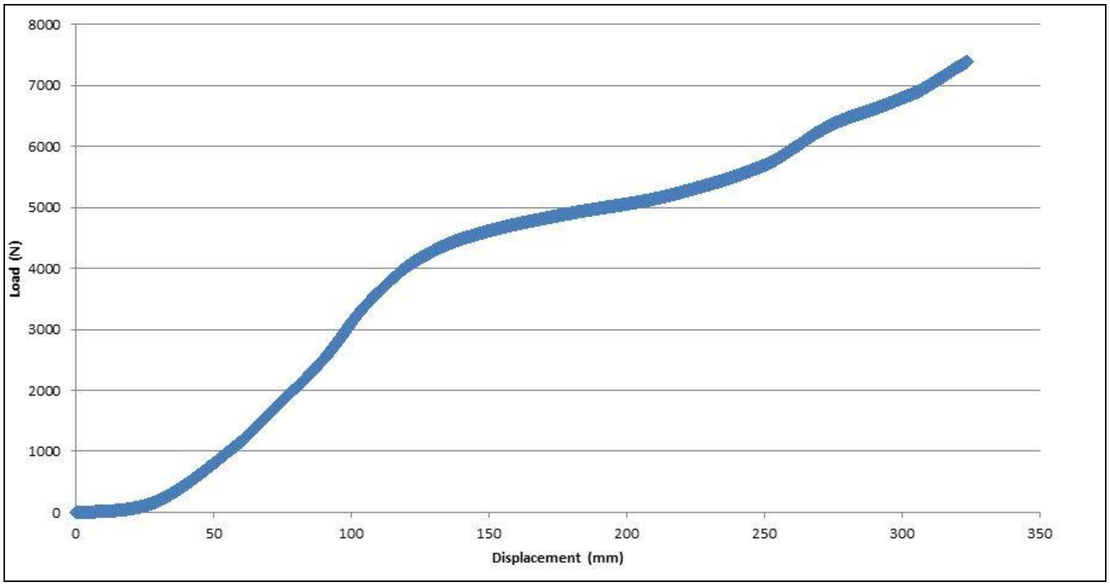

Figure 2: Energy-Displacement Curve (dynamic tests must show displacement during collision and after v=0)

Figure 3: Attenuator as Constructed

Figure 4: Attenuator after Impact

Energy Absorbed (J): Must be >= 7350 J	7390.1	Vehicle includes front wing in front of front bulkhead?	Yes
IA Max. Crushed Displacement (mm):	324	Wing structure included in test?	No See page 4
IA Post Crush Displacement - demonstrating any return (mm):	95.25	Test Type: (e.g. barrier test, drop test, quasi-static crush)	Quasi-static crush test
Anti-Intrusion Plate Deformation (mm)	0	Test Site: (must be from approved test site list on website for dynamic tests)	Cal Poly Civil Engineering Department

Energy absorption calculation

Note: Data was recorded every 0.009525 mm

Energy = Force · displacement

$E_{data\ point\ 1} = F_1 \cdot d_1$

$E_1 = (454.9\ N)(0.009525\ mm) = 4.333\ mJ = 0.00433\ J$

$E_{total} = \sum_{n=1}^{N} E_n$ where N is total number of data points

$E_{total} = 7390.1\ J$ $> 7350\ J$ ✓

Average deceleration calculation

Average force $F_{avg} = \dfrac{\sum_{n=1}^{N} F_n}{N}$

$F_{avg} = 22.813\ kN$

$a_{avg} = \dfrac{F_{avg}}{W} = \dfrac{(22.813\ kN)}{(300\ kg)(9.81\ m/s^2)}$

$a_{avg} = 7.75g$ $< 20g$ ✓

Peak deceleration calculation

$F_{max} = 64.31\ kN$

$a_{peak} = \dfrac{F_{peak}}{W} = \dfrac{(64.31\ kN)}{(300\ kg)(9.81\ m/s^2)}$

$a_{peak} = 21.87g$ $< 40g$ ✓

See page 4 for front wing mounting inclusion

Peak force including front wing calculation

Peak force from quasi-static crush test of impact attenuator
$F_{peak} = 64.31\ kN$

Front wing is mounted using 4 AN3 bolts
See Figure 8

Failure load of 1 AN3 bolt $F_{failure} = 9.452\ kN$ (shear failure)

Total load required to fail assembly

$$F_{failure,total} = N_{bolts} \cdot F_{failure} = 37.8\ kN$$

$$F_{max} = \underbrace{F_{failure,total}}_{\text{from wing failure}} + \underbrace{F_{peak}}_{\text{from testing}}$$

$$= (37.8\ kN) + (64.31\ kN) = 102.1\ kN$$

$$a_{max} = \frac{(102.1\ kN)}{(300\ kg)(9.81\ m/s^2)} = 34.7\ g < 40\ g \ \checkmark$$

Even with the front wing failure load added to the peak force from the test, the maximum deceleration is still less than 40g.

APPENDIX T-2
2015 FSAE® IMPACT ATTENTUATOR DATA REPORT

University Name: California Polytechnic State Univ - SLO   Car Number(s) & Event(s): 025 FSAE Lincoln

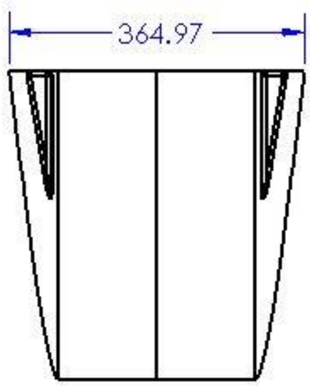

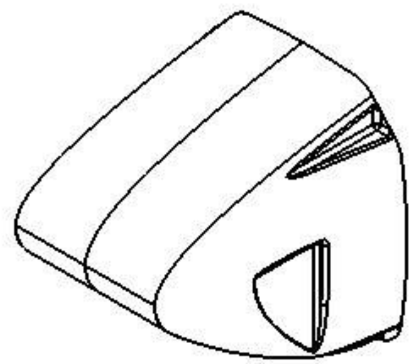

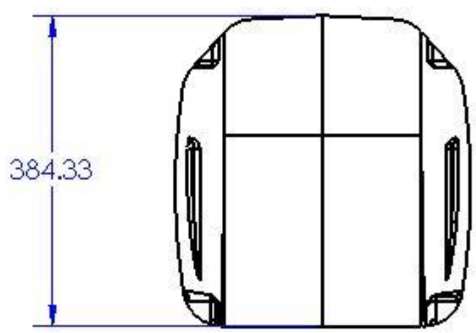

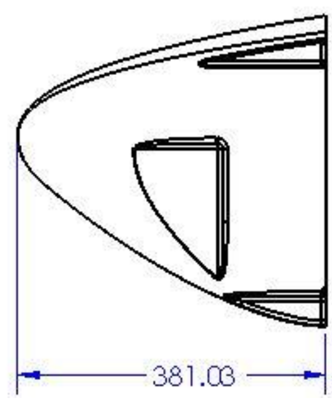

Length (fore/aft direction): 381 mm (>=200mm)
Width (lateral direction): 365 mm (>=200mm)
Height (vertical direction): 384 mm (>=100mm)
Attenuator is at least 200mm wide by 100mm high for at least 200mm: Yes
Attach additional information below this point and/or on additional sheets

Test schematic, photos of test, design report including reasons for selection and advantages/disadvantages, etc. Additional information shall be kept concise and relevant.

University Name: California Polytechnic State Univ - SLO   Car Number(s) & Event(s): 025 FSAE Lincoln

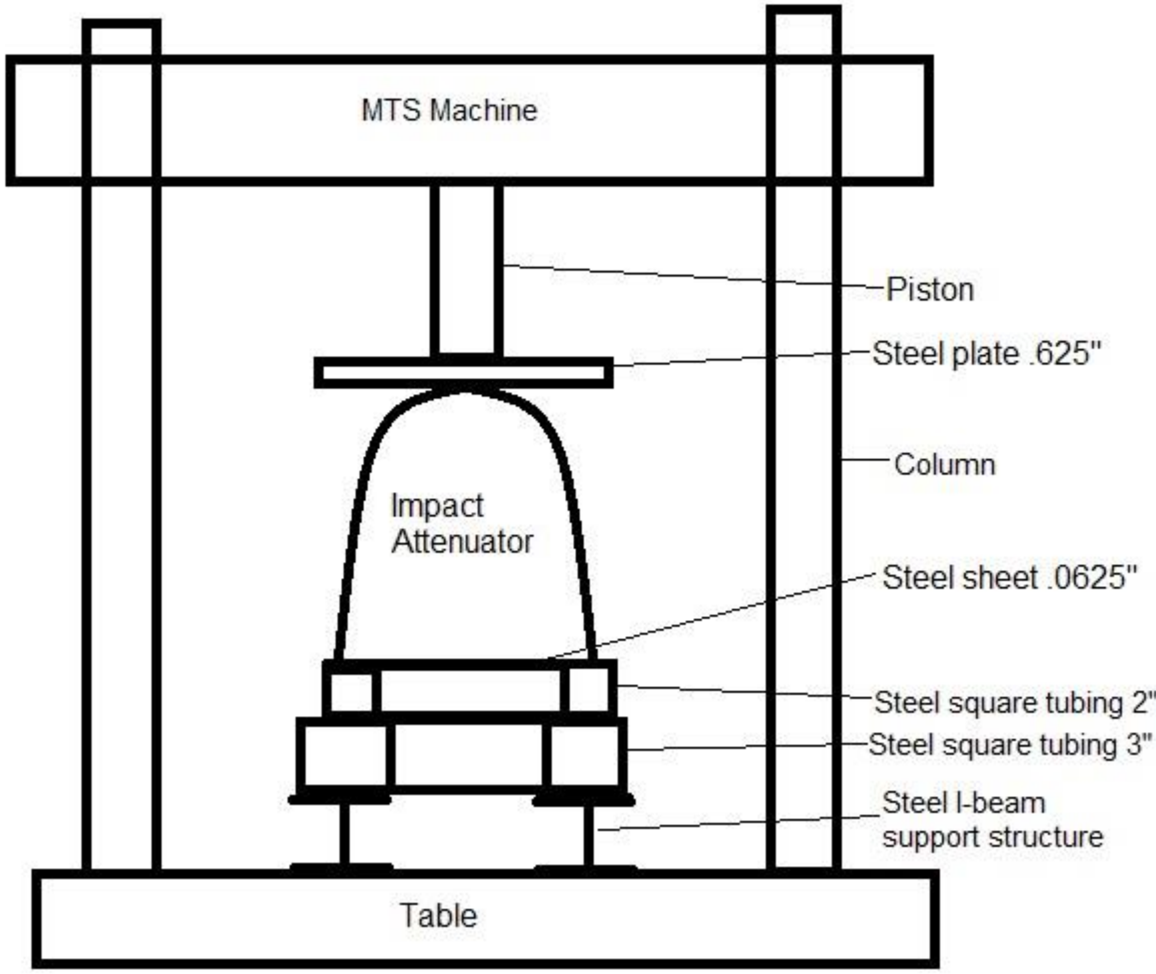

Figure 5: Quasi-static crush test setup.

University Name: California Polytechnic State Univ - SLO Car Number(s) & Event(s): 025 FSAE Lincoln

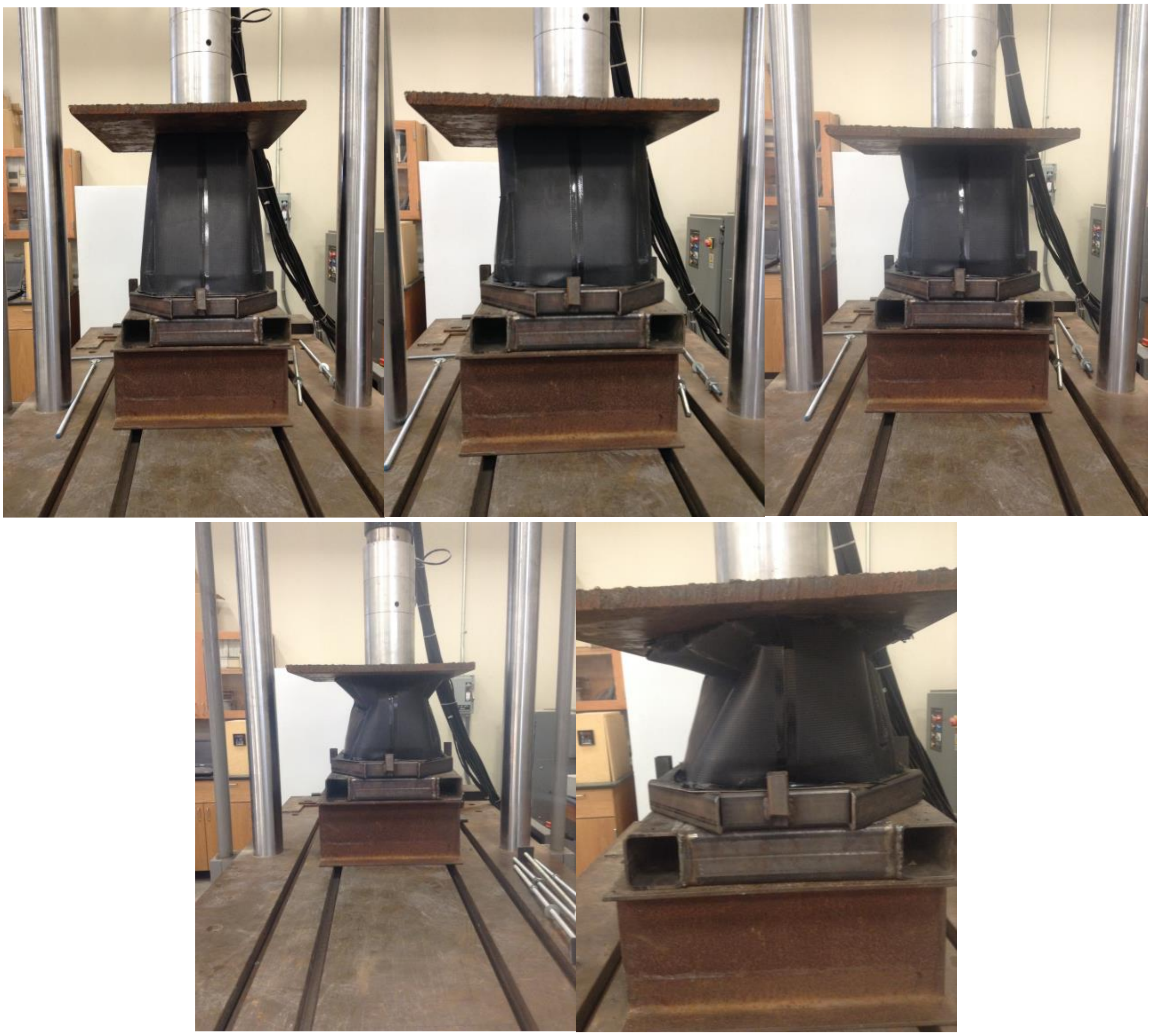

Figure 6: Photos of quasi-static crush test.

University Name: California Polytechnic State Univ - SLO   Car Number(s) & Event(s): 025 FSAE Lincoln

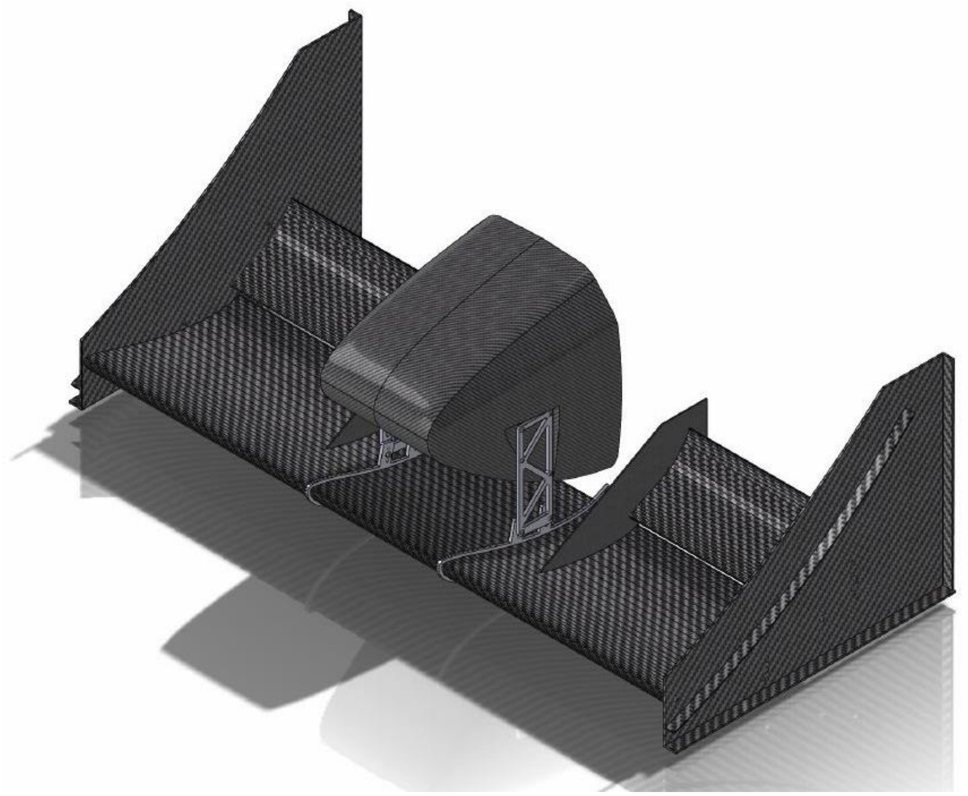

Figure 7: Front wing mounting configuration.

Figure 8: Front wing mounting configuration. Note the AN3 bolts (2 per side, 4 total) fastening the wing to the truss structure. Note endplates are not shown.

Appendix P

Impact Attenuator Test Additional Photos

Figure P1. Nosecone crush testing revealed the failure mode to be fiber bending stress concentrations created by the wing mount flat sections (indicated with red arrow). Eliminating these flats or providing additional localized reinforcement would reduce the overall weight of the nosecone.

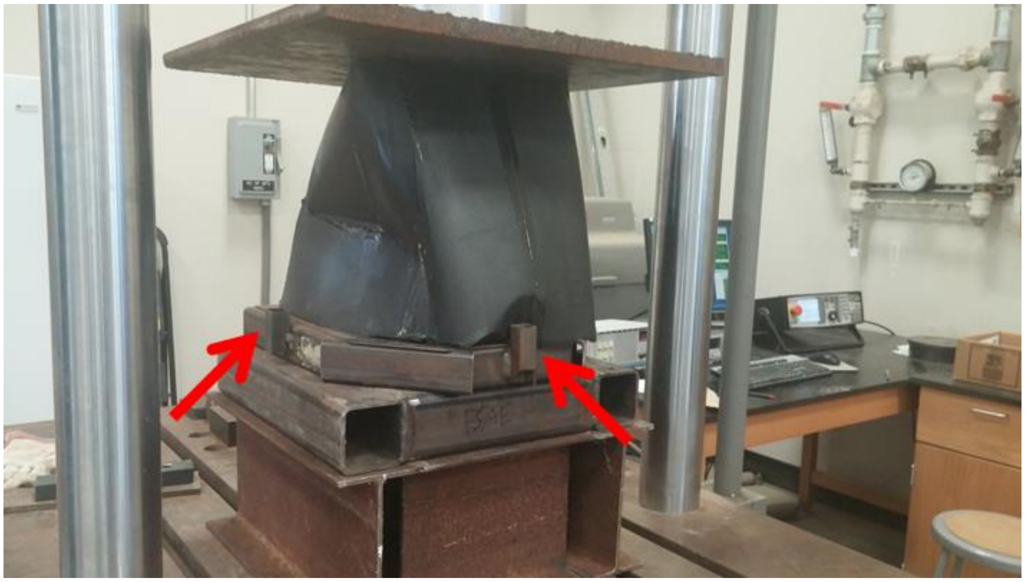

Figure P2. The rectangular tube (indicated by red arrows) was used to constrain the nosecone in the horizontal plane. However, these tubes created an undesired secondary failure mode for the nosecone. This lowered the overall strength and was remedied by the addition of plies. Creating a continuous perimeter around the nosecone would allow the reduction of these stress concentrations and a lighter part. However, in the interest of driver safety, the best method for securing the nosecone to the fixture is the actual hardware type and location as found on the vehicle.

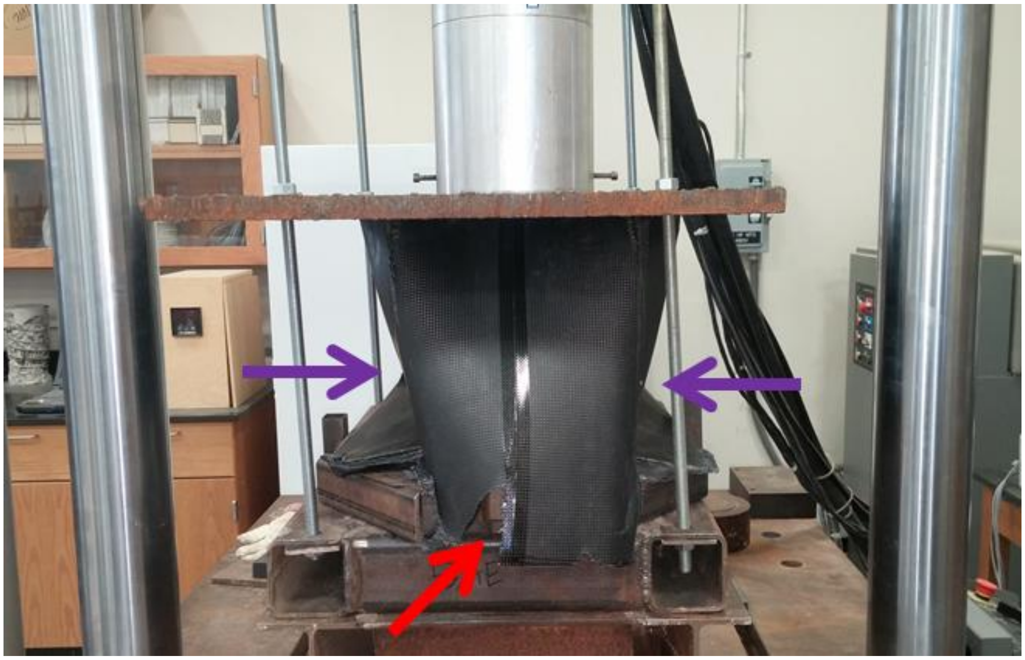

Figure P3. With increased displacement of the impact head the nosecone broke past the rectangular tube (shown with red arrows) and the edge protruding beyond the fixture lost ability to carry significant load. The primary failure mode continued to be the wing supports at this stage as indicated by the purple arrows. Note that the threaded rod was only used for repositioning the test machine head, not during dynamic testing.

Figure P4. The recesses for the bolt/attachment flanges (one of four shown with the red arrow) held nearly 775lb of force over 4” total of travel. This value could be improved by bolting the flanges onto the fixture as they began to tilt prematurely. The geometry’s resistance to buckling and ability to raise load-holding capability far into the displacement spectrum can be exploited by future teams to help meet energy requirements.

Appendix Q

Standard Operating Procedure for Test Panel Manufacturing

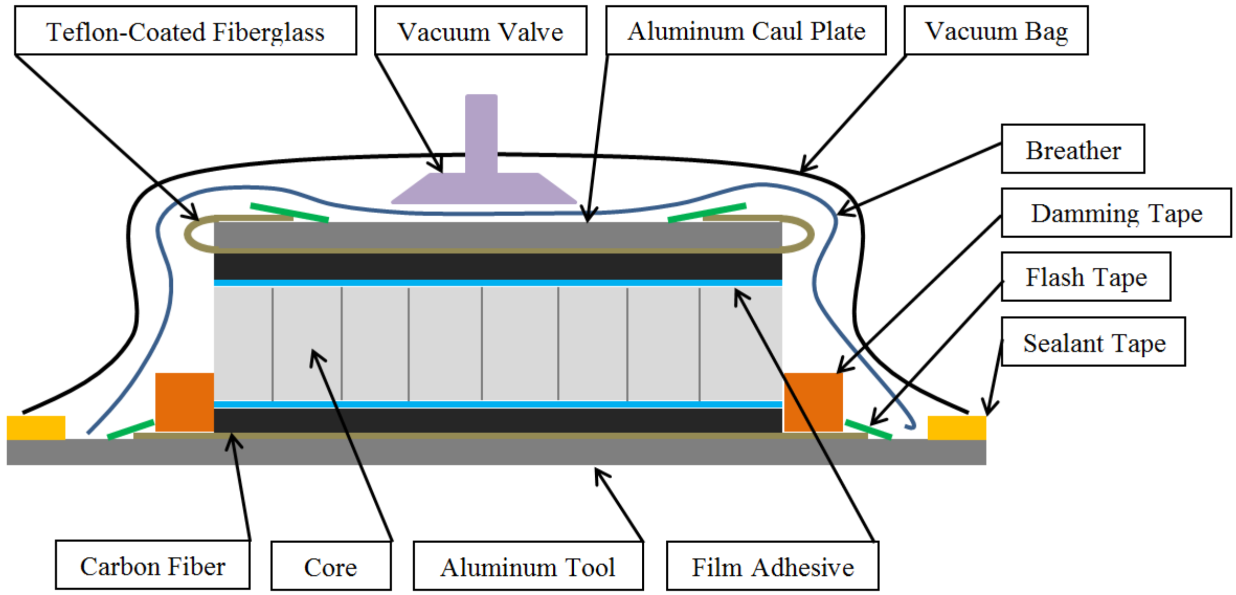

Figure Q1. A typical flat panel prepreg layup for the FMD project shown with all materials except fiberglass tows.

Part I: Preparation

Mold Tool

Step 1: Size aluminum mold tools based on testing panel dimensions. Select a mold tool with at least 3.5" of extra material on each side of the laminate (1" for sealant ["tacky"] tape, 1" for taping release film, 1" for edge dam leaves 0.5" clearance). Note that the laminate size will vary significantly from the test panel size as laminates will be trimmed after cure. Mold tool should be at least 0.70"-0.25" thick. Thicker tools promote flatter panels.

Step 2: Clean excess resin from the surface of the aluminum mold using a razor blade. Be careful not to score the surface of the aluminum with the blade. Wipe the mold with acetone using a paper towel.

Step 3: Apply sealant tape to the edge of the aluminum plate, leaving the paper backing on one side to prevent dust from collecting on the surface.

Step 4: Cut Teflon-coated fiberglass (Airtech Release Ease 234 TFNP) or nonporous FEP to cover the aluminum mold surface. Cover the surface up to about ¾" offset inward from the inside edge of the sealant tape. Use flash tape to secure the release film to the tool at each corner and midpoint of each long edge. If FEP is used, take care to tension the FEP to remove all ripples.

Cutting Prepreg Cloth, Tape, and Film-Adhesive

Step 1: All resin-containing materials should be thawed for 1-2 hours at room temperature in sealed bags (which should contain moisture absorbing desiccant pouches) to prevent moisture buildup on part. Out of autoclave panels are especially sensitive to moisture and should be handled accordingly. Out times for each roll should be recorded so that material does not exceed its projected "out life." Plan layups accordingly.

Step 2: Open the bag containing the desired roll of prepreg or film-adhesive. If possible, unroll desired amount of material to cut on a clean, smooth surface. Use a metal straightedge and a razor blade to cut major pieces of material from which smaller pieces will be cut. Then replace prepreg roll back into bag. Reseal with desiccant inside, and replace in freezer. This process minimizes out time for the roll overall.

Step 3: Use a caul plate as a cutting template for individual pieces. Use a razor blade to carefully cut along the edge of the caul plate, ensuring a straight cut.

Caul Plate

Note: Must be completed **after** all core, film-adhesive, and prepreg materials are cut.

Note: Based on 2015 SES rules, Hexcel guidelines, and ASTM codes for laminate testing, the following sized caul plates should be used (values in parenthesis indicate the actual trimmed size of the panel). See Figures Q2-Q6 for graphical representations of these size requirements.

- For long beams: 12.0" x 21.0" (10.8" x 19.7")
- For perimeter shear: 5.0" x 5.0" (4.0" x 4.0")
- For cockpit pullout: 12.0" x 12.0" (11.0" x 11.0")
- For short beams with core: 3.0" x 7.0" (2.0" x 6.0"). Note that since short beam panels are easily made in large numbers and easy to cut with the tile saw, 7.0" x 7.0" caul plates can be used to make 3 short beams for statistical analysis.
- For short beams without core: 2.0" x 3.0" (1.0" x 0.25")

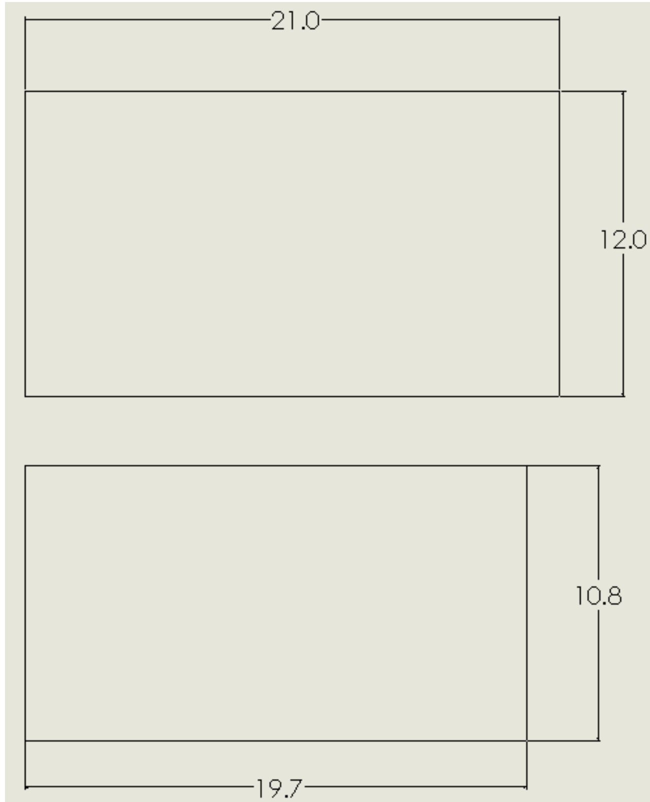

Figure Q2. Long beam panels as laid up (top) and after trimming (bottom). All dimensions are in inches. Height varies based on core and facesheet thicknesses.

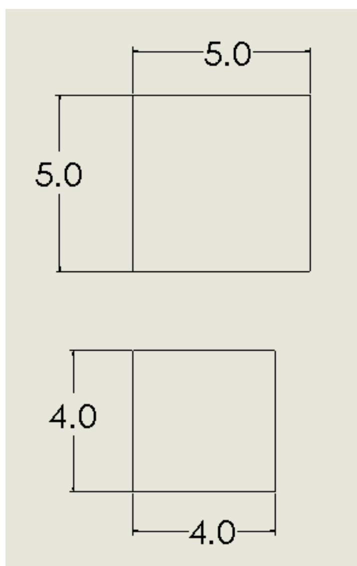

Figure Q3. Perimeter shear panels as laid up (top) and after trimming (bottom). All dimensions are in inches. Height varies based on core and facesheet thicknesses.

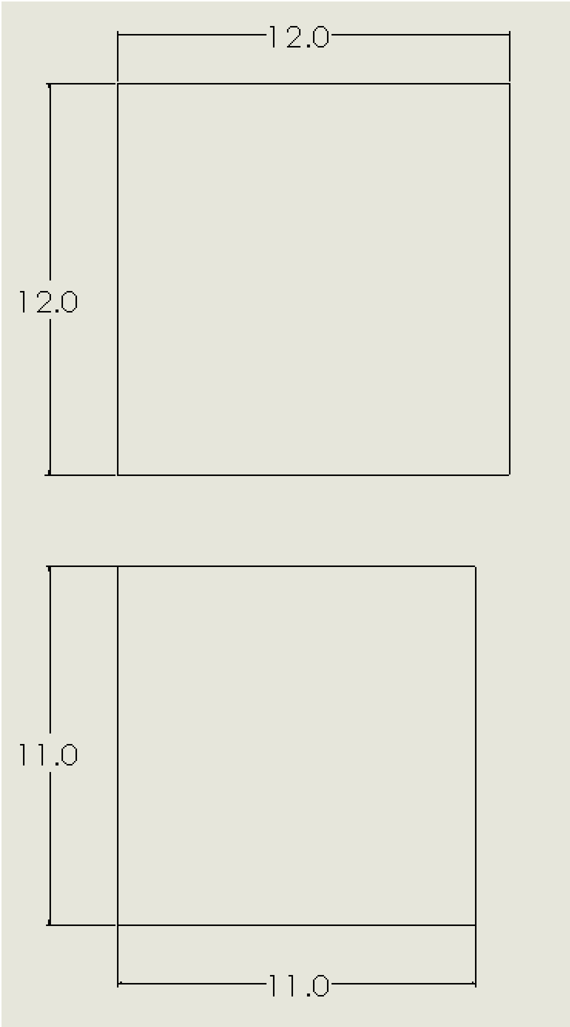

Figure Q4. Cockpit pullout panels as laid up (top) and after trimming (bottom). All dimensions are in inches. Height varies based on core and facesheet thicknesses.

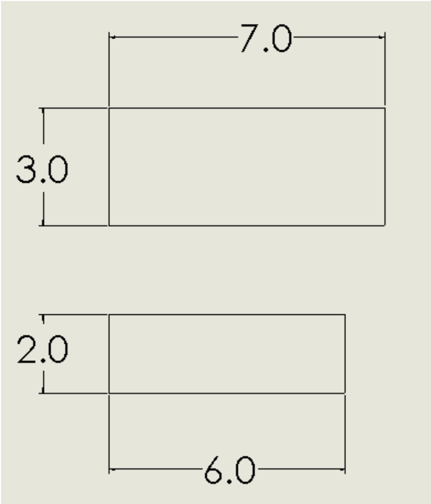

Figure Q5. Short beam shear panels with core as laid up (top) and after trimming (bottom). All dimensions are in inches. Height varies based on core and facesheet thicknesses.

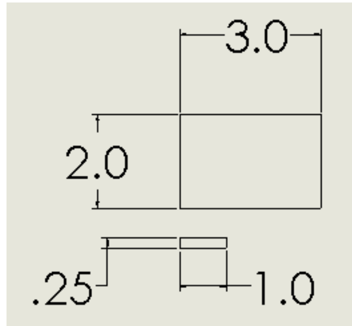

Figure Q6. Short beam shear panels without core as laid up (top) and after trimming (bottom). All dimensions are in inches. Height varies based on core and facesheet thicknesses.

Step 1: Clean excess resin from the surface of the aluminum caul plate using a razor blade. Be careful not to score the surface of the aluminum with the blade. Wipe the mold with acetone using a paper towel.

Step 2: Cut Teflon-coated fiberglass or nonporous FEP to cover the aluminum mold surface, cutting approximately 1.5” extra material on each edge.

Step 3: Fold the 1.5” extra material over the back end of the caul plate, taking care to tension the release film so no ripples are present. Use flash tape to secure the release film on the back of the plate so that the flash tape will not contact the completed laminate.

Fiberglass Tow Application (Vacuum Bag Only Parts)

Note: Fiberglass tows are only placed between consecutive plies of laminated prepreg material. They are not placed between laminate and film adhesive, or between film adhesive and core. The inclusion of fiberglass tows aids in laminate gas evacuation in out of autoclave application.

Step 1: Placement of fiberglass tows is determined prior to layup as it impacts laminate, tool and caul plate sizes. Fiberglass tows must have at least 3” of extra length extending past each end of their respective laminate edge so they can extend past the damming material and facilitate edge breathing. Cut fiberglass tows using scissors, ensuring that no smaller strands become separated from the main strand. Alternatively, pull tows from dry fiberglass cloth and cut to length.

Step 2: Remove the polyethylene or paper backing sheet from the top of the prepreg ply.

Step 3: Carefully place the fiberglass tows along the desired edges of the laminate, ensuring that contact is restricted to the edges. First, hold the tows taut above the edge of the part. Then, carefully press the tows onto the part, to prevent wrinkling.

Step 4: Remove the backing material from the next prepreg ply.

Step 5: Place the next prepreg ply over the fiberglass and previous ply.

Core Material

Step 1: Nomex core material must be heated to 250° F in order to evaporate volatiles and reduce moisture during cure. Aluminum core material does not need to be heated.

Step 2: Using a caul plate as a template, cut core material using a razor blade, ensuring that the ribbon direction (direction of the pointed ends when using a hexagonal honeycomb core) follows that specified in the layup schedule.

Step 3: For aluminum core, "scuffing" the core with Scotch-Brite has been shown via short beam shear tests to increase bonding strength. Lightly pass the Scotch-Brite along both sides of the core. Next, use a high-powered hair dryer to blow air over the core and evacuate Scotch-Brite particulate. Do not use shop air as it is most and may contain oil. Finally, lightly wipe the surface with acetone.

Part II: Layup

Layup Stacking

Step 1: Remove backing from first ply in the layup sequence and place onto a smooth surface covered with a release film. Note the 0° ply direction relative to the short or long edge (as specified in the layup schedule) using a marker on the release film.

Step 2: Place subsequent plies, using fiberglass tows if necessary, following the angle patterns specified in the layup schedule. Ensure careful alignment of each ply. Because ply size varies slightly, line up all panels at one corner for each layer.

Step 3: With the protectant film still on the plies, roll a 1" OD steel tube cleaned with acetone over the laminate as one would use a bread roller. An actual bread roller deflects too much and applies uneven pressure to the laminate.

Step 4: Place in debulking setup for at least 15 minutes every three plies. A debulking setup is a resealable vacuum bag that can apply vacuum pressure to the laminate.

Film adhesive and Core Application

Step 1: Place film adhesive onto the side of the face sheet to be bonded to core, following the same alignment procedure specified in Step 2 of the "Layup Stacking" procedure. Fiberglass tows should not be placed between the film adhesive and the laminate.

Step 2: Carefully peel away backing paper, leaving film adhesive on the surface of the laminate.

Step 3: Place core on the film adhesive, following the same alignment as specified in step 2 of the "Layup stacking" procedure. Ensure that the ribbon direction matches the one specified in the layup schedule.

Step 4: Follow the same process to place the corresponding face sheet on the other side of the core.

Part III: Bagging and Cure

Edge Dam Placement

Step 1: Place completed laminate on release film, then select edge dam pieces to box in the laminate.

Step 2: Place the silicon edge dams as close to the edges of the laminate as possible. Ensure that there are no holes in the "fence" around the laminate, as this will allow resin to flow out of the part. If fiberglass tows are used, ensure that they continue over the edge dams.

Step 3: Use flash tape to hold the silicon dams in place.

Caul Plate and Breather Placement

Step 1: Place a caul plate over the laminate.

Step 2: Place two layers of breather cloth in bagging sequence, making sure it contacts the fiberglass tows (if any).

Vacuum Bag and Line Setup

Step 1: Disassemble vacuum end insert and place lower piece on the breather cloth, ideally not over a caul plate.

Step 2: Carefully seal vacuum bag over the tool. Start at the short edge of the part, and then slowly and evenly seal the bag by pressing it against the tape, while keeping the bag in tension. If necessary, use additional sealant tape to seal any "dog ears" of extra vacuum bag material.

Step 3: Use a razor blade to cut a hole in the vacuum bag over the hole in the lower piece of the vacuum end insert.

Step 4: Insert the upper half of the vacuum end insert and twist clockwise to seal.

Step 5: Turn on vacuum pump, then attach the universal hose end seal to the upper end of the insert.

Step 6: Check for a minimum of 25 in-Hg vacuum pressure and seal any leaks as required.

Cure

Step 1: Obtain material datasheet for recommended cure cycle

Step 2: Select the oven if using a large mold or want to replicate heat transfer properties for "blob" layup testing. Select the autoclave (with or without pressure) if part consistency, ease of use, and quality are the primary concerns.

Step 3: Place thermocouples (if desired) on the parts to be cured. Note the corresponding jack numbers.

Step 4: Follow instructions provided by Dr. Mello for either the oven or the autoclave.

Step 5: Upon completion of the cure, remove the part from the bag and mark with a permanent marker the tool side and the caul plate side.

Step 1: Since the panels were made larger than needed, they must be cut to size. Size requirements may be dictated by SAE, Hexcel, or internal standards.

Step 2: Most panels will fit in the tile saw located in the rear of the Mustang '60 machine shop. This is the preferred method of cutting as the edges are clean and straight and the water from the saw reduces airborne carbon particulate. Ensure the saw and blade are in good working order and the water level is above the uppermost surface of the sump. Before using the saw, put on a half-face respirator with filters suitable for carbon particulate. Also ensure safety glasses or goggles are worn.

Step 3: Use a square and a paint pen as a guide to cut the panels to size. Initial cuts with the tile saw to remove larger sections of excess material may be required to fit the panel flush onto the saw bed.

Step 4: Confirm dimensions are as marked/required since the SAE tests have specific dimensions that are checked during technical inspection.

Step 5: Unplug and clean the saw using shop towels. Wipe the saw blade cover, motor, and table. Refill water if level is below the sump's uppermost surface. Remove any debris on the floor.

Step 6: Dry panel with a shop towel, taking care to avoid splinters. The panel is now ready for destructive testing.

Appendix R

Meguiar's Mold Release Wax #8 and Loctite Frekote 770-NC Application

Standard Operating Procedure

Part I: Preparation

Step 1: Remove lose debris and dust from inside mold using a shop vacuum. Cup a hand around the shop vacuum nozzle to prevent the mold surface from being scratched by the hard plastic.

Step 2: Don nitrile gloves and safety glasses

Step 3: Apply a moderate amount of acetone to a WypAll disposable towel if available or a regular paper towel. The WypAll towels are softer than the paper towels available at the university and are tear-resistant. Wipe the mold surface with acetone anywhere that Duratec or other gel-coating is present.

Step 4: Repeat Step 3 until no residue appears on the paper towel.

Part II: Wax Application

Step 1: Apply a moderate amount of wax to an automotive wax applicator pad. Rub the wax in a circular motion on the mold surface. Immediately after the wax begins to haze, use a clean microfiber towel to buff the wax coat by briskly rubbing it in a circular motion. Note that wax should be applied beyond the region where the laminate is intended to be placed to account for errors in the layup process; however, wax should not be applied where vacuum bag sealant tape it to be used.

Step 2: Repeat Step 5 until the mold has a thick, even layer of wax. Good results had been achieved with **0.75oz/1ft^2** of mold surface. Take care to buff the final coat to a highly-smooth finish as this has a large effect on the part smoothness.

Part III: Frekote 770NC Application

Step 1: Frekote can be used with or without mold release wax. Should wax be used, apply the Frekote onto the wax without cleaning the waxed surface. Cleaning will strip wax and damage the buffed finish from Step 2 in Part II: Wax Application. If wax is not used, just follow the procedures in Part I: Preparation.

Step 2: Frekote produces noxious vapor, so ensure the room is well-ventilated and that a half-face respirator suitable for gases is being worn.

Step 3: Invert the bottle of Frekote onto a WypAll or standard paper towel. Take care not to saturate the towel as excessive release agent will leave swirls on the final parts. Lightly rub the mold with the towel. Replace the towel if it tears.

Step 4: Wait 10 minutes and apply the next coat as done in Step 3.

Step 5: Steps 3 and 4 can be repeated for a total of 3-5 coats depending on mold value, part value, and tool porosity.

Step 6: Wait 30 minutes after the last coat before applying the first layer of the laminate.

Step 7: Note that Frekote is self-building and less layers can be applied on subsequent parts. However, if wax is used, the full process must be performed.

Part IV: Post-Layup Cleaning and Mold Storage

Step 1: To make future layups quicker and easier, molds should be cleaned after the part is pulled from them. In addition to marking the pull count on the mold, the entire surface should be cleaned with acetone as described above. Acetone will generally remove resin, though firmer wiping may be required than for an unused mold.

Step 2: Apply sealant tape to the mold as far "off-part" as possible.

Step 3: Place a packet of desiccant inside the sealant tape boundary.

Step 4: Apply vacuum bag over the mold and secure it to the sealant tape. By keeping the mold surface clean and dry, less labor will be required for future pulls and the tool will be less likely to be damaged from water expansion during the next curing cycle.

Appendix S

Core Failure Repair Process Photos

Figure S1. First a small opening was made with a rotary tool to inspect the core for damage.

Figure S2. When full core failure was observed, the repair began and a 2" x 2" square was cut using a rotary tool and cutoff wheel.

Figure S3. A sample of the failed core shows the results of continued out of plane loading after the core sheared loose inside the sandwich structure (shown later).

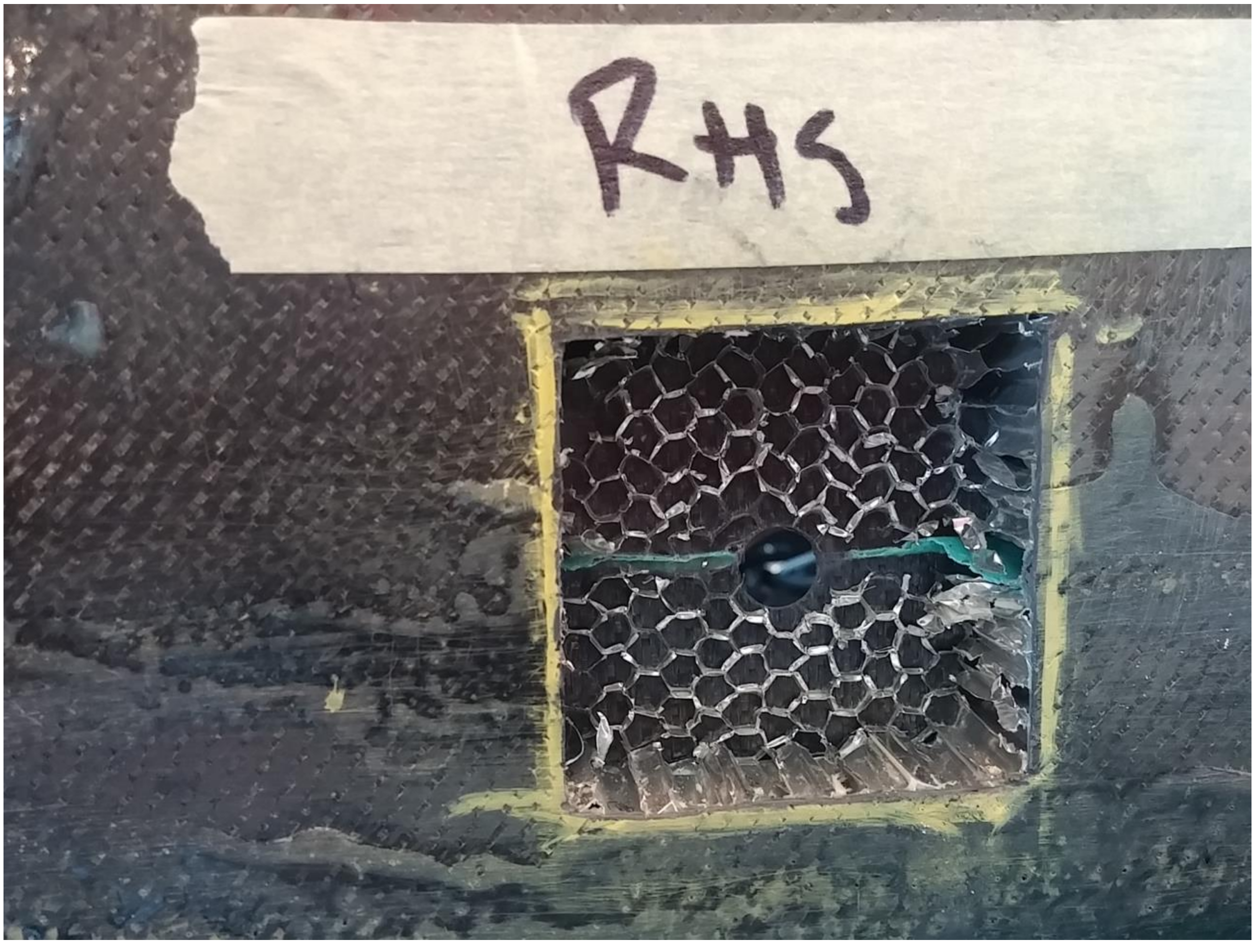

Figure S4. The core sheared loose from the inner facesheet. Balsa wood or another solution that provides higher compressive strength is highly recommended for future vehicles. Prior to bonding in a balsa wood insert, the remnants of the sheared core were removed by pulling a shard razor blade along the affected region. The blade was not pushed in an effort to reduce cutting fibers.

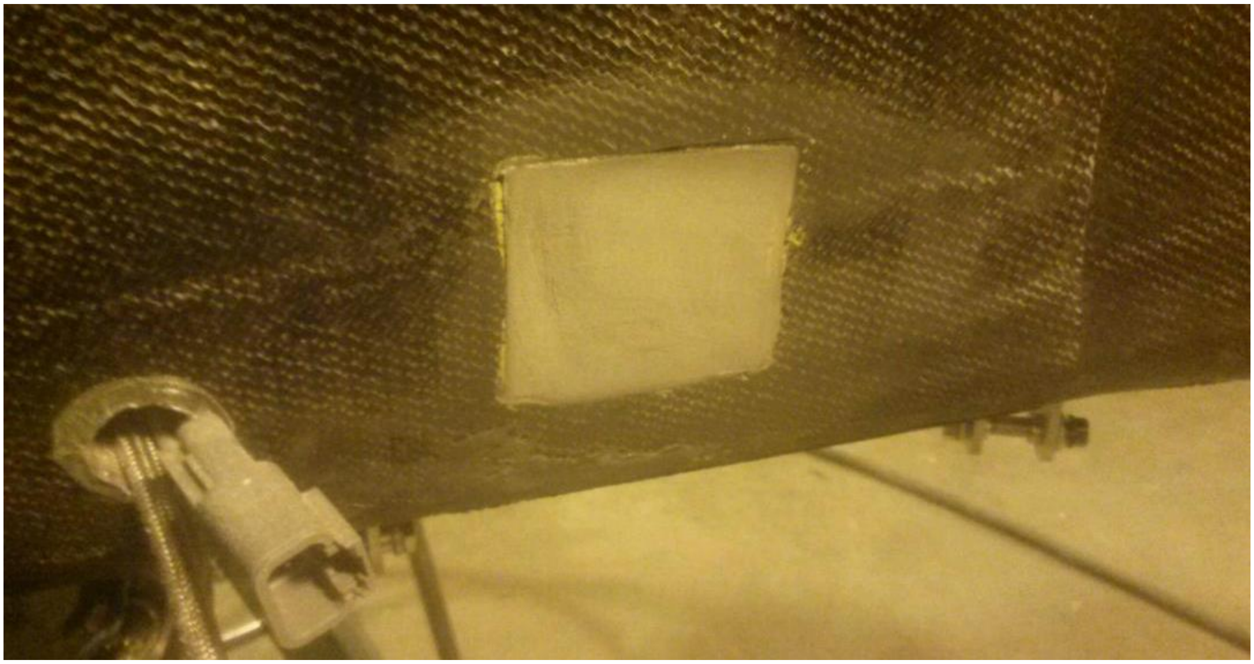

Figure S5. 0.750" thick end-grain balsa wood was cut into a 2"x 2" square and test fit in the cavity. Next it was scuffed with sandpaper and wiped clean with a new towel.

Figure S7. Following preparation of the balsa plug, resin and microballoons were mixed to a frozen-yogurt consistency (to allow for flow into the core). An excess amount of the resin and microballoons were inserted into the cavity to reduce potential voids in the dried slurry. The excess protruding beyond the facesheet was then wiped flush before curing.

The next steps are not pictured but included the following:

1. Cover balsa wood plug with FEP.
2. Pull FEP taut and tape it onto the surrounding monocoque.
3. Place wooden blocks on top of the FEP and use a ratchet strap to apply firm pressure onto the balsa wood.
4. Let resin cure and sand excess resin and balsa wood flush with the monocoque's outer facesheet.

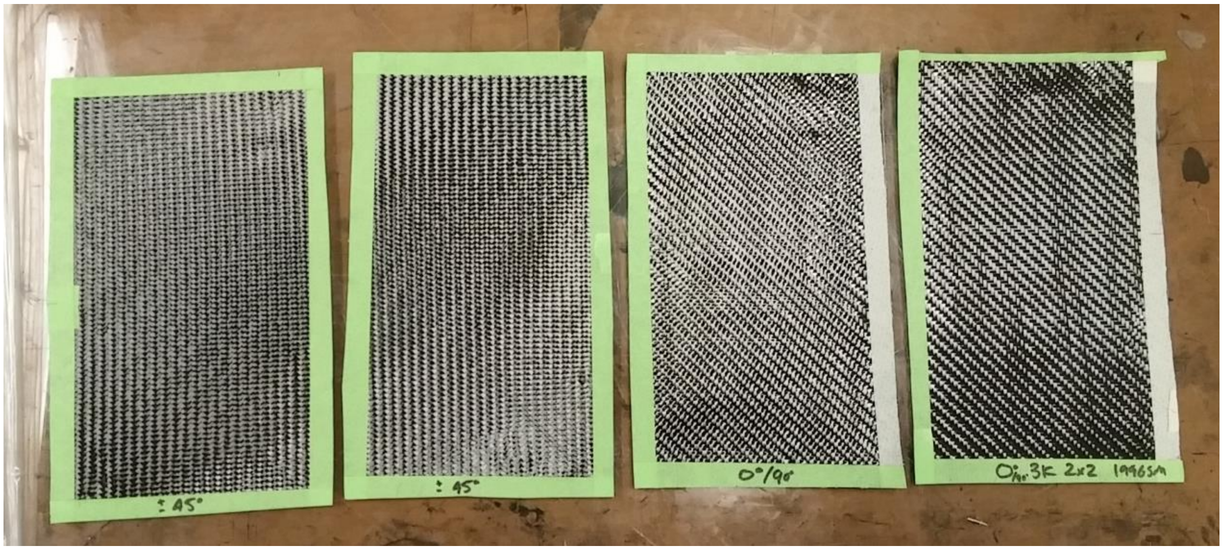

Figure S8.The carbon fiber used to cover the balsa wood was labeled carefully to prevent improper ply orientation.

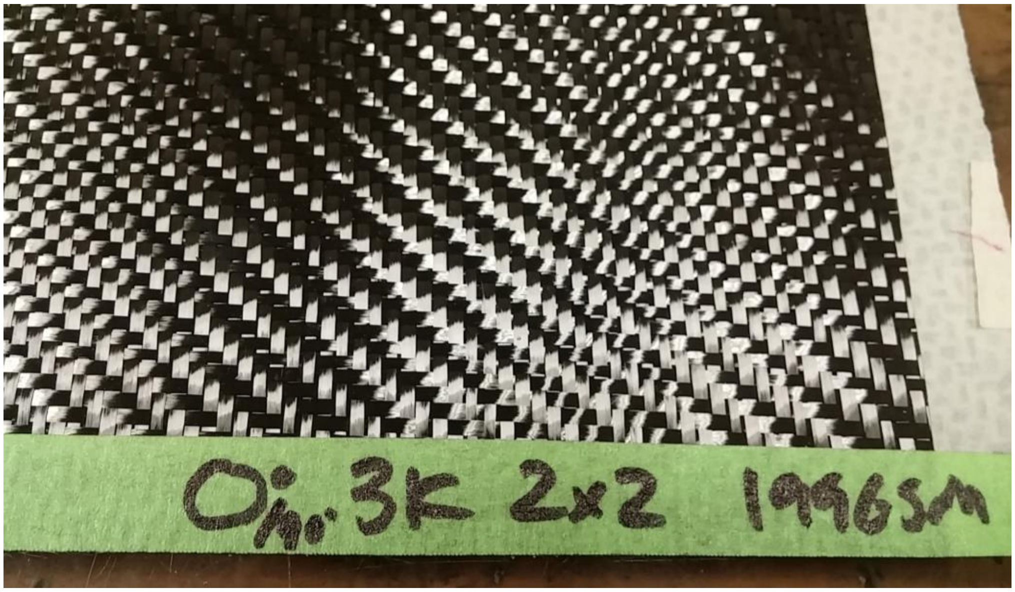

Figure S9. A 2x2 twill, 3K, 199 GSM, 640 KSI Aerospace fiber manufactured by Soller Composites was used for the repairs due to its strength properties and the team's prior positive experiences with the fabric.

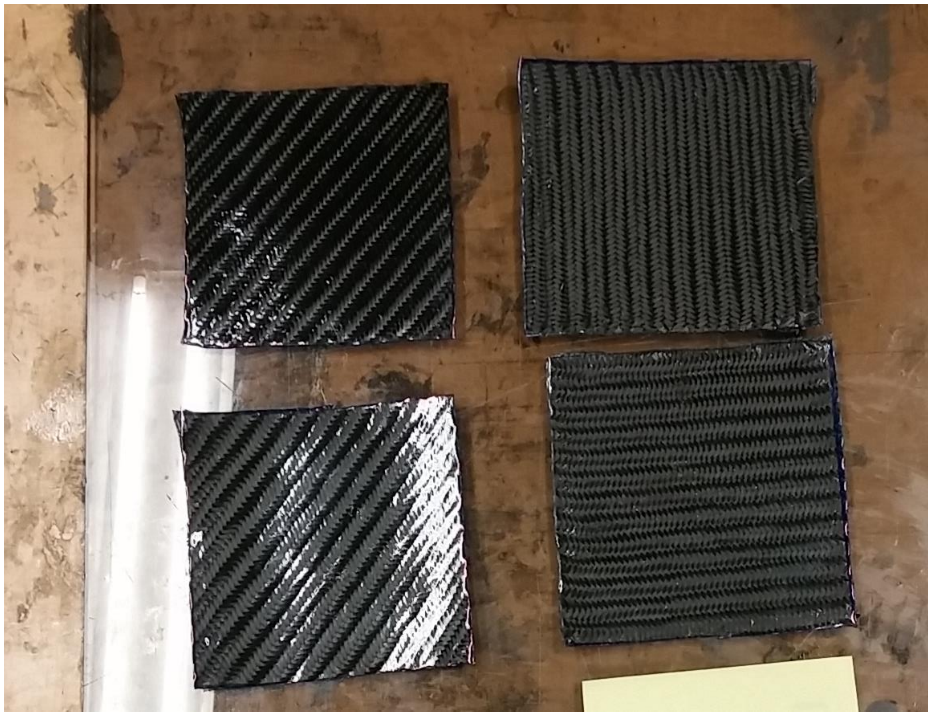

Figure S10. Tapering was used in accordance with Bailie's et al. recommendations for reducing delamination.[Ref 1] The ±45° plies were placed on the outside and the 0°/90° plies were placed on the inside to mimic the prepreg layup in the associated region. The interior plies had 0.75" overlap and the exterior plies had 1.0" overlap.

Figure S11. The tapered stack prior to application onto the monocoque. FEP was used to apply pressure to the fabric since the facesheet would not hold vacuum and bagging the entire vehicle was not possible. West Systems 105 resin and 207 hardener were applied to the fabric.

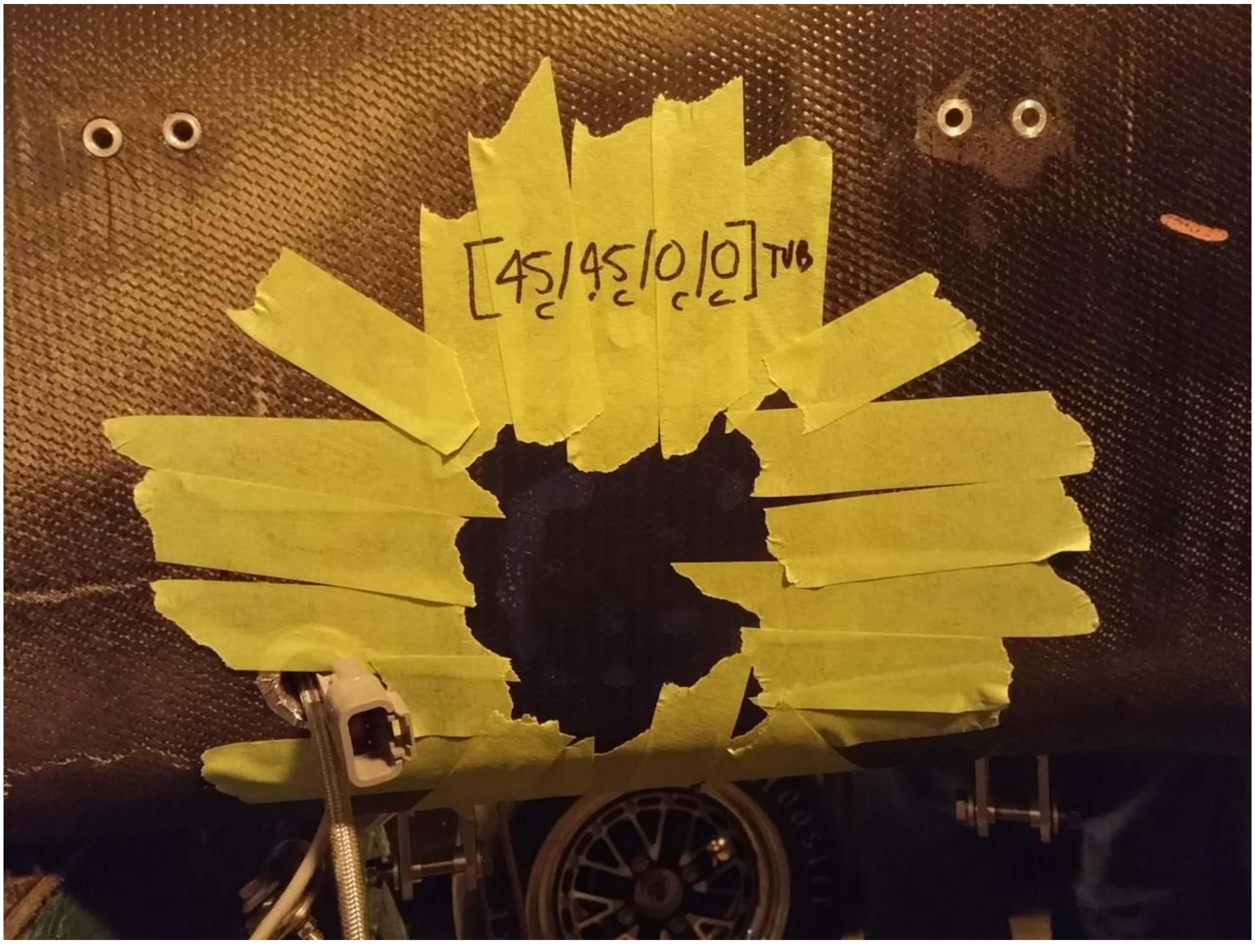

Figure S12. The stack was placed onto the monocoque and pulled taut with FEP and tape. Resin and fabric were mixed at a 1:1 ratio allowing for the elimination of peel ply. The FEP is slightly porous which aids in achieving a proper cure.

Appendix T

Pursuing the Alternative Frame Rules

The alternative frame rules require that a full FEA model of the chassis meet the strength and stiffness requirements set forth by several loading conditions (summarized in Table T1). Under each loading condition, the chassis must not deflect more than 25mm, nor can any region of the chassis fail. See Appendix U for full details on the loading conditions and structural requirements.

In order to gain clearance from SAE to pursue the AF rules, FMD was required to model a sample chassis, apply the applicable loadings, and submit the results to SAE. FMD managed to submit several iterations of the sample chassis model, but all were rejected because elements were missing from the NASTRAN output files they requested. A summary of the sample AF chassis results can be found in Appendix V.

Table T1. Summary of Alternative Frame loading tests

Test Number	Evaluated Chassis Region
AF1	Main Roll Hoop, Bracing and Bracing Supports
AF2	Front Roll Hoop
AF3	Side Impact
AF4	Front Bulkhead & Bulkhead Support
AF5	Shoulder Harness Attachment
AF6	Lap & Anti-Sub Harness Attachment
AF7	Front Bulkhead & Bulkhead Support Off-Axis

The model utilized in the simulations is an assembly of four components: the monocoque, subframe, suspension, and front bulkhead. The monocoque and front bulkhead are modeled as composite shells. The subframe is composed of beam elements, and the suspension is made of truss elements. What differentiates the AFR model from the torsional stiffness model is the fact that the front bulkhead is tied to the front of the monocoque in order to better reflect the frame's performance under the off-axis frontal impact load. The addition of the front bulkhead was not transitioned to the torsional stiffness model.

Table T2. Alternative Frame test results

Test Number	Maximum Measured Deflection (in.)
AF1	0.1492
AF2	0.8885
AF3	0.3605
AF4	0.1363
AF5	0.1569
AF6	0.01987
AF7	0.8457

The results of each test (Table T2) show a maximum frame deflection of less than 25 mm, which indicates sufficient stiffness. Contour plots of each test can be referenced in Figures T1 – T7.

The individual ply stiffnesses incorporated in the model were derived from manufacturer's prepreg and core data sheets. The FSAE rules body notified the team that laminate properties needed to be based on the 3-point long beam test data, and that inputting individual ply properties from manufacturer data sheets did not fall in line with the rules. In order to be rules compliant, the results of a long beam test needed to be inputted into the SES in order to calculate overall laminate strength and stiffness in both the 1 and 2 directions. Then, an FEA model could be composed that incorporated a single-ply monocoque with the new SES-derived material values. Once that news reached us, the team had already decided to halt the pursuit of the AF rules, since doing so would likely put significant delays on the monocoque layup.

Future teams pursuing the AF rules should first re-confirm the method of tying the testing data to the creation of the FEA model, as the AF ruleset is in a state of constant evolution. Also, teams are encouraged to submit AF rules queries very early, as there is considerable lead time on any response.

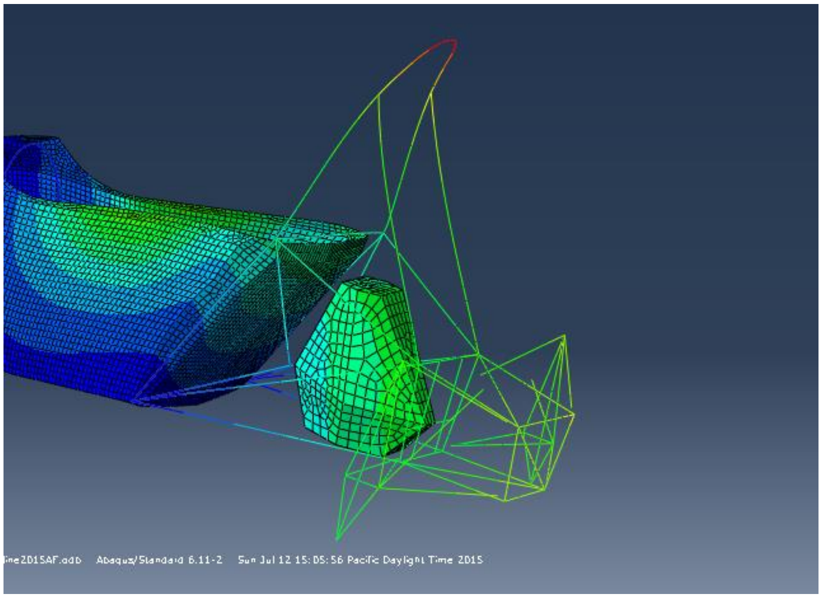

Figure T1. Deflection contour plot for test AF1.

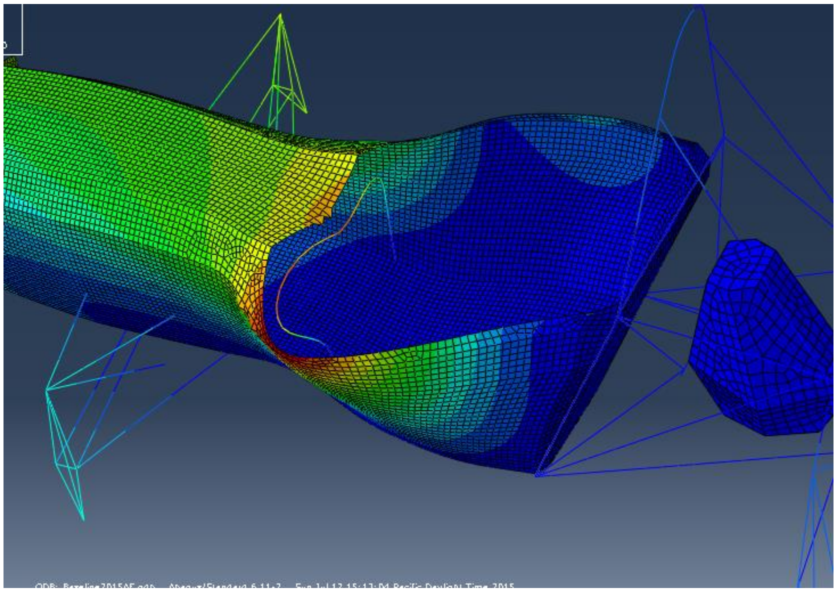

Figure T2. Deflection contour plot for test AF2

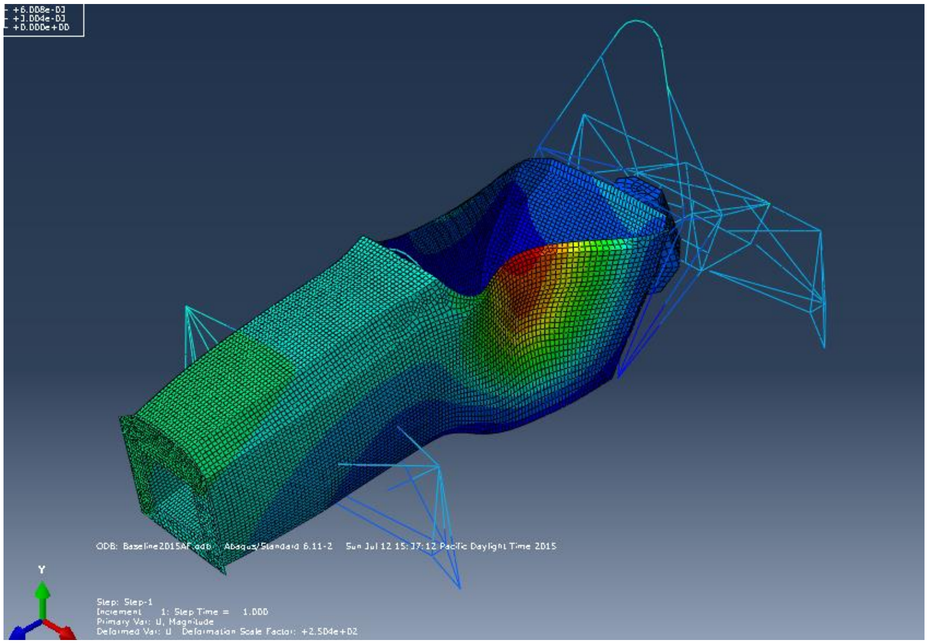

Figure T3. Deflection contour plot for test AF3

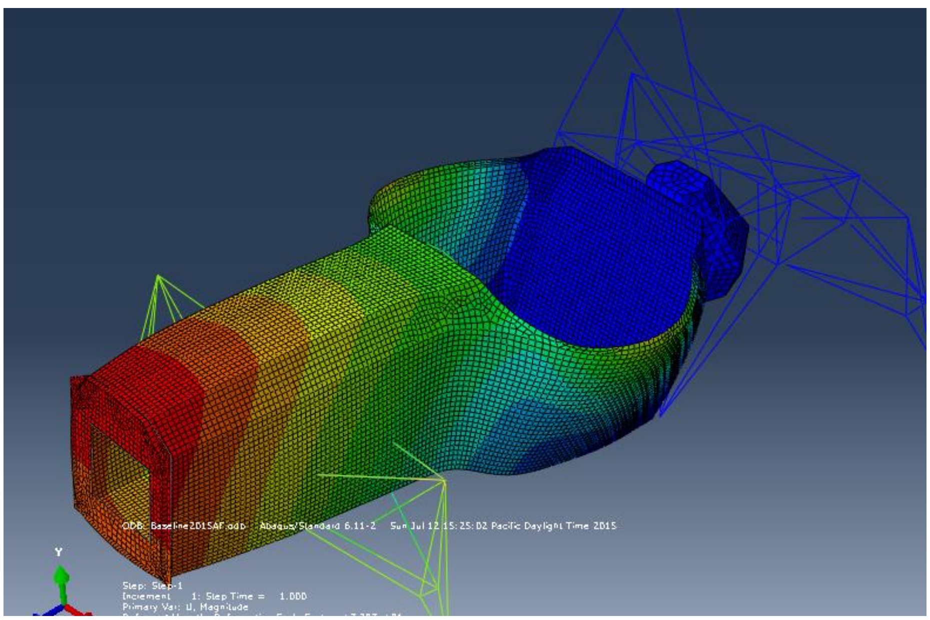

Figure T4. Deflection contour plot for test AF4

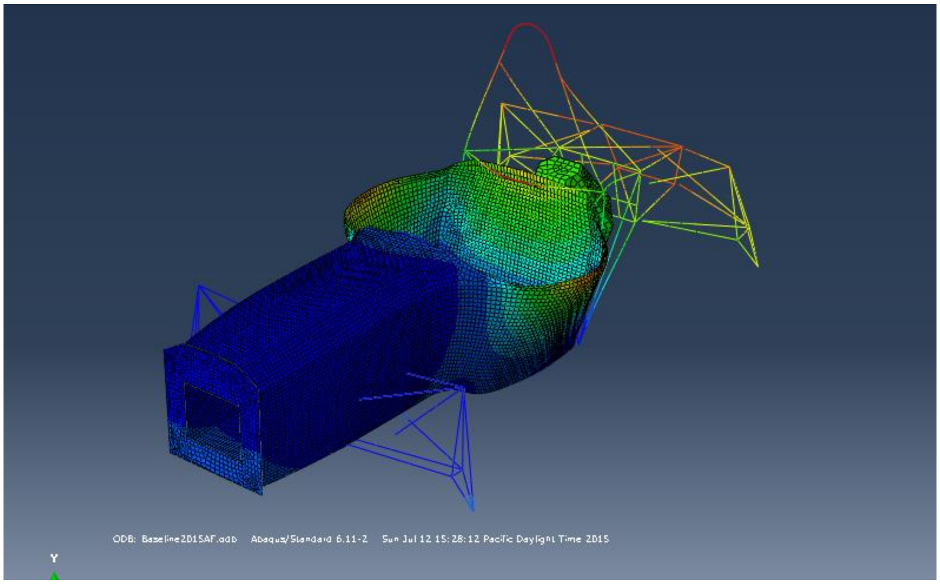

Figure T5. Deflection contour plot for test AF5

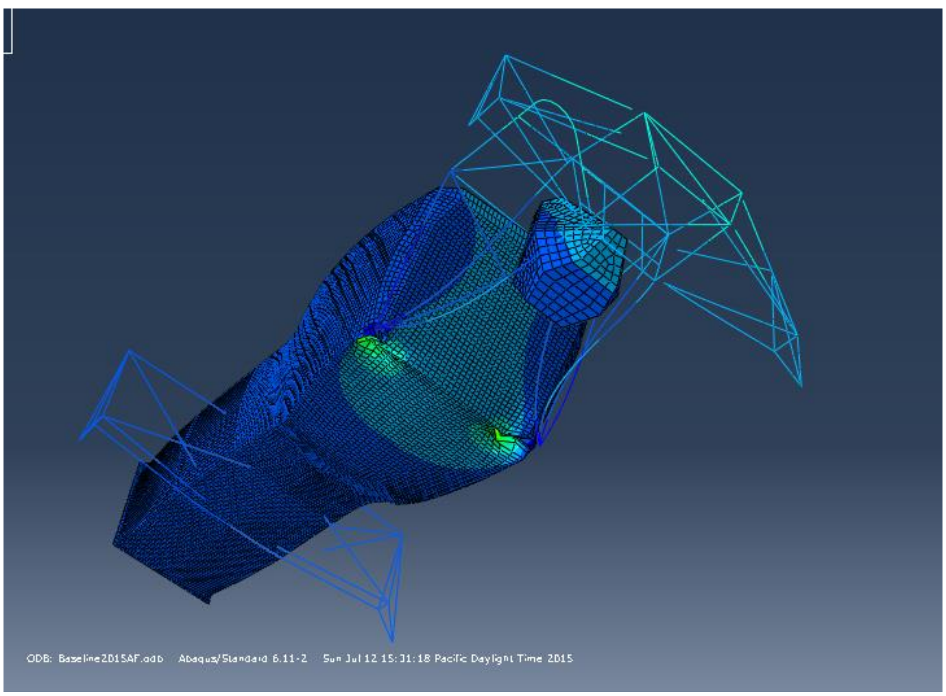

Figure T6. Deflection contour plot for test AF6

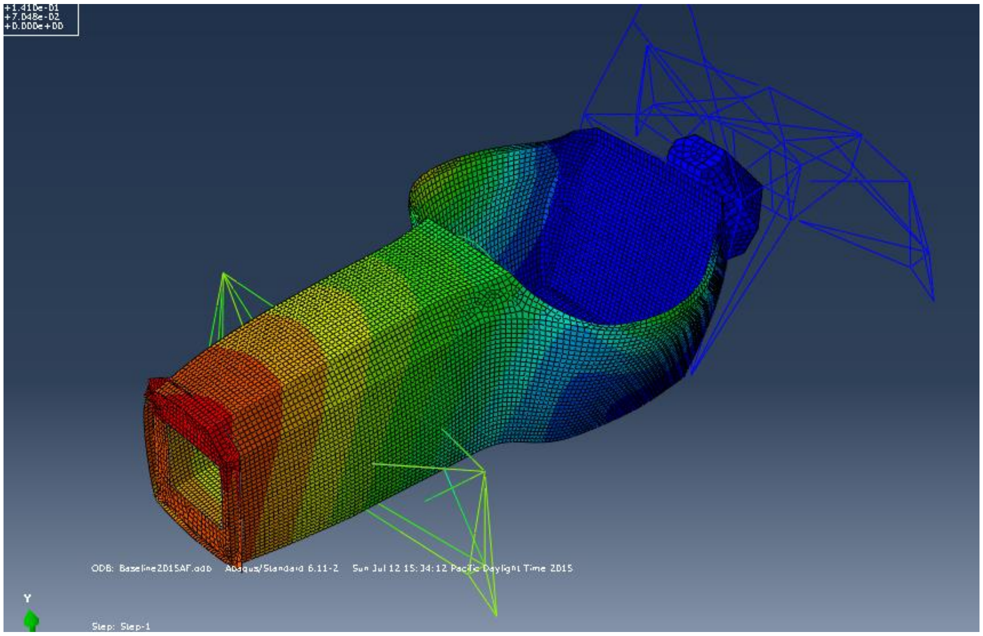

Figure T7. Deflection contour plot for test AF7

Appendix U

Alternative Frame Loading Conditions and Structural Requirements

The following alternative frame loading conditions were taken from the pages 76 through 79 of the 2015 FSAE rules

ARTICLE 3: DEFINITIONS

The following additional definitions apply throughout the Rules document in addition to the ones listed in T3.3

a. Failure - Tensile, compressive, shear load or buckling critical load lower than the specified load. All failure modes have to be considered for every load case.

b. Directions – The following coordinate system and labeling convention is used within these rules

- Longitudinal (X)

- Transverse (Y)

- Vertical (Z)

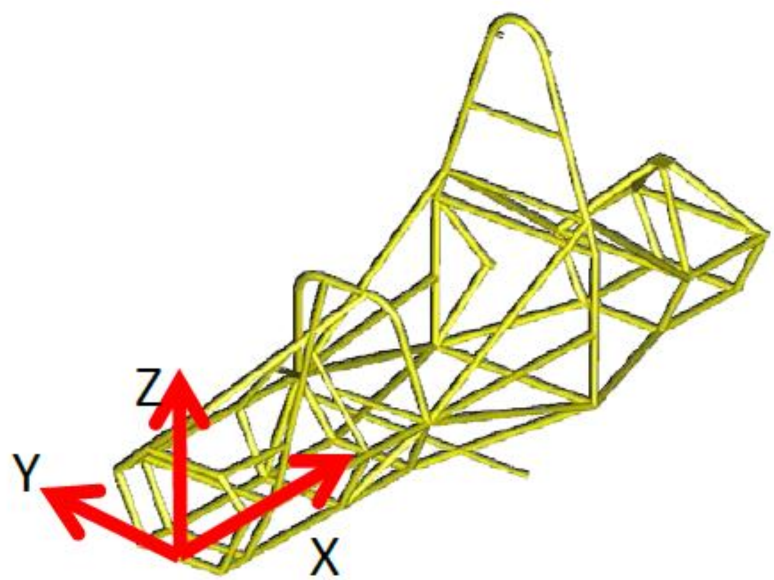

ARTICLE 4: STRUCTURAL REQUIREMENTS AF4.1 Main Roll Hoop, Bracing and Bracing Supports AF4.1.1 Load Applied: Fx = 6.0 kN, Fy=5.0 kN, Fz=-9.0 kN

AF4.1.2 Application point: Top of Main Roll Hoop

AF4.1.3 Boundary Condition: Fixed displacement (x,y,z) but not rotation of the bottom nodes of both sides of the front and main roll hoops.

AF4.1.4 Max Allowable Deflection: 25mm

AF4.1.5 Failure must not occur anywhere in structure

AF4.2 Front Roll Hoop AF4.2.1 Load Applied: Fx = 6.0 kN, Fy=5.0 kN, Fz=-9.0 kN

AF4.2.2 Application point: Top of Front Roll Hoop

AF4.2.3 Boundary Condition: Fixed displacement (x,y,z) but not rotation of the bottom nodes of both sides of the front and main roll hoops.

AF4.2.4 Max Allowable Deflection: 25mm

AF4.2.5 Failure must not occur anywhere in structure

AF4.3 Side Impact AF4.3.1 Load Applied: Fx = 0 kN, Fy=7 kN, Fz 0 kN. Vector direction of lateral load to be in toward the driver.

AF4.3.2 Application point: All structural locations between front roll hoop and main roll hoop *that are also required by AF6.4 (intrusion protection). Load may be distributed by the overlap of the impactor circle to the structural members. In Nastran this can be best accomplished through a "RBE3" (zero stiffness multi-point constant) with the dependent node at the circle center and the independent nodes being all remaining nodes within a 5" (127 mm) radius. Most solvers have a similar type of element*. The analysis may show worst case only but need to support choice of location to justify why it is worst.

AF4.3.3 Boundary Condition: Fixed displacement (x,y,z) but not rotation of the bottom nodes of both sides of the front and main roll hoops.

AF4.3.4 Max Allowable Deflection: 25 mm

AF4.3.5 Failure must not occur anywhere in structure

AF4.3.6 *Accumulator Side Impact protection (EV cars only) use AF4.3 to satisfy EV3.4.4.*

AF4.3.7 *Tractive System Side Impact protection (EV cars only) use AF4.3 with a 5.5 kN load instead of 7 kN to satisfy EV4.2.2.*

AF4.4 Front Bulkhead & Bulkhead Support AF4.4.1 Load Applied: Fx = *120* kN, Fy=0 kN, Fz 0 kN.

AF4.4.2 Application point: use the actual attachment points between the impact attenuator and the front bulkhead

AF4.4.3 Boundary Condition: Fixed displacement (x,y,z) but not rotation of the bottom nodes of both sides of the main roll hoop and both locations where the main hoop and shoulder harness tube connect. Monocoques should use both sides of the bottom of the main hoop and both sides of the upper attachment point between the main hoop and monocoque.

AF4.4.4 Max Allowable Deflection: 25mm

AF4.4.5 Failure must not occur anywhere in structure

AF4.5 Shoulder Harness Attachment AF4.5.1 Load Applied: 13- kN *load for Monocoque chassis or 7kN load for steel space frames applied at each hardness attachment point with the worst case for the range of angles specified in T5.4.4.*

AF4.5.2 Application point: Both harness attachment points simultaneously

AF4.5.3 Boundary Condition: Fixed displacement (x,y,z) but not rotation of the bottom nodes of both sides of the front and main roll hoops.

AF4.5.4 Max Allowable Deflection: 25mm

AF4.5.5 Failure must not occur anywhere in structure

AF4.6 Lap & Anti-Submarine AF Harness Attachment AF4.6.1 Load Applied: *13kN load applied at each lap belt attachment point with the worst case for the range of angles specified in T5.3.5. 6.5 kN load applied at each sub-marine belt attachment point with the worst case for the range of angles specified in T5.3.5. If the lap and sub-marine belts share the same attachment points, then a 19.5 kN load is applied at each belt attachment point with the worst case for the range angles specified in T5.3.5.*

AF4.6.2 Application point: All harness attachment points simultaneously (same load case)

AF4.6.3 Boundary Condition: Fixed displacement (x,y,z) but not rotation of the bottom nodes of both sides of the front and main roll hoops.

AF4.6.4 Max Allowable Deflection: 25mm

AF4.6.5 Failure must not occur anywhere in structure

AF4.7 Front Bulkhead & Bulkhead Support Off Axis AF4.7.1 Load Applied: Fx = *120* kN, Fy=*10.5* kN, Fz 0 kN.

AF4.7.2 Application point: Create load application node in the front bulkhead plane at the center of the front bulkhead. Load application node may be rigidly connected to the front bulkhead and impact attenuator attachment points.

AF4.7.3 Boundary Condition: Fixed displacement (x,y,z) but not rotation of the bottom nodes of both sides of the main roll hoop and both locations where the main hoop and shoulder harness tube connect. Monocoques should use both sides of the bottom of the main hoop and both sides of the upper attachment point between the main hoop and monocoque.

AF4.7.4 Max Allowable Deflection: 25mm

AF4.7.5 Failure must not occur anywhere in structure

2015 Alternative Frame Rules

Notice of Intent

Cal Poly SLO FSAE Team

Introduction

This is Cal Poly's FSAE team proposal to use the Alternative Frame Rule set for the 2015 North America competitions. The purpose of this notice is to demonstrate our team's finite element capability when analyzing our vehicle. Through the sample problem given by the FSAE committee, we hope to prove we are able to meet the analytical requirements specified in the rules. The software used to conduct all of the finite element analysis was done in ABAQUS 6.11.

Procedure and Requirements

Given a list of coordinates and tube number, a solid 3D curve was used in Solidworks to generate the sample chassis profile, shown in Figure V1. Since we will be using composites, the chassis profile in Figure V1 has its two side impact and two front bay diagonals removed for the composite plates that will used instead. This profile was then saved as a wireframe, IGES file and imported into ABAQUS.

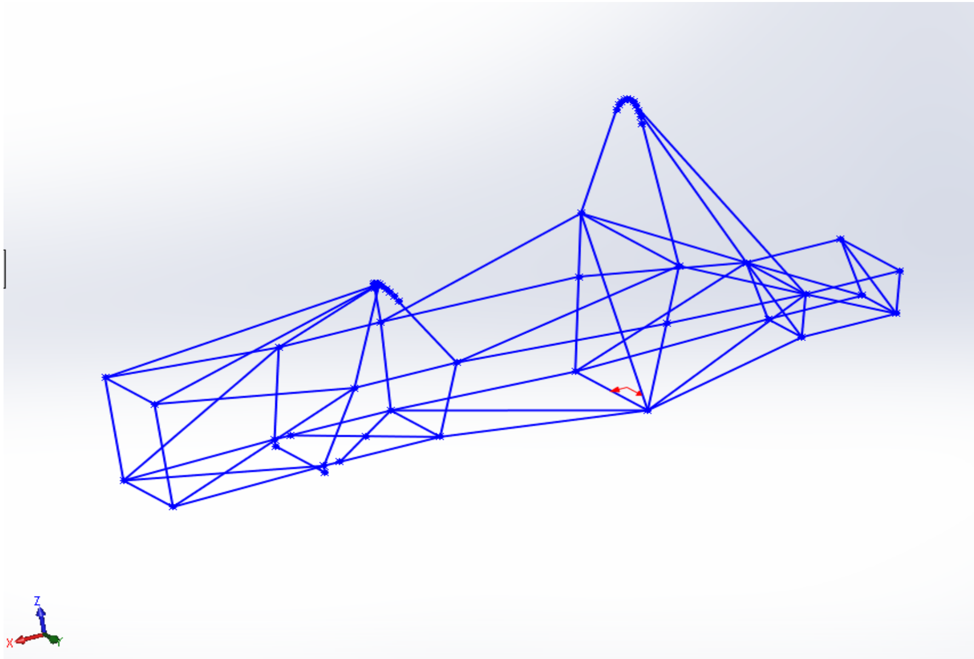

FigureV1. Solidworks model of sample chassis with the side impact and front bay diagonals removed.

Once the file was imported, the material property of the specified core, skin and steel (E = 29,000 ksi) were created. Then the frame profiles and material were created and assigned to their appropriate sections. The four required composite plates were made and assigned with the specified composite layup. The plates were constrained using the tie function and the assembled was made. A meshed image of the chassis without the plates is shown in Figure V2. According to the rules, the tubes with a thickness of less than 0.047 inch, shown in pink, are excluded from the mesh and will not be included in the analysis. Specified boundary conditions and loadings are then applied, analyzed, and recorded.

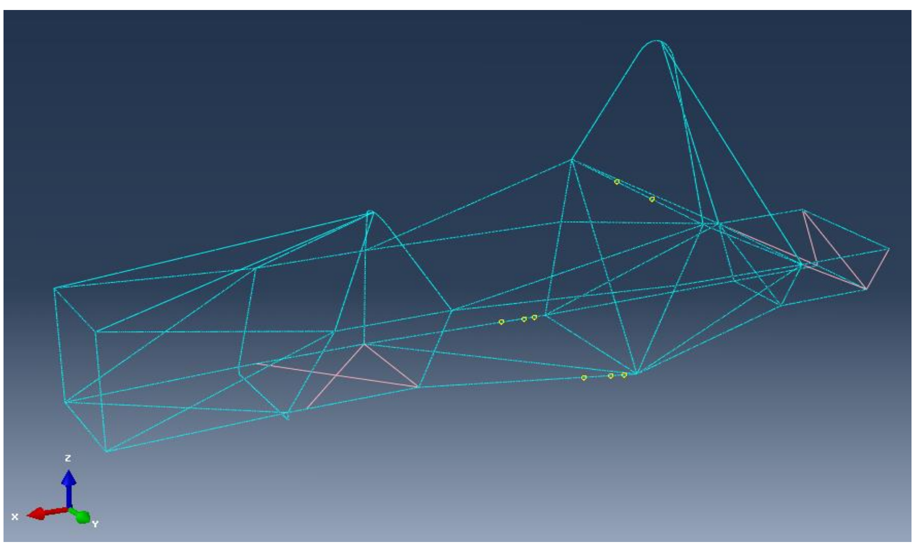

Figure V2. ABAQUS model of the sample without the composite plates. Unmeshed regions (pink) are excluded because of FSAE rules.

Results

A brief mesh convergence study was used to determine our seed size and element type. Shown in Table V1, convergence was achieved using quadratic elements but not linear. Thus, our results are analyzed using a seed size of 0.75 and quadratic elements for all parts. The steel frame is made of B32, 3-node quadratic beam elements, while the composite plates are meshed with S8R, 8-node doubly curved thick shell, reduced integration elements. The boundary conditions used were fixed in the U1, U2, and U3 directions for every location specified. This pin constraint will prevent the node from translating but allow for rotation in the three directions.

Table V1. Mesh convergence study on FSAE sample problem.

Element Seed Size - Linear	DOFs	Max Displacement (in.)
2	33216	0.1533
1.75	33864	0.1536
1.5	34842	0.1542
1.25	36336	0.1545
1	39180	0.1542
0.75	44550	0.1547
0.5	60882	0.1556
Element Seed Size - Quadratic	**DOFs**	**Max Displacement (in.)**
2	37248	.1535
1.75	39132	.1536
1.5	41958	.1531
1.25	46350	.1536
1	62868	.1541
0.75	68792	.1540
0.5	68388	.1540

The mesh convergence analysis was done using only the Main Roll Hoop boundary and loading conditions in order to keep everything constant. Since the linear elements were unable to converge, quadratic elements were used. The purpose of this study was to define the number of elements used is the sufficient minimum and to prove that our values are at its converging point.

Table V2. Max deflection and max Mises stress for the following load and boundary cases.

Rule Number	Rule Description	Max Deflection (in.)	Max Mises Stress (ksi)
AF4.1	Main Roll Hoop	0.154	29.9
AF4.2	Front Roll Hoop	0.451	46.9
AF4.3	Side Impact	0.663	57.6
AF4.4	Front Bulkhead & Supports	0.264	69.7
AF4.5a	Shoulder Harness 0°	0.753	152
AF4.5b	Shoulder Harness 10°	0.760	152
AF4.5c	Shoulder Harness -20°	0.733	152
AF4.6a	Lap & Anti-Submarine Belts 45°	0.025	42.2
AF4.6b	Lap & Anti-Submarine Belts 55°	0.031	47.6
AF4.6c	Lap & Anti-Submarine Belts 65°	0.036	51.5
AF4.7	Front Bulkhead Off-Axis	0.703	96.5

The smallest, median, and largest angle were analyzed to produce the worst case scenario for the Shoulder Harness and Lap & Anti-Submarine Belt case. That will be the Shoulder Harness at 0° and Lap & Anti-Submarine Belts at 65°.Smaller individual loadings were distributed in different to match the magnitude that is specified. From here, only the worst case for those loading case will be displayed. For the side impact load, a pressure load is applied on a 10 inch diameter circle representing the impactor on the center of the side impact plates. The equivalent force is calculated by dividing the specified force by the area of the circle.

Table V3. Factor of safety for both deflection and stress.

Rule Number	Rule Description	Deflection Factor of Safety	Stress Factor of Safety
AF4.1	Main Roll Hoop	6.39	1.48
AF4.2	Front Roll Hoop	2.18	0.94
AF4.3	Side Impact	1.48	0.77
AF4.4	Front Bulkhead & Supports	3.72	0.63
AF4.5	Shoulder Harness 10°	1.30	0.29
AF4.6	Lap & Anti-Submarine Belts 65°	27.6	0.46
AF4.7	Front Bulkhead Off-Axis	1.40	0.86

The stress factor is calculated by $SF = \frac{Max\ Allowable\ Stress}{Max\ Mises\ Stress}$, where the max allowable is specified in the rules to be 44.2 ksi. Similarly, the deflection safety factor is calculated by $SF = \frac{Max\ Allowable\ Deflection}{Max\ Deflection}$, where the max allowable deflection is 25mm or 0.9843 inches.

Table V4. The individual constraint reactions at each load for each loading case.

Rule Number	Rule Description	Constraint Reactions (lb_f)
AF4.1	Main Roll Hoop	RFRH 1922 LFRH 1452.2 LMRH 1661.16 RMRH 4601.35
AF4.2	Front Roll Hoop	RFRH 1023.04 LFRH 550.259 LMRH 559.259 RMRH 1873.31
AF4.3	Side Impact	RFRH 1217.7 LFRH 1108.44 LMRH 1045.39 RMRH 1191.07
AF4.4	Front Bulkhead & Supports	RSH 6474.27 LSH 6420.01 LMRH 7198.2 RMRH 7278.16
AF4.5	Shoulder Harness 10°	RFRH 1586.12 LFRH 1474.61 LMRH 1738.26 RMRH 1679.45
AF4.6	Lap & Anti-Submarine Belts 65°	RFRH 409.261 LFRH 240.925 LMRH 4242.37 RMRH 4332.2
AF4.7	Front Bulkhead Off-Axis	RSH 8806.4 LSH 4013.66 LMRH 10871.1 RMRH 3690.95

The constraint reactions measure the loading at each of the four nodes where the boundary conditions are placed. The three different acronyms are: FRH – Front Roll Hoop, MRH – Main Roll Hoop, and SH – Shoulder Harness. The preceding letter of each acronym defines whether it is left or right, looking from the back of the car.

Table V5. The first three positive eigenvalues for buckling produced in ABAQUS.

Rule Number	Rule Description	First Three Positive Modes	Buckling Eigenvalues
AF4.1	Main Roll Hoop	Mode 2	8.91
		Mode 4	9.15
		Mode 6	9.80
AF4.2	Front Roll Hoop	Mode 1	7.35
		Mode 2	8.52
		Mode 3	8.88
AF4.3	Side Impact	Mode 1	12.54
		Mode 2	13.16
		Mode 3	13.37
AF4.4	Front Bulkhead & Supports	Mode 1	2.74
		Mode 2	3.02
		Mode 3	3.16
AF4.5	Shoulder Harness 10°	Mode 1	9.89
		Mode 2	10.14
		Mode 3	10.86
AF4.6	Lap & Anti-Submarine Belts 65°	Mode 7	12.75
		Mode 10	16.19
		Mode 14	17.84
AF4.7	Front Bulkhead Off-Axis	Mode 1	2.33
		Mode 2	2.49
		Mode 3	2.98

Here are the first three positive eigenvalues produced for each loading case. Negative eigenvalues are excluded because there is a possibility that those modes are not possible and are irrelevant. The smaller the eigenvalues, the more likely it is for the part to buckle.

Attached here is an image of each loading case showing deflection and a caption describing the loading case.

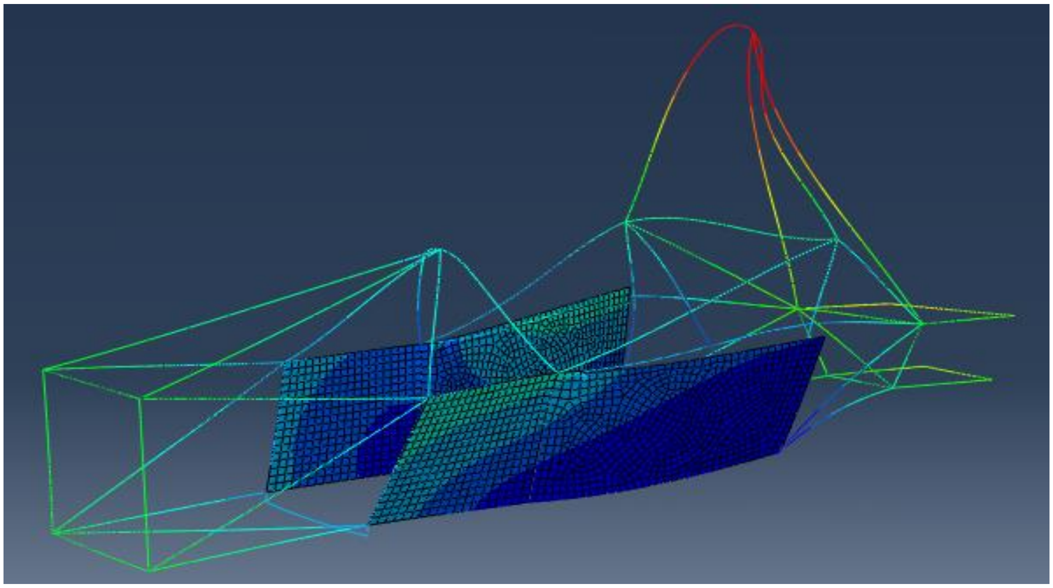

Figure V3. Main Roll Hoop, point load on top of main roll hoop.

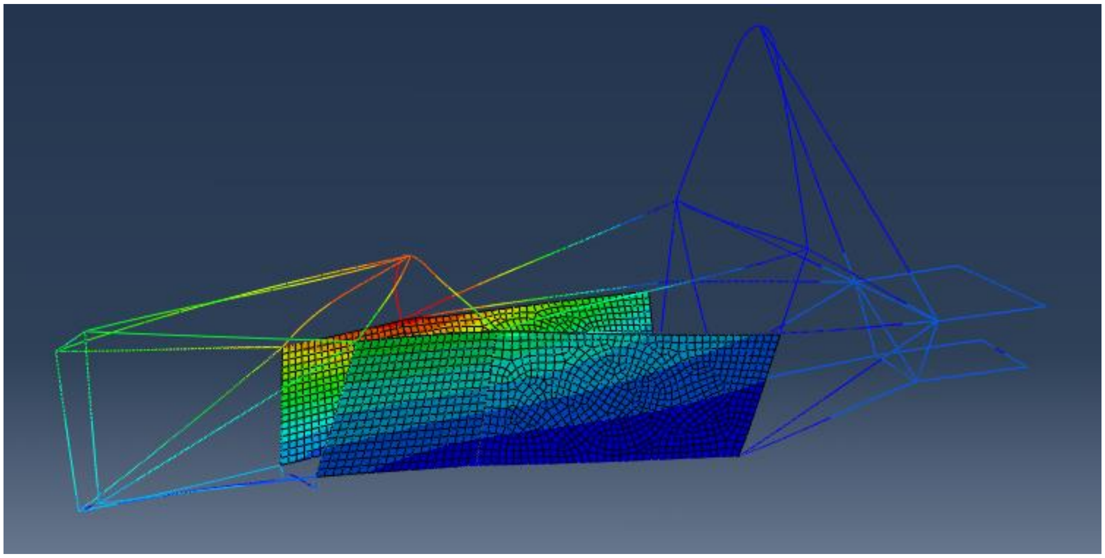

Figure V4. Front Roll Hoop, point load on top of front roll hoop.

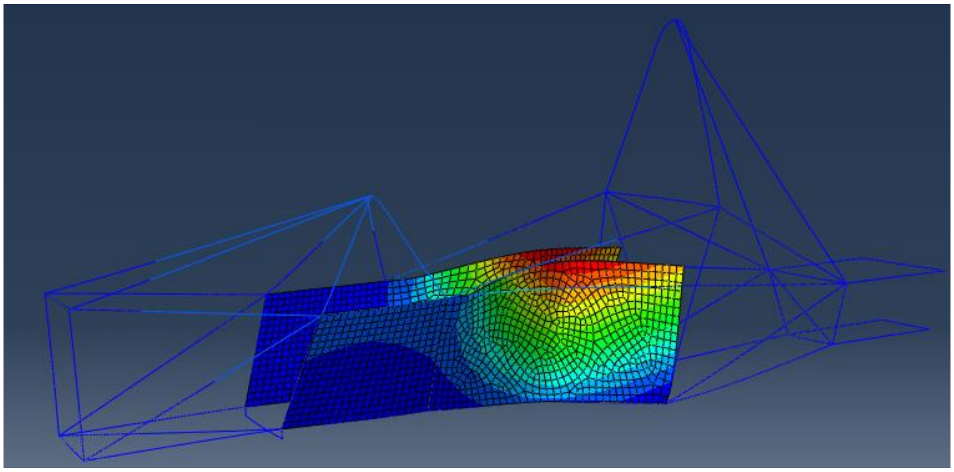

Figure V5. Side Impact Plates, 10” circular pressure load on each plate

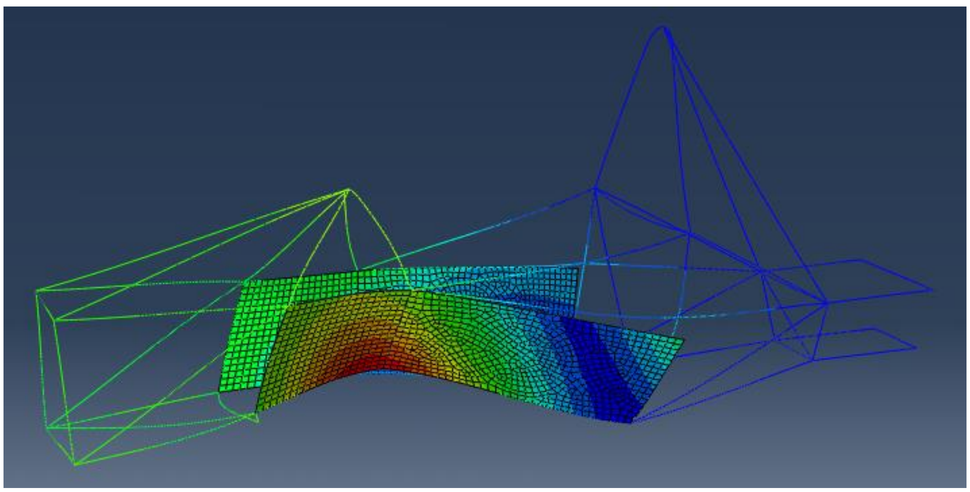

Figure V6. Front bulkhead/Support. Loading placed on the four nodes of the front bulkhead/attenuator.

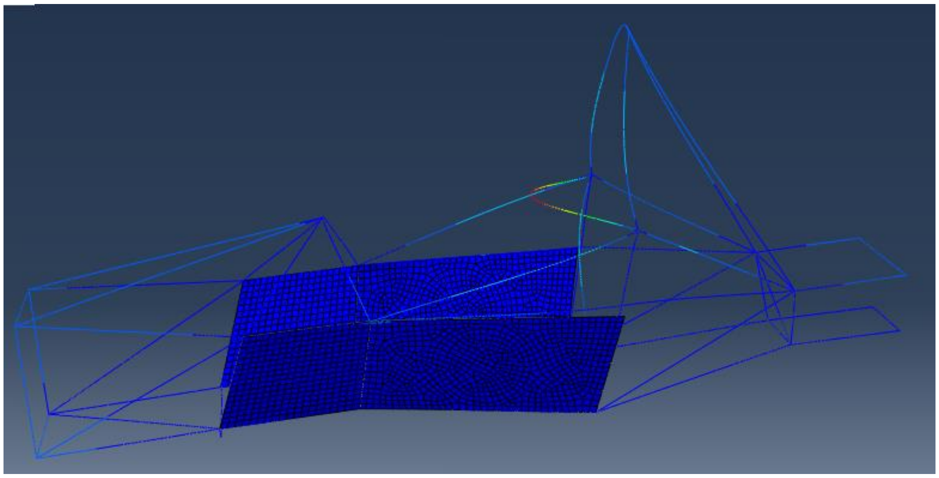

Figure V7. Shoulder Harness Attachment load applied 8 inch apart

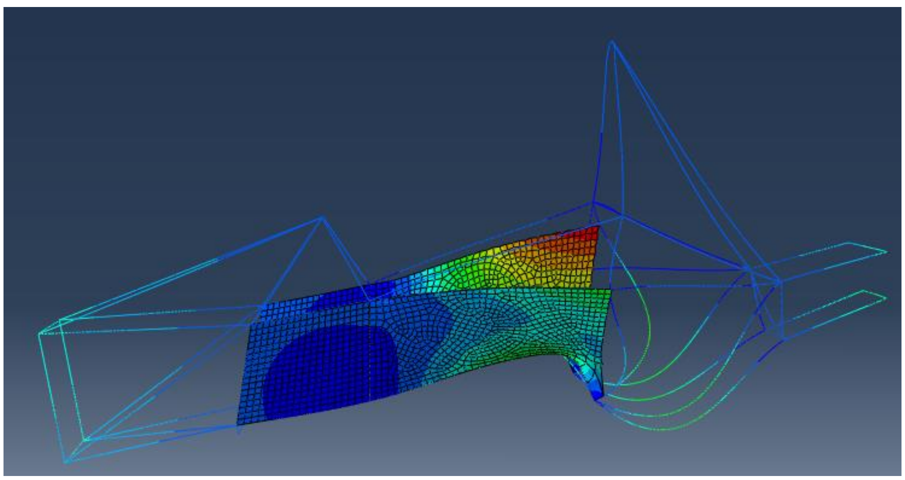

Figure **V8.** Lap & Anti-Submarine Harness Attachment. Load applied 1.62 inches away from both sides of the bottom of the main roll hoop.

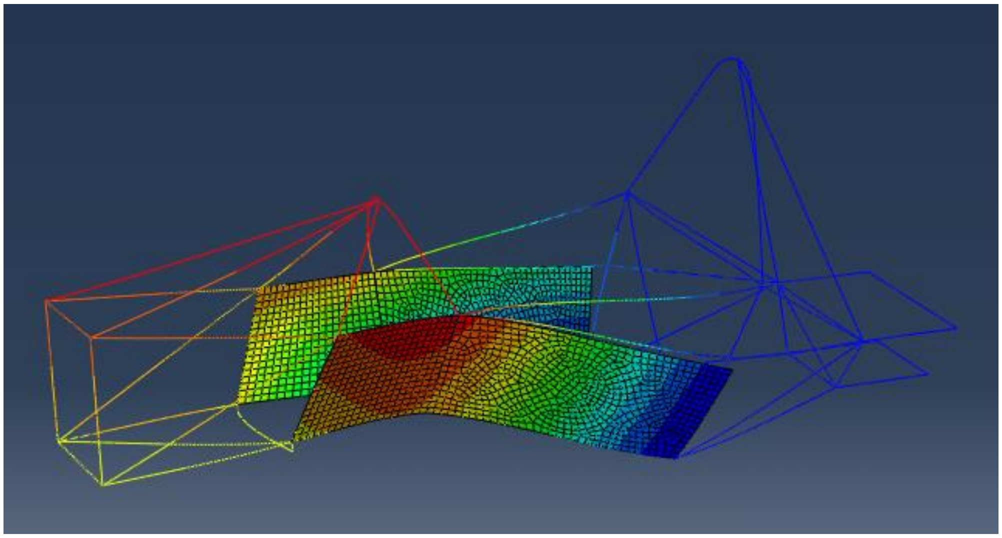

Figure V9. Front Bulkhead/Support with an off axis loading at the center of the front bulkhead. A reference point was used along with a coupling constraint to allow application of laod.

Appendix W

CP Speed Torsional Test Results

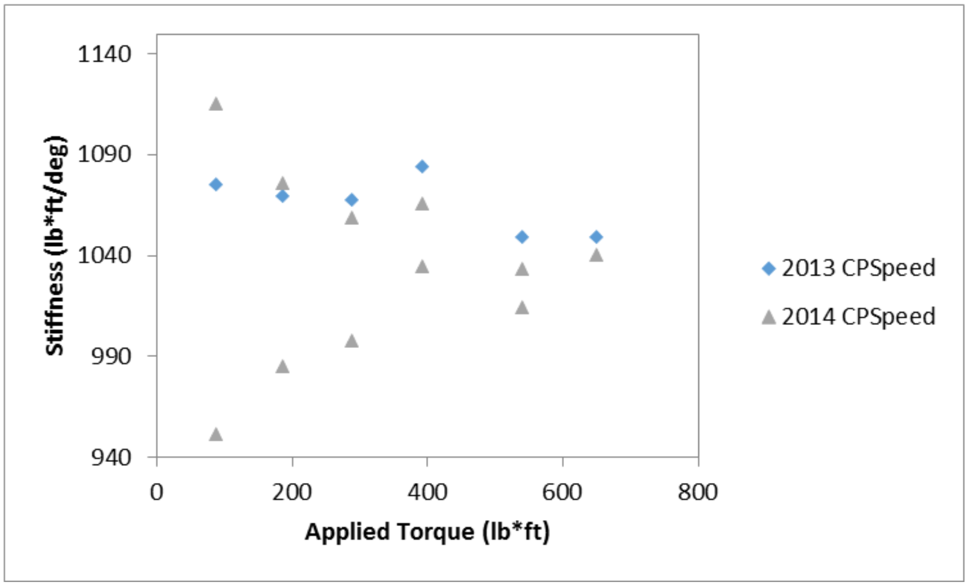

Figure W1. Senior project CP Speed reported torsional stiffness values slightly different than FMD. This data gathered by CP Speed shows that removing weight during the torsional test resulted in high hysteresis, skewed toward the compliant end of the spectrum. When computing the average stiffness, only the values from adding weight were used in the 2013 number; whereas, the 2015 average included the data points collected after removing weight.

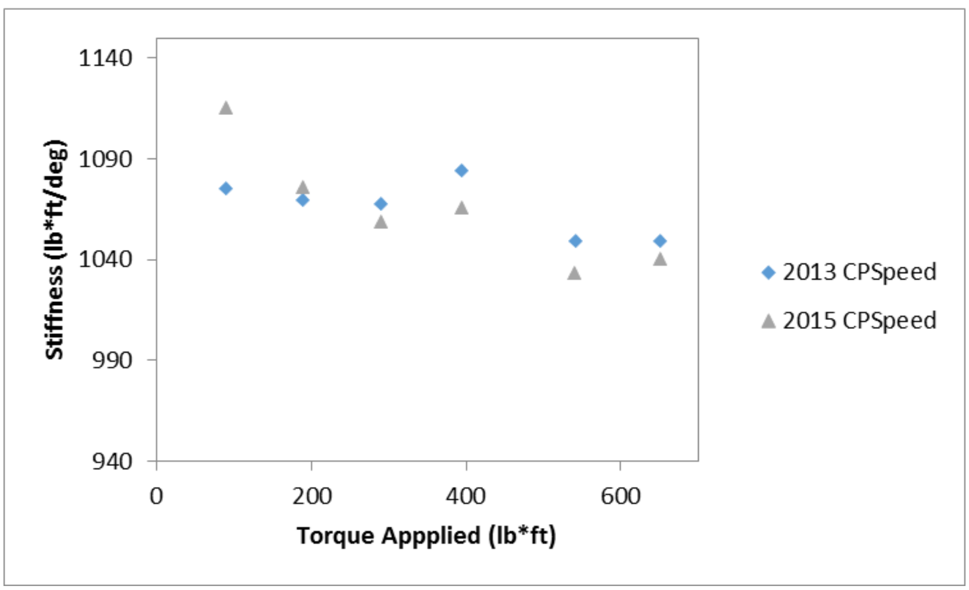

Figure W2. When the values for the same data are used but excluding the points collected when removing weight, it is clear that the two stiffnesses are much more similar than originally reported. The average value for the 2013 vehicle is 1067 lb*ft/deg whereas the 2013 chassis is 1065 lb*ft/deg. More work can be done to examine the effects of hysteresis and to explore methods to reduce it such as lubrication of bolted joints and higher-quality dial indicators.

Appendix X

Laminate Stacking Order Drawings

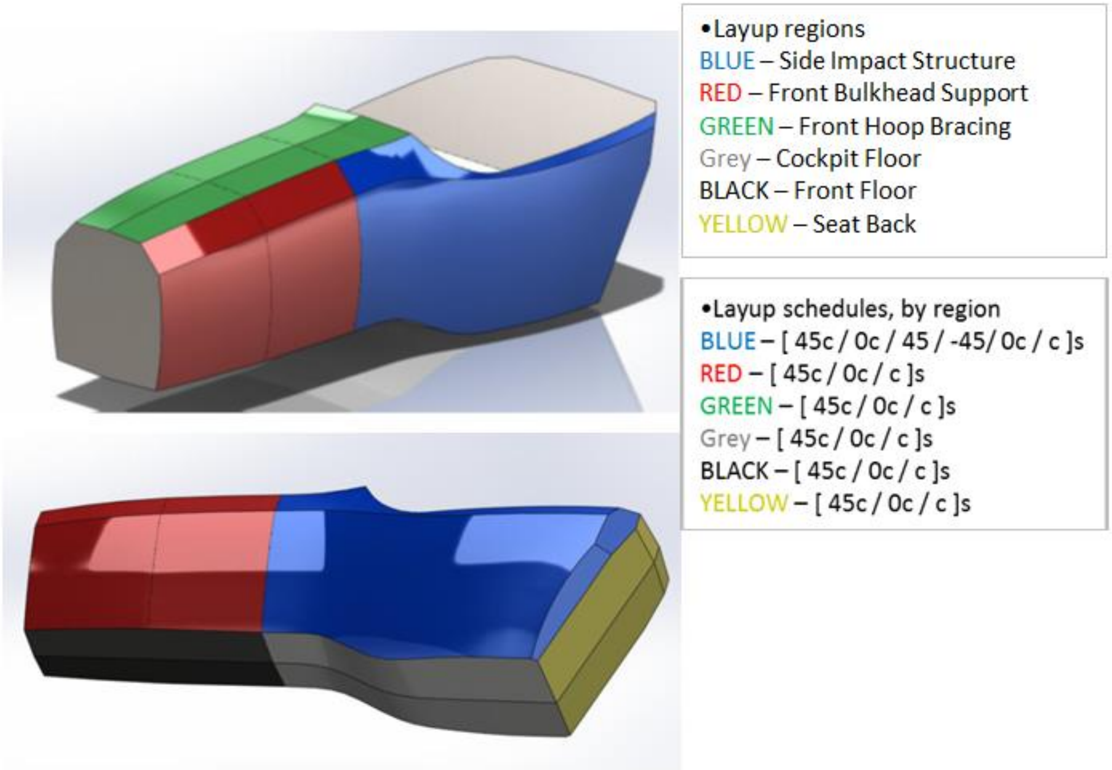

Figure X1. Laminate schedules for the regions of the monocoque dictated by SAE. Cloth is TenCate TC250-AS4 and unidirectional tape is Umeco MTM49-M55J. Core is Plascore PAMG-XR1 5052

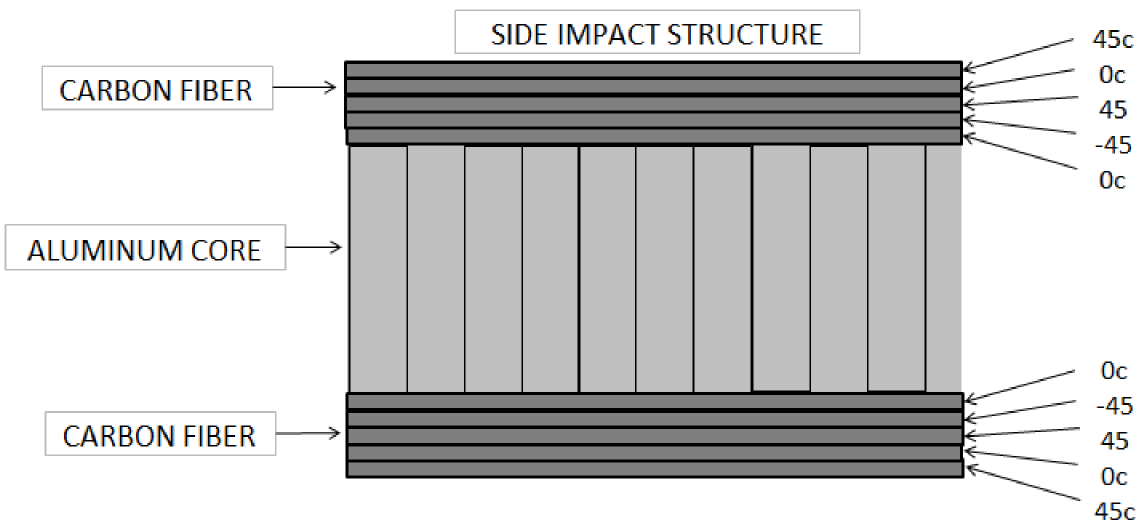

Figure X2. The side impact structure laminate was the thickest with 3 plies of cloth and 2 plies of unidirectional tape. Core was 0.700" thick.

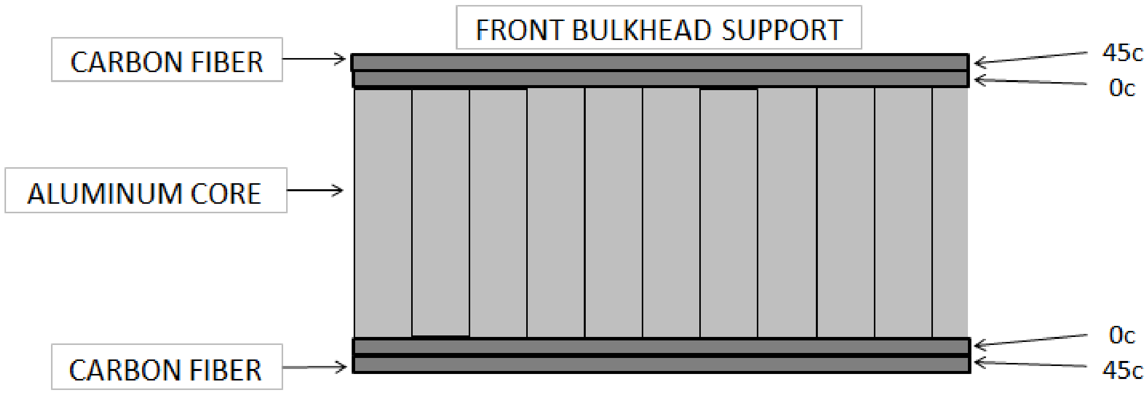

Figure X3.The front bulkhead laminate utilizes 2 plies of cloth and 0.700” thick core.

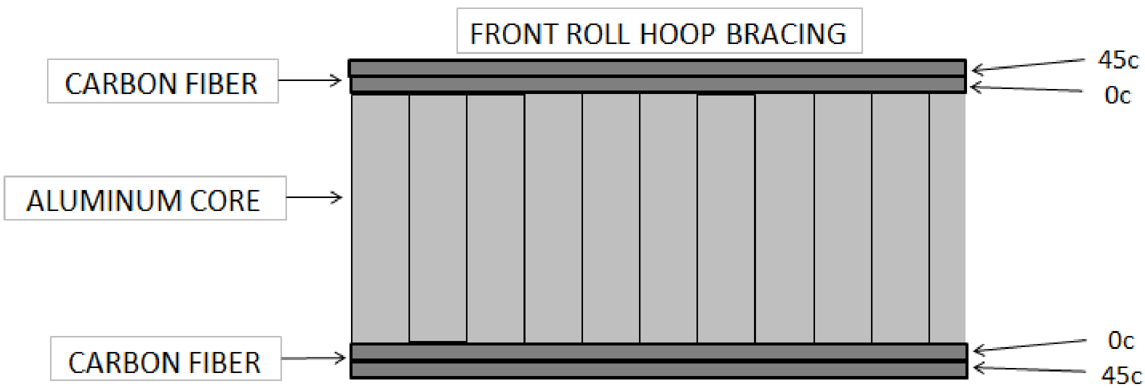

Figure X4. The front roll hoop bracing laminate utilizes 2 plies of cloth and 0.700” thick core.

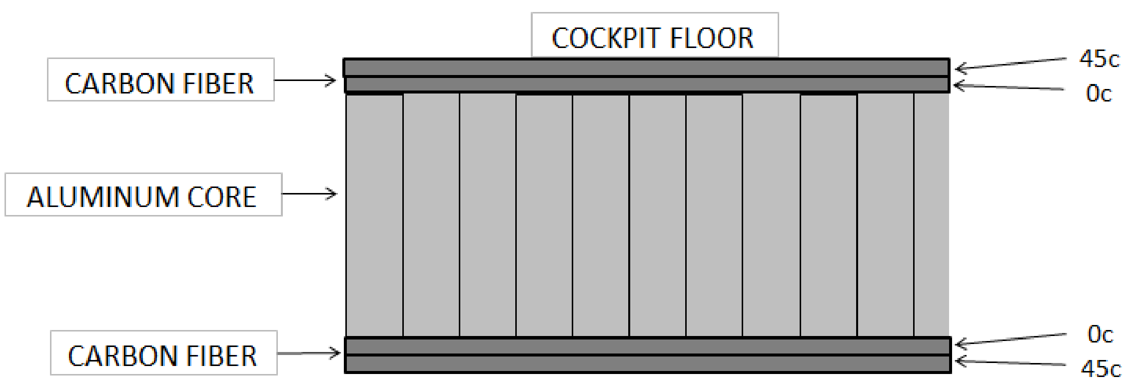

Figure X5. The cockpit floor laminate utilizes 2 plies of cloth and 0.700” thick core.

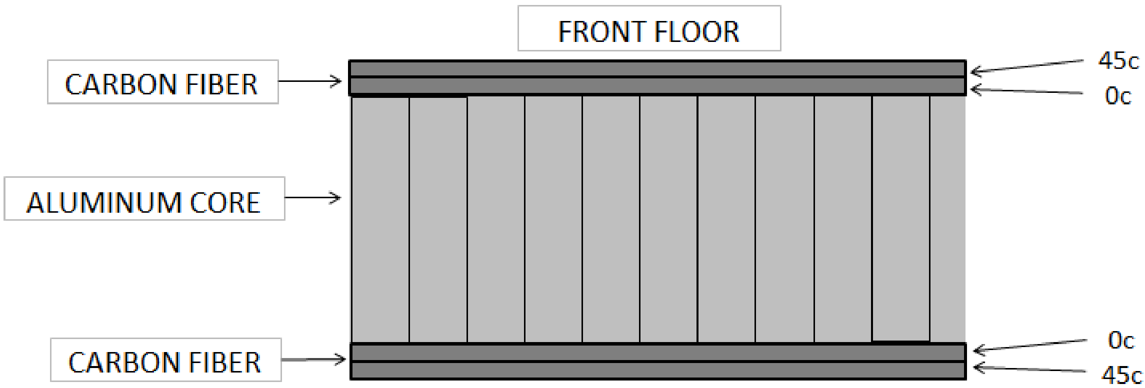

Figure X6. The front floor laminate utilizes 2 plies of cloth and 0.700” thick core.

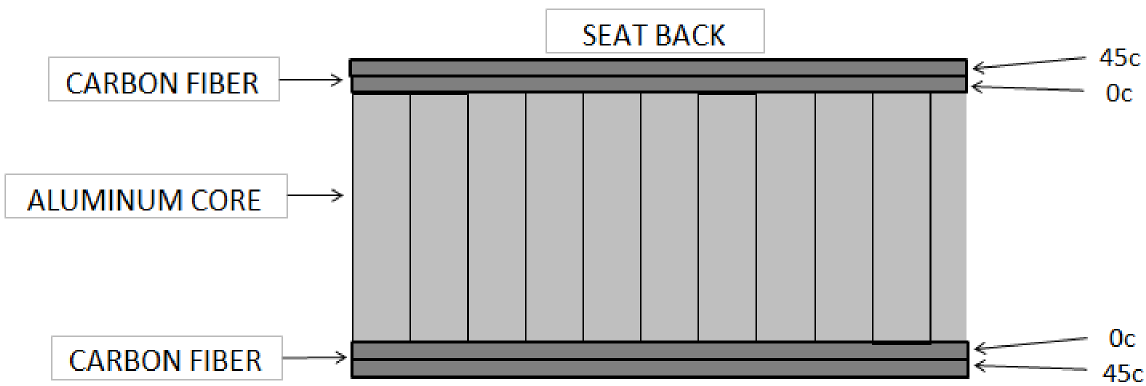

Figure X7. The seat back laminate utilizes 2 plies of cloth and 0.700” thick core.

Appendix Y
Additional Core Preparation Information

Core-Splicing

Figure Y1. One method of core-splicing that was explored was butting two sections of core together and using a mallet to smash a third small piece into the cells adjacent to the butt. This method was suggested by an aerospace contractor at AASC in Stockton. Most samples joined well, but FMD was unwilling to hammer the joint together on the mold as would have been required. In this sample, 2 cells on each side were overlapped by the third piece and offset into the middle of the hexagon.

Figure Y2. Another example of core-splicing using a third piece hammered into the joint. Not offsetting the third piece kept the most cells intact. This was the best way FMD found to execute this method.

Figure Y3. This section showing the bottom side shows poor joining at the seam. Aligning the smashed-down pieces cells reduced this splitting effect.

Figure Y4. Two pieces of core butted together with the third piece ready to be smashed into the joint.

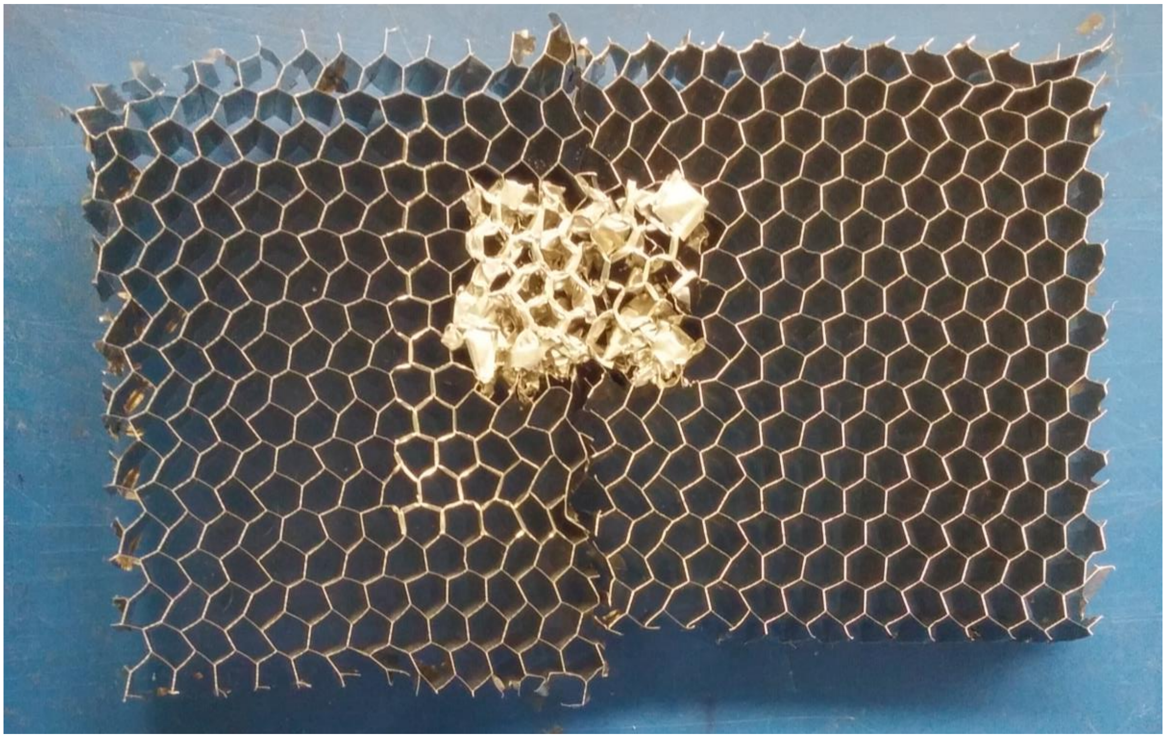

Figure Y5. The third piece smashed in shows a flat upper surface. The bottom surface was typically flat as well when the cells of the third piece were aligned with the other two pieces.

Figure Y6. Simply overlapping two pieces and hammering down was unpredictable. Some samples joined exceptionally well and others poorly when the top piece moved downward at an angle.

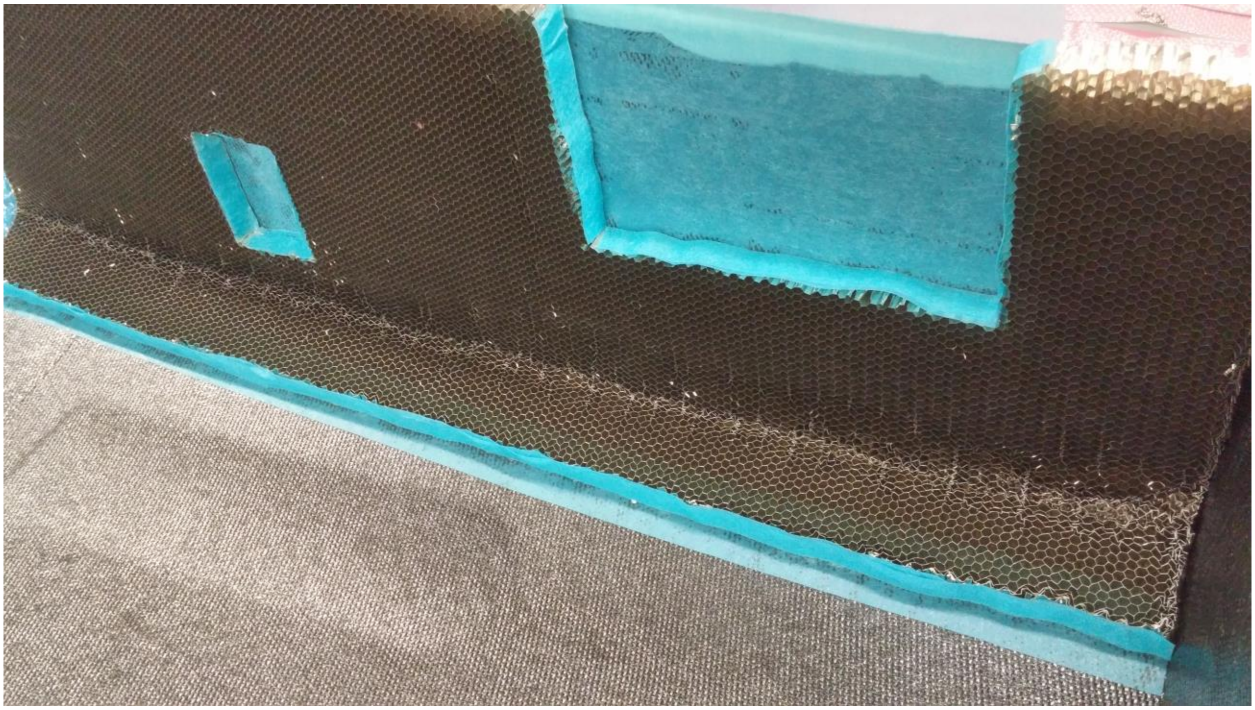

Figure Y7. Film adhesive was placed at every surface where balsa joined with aluminum core.

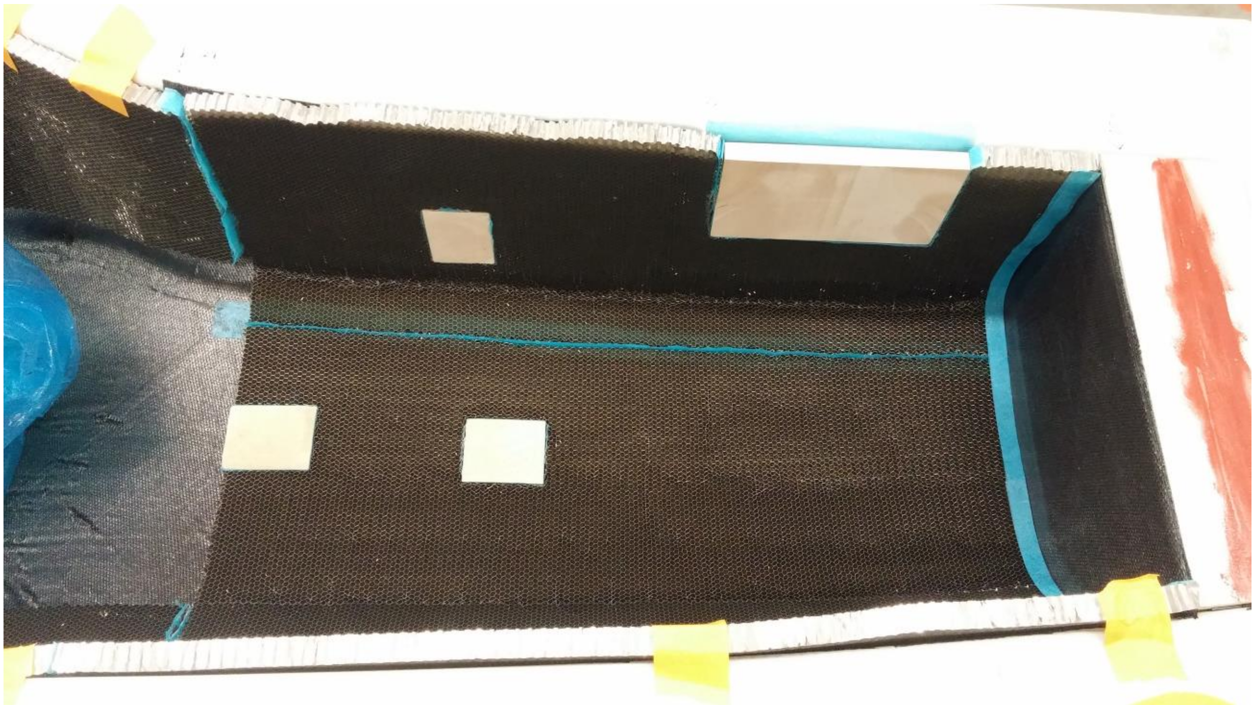

Figure Y8. Balsa inserted into the recesses of the core.

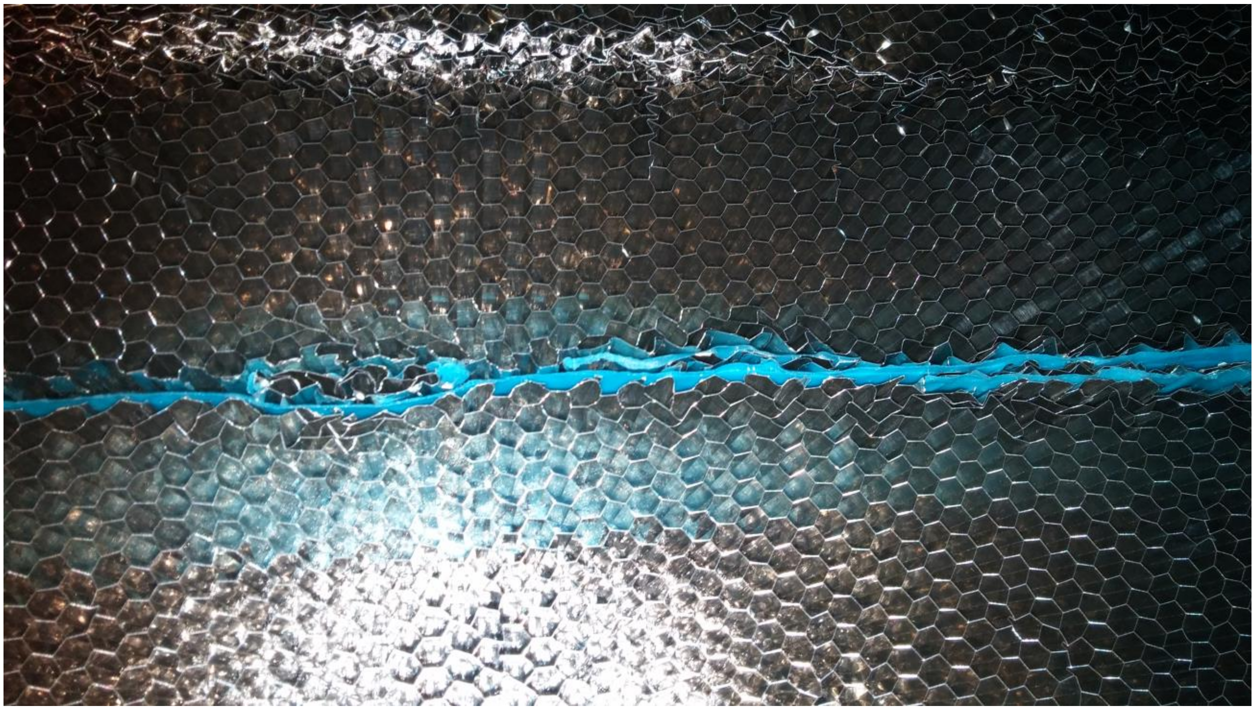

Figure Y9. Core splices were a tedious process of pulling back core at the joint, inserting thin, compressed strips wrapped in film-adhesive and manually expanding the previously-compressed cells (one-by-one). Foaming core splice is recommended.

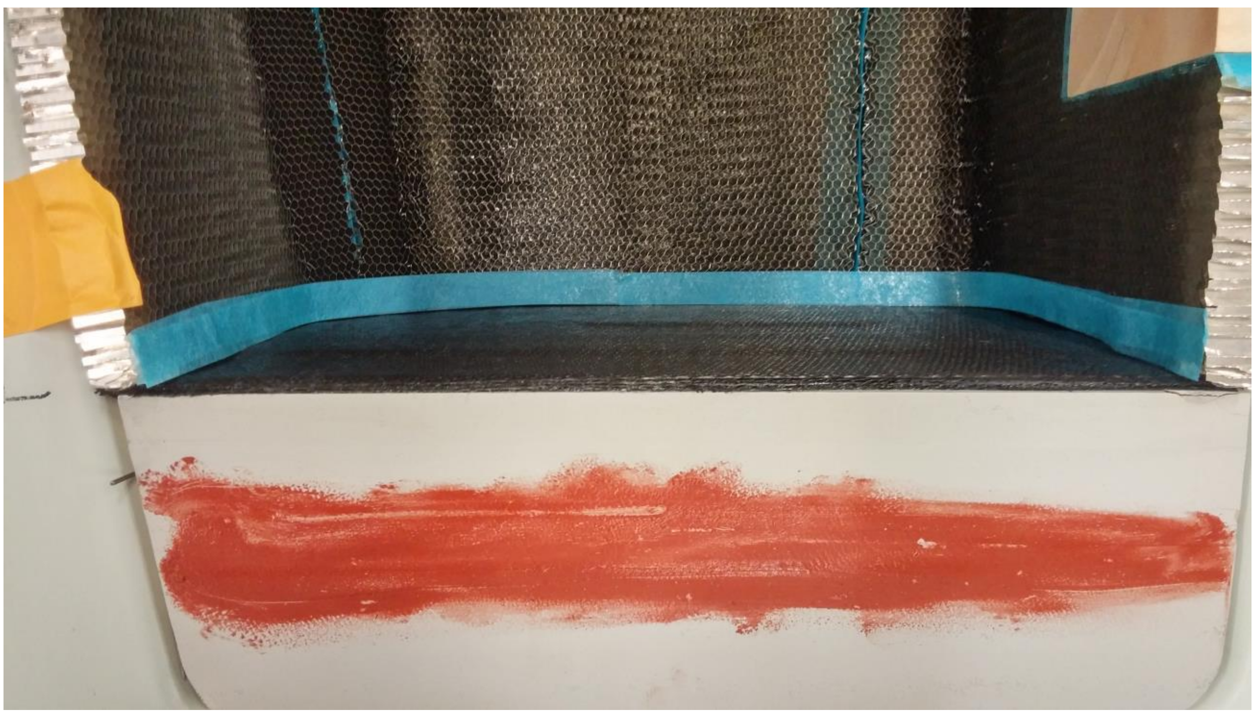

Figure Y10. Film adhesive was used where the front bulkhead core was placed as well.

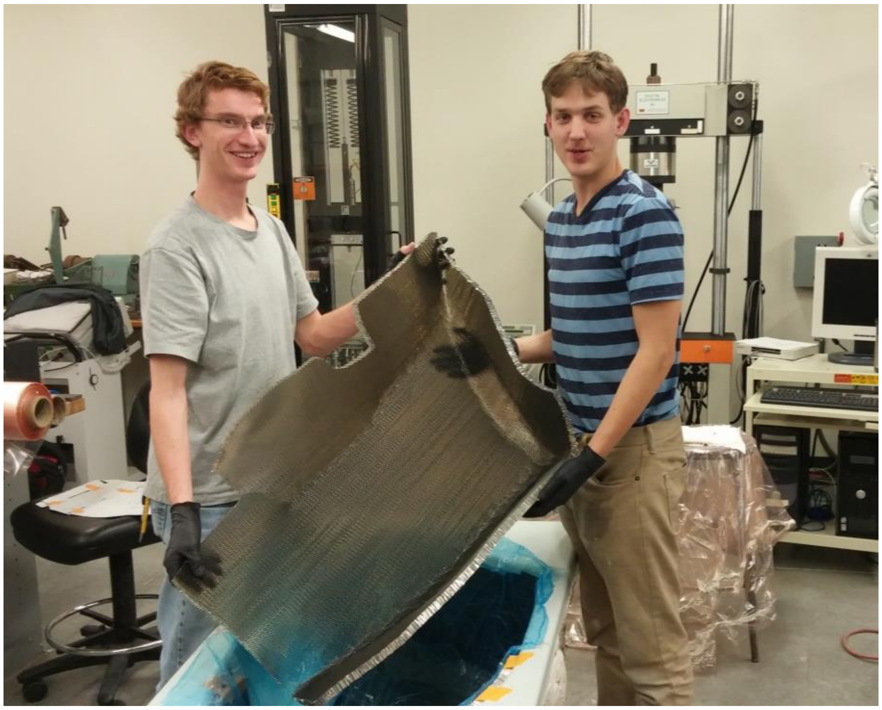

Figure Y11. The core for the SIS was formed out of one continuous sheet to reduce splices. This method worked very well.

Figure Y12. The single-piece SIS core in-place.

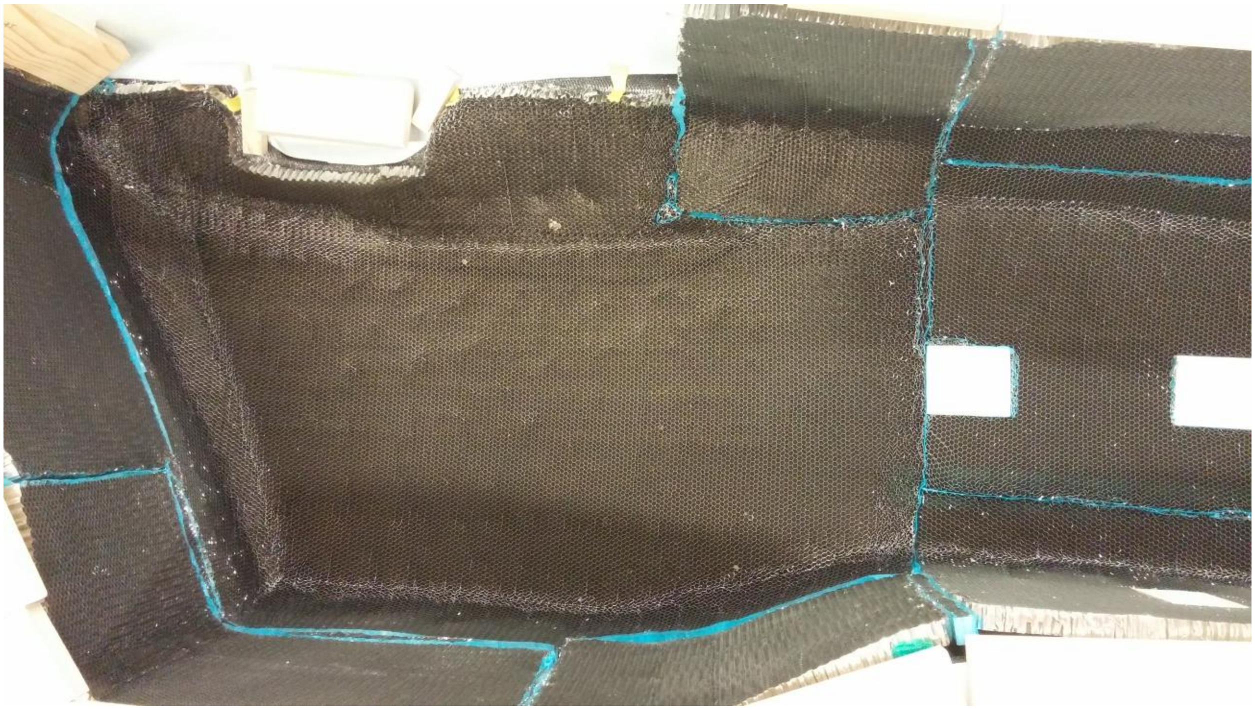

Figure Y13. The core templates were different than the carbon templates in order to minimize compound bends.

Figure Y14. Wood was inserted at the edges of the core by the cockpit opening (shown) and all other edges (not pictured) to prevent core from crushing while under vacuum in the debulking and cure cycles.